Morphodynamics and sediment transport in a wandering gravel-bed channel: Fraser River, British Columbia

by
Darren Gary Ham

B.Sc. (Hons.), University of Victoria, 1990
M.Sc., The University of British Columbia, 1996

A thesis submitted in partial fulfillment of
the requirements for the degree of
Doctor of Philosophy

in
THE FACULTY OF GRADUATE STUDIES
(Geography)

The University of British Columbia
July, 2005

Abstract

This study investigates the relation between sediment transport and channel deformation on a 70 km long wandering reach of lower Fraser River, British Columbia. The reach is characterized by an irregularly sinuous single-thread channel split around large bar and island complexes. An extensive network of secondary channels, produced from channel shifting and abandonment, is found within these complexes and along the adjacent floodplain. Most material accumulates within wide 'sedimentation zones' where deposited sand and gravel create an obstruction to downstream flow conveyance, and in areas of flow expansion where shear stress declines. These sites correspond to the location of prominant diagonal riffles. Changes to reach morphology are dominated by the transfer of coarse alluvial sediments. Small gravel sheets are attached to existing lateral and mid-channel bars, forcing compensating erosion across the channel and propagating instability downstream. Over periods of several decades, entire bars and bar / island complexes migrate downstream in association with the riffles.

Sediment budgets constructed for several periods between 1952 and 2003 show that the transport rate into the reach is highly variable over time and does not correlate well with the magnitude or frequency of large floods. Influx into the reach has apparently increased over time, from 180,000 m^3/yr from 1952 to 1984 to 494,000 m^3/yr from 1999 to 2003. The present high rates are associated with channel alignment upstream of Agassiz-Rosedale Bridge that causes extensive erosion at lower Herrling Island. This sequence is apt to be disrupted within the next several years as the island becomes bissected, and transport rates should subsequently decline. The long-term (1952-1999) rate of 212,000 m^3/yr appears to be the more conservative figure for applied gravel management strategies. This budget also indicates that channel reaches upstream of the bridge have degraded. It is probable that sedimentation in the gravel reach during most of the 20th century was influenced by placer mining in the Fraser Canyon which introduced significant (though unknown) quantities of bed material to the river. More recent factors such as development of the Coquihalla Highway and numerous pipeline and transmission lines may also have led to higher inputs than would be expected in a natural, undeveloped system (Church et al., 2001). However, it is difficult to confirm that these activities continue to impact the gravel budget, or that recent degradation is in fact a response to an exhaustion of upstream sediment supply.

Although the gravel reach remains a relatively pristine environment relative to most large navigable rivers in populated regions, the isolation of several large sloughs and backchannels, lateral confinement through bank hardening, and removal of sand and gravel from the channel have

cumulatively reduced the complexity of channel morphology and reduced the channel gradient. Despite evidence that recent morphologic evolution is trending towards a more stable single-thread meadering habit, considerable downtream instability is expected to continue for several decades as this pattern continues to develop. The relations between sediment transport and channel deformation developed in this thesis should provide better tools to facilitate sound riverine management during this period, but additional survey is required to evaluate such change.

Table of Contents

List of Tables

List of Figures

Acknowledgments

First and foremost, I wish to express my sincere thanks to my supervisor, Dr. Mike Church, for his invaluable contributions and support during the completion of this thesis. Because of his always thoughtful commentary, thorough review, and stimulating questioning, I have become a better writer and scientist. I should also like to express my gratitude to the other members of my committee: Dr. Ted Hickin, Dr. Brian Klinkenberg and Dr. David McLean for their input and review.

Thanks are extended to Mr. Terry Keenhan, formerly of the Ministry of Environment, Lands and Parks, for initiating interest on the gravel management concern in lower Fraser River, and to Mr. Ron Henry, senior hydraulic engineer responsible for lower Fraser River (also with MoELP, later Ministry of Water, Land and Air Protection) for his continued interest in the project. I am appreciative for the efforts of Karen Kranabetter and Jason Barraclough with regard to the monumental task of digitizing so many airphotos, and to Hamish Weatherly for his assistance with the early formulation of the sediment budget. I would be remiss if I did not also thank Scott Paper for access to their archival materials, the Fraser Basin Council for their interest and support of this project and to Kevin and Rosemary in the GIC for always being helpful in accessing materials. Finally, I am grateful to my friends and family, especially my parents, who so strongly supported my decision to undertake a PhD.

Financial assistance for this project was provided by the British Columbia Emergency Flood Protection Program, The City of Chilliwack and a National Sciences and Engineering Research Council strategic grant awarded to Dr. Mike Church. The project could not have been completed without this assistance.

Chapter 1: Introduction

1.1 Problem statement

The floodplains of large alluvial rivers have long been a focus of human settlement, providing ideal locations for development and agriculture, important sources of food and building materials, and vital conduits for transportation and commerce. For as long as such areas have been populated, flooding and channel erosion have prompted river engineering solutions to minimize these impacts, and costly maintenance programs to ensure effectiveness (Schumm and Winkley, 1994). Consequently, many rivers have been altered to some extent to accommodate the needs of people, usually to the detriment of the natural environment. As population growth fuels the need, and technological advances continue to enhance our ability to modify riverine environments, it becomes increasingly important to recognize the processes that govern river behaviour and to understand the resultant morphological response over appropriate spatial and temporal scales. Failure to do so will undermine efforts to effectively manage alluvial channels while preserving ecosystem health and diversity.

Attempts to relate form and process relations on alluvial channels have been a dominant theme in fluvial science for the past half-century (Leliavsky, 1955, Leopold, Wolman and Miller, 1964). This avenue of study is complicated by the large number of variables involved, the broad range of possible channel adjustments and the scale of investigation. Over periods of years to decades (the timescale of central interest in this thesis), alluvial channels can exhibit a wide variety of distinct morphologic forms in response to the complex interaction of various governing conditions. Along the length of a channel network, the presence of a given morphology within a homogenous reach[1] is dominantly influenced by the local flow and sediment regimes (cf. Mollard, 1973; Kellerhals et al., 1976; Richards, 1982; Church, 1992) and by valley gradient (Carson, 1984; van den Berg, 1995). Further, land use patterns (Dykaar and Wigington, 2000; Kondolf et al., 2002), riparian vegetation (Hickin, 1984; Millar, 2000), bank strength (Schumm, 1963; Millar and Quick, 1993) and anthropogenic modifications (Kellerhals and Church, 1989; Collins and Dunne, 1990) have been identified as secondary factors that locally influence adjustments to channel shape, position and pattern. Together, these variables directly influence the entrainment, transport and deposition of clastic sediments, and hence the morphology of alluvial channels.

1. Reaches are variable lengths of channel within which the dominant factors that influence morphology do not change appreciably such that channel pattern remains reasonably uniform.

The direct association between sediment transport[2] and morphology has not been widely pursued until relatively recently. Although the basic relation is well established (following the sediment continuity equation), a complete solution requires a reliable estimate of sediment transport (Hickin, 1983). This problem has itself been a subject of extensive study over the past century, yet has not been satisfactorily resolved (Carson and Griffiths, 1987; Reid and Frostick, 1994). Fluvial scientists have long sought to develop functional relations that correlate transport rates to some property of flow. Attempts to relate sediment transport and morphologic development to hydraulic variables in rivers have been largely unsuccessful, however, due to the non-uniformity and unsteadiness of flow (Gomez, 1991; Ferguson and Ashworth, 1992). Ashmore and Church (1998) point out that functional relations are statements of equilibrium conditions, which are rare in nature. Consequently, predictions may be grossly over-estimated in supply-limited channels, especially where bed structures increase the force required to mobilize clasts (Brayshaw, 1984; Church et al., 1998). Similarly, under-predictions are common where input parameters such as peak instantaneous flow (hence shear stress) and channel dimensions are averaged over larger temporal and spatial scales. In particular, most bedload equations fail to adequately perform on systems for which they were not developed, having been calibrated for a particular grain size distribution and set of flow parameters that may simply not translate to other systems.

Furthermore, any approach that stresses equilibrium conditions is not suitable for understanding river behaviour over longer timescales, although this is the period over which management concerns become pronounced. Perhaps more importantly, such approaches to the problem do not emphasize the important links between sediment transport and morphology which are often central to investigations of channel stability (Ashmore and Church, 1998; Hooke, 2003) and which provide the physical basis for aquatic habitat (Lisle, 1989; Kellerhals and Miles, 1996). Nevertheless, their use remains critical in numerical modeling studies where a sediment transport function is specified, though uncertainty in the reliability of such functions may require an independent means of calibration if the models are to be used in predicting bed level changes (cf. Li and Millar, 2004).

---

2. The morphology of a channel is determined by the bed material load, or sediment that comprises the bed and lower channel banks. Bed material is mainly transported as bedload, where particles travel by rolling or sliding along the bed, but may also include sediments moving in suspension. The bed material load is distinguished from the wash material load, which consists of sediments that mainly travel through a reach in suspension, are deposited only on overbank surfaces during floods, and have minimal influence on channel morphology.

Numerous attempts have been made to measure bedload transport directly using a variety of sampling devices and traps. This approach requires an extensive field effort because the spatial and temporal variability associated with its movement makes observation and collection of transported sediment exceedingly difficult (see reviews in Hubbell, 1987; Gomez, 1991). It is necessary to integrate a large number of samples over a wide range of flow conditions to adequately characterize a river's sediment transport regime. This is especially true of larger rivers, where adjustments may occur over decades for example, and similarly require long-term monitoring programs (Macklin et al., 1998). Sampling difficulties are amplified by the fact that most sediment transport in gravel bed rivers occurs during high flow events when direct observation and mensuration is difficult, even dangerous. Consequently, most direct sampling programs have been limited to fairly small channels (though measurements on Fraser River provide an unusual exception). Concern over the accuracy of the sampling devices themselves raises an additional problem that requires sampler calibration and adjustment for trapping inefficiencies (Hubbell, 1987; McLean et al., 1999; Sterling and Church, 2002).

Although many researchers continue to pursue theoretical, empirical and direct approaches to estimating bedload transport, an alternative strategy has emerged in recent decades which emphasizes the obvious association between sediment transport and morphologic change. Since the morphology displayed by a channel reach is a direct consequence of sediment transport (McLean and Church, 1999), observations of channel deformation can reveal details of sediment transfer in rivers (cf. Ashmore and Church, 1998). The association between morphologic measurement and sediment transport was first recognized by Popov (1962) but the study did not clearly demonstrate how they were related (Neill, 1971). Neill (1971) presented a more formal approach, demonstrating that an estimate of sediment transport along a meandering channel could be made by measuring bank erosion volumes over time. Church et al. (1987) provided a more general statement of Neill's approach and adapted the technique to estimate sediment transfer on rivers with more complex morphologies. More recent studies have modified the technique to describe temporal changes in local bed material transport rates for a variety of river types and sizes (McLean, 1990; Ferguson and Ashworth, 1992; Goff and Ashmore, 1994; Lane et al., 1995; Ham and Church, 2000; Lane et al., 2003). Refinements in measuring techniques have been an integral part of this progress.

Although there are circumstances in which the morphologic approach fails to provide a reliable estimate of sediment transfer, the technique reveals details of spatial and temporal channel

change that other approaches do not. Since the underlying principle relating sediment transport to morphologic change involves intersurvey comparison, useful information on rates and locations of morphologic change can be derived as a consequence. McLean (1990), Ham and Church (2000) and Gaeuman et al. (2003) provide examples for bank erosion, channel widening and changes in channel morphology utilizing planimetry-based studies. Other researchers have demonstrated the magnitude and dynamics of channel scour and fill along surveyed cross-sections (Ferguson and Ashworth, 1992; Goff and Ashmore, 1994; Hickin, 1995; Martin and Church, 1995; Paige and Hickin, 2000). Increasingly, three-dimensional surfaces of difference have been generated to illustrate complex patterns of sediment erosion and deposition distributed along entire channel reaches (McLean, 1990; Eaton and Lapointe, 2001; Lindsay and Ashmore, 2001; Lane et al., 2003). These efforts have begun to reveal details of the association between channel form and process rates on braided rivers (Ferguson and Ashworth, 1992; Lane et al., 1995; Brasington et al., 2000; Gaeuman et al., 2003). While such developments remain incomplete, it appears clear that observations of morphodynamic changes may usefully provide a means to better understand form and process relations in alluvial rivers. As such, the approach provides a valuable tool for monitoring and evaluating the sensitivity of riverine systems to environmental changes, hence to predict channel response to disturbance.

The purpose of this research is to elucidate the relation between sediment transfer and channel morphodyamics on the 75-km long wandering gravel-bedded reach of lower Fraser River, British Columbia. It is intended that this research will improve our scientific understanding of the style and rate of instability along large wandering channels and provide better tools to facilitate management decisions that impact channel development. At present, our knowledge of the spatial and temporal behaviour of these systems at the channel scale is incomplete. Although it is known that channel morphodynamics is connected to the downstream staging of bed material, the variability of sediment transport has hindered scientific progress towards defining this association.

1.2 Wandering channels

Lane (1957) noted that although there is nearly an infinite variety of possible stream forms, similar combinations of the major controlling variables produced similar principal patterns, which he classified as meandering or braided types. Leopold and Wolman (1957) added that channel planform formed a continuum, and introduced straight, meandering and braided channels as quasi-equilibrium forms. Both works are notable for introducing standardized definitions such that

different rivers could be classified and compared between regions, and for an attempt to relate channel form to principal controlling factors. Both are largely remembered for the development of discriminating functions distinguishing meandering from braided channels on the basis of slope and discharge (Ferguson, 1987).

Although the classification introduced by these authors, particularly that of Leopold and Wolman, has since become firmly entrenched in the literature, it has also been criticized for being too restrictive. Fluvial scientists now recognize a much broader range of planform types, including variations of the original tripartite classification, several transitional forms and a variety of multi-channel forms where the flow is separated around semi-permanent vegetated islands. Mollard (1973) presented 17 example channel morphologies illustrating the intergrading between classical end-member types and attempted to link channel and floodplain form with the variables that influence them. Mollard (1973) also gave examples of wandering channels, but reserved the term 'anastomosing' to describe high-energy, low-sinuosity streams split around wooded islands. A similar classification was given by Schumm (1985), although the term 'anabranching' was adopted to characterize channels split around large islands, while anastomosing channels were not considered to be a distinct type because individual channel branches could exhibit straight, meandering or braided patterns.

More recently, Church (1992) presented a conceptual classification scheme for large rivers that combined concepts from Mollard (1973) and Schumm (1985) but which emphasized in-channel sediment storage. The style of lateral channel stability (after Kellerhals and Church, 1989) was presented as an additional parameter for classification. Church (1992) distinguished wandering from anastomosing channels on the basis of sediment calibre, with the latter type conveying a much finer load. The importance of sediment load (suspended, mixed, bedload) in influencing channel type was also explicit in Schumm's (1985) work. More recently, Nanson and Knighton (1996) have nominated multiple-channel forms as types of anabranching rivers in an attempt to clarify confusing nomenclature. This categorization includes laterally-active, gravel-dominated rivers, more commonly referred to as wandering channels. They are largely discriminated from other anabranching channels by greater specific stream power, larger sediment size and less cohesive banks.

The term 'wandering' was originally used to describe the process of thalweg migration between channel banks (Leopold and Wolman, 1957) and amongst semi-permanent bedforms (Kopaliani and Romashin, 1970). Neill (1973) first formally nominated the term to characterize a

distinct channel planform type in a discussion of the characteristics and behaviour of the gravel-bedded Athabasca River, Alberta. Wandering gravel-bed channels are now commonly recognized throughout mountainous and piedmont regions of Western Canada (Desloges and Church, 1989) and have further been identified in China, Europe, New Zealand, Russia and western United States. These rivers typically form part of a downstream continuum of channel planform types between braided and meandering reaches and develop in response to environmental controls that vary downstream (Church, 1983a; Brierley, 1989).

Wandering channels possess similarities to both braided and anastomosed systems (Knighton and Nanson, 1993) but exhibit several distinguishing characteristics. They commonly flow in irregularly sinuous single-thread channels but are frequently split around large wooded islands, even at peak flows. Reach morphology is dominated by the erosion and mobilization of stored floodplain sediments, though tributary streams may contribute significant loads. Coarse sediments accumulate in locally unstable 'sedimentation zones' (cf. Church, 1983a) which may exhibit low-order braiding, and which are separated by narrower, stable 'transport zones.' Aggradation along the channel is spatially and temporally discontinuous – both the location and number of sedimentation zones are apt to evolve over time. Sedimentation zones locally increase water-surface elevations, causing overbank flooding, and direct flows around them resulting in bank instability and channel shifting. Over time, these processes typically produce an extensive network of seasonal, perennial and abandoned sidechannels along the adjacent floodplain. These pathways delineate positions where the active channel flowed in the past, and are subject to avulsions and cutoffs during high flows (Desloges and Church, 1987). Bedrock or erosion-resistant bank materials commonly abut channel margins along transport zones, creating deep scour holes.

Floodplain modification and channel instability along wandering rivers are directly related to the downstream transfer and storage of coarse alluvial sediments, although the association is not well understood. Along lower Fraser River, British Columbia, these natural processes create significant management concerns for infrastructure developments, silvicultural investments, aquatic habitat diversity, navigation and can even limit recreational opportunities. Insofar as applied management strategies (i.e. dyking, placement of riprap and gravel removals) may conflict with the maintenance of aquatic habitat for the spawning, rearing and migration of numerous fish species, including great runs of Pacific salmon, mitigating potential environmental, economic and engineering conflicts requires an increased understanding of the links between channel and floodplain morphodynamics and the contemporary sediment cascade. This knowledge has

practical implications for successful land-use and riverine management along other wandering channels where similar conflicts are shared or expected.

1.3 Research Hypotheses

Although bed material generally represents only a small fraction of the total load carried by most alluvial rivers (Church 1985; Meade et al., 1990), the staging of coarse sediment along a river channel directly alters channel morphology. As a consequence of spatial and temporal displacements in channel form, both natural and anthropogenic systems may be directly impacted. Excessive scour or fill can have a detrimental influence on the amount and quality of spawning gravels (Reiser, 1998) and can reduce the diversity of available habitat types by changing the distribution of flow depth and velocity (*sensu* Hogan and Church, 1989). Erosional processes may also undermine riprap revetments, flood protection structures, bridge piers or pipelines and lead to the loss of developed lands, while depositional processes can fill reservoirs, increase the flood risk, and create navigational problems. Providing reliable estimates of rates of bed material erosion, transport and deposition along river channels, therefore, has a number of practical environmental and engineering applications.

Along unconfined alluvial channels, rivers typically modify their pattern through the downstream progression of bank erosion and sediment deposition in channel bars (Church, 1983a). Neill (1971, 1987) recognized this association on rivers displaying a regular downstream progression of meanders and used it to estimate the rate of bed material transport on a large braided river. Along meandering rivers, quantitative theories have been sufficiently developed to predict facies patterns and planform evolution (Allen, 1965, Ferguson and Ashworth, 1992). Bend migration has been found to relate to bank erosivity, channel width and bend curvature (Hooke, 1980; Hickin and Nanson, 1984) and has been partly described by kinematic wave models (Beck, 1984; Mosselman et al., 1995; Gilvear et al., 2000). The relations between braided channel morphology and causative variables has received comparatively less attention (Ferguson and Ashworth, 1992), although the conditions necessary for braiding and mechanisms of braid development appear fairly well known (Miall, 1977; Ashmore, 1991; Knighton, 1998). Recent studies (Ferguson and Ashworth, 1992; Goff and Ashmore, 1994; Lane et al., 1995; Murray and Paola, 1994) have begun to reveal details of the spatial patterns of sediment transport and morphologic development in small braided streams and attempts at predicting channel evolution in braided rivers have been made (Lane et al., 1995; Paola, 2001; EGIS, 2002).

In comparison to the classic forms of meandering and braided channels, the style of instability along wandering rivers remains poorly described. Quantitative models of deformation along wandering channels do not currently exist. These rivers are not easily amenable to scale model studies (e.g. compared to flume studies of straight or braided channels) given the difficulties of adequately representing a vegetated channel-floodplain system (although recent work by Gran and Paola, 2001 demonstrates progress). As a result, the physical processes which determine channel form and development have not been well addressed. The most suitable approach to observe and measure patterns and rates of sediment transfer and morphologic development along large rivers involves mensuration of channel and floodplain processes at appropriate temporal scales. This appears to be years to decades along lower Fraser River, which corresponds to the persistence of major sedimentation zones (McLean, 1990; McLean and Church, 1999). This extended timescale occurs because the volume of bed material that is mobilized along wandering channels is modest relative to that stored within the channel and floodplain (Desloges and Church, 1989; Ham and Church, 2000). As a consequence, many years of persistent erosion or deposition are required to cause significant changes to the morphology. Similarly, large floods may complete or accelerate channel changes currently in progress (McLean and Church, 1999) but are not necessarily associated with major, distinct morphologic developments. Insofar as the patterns of sediment transfer and morphologic evolution occur relatively slowly, archival data records provide the appropriate temporal resolution for investigating this behaviour. The matter is discussed in further detail at the end of the chapter.

The main objective of this study is to elucidate the association between the staging of sediment and the style of morphologic change along a large, wandering gravel-bedded channel. The lower Fraser River is an ideal site for this investigation because historic documentation of the river is extensive. Planimetric maps and aerial photographs date back more than a century, while topographic surveys of the channel bed and banks are available since 1952. As well, the river has been continuously gauged since 1912, while prior information on sediment flux is available from a period of direct measurement (Tywoniuk, 1973; McLean et al., 1999) and from a comparison of computational formulae with morphologic estimates (McLean, 1990).

The specific research hypotheses to be examined are:

1. that the spatial and temporal variability of sediment transport on lower Fraser River can be directly related to observable sequences of channel morphodynamics;

2. that historic patterns of morphodynamic change can be used to predict locations and rates of future instability; and
3. that past gravel removals, construction of flood dykes and riprap bank protection, and a reduction of naturally occurring woody debris deposits have significantly altered the sediment transport and morphology regimes of the river over the past century, and may have caused degradation of the channel

The remainder of this chapter reviews the potential for inferring channel morphodynamic changes from survey data, including historic maps, aerial photographs and hydrographic surveys. The following chapter provides an overview of the physiographic setting of the study area and includes a detailed description of major anthropogenic changes that have occurred since early European settlement of lower Fraser Valley. Chapter 3 gives details on the data available for this study and explains how these data are analyzed for subsequent use. The interpretation of this information is given in Chapter 4, where quantitative analysis of channel change over time is provided, and in Chapter 5, where the association between the processes which transport bed material and the deformation of the channel is used to provide a detailed bed material sediment budget. Chapter 6 investigates how sediment is staged through the reach and relates this movement to spatial and temporal patterns of morphologic change. The final chapter discusses probable future evolution of the river based on observed patterns and trends and presents implications for successful management of the system in the future.

1.4 Morphodynamic changes from survey data

Rivers of different size and morphology exhibit a wide variety of depositional forms in response to the calibre of sediment being transported. Accordingly, any successful attempt to model these forms and record their displacement requires that the resolution of channel surveys corresponds to the deformation style of a given river. Application of the morphologic approach, therefore, requires some a priori knowledge on the details of sediment transport and storage. By definition, efforts to relate sediment transport to channel deformation are limited to the movement of bed material only, that is sediments which comprise the bed and lower banks of alluvial channels (cf. McLean et al., 1999). Along gravel-bedded channels, this material typically consists of coarse sand and larger particles which move relatively short distances during flood events. Finer sediments may be introduced to the system from erosion of channel banks and islands, where such

materials may constitute a significant proportion of overbank flood deposits. Once entrained, however, these sediments are mainly transported long distances in suspension, though some fraction is deposited interstitially within the bed. Suspended sediments do not appreciably influence channel morphology except where they enhance upper bank strength (Martin and Church, 1995).

Since sediment erosion, transfer, and deposition result in deformation of the channel, a measurement technique must provide a means to capture this deformation in sufficient detail to prevent, or at least minimize, unmeasured changes that otherwise occur between successive surveys. While methods to continuously monitor the movement of bedload at fixed locations have been developed (cf. Rennie et al., 2002; Rennie and Millar, 2004) no method currently exists for measuring real-time deformation at the reach scale. Bed material exchanges along rivers primarily include scour and fill along the channel bed, erosion and deposition along islands and channel banks, and sediment accumulations and movements amongst bed and bar forms. As movement of this material is known to exhibit high spatial and temporal variability (Meade, 1985; Hubbell, 1987; Gomez, 1991; Nicholas et al., 1995), morphologic estimates provide a reasonable means to average this variability over the reach scale provided sufficient survey detail is available (Knighton, 1998; Fuller et al., 2003).

Along gravel-bed rivers, most transported bed material is stored in large-scale bars (Neill, 1987) which scale to channel width or greater and have thicknesses comparable to mean bankfull depth (Church and Jones, 1982). The frequency with which bar migration occurs varies enormously by channel type and scale. Along small meandering and braided channels, changes in morphology have been observed daily (Meade, 1985; Goff and Ashmore, 1994; Lane et al., 1995). Conversely, detectable change along large wandering channels may take several years if there are no large floods, although some minimum volume of transport usually occurs seasonally. Ideally, survey data would be available at a resolution appropriate to record this displacement. However, most studies must make use of commonly available survey data, including available maps, aerial photographs, satellite imagery[3] and cross-section surveys, though application of emerging remote-

3. Satellite imagery can provide information similar to that derived from conventional aerial photography, although multiband sensors allow individual spectral signals to be combined for increased interpretive capabilities. Few riverine studies make use of this technology, however, because commercially available images date back only to the 1970s, and coarse spatial resolution limits application to very large rivers only. Given recent improvements in spatial resolution, their use may become increasingly common for geomorphologic studies. However, since the spatial and temporal limits of airphotos can be extended to include satellite images, the latter are not specifically discussed herein.

sensing technologies is becoming more common. The technical and practical limits of these different techniques for measuring changes in sediment storage, hence estimating bed material transport rates, are discussed below.

1.4.1 Planform data and analysis

The use of historic sequences of maps and aerial photography for quantifying channel changes is well-established in the geomorphic literature. Maps have particular utility for channel change mapping because this type of record extends further in time than any other type of riverine record (see Chapter 3). Aerial photographs have a much more limited temporal coverage, but their use eliminates cartographic biases often associated with maps. As well, photographs frequently allow measurements to be made over much greater spatial scales than is generally practical in the field. Along rivers, their use is largely restricted, however, to phenomena that can be observed in planform above the subaqueous zone. Typically, the main application has been to measure changes in channel width and lateral bank erosion over some length of channel (Hooke, 1980; Hickin and Nanson, 1984).

Neill (1971; 1987) first formally demonstrated that an estimate of sediment transfer could be made on meandering rivers by measuring average bank recession rates from maps and airphotos. Assuming that the height of the bank could be measured, the only limiting assumption is that an estimate of average travel length can be made (given by Neill as half the meander wavelength on a meandering channel). Neill (1987) cautioned, however, that the method would underestimate actual transport volumes when the assumed transfer length was too short; similarly, the technique will overestimate actual short-term transport volumes if material moves only locally (Ashmore and Church, 1998). McLean (1990) tested the approach on an eroding island on Fraser River that exhibited similar progressive meandering over a 20-year period and compared eroded volumes over time to estimates of bed material transport at an adjacent gauging station where bedload samples were available. McLean found the approach underestimated actual transport values because migrating gravel sheets passed undetected through the study area, suggesting the technique is further limited along rivers that exhibit multiple modes of sediment transport. This bias of undetected sediment transfer obviously is magnified as the intersurvey period increases.

Carson and Griffiths (1989) applied the travel distance approach to a 5-km section of the braided Waimakariri River, New Zealand. Travel distance was assumed equivalent to the average distance between zones of scour and fill along the reach. Erosional and depositional areas were measured from overlays of photos taken at different dates over 16 months, and converted to

volumes using representative scour and fill depths from repeat cross-sections. The authors noted that, by acquiring photographs following each significant flow event, undetected throughput should be minimized (assuming throughput is actually proportional to discharge), but added that the morphologic approach can provide only a lower bound estimate. Ham and Church (2000) demonstrated the magnitude of unmeasured flux due to compensating scour and fill along a 49-km length of the wandering Chilliwack River, British Columbia. Estimates of bed material transport measured at intervals of 7 to 14 years were compared to shorter-term estimates along a single downstream reach. The study revealed that long-term average transport rates clearly underestimate the magnitude of short-term transport because sites of distinct erosion and deposition are masked by compensating scour and fill. This circumstance is a consequence of the timing of individual floods. Photographs would ideally be available after each major flood to reduce unmeasured scour and fill over longer periods. This would also ensure that channel morphology was sufficiently modified to be detected, hence measured.

Assuming photos are available at suitable dates, reliable estimates of sediment transport are mainly affected by errors in storage change estimates. This largely results from uncertainty in measuring the thickness of deposited bed material (Ham and Church, 2000; Gaeuman et al., 2003) since planimetric (mapping) errors are comparatively small. The uncertainty can be reduced where repeat cross-sections are available, but otherwise requires sufficient field measurements to establish reach-averaged or denser estimates of bar and bank heights. However, Ham (1996) recognized that planimetric errors could dominate between successive dates if water levels (discharges) were significantly different. A condition of low water on the first map, and high water on the second results in the interpretation of erroneously small deposition zones, and correspondingly large erosional zones, leading to an apparent [false] impression of net scour, even if no sediment was actually moved. Church et al. (1987) demonstrated a technique for resolving this issue by relating areal exposure to stage, but recognized the approach was limited by several general assumptions and a lack of sufficient data. Their technique was modified by Ham and Church (2000) for wide, shallow reaches by replacing flow depth with flow 'area'. While this adjustment resolves most of the limiting assumptions, the procedure has not been tested on different morphologies.

1.4.2 Limits of topographic data and analysis

Most morphologically-based studies have been based on between-survey comparisons of topographic data collected through regularly-spaced cross-sections, ground survey, or remote

sensing, though tracers and scour chains have been used to measure deformation on very small channels (Hassan and Church, 1992; Haschenberger and Church, 1998). Through the comparison of interpolated surfaces, a distributed, three-dimensional view of erosion and deposition is provided, which can reveal details on the links between flow hydraulics, channel topography and sediment transport (Ferguson and Ashworth, 1992; Goff and Ashmore, 1994, Lane et al., 1995). The obvious advantage of this pursuit is that it captures details of bed deformation that are not detectable by planimetric means. Nevertheless, there are a number of concerns relating to the spatial and temporal resolution of the surveys that can limit applicability, though recent advances in data acquisition techniques have begun to address these. It is also important to recognize that historic data sources may be sparse, even non-existent, so longer-term trends in channel deformation can not always be determined.

Neill (1987) suggested that the approach developed for channels with systematic meander shifting could be adapted for channels characterized by large-scale bar migration. Given that this process results in thalweg shifting, repeat cross-section surveys could be used to measure scour and fill volumes across the channel. Though not explicitly stated, the approach also assumes that cross-sections are taken at the same fixed locations, limiting use to smaller channels. Large rivers are conventionally surveyed by depth sounding, and sampling positions are seldom replicated over time. Church et al. (1987) were able to roughly compare sounding surveys over two periods by subtracting averaged depth values to calculate net storage change. McLean (1990) followed this procedure along the gravel-bed reach of lower Fraser River using more sophisticated computerized modeling to interpolate and compare surfaces generated from two bathymetry surveys and was able to both illustrate and calculate spatially distributed volumes of scour and fill.

More recent studies have taken advantage of improved data collection and analysis techniques to more fully explore the spatial and temporal limits of data acquisition that ‘constrain practical application of the morphologic approach and limit the precision of results’ (cf. Ashmore and Church, 1998). Ferguson and Ashworth (1992) and Goff and Ashmore (1994) used closely spaced cross-sections to interpolate distinct sites of erosion and deposition, but it was found that intervening scour and fill or channel migration can mask the distinctiveness of erosion and deposition sites on small braided channels even within a few days. Lane (1997) was able to quantify the effects of changing temporal resolution, demonstrating an apparent time-dependent bias where the magnitude of net volumetric change decreased as the volume of water through a reach increased. While unmeasured scour and fill represent a negative bias in volume change

estimates (cf. Ashmore and Church, 1998), event-based surveys may not always be practical or necessary. On large rivers dominated by snowmelt floods, annual surveys may be adequate (Ashmore and Church, 1998). Correspondingly, ideal boundary conditions (i.e. zero or minimal downstream transport) can eliminate, or at least greatly reduce, temporal bias.

Several studies have identified the magnitude of loss of information that results from decreased survey spacing (McLean, 1990, Lane et al., 1994; Martin and Church, 1995) although Lane et al. (1995) noted that larger cross-section spacing may be appropriate in larger rivers. It is therefore reasonable to assume that increased survey density should obviously produce the opposite effect. Lane (1998) suggested that this issue had not been fully explored because of the legacy of at-a-station hydraulic geometry, but there were more practical constraints: until recently, there was simply no method available by which spatially distributed data could be economically or conveniently collected. Existing approaches, including manual photogrammetry and hand-logged field survey were simply too time-consuming to collect distributed topographic data over large spatial scales or short temporal intervals. Lane et al. (1994) attempted to resolve this problem by collecting topographic data using a combination of close-range photogrammetry for exposed regions with tacheometric survey of the subaqueous zone, recognizing that widely spaced cross-sections are insufficient to reveal details of within-reach erosion and deposition. This approach overcame the traditional trade-off between collecting data at higher spatial densities over large areas and the frequency of repeat survey (Lane et al., 1995).

Several researchers have since followed this work using electronic total stations (Milne and Sear, 1997; Eaton and Lapointe, 2001; Fuller et al., 2003) and kinematic GPS surveys (Higgitt and Warburton, 1999; Brasington et al., 2000). Not only do these techniques help overcome spatial and temporal limitations of data collection, but because they are explicitly field-based, collection procedures can be modified on-the-fly to account for complex terrain or features of particular interest such as banklines. There is of course a lower limit for temporal spacing set by the precision with which any detectable change can be made for a particular morphology (Ashmore and Church, 1998). Surveying may be limited by fast or deep water, limiting use to small, wadeable systems.

Chandler (1999) demonstrated the use of automated digital elevation extraction for quantifying landform topography using vertical and oblique photographs, an approach followed by Lindsay and Ashmore (2002) to measure scour and fill on a model braided river over periods as short as ten minutes. Accurate topographic reproductions of the landscape may be limited by vegetative cover (though analytical techniques can largely resolve this issue) so the use of photos

remains limited to exposed surfaces. Applications of through-water photogrammetry have been explored on shallow braided channels (Westaway et al., 2000) including shallow, modestly turbid waters (Westaway et al., 2003) but deep water, surface turbulence and high turbidity levels limit practical adoption along rivers where such conditions may be common. Water also represents a measurement barrier to conventional LiDAR (light detection and ranging), an emerging technology that uses pulsed laser to measure the distance from an aircraft to the ground. LiDAR has demonstrated potential to rapidly survey large areas at high spatial resolution (Charlton et al., 2003; French, 2003). Further, the technique is unaffected by shadows, interpolation schemes can estimate ground elevations beneath the vegetation canopy, and data collection appears more cost-effective than other approaches, an advantage which increases with areal coverage. An alternative type of blue-green LiDAR known as SHOALS (scanning hydrographic operational airborne lidar survey) uses multiple survey frequencies to survey up to 60 metres depth in clear water, but is currently restricted to a maximum of 2-3X the Secchi depth (http://shoals.sam.usace.army.mil; see also Guenther et al., 2000). While such advances show promise, large turbid rivers (including Fraser River) still require survey of subaqueous regions using more conventional approaches. As such, there will be an obvious mis-match in survey frequency above and below the water line that will affect the overall quality of individual digital elevation models (DEMs).

Current research has also begun to explore the accuracy by which irregularly spaced topographic data can be converted to a digital representation of a geomorphic surface, either in the form of a triangulated irregular network (TIN) or regular array of interpolated grid cells. There are several issues to consider, including the accuracy of individual survey points (Lane et al., 1994; Chandler, 1999) and the density and distribution of points (Brasington et al., 2000). The size of interpolated grids is also important (Milne and Sear, 1997; Fuller et al., 2003), especially where TIN facets are converted to a regular grid array. Studies have also examined the validation of individual DEMs, a process which involves comparing modeled elevations to independently surveyed checkpoints (Westaway et al., 2000; Brasington and Smart, 2003) and error propagation between DEMs of difference (Lane et al., 2003). Such comparisons are not only important for producing reliable estimates of volumetric changes, but they identify the lower limit from which morphologic change can be detected (cf. Lane et al., 2003). Somewhat surprisingly, the choice of an appropriate modeling strategy has been poorly investigated. Although the effects of interpolation accuracy are related to data density (and can largely be ignored for spatially dense datasets), there can be significant differences in apparent storage volumes when the different

models are applied to well-spaced points, such as along individual cross-sections. This concern is analyzed in greater detail within Chapter 3.

Extending measures of net volumetric changes to estimates of sediment transport is also complicated by assumptions about the transport lengths of particles during transport or by the need to define an upstream or downstream transport rate (Lane, 1997; Ashmore and Church, 1998). Neill (1987) recognized that reliable application of the approach required knowledge of an appropriate sediment step length, with surveys taken at closely spaced spatial and temporal intervals. Church et al. (1987) presented a more generalized method by which information on net storage changes could be combined with a local estimate of the transport rate to extend transport estimates upstream and downstream, termed a sediment budget approach. For some length of channel, the transport rate out of a reach was determined as the transport volume entering, minus the change in volume stored. This procedure eliminates the requirement that the transport step-length be known, provided the surveys are sufficiently dense to define loci of erosion and sedimentation (Lane et al., 1995) and the length of the study reach exceeds typical transport distances (Eaton and Lapointe, 2001). Although Church et al. (1987) lacked sufficient data to construct a sediment budget, the approach has since been widely pursued.

Ferguson and Ashworth (1992) and Goff and Ashmore (1994) prepared within-reach sediment budgets using a bounding transport estimate. Their efforts were confounded, however, by the requirement to identify a reference transport, which both studies identified as a weakness in the approach that biases the estimates, especially along active braided channels that change quickly. A flux rate must be determined at some location along the channel to propagate transport rate estimates. Martin and Church (1995) also used prismatic approximation (cf. Goff and Ashmore, 1994) to estimate volumetric bed changes between cross-sections along a larger wandering channel. Since the study river had an assumed zero transport boundary, the authors were able to extend reach-scale transport beyond the bar scale estimates following a sediment budget approach. However, the calculation of negative transport rates for some dates demonstrated that even under more ideal circumstances, the approach still provides only a lower-bound estimate of actual transport. A violation of the zero transport assumption, imprecision in the volume calculations or unreported dredging were suggested as possible explanations for the unexpected results.

Since the downstream end of the gravel reach of lower Fraser River is also characterized by zero gravel transport (transition to a sand-bed river), McLean (1990) was able to extend

transport calculations upstream from this reference point by 2-km long cells (reaches) and illustrate spatial variations in the gravel transport rate over a 32 year period. Although the survey interval is large, there is no practical upper limit on rivers with no downstream transport since all material becomes trapped. Although this eliminates the problem of unmeasured bed material throughput that otherwise occurs, compensating scour and fill between surveys masks shorter-term details of spatial and temporal trends in bed material transport within the reach.

The active pursuit of topographic data collection at increasing spatial and temporal scales has provided unprecedented views of form and process feedback relations along alluvial rivers. This advance, however, has been largely restricted to relatively short lengths of fairly small channels. To the extent that these approaches can be modified for, or extended to large rivers remains unclear. Although Lane et al. (2003) and Westaway et al. (2003) have demonstrated progress for capturing fully-distributed three-dimensional topography on a large braided river, the techniques have not been tested on rivers with greater vertical relief and greater flow depths. It is also important to recognize that survey comparisons are limited by the accuracy, density and availability of the poorest quality data set. On very large channels like lower Fraser River, limitations include aerial photographs taken with non-metric cameras and bathymetric data surveyed at low-density along widely spaced cross-sections. However, we can not ignore these data because large channels are modified over timescales that necessitate the inclusion of such information if we are to arrive at a meaningful understanding of channel morphodynamics at appropriate scales of investigation. This perspective is developed in the following chapters.

Chapter 2: Physical setting

2.1 Introduction

The Fraser River drainage basin encompasses an area of 233,000 km^2, nearly one-fourth the land surface area of British Columbia, and is the largest watershed located essentially within provincial boundaries (see Figure 2-1). The headwaters are located near Yellowhead Pass along the British Columbia / Alberta border, from where the river flows northwest along the Rocky Mountain trench to Prince George, south to Hope townsite in a deeply incised channel through the Interior Plateau and west through a broad alluvial plain to its delta on the Pacific Ocean, a total distance of nearly 1400 km.

Along much of its length upstream of Hope, the course of the river is structurally controlled and lateral movement is commonly restricted by bedrock or Pleistocene terraces. Below Hope, however, the channel becomes largely unconfined, coarse sediments are deposited as gradient declines and the river has formed a laterally-active wandering channel that extends downstream to Mission. Sediment transfer and deposition in this gravel-bedded reach of Fraser River dominates the stability, hence morphology, of the channel and adjacent floodplain, and presents a variety of management concerns.

This chapter provides an overview of basin physiography and hydrology. Flow and sediment regimes within the gravel reach are a reflection of upstream controls established [chiefly] by the Quaternary history of the province, and are manifested in the contemporary channel morphology. The remainder of the chapter examines anthropogenic influences on channel morphology within the gravel reach – activities that have altered the natural riverine environment over the past century.

2.2 Physiography and hydrology

The Fraser River basin lies wholly within the Canadian Cordilleran Region, one of five major physiographic subdivisions of Canada (Holland, 1964) and has been further sub-divided into major units including the Rocky and Columbia Mountains, the Interior Plateau, the Coast and Cascade Mountains and the Fraser Lowland. The basin was repeatedly covered by the Cordilleran Ice sheet during the Pleistocene Epoch and thick deposits of Quaternary sediments were deposited in main valleys and lowlands during both glacial and nonglacial periods (Clague, 1989). The most recent (late Wisconsinan) Fraser glaciation terminated about 13,000 years ago (BP) (Armstrong,

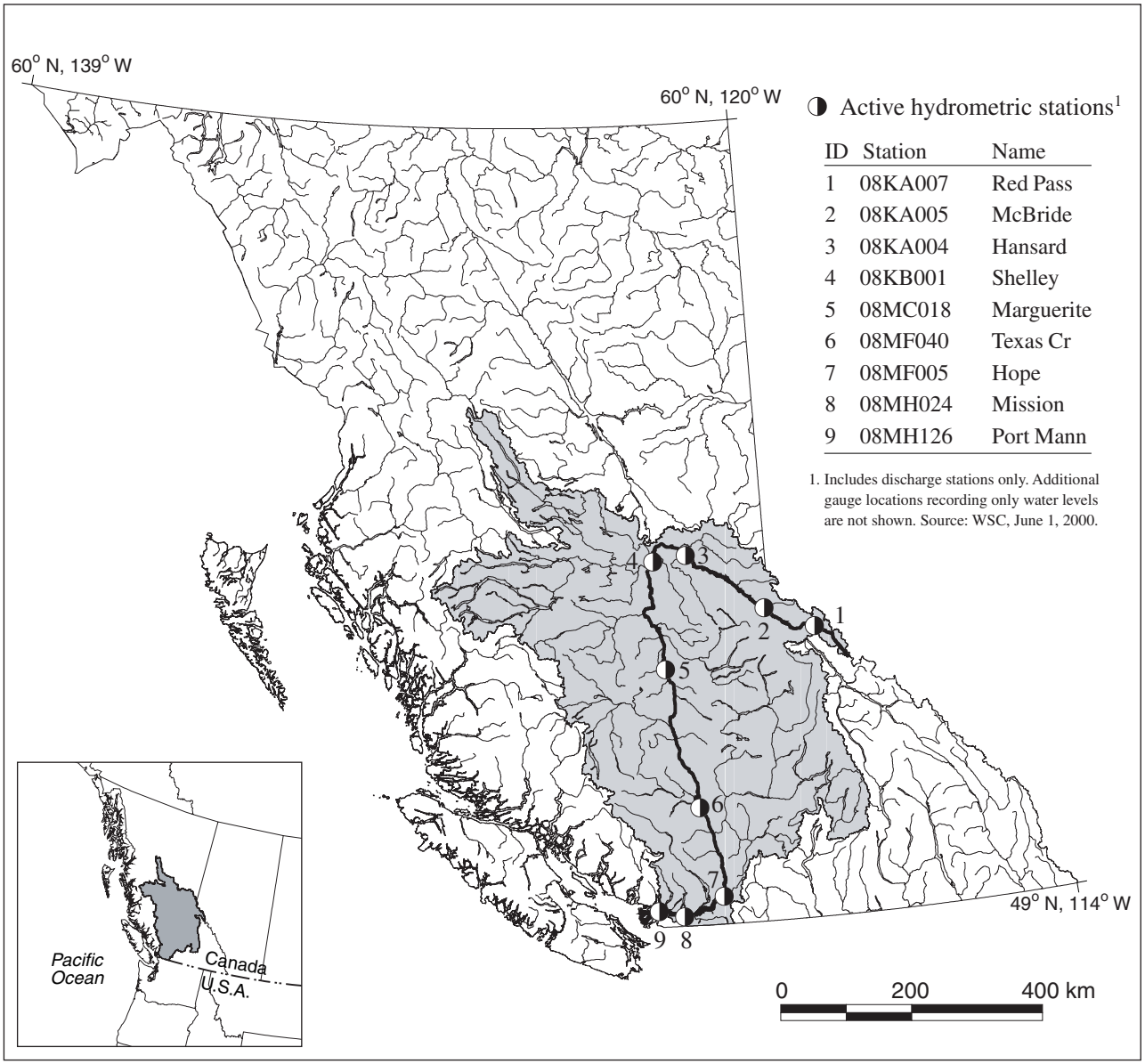

Figure 2-1. Location map and boundary of Fraser River watershed. Principal hydrometric stations are shown. The gravel reach extends from station 7 to 8. Base maps from B.C. GIS warehouse (Ministry of Sustainable Resource Management).

1981). Fraser glaciation drift consists mainly of till overlain and underlain by glacial fluvial and glacial lacustrine deposits, while glacial marine sediments are common in some coastal areas (Ryder and Clague, 1989). Repeat cycles of sedimentation followed by partial or complete excavation have resulted in a complex reworking of Quaternary sediments in most lowlands and valleys, making it difficult to correlate discontinuous statigraphic units in the absence of dating techniques (Ryder and Clague, 1989).

Following deglaciation, mass wasting and fluvial processes began to rapidly redistribute the vast volumes of unstable, unvegetated drift that were left behind. Initially, this resulted in the formation of large alluvial and colluvial fans and aggrading valleys, while finer sediments were commonly transported and deposited in lacustrine or marine deltas and offshore sediment basins (Ryder and Clague, 1989). As slopes began to stabilize, vegetation was established and the supply of drift declined. Many streams, including Fraser River and its major tributaries, incised into their former floodplains creating deep valleys cut into Quaternary fills (Clague, 1993) and producing relict terraces and dissected fans (Ryder and Clague, 1989). The rate of incision along lower stream courses may have been accelerated by the effects of isostatic rebound following final ice retreat (Holland, 1964). An observed downstream increase in sediment yield within the Fraser River watershed (Church and Slaymaker, 1989; Church et al., 1999) demonstrates that degradation of Quaternary valley fill in the Interior Plateau (cf. Church, 1990) continues today. These sources produce mainly fine grained sediments as banks are eroded during high flows (Church and McLean, 1994). Annual total suspended yields are strongly correlated to the size of the freshet, and average roughly 17 million tonnes below Fraser Canyon (McLean et al., 1999). In comparison, upland regions are not prolific sediment sources, as these areas are poorly connected to the channel network (Church, 1990).

The major alluvial reaches of Fraser River are located within the Fraser Lowland, a triangular region of roughly 3000 km^2 that extends westward from Hope and forms the southwest corner of the province, including part of northwestern Washington State (Holland, 1964). The valley preserves evidence of three intense late Pleistocene glaciations that left deposits of unconsoliated Quaternary sediments up to 300 metres thick above Tertiary and Cretaceous bedrock. Fraser River forms the dominant geomorphologic feature of the lowland, occupying a late glacial and post-glacial valley up to 5 km wide and 225 metres deep fronted by an extensive, growing delta (Armstrong, 1984). East of Mission, the valley is comprised mainly of Salish and Fraser River (Holocene) sediments, including sand, gravel and overbank fines. West of Mission,

sand and silt become the dominant floodplain material. Aggradation on the floodplain continues today, probably at a lower rate than during the early Holocene (Ryder and Clague, 1989; Church, 1990) but there are almost no contemporary records of sedimentation for comparison (Church and Ryder, 1972). Further, since the floodplain is almost entirely isolated from the river, fine sediment deposition is largely restricted to vegetated islands.

From Hope downstream to Laidlaw, the river is nearly continuously confined by bedrock, landslides or Pleistocene terraces (McLean et al., 1999). Below Laidlaw, the river exhibits a wandering channel planform within a partly confined floodplain that extends 55 km downstream to Sumas Mountain (Church and McLean, 1994). The deposition of gravel in this reach is a consequence of a reduction in channel gradient below the steep confines of the Fraser Canyon. The terminus of gravel deposition is marked by an additional (order-of-magnitude) decrease in gradient and transition to a single-thread sand-bed river. The typical thickness of the active gravel layer is estimated as 5 to 15 metres along much of the reach (Armstrong, 1981). GPR profiles of large bar complexes within the reach (cf. Wooldridge, 2002) show alluvial sediments 8 - 24 metres thick, underlain by steeply dipping deposits interpreted as former positions of a prograding delta front following deglaciation. Similar measurements on the wandering Squamish River (Wooldridge, 2002) provide additional evidence to support Desloges and Church's (1987) assertion that the wandering planform appears vertically stable. Although the gravel reach of Fraser River is known to be slowly aggrading at present, channel behaviour, hence morphology, appears to be dominated by lateral migration within the floodplain. Therefore, anthropogenic modifications such as bank hardening may have important implications for both recent and future channel development along the reach.

Despite extremes in climatic diversity that arise from the watershed's large and varied geography, the hydrologic regime is strongly characterized by nival flows. Elevations in the watershed range from near sea level at the delta and lower Fraser Valley to 3600 metres in the headwaters. Hypsometric calculations reveal that half of the watershed lies at elevations above 1150 metres, while 1.2% of the watershed remains glaciated with the greatest concentration in the Coast and Cariboo Mountains (Figure 2-2). Although autumn and winter maritime air masses produce heavy rains at lower elevations, snowfall is common at higher levels and interior locations where these masses encounter colder arctic air. Two-thirds of annual precipitation in the basin falls in the form of snow (FBMP, 1994) so widespread, prolonged melting of the accumulated snowpack dominates runoff patterns (Moore, 1991). Large rainstorms can increase runoff in the

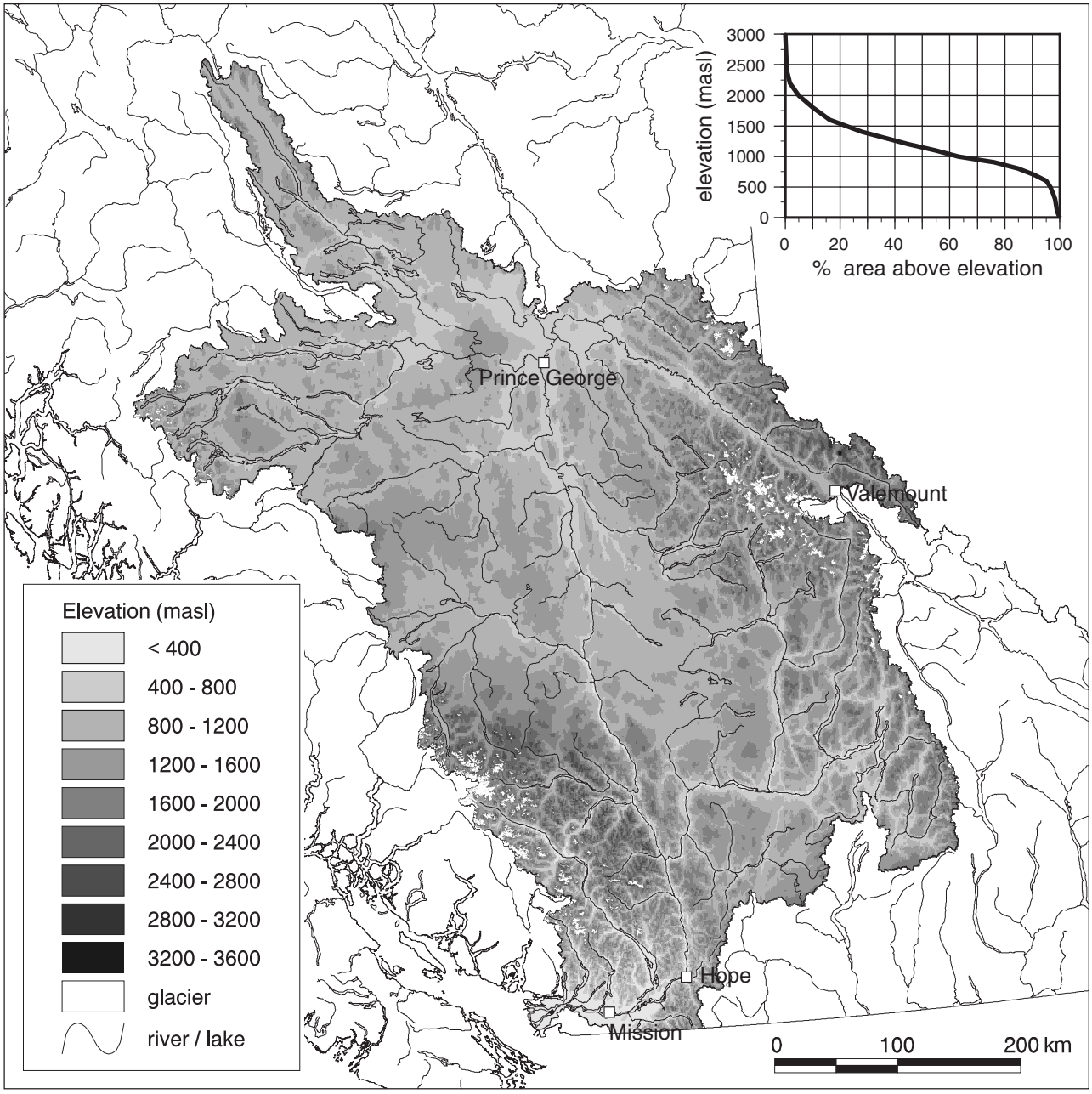

Figure 2-2. Relief map of Fraser River watershed. The location of existing glaciers and a hypsographic curve are shown for reference. Data are derived from Provincial 1:250,000 base mapping.

summer to autumn period and even prolong the freshet (i.e. as occurred in 2001) but rarely generate flows at or near bankfull discharge. The annual freshet occurs from May to July (median date is June 13) and commonly takes the form of a single-event hydrograph (Church and McLean, 1994; see example, Figure 2-3). Most gravel transport, hence morphologic change, occurs during this time.

The mean annual flood at Hope, site of the longest continuously operating gauge in the watershed (since 1912) is 8750 m^3/s. For comparison, the mean minimum discharge is 600 m^3/s – the ratio between them (14:1) is typical of large rivers and reflects the attenuation of snowmelt and rainfall inputs over large areas (cf. Dunne and Leopold, 1978). Mean annual flow is 2700 m^3/s, while major tributaties, including Coquihalla, Chilliwack and Harrison Rivers, increase discharge to 3350 m^3/s at Mission, located at the distal limit of the gravel reach[1]. The known flood of record, in 1894, was estimated from local high water marks as 17,200 m^3/s (at Mission) and the measured flood of record was 15,200 m^3/s in 1948 (at Hope). Other major floods that pre-date the gauging record occurred in 1876, 1882, 1896, and 1903 (Johnston, 1921). The historic sequence of annual peak flows is shown in Figure 2-4A. The largest floods occur when cool spring temperatures give way suddenly to extended warm periods, such that melt occurs quickly rather than over a protracted period. These conditions were the principal cause of the 1894, 1948 and 1972 floods, with significant rain amplifying the 1948 and 1972 events. A large snowpack with high water equivalent, above-freezing overnight temperatures at high elevation and heavy rainfall have been identified as additional factors which increase the rate and volume of runoff during the melt phase (FBMB, 1994).

Discharge in the watershed is partly regulated by a number of storage facilities for hydro-electric power generation. The largest of these is a diversion located on the Nechako River (completed 1952), which effectively reduced the size of the basin by 14,000 km^2 (5.6%) and mean annual flows by 3% (Moore, 1991). Smaller hydro reservoirs are found on the Bridge River system, lower Fraser Valley tributaries and Mabel Lake. During the 1972 flood, it is estimated that that utilized storage capacity at the Nechako and Bridge River facilities reduced the peak flow at Hope by 1130 m^3/s and peak flood crest elevation at Mission by 0.3 metres (FBMB, 1994). The attenuation effects of water storage have contributed to a reduction of the mean annual flood by

1. Annual maximum discharge at Hope (WSC gauge 08MF005) is calculated for the period 1912 to 2002, while mean annual flows are availabile since 1913. The Mission gauge (08MH024) has been in continuous operation since 1965 but the reported figure is based on published data available for the period 1966-1992 inclusive.

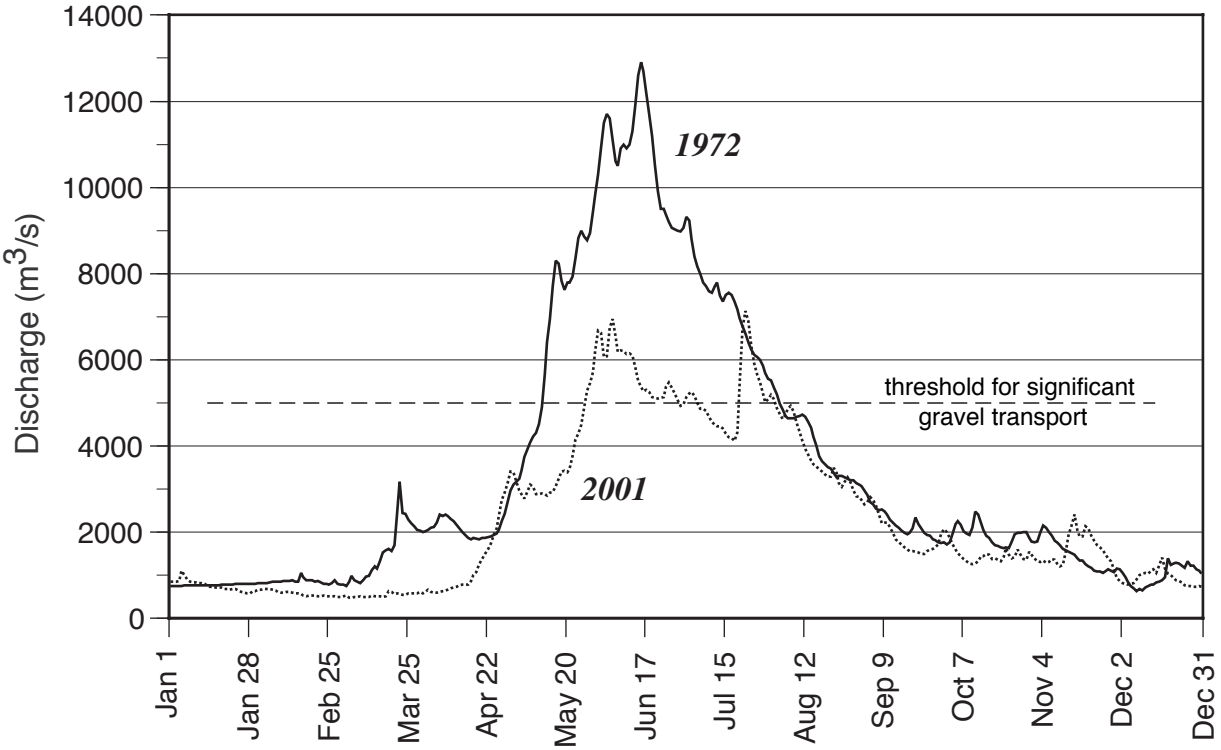

Figure 2-3. Example annual hydrographs, Fraser River at Hope, 1972 and 2001.

13% over the 50 years since 1952, though natural long-term climatic variability confounds such a simple conclusion. Over the complete record, flood flows have declined nearly 5% while, surprisingly, the mean annual discharge has actually increased by the same proportion. This trend may in fact be a signal of glacial retreat throughout the watershed (D. Moore, *pers comm.*, 2004).

Individual floods are not as important in influencing channel morphology on large rivers as are longer-term trends in flood flows. McLean (1990) found that individual floods may accelerate local changes such as bank retreat, but do not directly influence large-scale morphologic patterns. because the volume of material stored in the river is so large relative to the capacity of the flow to erode and transport the stored sediment during a single freshet. This effect can be observed qualitatively by comparing low-water photo series in 1943 and 1954 (McLean, 1990) and from the early 1940s to 1949 (Church and Ham, 2004) — these show a surprising lack of major channel shifting and erosion compared to that observed since 1928 despite the magnitude of the 1948 flood (examples are provided in Appendix B). In order to better understand long-term patterns of channel behavior, it is neccessary to relate observed changes to long-term trends in flood flows. Plots of cumulative departures for the annual maximum and mean flow series are given in Figure 2-4 B. Mean flows were generally above the long term average to 1922, below average to 1952, and above average to 1977. Flows have generally been below average since, but there is limited evidence to suggest that they have been increasing since the mid-1990s. These dates reveal shifts in climatic regime, and are thought to coincide with the Pacific Decadal Oscillation (Mantua et al., 1997, in McLean and Church, 1999). Flood flows follow a broadly similar pattern, but dates of major regime changes do not conform with mean flows and intervening flow trends exhibits greater variability. Nevertheless, it is expected that major changes in bed material transport, and hence changes in channel morphology, should correspond with trends in flood flows.

2.3 Anthropogenic influences on morphology

The lower Fraser River remains today a relatively pristine environment compared to many large rivers that flow through heavily urbanized regions. Nevertheless, efforts have continued since the late 1800s to protect developed areas and infrastructure along the river from flooding and erosion through a system of dykes, bank protection structures, channel dredging and removal of woody debris. The known history of these developments is summarized in the following sections. It is probable that these efforts have influenced morphologic development over this same period. The sensitivity of channel response to anthropogenic disturbance is examined in Chapter 4.

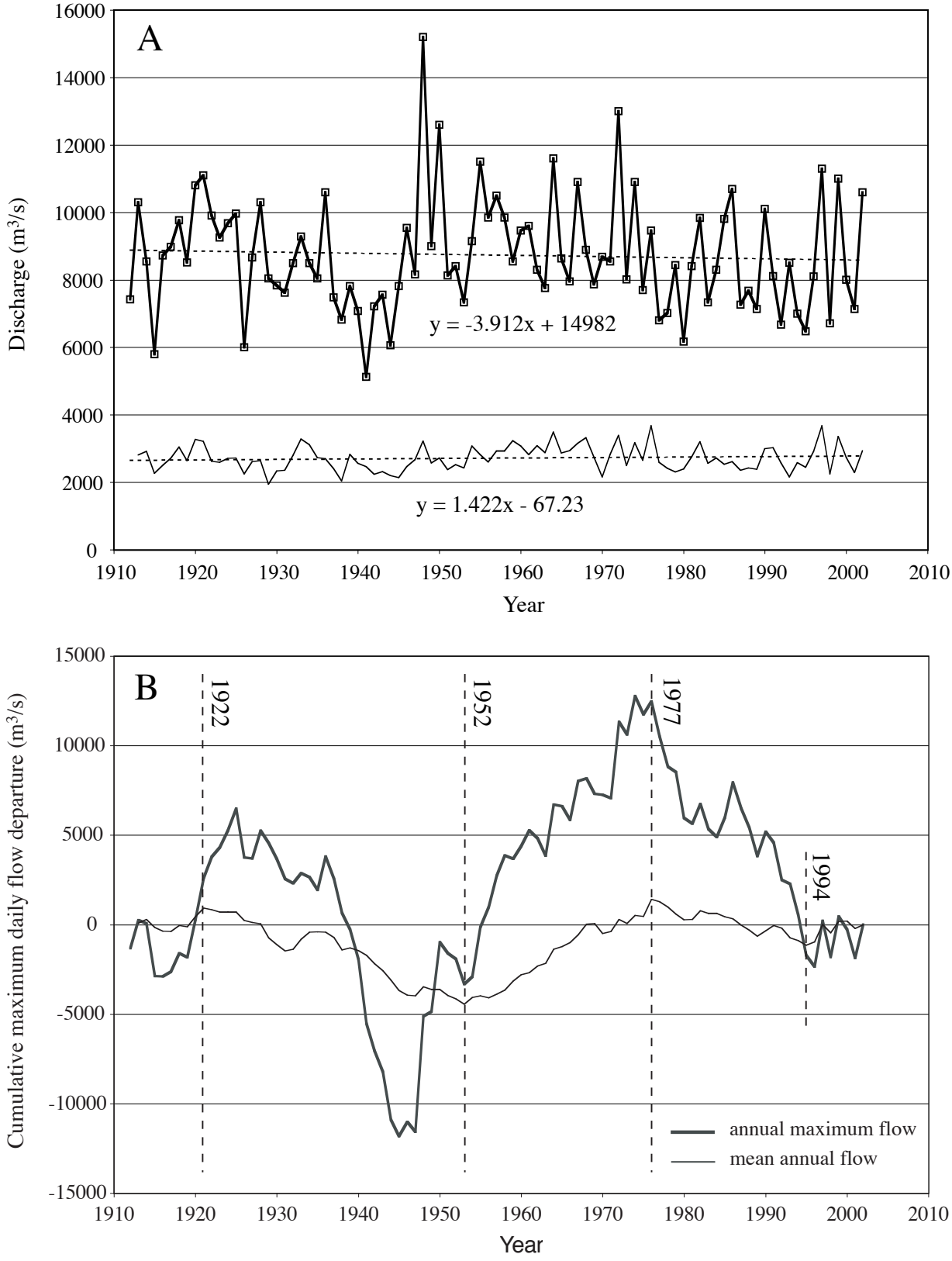

Figure 2-4. Annual maximum and mean daily discharge, Fraser River at Hope (08MF005). A. Annual flow series with best-fit trend lines. B. Accumulated departure series showing major trends in mean and flood flows over the period of gauging. An ascending plot indicates periods of persistently above-average flows, a descending plot indicates periods of persistently below-average flows, and a level plot indicates flows near the long-term mean. See text for discussion.

2.3.1 Flood protection structures

Much of the initial European settlement of lower Fraser Valley was established on low-lying areas along the Fraser River floodplain, largely because of the high demand for suitable agricultural lands. These areas were also at risk of flooding during freshet in most years. North and Teversham (1984) note that early farmers recognized the need to lower the water table and protect their planted crops and grazing lands from damaging floods and many responded by building small dykes along their property (Sewell, 1965). Following a major flood in 1876, an act was passed [1878] to build privately-financed dykes at Chilliwack, Sumas and Matsqui in exchange for land, but the project was discontinued (Winter, 1966). Also in 1878, a separate plan was initiated to drain the seasonally-flooded Sumas Lake in an attempt to reduce the area of floodplain that was inundated, create additional arable land, and open east-west travel corridors. However, the project was not completed until 1923 (Siemens, 1966). In 1892, earthen dams were built to close several small sloughs and the upstream end of the major slough at Nicomen Island (Public Works Canada, 1949). Additional dams were built at Hope Creek and Camp Slough near Chilliwack (Sinclair, 1961). Despite these efforts, the dyking system was discontinuous, often built without engineering advice, and many sections had been abandoned during construction (Sewell, 1965). The devastating 1894 flood emphasized these problems, and spurred efforts to protect newly developing areas from future flooding by establishing an integrated system of dykes. Through substantial government assistance, most flood-prone areas had been protected within ten years (Siemens, 1966).

There were no significant improvements to the dyking system in following decades, although additional flood dykes were built to support the draining of Sumas Lake. This inaction was largely due to financial difficulties, as most local municipal districts did not have sufficient revenues to both service accumulated debts and finance dyke construction and maintenance. As a result, many of the dykes were never completed to recommended engineering standards and commonly fell into disrepair (Sewell, 1965). Fortuitously, there was a lack of damaging floods during this same period, and this circumstance likely reinforced the status quo. A major program to repair and upgrade existing dykes was, however, initiated following the disastrous 1948 flood, which breached and damaged much of the existing flood-protection framework, resulting in considerable economic loss and disruption. The upgrades were sufficient to withstand a second, less severe flood in 1950, but engineering tests revealed that the desired design elevation was not being met (Fraser River flood control program, 1968). As a result, another major program of dyke

upgrades and flood control works was initiated under the plan of protection outlined in the 10-year Federal-Provincial Flood Control Agreement of 1968. Much of the work in the gravel reach involved new or improved bank protection works where lateral erosion threatened to undermine dykes or cause loss of developed lands. The program also provided funds for improvements and additions to the pumping / ditching system designed to provide internal drainage of lands enclosed within the dykes (Fraser River flood control program, 1968). Notably, there were no planned extensions to the existing 130 km of flood dykes within the gravel reach and, since then, the only major addition to the system has been a 3.4 km branch dyke along Island 22 near Chilliwack. The current network of flood dykes is shown in Figure 2-5.

Along much of the floodplain, the dykes are set back a sufficient distance from the margins of the active channel zone such that they do not directly interfere with morphologic development of the river. One of the main impacts has been the separation of many prominent sloughs and backchannels from the main channel. McLean (1990) notes that several of these have since filled with finer sediments and vegetation has encroached. This has resulted in a loss of aquatic habitat, and water once conveyed through these secondary channels at high flows has since been forced back into the main channel. The primary impact of the dykes on channel morphology has been indirect. As the river has long been recognized as being laterally unstable, bank protection works have been used to restrict erosion where the dykes are vulnerable.

2.3.2 Bank hardening

The construction of bank protection structures within the gravel reach dates back to 1892 when crude buttresses of brush and rock were sunk along wood pilings to limit erosion at Miller's Landing near Sumas (Public Works Canada, 1949). By 1910, additional similar structures had also been placed at Sumas and Matsqui, while a wing dam was built at Chilliwack. In 1914, severe bank erosion along Nicomen Island resulted in several attempts to limit erosion using brush, rock, and pilings, but all measures were unsuccessful. The erosion was not stopped until a channel was dredged to divert flow away from the sharp developing bend, although the diversion channel was not actually adopted by the river until 1922 (Public Works Canada, 1949). Other major projects included placed rock at Rosedale (1928 to 1939) and installing pile groins followed by placed rock near Agassiz (1928 to 1948). As McLean (1990) points out, there is little specific documentation of these early protection measures. Much of the work completed to protect the dykes and settled land from bank erosion likely took place after the late 1920s, when the federal government made its first financial contribution to flood control (Winter, 1966). By the date of signing of the 1968

Summary of bank hardening between Mission and Hope

Reach	Total bank length (m)[1]	Railway[2]	Dykes	Riprap[3]	Bedrock[4]	Total protected[5]	% protected
Sumas	31 925	4 715		13 760	4 873	23 348	73.1
Chilliwack	35 739		173	14 898	6 525	21 596	60.4
Rosedale	26 346	4 091		14 202	833	19 126	72.6
Cheam	42 501	18 358		11 739		30 097	69.2
Hope	32 202	6 207		8 692	2 314	17 213	53.5

1. outer banks of main channel only; does not include island shoreline
2. railway protects many banks that otherwise would be classified as bedrock
3. riprap includes 2907 m of rock berms, mainly in Cheam reach
4. bedrock includes non-alluvial, non-erodible banklines (eg. Mission bend)
5. all categories are exclusive (i.e. any length is counted in one category only); total protected (and % protected) includes bedrock

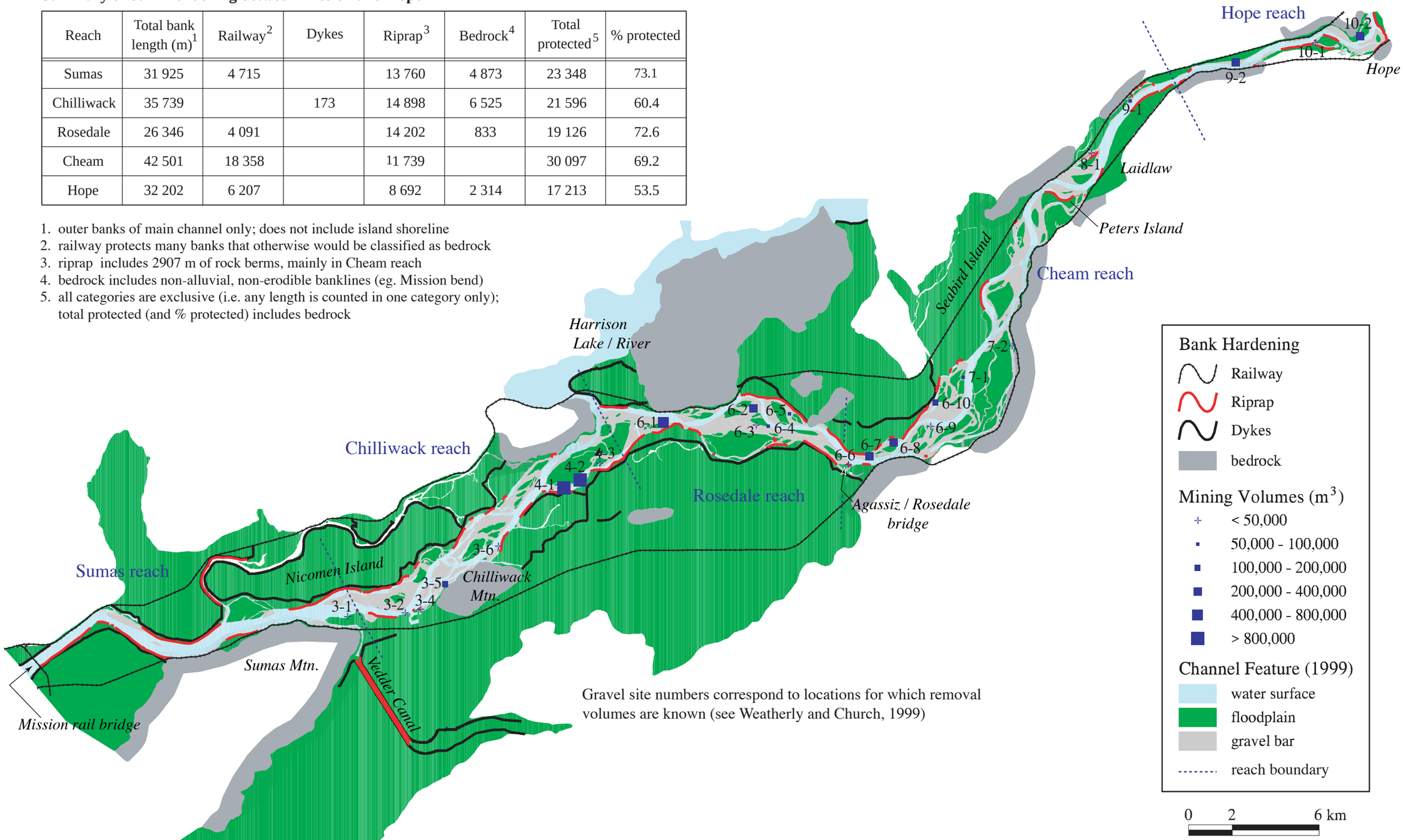

Gravel site numbers correspond to locations for which removal volumes are known (see Weatherly and Church, 1999)

Figure 2-5. Location and summary (inset table) of bank hardening along lower Fraser River. The location of known gravel mining sites is also shown.

Federal-Provincial Flood Control Agreement, 36 km of shoreline were protected by riprap (McLean, 1990), of which 13 km was slated for upgrading and an additional 9.4 km was proposed (Fraser River flood control program, 1968). Roughly 55 km of bankline are currently protected, including 1.9 km along Peters Island (Figure 2-5).

Bank protection structures have also been used throughout the gravel reach to protect railway lines from bank erosion. Construction on the transcontinental Canadian Pacific Railway began in 1880 near Yale, then the head of navigation on lower Fraser River, and by 1885 the line extended downstream to Port Moody (Roy, 1966). Additional railways established several new lines in the Fraser Valley at the turn of the century to provide service to communities along the southern shore of the river, but these generally extended north-south, or ran close to the U.S. border. A second transcontinental railway (Canadian Northern Railway, now Canadian National) was completed in 1914 and connected Hope with New Westminster along the southern side of the river (Roy, 1966). Both the CP and CN railway lines parallel the river through lower Fraser Valley and run adjacent to the active channel in several locations (see Figure 2-5). Since the railways are vital transportation and economic corridors, the rail bed has been heavily engineered with riprap to protect against undercutting or lateral erosion by the river. It is estimated that the railways currently protect 33 km of floodplain from erosion. Upstream of Agassiz, the railway also functions as a flood dyke since the rail bed has been built to sufficient height along the floodplain to maintain rail transport during high-water events.

Lateral channel movement is further restricted at several locations by natural phenomena. Between Hope and Laidlaw, the river is almost continuously confined by bedrock, landslides and Pleistocene terraces (McLean *et al.*, 1999) and there is little adjacent floodplain. Downstream of Laidlaw, bedrock is found adjacent to the active channel margins along the Skagit Range near Herrling Island and at Hopyard Hill, Mount Woodside, Harrison Knob, Chilliwack Mountain and Sumas Mountain. Terraces are also found at Mission, near the downtream limit of the gravel reach. The shape and extent of the modern floodplain, therefore, is strongly affected by the presence of these features (it is effectively a confined alluvial fan). This circumstance is not unusual along wandering gravel-bed channels (cf. chapter 1). The location of natural constrictions (for mapping convenience, all are plotted as bedrock) is also shown in Figure 2-5. In total, 14.5 km of channel are protected by natural constriction or confinement. A summary of bank hardening, including the percentage of outer banks that are currently protected, is summarized as an inset table in Figure 2-5. As it is known that the net effect of this bank hardening has been to narrow the width of the

channel zone (the average width between outer banks) along all reaches (cf. Ham and Church, 2002) major adjustments in active channel width must result from erosion or construction of channel islands. Forced channel narrowing may also lead to deeper, faster currents in order to maintain flow conveyance, which has implications for sediment transport capacity, hence overall channel stability. This possibility is reviewed in Chapter 5.

2.3.3 Sediment removals

Sediment has been dredged from the channel since at least the start of the 20th century when steam-operated hydraulic suction dredges became available. The purpose of these removals was to maintain a safe navigable channel for shallow-draft vessels (that once extended upstream to Yale). Earlier removals may have taken place, but the volumes would have been very modest given the limited available means that would have existed to physically dredge and transport the material. Public Works Canada (1949) reports that 3.77 million cubic yards (2.88 million m^3) of material (bulk volume) were dredged between the delta and Chilliwack during the period 1901-1910. Given that these removals extended well into the gravel reach, and the diameter of the suction pipe (20 inches, or 508 mm) exceeds that of the largest mobile clasts in the channel, some gravel is likely to have been extracted along with sand and finer materials. The records are nonetheless inadequate to estimate the proportion of the total volume removed that was taken upstream of Mission. The only other documented early extraction is the 393,000 m^3 dredged between 1914 and 1922 for the diversion channel at Nicomen Island, but this material was replaced within the channel. Gravel was also dredged from the river during the construction of railways and roadways where this infrastructure was located in close proximity to the active channel (several examples are documented in Weatherly and Church, 1999). Some gravel may also have been obtained for dyke construction, but borrow pits were usually located on the landward side of the dykes (Sewell, 1965). Large scale channel removals certainly took place for dyke upgrades following the 1948 flood, however, since extraction pits and heavy trucks are directly visible on 1949 aerial photographs (eg. near Minto Channel). However, as there was no documentation of these removals, it is not possible to reliably estimate the total volume taken.

The earliest summary inventory of gravel extraction in the river was completed by Kellerhals Engineering Service Ltd. (1987) for the period 1973-1986. The report gathered information given by local gravel operators and representatives from various government agencies. Weatherly and Church (1999) note that, as gravel extraction has been regulated since 1974 by British Columbia Assets and Land Corporation, the Kellerhals inventory appears fairly accurate.

However, the authors caution that the records may be incomplete because of (1) inaccurate self-reporting of amounts removed by gravel operators, (2) the lack of documentation of gravel removals by the Ministry of Transportation and Highways, which had established gravel reserves but was not subject to regulation, and (3) unregulated removals on private lands. The latter includes removals on Indian Reserves, for which records appear non-existent. The completeness of extraction records has improved since 1980, when the Department of Fisheries and Oceans first required permits for any removal because of fisheries concerns (McLean, 1990; Weatherly and Church, 1999). As well, pre- and post-extraction surveys were sometimes requested to verify removal volumes, adding credibility to reported figures.

Gravel removal volumes presented herein are primarily based upon the 1999 Weatherly and Church report, which provides an update to the existing Kellerhals inventory, and extends the reporting period from 1964 to 1998. As the authors were able to contact a number of individuals, additional information was obtained for pre-regulation commercial operations and removals related to road and dyke construction. A second report (Kerr Wood Leidal, 2001) was used to extend the inventory to 1999 and amend reported [1998] values at Hamilton Bar and Powerline Island. A total of 4.2 million m^3 of gravel (bulk volume) is documented to have been removed between Mission and Laidlaw during the period 1964-1999, an average of 120,000 m^3 per year. The total extraction increases to 4.8 million m^3 if extended upstream to Silverhope Creek near Hope, or 138,000 m^3 per annum. Although far more gravel was removed in 1995 (428,000 m^3) than in any other year of record, maximum removal volumes generally took place from the early 1970s to the early 1980s. The dominant location of these removals has been along Minto Channel, though large removals have also occurred at Foster Bar and Powerline Island. A nearly complete record of known gravel extractions between Mission and Hope is summarized in Weatherly and Church (1999) and is also reported in the sediment budget tables (Chapter 5). Corresponding site locations are shown in Figure 2-5.

Of particular interest in this thesis are those removals which took place between the years 1952 and 1999, as this corresponds to the period for which estimates of sediment transport are given (see Chapter 5). The incomplete information on gravel mining prior to industry regulation, and missing information on removals between 1952 and 1964 represents a negative bias for estimates of total bed material transport in the gravel reach. The magnitude of this bias remains unknown, but may be small, given that individual recollections of these early extractions typically report modest volumes (cf. Weatherly and Church, 1999).

While scuffle dredging along shallow riffle zones was until recently practiced to maintain navigational safety, most current removals are conducted as commercial operations. Sand and gravel is taken from targeted locations where deposition is thought to cause local increases in water-surface elevation. The sediment is sorted to eliminate smaller grain sizes, and the gravel is sold for profit, both offsetting removal costs and providing crown royalties. The success of this practice in actually reducing water levels for a given discharge on Fraser River has been examined by UMA (2002, 2004). It was found that reported sand and gravel removals from 1952 to 1999 lowered the flood profile up to 20 cm between Chilliwack and the Agassiz-Rosedale Bridge, but that channel alignment appears equally important in determining the flood profile.

2.3.4 Woody debris

The removal of woody debris (snags) from the gravel reach dates to the early 1870s when the river was a principal conduit for transportation and commerce. A total of 2300 snags were removed by 1894 to improve navigational safety along the lower 135 kilometres of channel (approximately to Agassiz). An additional 35,400 snags had been removed by 1949 between the delta and Harrsion River confluence (Public Works Canada, 1949). Despite these efforts, woody debris jams still acumulated along the upstream margins and distributary channels of major bar/island units, as visible in historic aerial photographs. By 1979, a boom to trap floating debris was established near Hope, replacing the boats that had previously been used. Hales (2000) reported that the trap has caught 90,000 m^3 of wood annually since that time, roughly 90-93% of all floating debris in the river. The continuous operation and greater efficiency of the trap has since resulted in a steady decline of deposited wood in the gravel reach. At present, both the gravel reach and the tidal flats (cf. Hales, 2000) are largely free of woody debris. Since woody debris is known to be an important nucleus for the establishment, growth and maintenance of channel islands and side-channels, there may be observable changes in both over the past two decades. The morphologic and ecologic implications of this practice are explored in Chapters 4 and 6.

Chapter 3: Data Compilation

3.1 Introduction

This chapter provides an overview of the primary data used for mapping and measuring morphologic changes and estimating sediment transport rates within the gravel reach of lower Fraser River. The pattern and rate of morphologic changes over time is measured from a sequence of historic maps and aerial photographs available for various dates since the early 1900s. Patterns of aggradation and degradation within the gravel reach are determined by comparing topographic surfaces of the channel bed and banks from hydrographic surveys completed in 1952, 1984, and 1999. The quantitative interpretation of this information is given in Chapter 4, while the links between observed changes in channel deformation and the processes that produce them are discussed in Chapter 5. A complete description of data collection and analysis procedures is provided in the following sections.

3.2 Channel and floodplain mapping

3.2.1 Data acquisition from old maps

The availability of old maps and charts represents a valuable resource from which to investigate the morphologic evolution of river channels. Their use is particularly relevant for large river systems, where significant changes may occur over timescales that exceed the temporal limits of available aerial photography (Lawler, 1993). By incorporating available maps, studies of channel migration and development can be extended by decades or even centuries beyond the photographic record. Braga and Gervasoni (1989) provide an exceptional example of chronologic evolution on the Po River, Italy, where migration of the channel within its floodplain was dated back to the 13th century at several locations. Similarly, Decamps *et al*. (1989) were able to track changes on the Garonne River at the city of Toulouse, France from the 17th century, while Sundborg (1956) was able to infer local details of bank erosion on farmland on River Klarälven, Sweden from local tax records over a similar timeframe. These studies demonstrate that archival records provide a means for evaluating the long-term stability of the magnitude and frequency of dominant channel forming processes (cf. Hooke, 1980) and can illustrate the nature of channel adjustment in response to natural (Vandenberghe and Maddy, 2000) or anthropogenic (Hooke and Redmond, 1989) influences. The availability of old maps is, however, commonly restricted to settled areas, limiting applicability at the reach or larger scale.

Quantitative assessments of channel changes can reasonably be made since the development of cadastral surveys in the 18th century (cf. Church, 1983b). However, the quantitative use of old maps is complicated both by the interpretive biases of the surveyors and cartographers who prepared them, and by the accuracy of the instruments used in map construction (cf. Leys and Werrity, 1999). Depicted channel features such as gravel bars and islands may also change over time due to changes in surveying practices, a concern further complicated by varying standards adopted by different mapping organizations (Hales, 2000). In practice, this means that maps may not only be inaccurate, but may not show all features that are of interest, or may show particular features in insufficient detail where such features are incidental to primary mapping themes. The level of detail also varies with map scale, since some generalization of information is neccessary when abstracting reality to a cartographic representation (cf. Vitek et al., 1996). Veregin (1988) adds that this process can further introduce conceptual (fuzzy) errors which affect the accuracy of spatial overlays.

The use of old maps in morphological studies can also be compromised by an inaccurate scale, a lack of referencing grids, or scale changes between different dates. These problems can be resolved by georeferencing all maps through the identification of common ground control points, a procedure which relates all data to a common frame of reference (Burrough and McDonnell, 1998). Positionally stable (fixed) points are assigned a set of cartesian coordinates which can be obtained, for example, from field surveys, planimetric maps, orthophotos, stereo aerial photographs, or differential GPS. The location of the digitized points is subsequently compared to the mathematical position of the assigned coordinates and a least squares fit is calculated. Large errors are usually caused by the inclusion of one or more incorrectly located points (or incorrectly recorded coordinates) but can be reduced by iteratively removing individual points until the 'fit' improves. Since older maps commonly suffer from unequal paper stretch (Burrough and McDonnell, 1998) an additional transform is generally required before any measurements can be collected. This step is known as "rubbersheeting", and is the mathematical stretching, rotating and translation of points along vectors linking the observed location of fixed points to their true location.

Despite potential difficulties, even qualitative assessments of gross planform changes such as channel shifting or the permanence of islands and major deposition zones can provide information about process changes on large rivers. A recent study on the Brahmaputra River (EGIS, 1997) compared the position of the modern channel to that depicted on a British admiralty

chart, revealing tens of kilometres of migration in response to tectonic effects nearly three centuries previous. Strahler and Strahler (1991) provide an example of bend migration and chute cutoff on the Mississippi River from 1765 to 1930, while Winkley (1994) notes that details shown on these same maps have been used to infer the effects of tectonics on river meandering and sedimentation. Even in cases where inferences of process changes can not be directly qualified, historic planform studies may provide valuable corraborative evidence to support other lines of inquiry.

Archival records in Western Canada are not nearly as extensive as in Europe. The first complete map of lower Fraser River dates to 1859, and merely provides a coarse snapshot of channel and floodplain conditions at that time. Although the detail shown is insufficient to characterize any channel changes that have since occured, the map usefully confirms that several of the major island groups within the river have been present for at least 150 years. More detailed maps are available through five early mapping projects in the Fraser Valley, completed using established surveying procedures (North *et al.*, 1977; North and Teversham, 1984). These include the Crown Colony and Royal Engineers town surveys from 1858-1863, the Provincial surveys from 1873-1877, the Dominion surveys from 1873 onwards, and the surveys of Indian lands. However, these surveys did not generally extend into the channel beyond the main river banks, so the condition of major deposition zones can not be assessed. An exception is the Indian land surveys, which were almost exclusively of channel islands (North *et al.*, 1977), but these surveys do not encompass the entire lower gravel reach. North and Teversham (1984) compiled a vegetation map of the islands and floodplain of lower Fraser River from the original land surveyor's ground coordinates, notes and sketches. Whilst the map represents the period 1859 to 1890, the authors note that most of the floodplain was surveyed between 1872 and 1878, a reasonably short timeframe on a large river from which a general morphologic assessment can be made. The reliability of this map must be questioned though, because the number of different surveyors who originally worked on the project introduces problems of interpretive bias and consistency in data collection practices which may have been translated into the final production map.

The first available map showing the complete gravel reach in sufficient detail to allow morphologic comparisons with more recent mapping was first published in 1905, and a modified version was reprinted as the "1913 Map of New Westminster District." The map was revised by land surveyors in 1912 from 'official sources' which appear to be the original township surveys, given the similarities to several maps shown in McLean (1990). The map provides a detailed

cadastral survey of sectional boundaries and property lots within the lower Fraser Valley. Since land title extended to active channel margins and included channel islands, it can be used fairly reliably to measure active channel width or to compare with more recent maps and photographs to calculate rates of bank advance or recession. Exposed gravel bars are also shown in locations where deposition would typically occur, such as where channel width increases or along the margins of larger islands. Additionally, the size, shape, orientation and variety of bars are consistent with established sedimentation patterns on wandering rivers, and on Fraser River in particular. Nonetheless, several areas within the channel, including lower Herrling Island and present day Queens Bar, are shown as having no accumulation of gravel at all, which is improbable. It is unknown whether the inconsistent mapping of channel bars is due to interpretive differences amongst surveyors, or simply reflects river conditions during high water periods when no bars would be visible. Although the map appears to reliably depict channel banks and island positions, the representation of channel bars is therefore ignored.

The 1912 map lacked both a coordinate system and a suitable number of well-spaced identifiable ground control points to allow rubbersheeting. However, a two-mile cadastral grid was drawn over most of the map surface area, providing a means to scale the map. Since the map was too large to be digitized in one piece, a set of 6 reference coordinates were arbitrarily established along both sides and the map centre (hence it was registered twice using common central coordinates). The location of outer channel banks and all channel islands was digitized along with the cadastral grid, then imported into the GIS for further processing. The map was scaled to real-world coordinates by converting the length of the 2-mile grid in millimetres to the representative length in metres. An artificial grid (2 miles by 2 miles) covering the same area as the map was generated and the scaled map was translated to overlap the dummy grid. Observed differences between the two grids clearly showed locations of distortion through paper shrinkage or expansion. To correct this, vectors were digitized at each grid intersection from the digitized map to the dummy grid, and a rubbersheeting transform was applied. The final step involved rotation and further translation to align the digitized map with a more recent (and positionally accurate) photogrammetric map, using the railway, Harrison River, backchannels and bedrock outcrops as a guide. Despite these efforts, correspondence between the 1912 map and the modern channel could not be completely resolved for all areas. In particular, that section of the map between Vedder Canal and Agassiz-Rosedale bridge did not align as closely as the remaining sections. Although the 2-mile grid was coincidentally absent over this same area, differences are attributed to

cartographic errors introduced during map construction since remaining displacement usually exceeded that associated with paper shrinkage observed elsewhere. The logistical difficulties of accurately surveying this section of river likely reduced the accuracy of cartographic representation relative to other mapped areas. Consequently, the 1912 map is primarily used for qualitative assessment of major channel changes only (Appendix B).

3.2.2 Data acquisition from aerial photographs

When available, aerial photographs should be used in preference to maps to minimize intrepretive or omission errors. They are available much more frequently than maps, an important consideration on dynamic rivers. Though primarily a two-dimensional resource, a wide variety of historical information can be derived from photographs depending on operator knowlege and available measuring devices. The qualitative use of aerial photographs for interpreting fluvial landforms is well-established, and a number of classification schemes have been developed for associating channel pattern with some combination of different formative variables (cf. Mollard, 1973; Kellerhals et al., 1976; Schumm, 1985).

Provided photo scale is known or can be determined, quantitative information such as channel width and sinuosity can also be estimated, but distortion (e.g. due to camera tilt, changes in topographic relief) limits accuracy. By orienting photographs relative to one another through common scaling (cf. Leys and Werrity, 1999), more precise measurements of change can be observed and measured, including the rate of change over time. Church et al. (1987) demonstrate a method for overlaying successive images using an optical projection system. Relative scaling was achieved by matching control points on successive images. This approach has the advantage that external survey control is not required, allowing large numbers of photographs to be analysed rapidly, but small angular deviations introduced during successive photo registration introduces displacement errors relative to 'true' map position. Nanson and Hickin (1986) and Piegay et al. (1997) follow a similar approach, but projected successive images to a reference map. However, even where control points are matched to topographic maps, image displacement due to camera tilting, high topographic relief and radial distortion can introduce positional errors that are not easily rectified.

More recently, computerized techniques have become widely available for georeferencing individual photos, either printed images on a digitizing tablet or scanned images on a computer screen, using simple image processing tools. The procedure involves registering control points by relating their location to known coordinates and computing a best-fit (least-squares) adjustment.

An additional processing step known as polynomial rectification (effectively a rubbersheeting procedure) rotates and positions imagery relative to the known coordinate space, making direct overlays possible. Further, image distortion due to camera tilt or lens distortion can be reduced if sufficient ground control points are identified to re-establish an orthogonal plane (Livingstone et al., 1999). Known coordinates can be determined from ground survey using conventional bearing and distance or GPS survey (Chandler, 1999), the latter technique being suitable for large spatial areas. Topographic maps are more commonly used, but the accuracy of absolute orientation may be compromised both by map scale and the ability to record points at fine resolution using rulers or digitizers. To fully remove the effects of image displacement caused by terrain relief requires the use of orthorectified imagery (geometrically correct image maps). While orthophotos permit more accurate mensuration, the additional cost of having them prepared relative to more simple georeferencing approaches may be difficult to justify, especially for mapping of relatively flat areas like rivers and floodplains.

Although there apppears to be no standard approach for calculating georeferencing errors, they are commonly reported using the RMSE statistic. Stated errors range from ±5-10 metres using recent large scale maps and photos (Winterbottom and Gilvear, 2000; Gilvear et al., 2000; Micheli and Kirchner, 2002; Gaeuman et al., 2003), but errors quickly rise as scales decrease and either map or photograph sources become dated. The accuracy with which photographs can be georeferenced is an important consideration in historic analysis because it establishes the resolution with which detectable change can be reliably determined. This limits effective measurement on small channels, over short time intervals, or on systems with modest rates of deformation. Use of the RMSE statistic has been criticized, however, as it is assumed to apply uniformly over the entire modeled surface (Burrough and McDonnell, 1998), masking the difference between the accuracy and precision of individual points (Lane et al., 2003).

As the photographic records on lower Fraser River are extensive, they are used as the primary source of information on channel morphodynamic changes in this thesis (see Table 3-1). The earliest photographs of the entire gravel reach were taken in July, 1928. However, as these photographs were taken at a large scale (1:10,000), individual frames often did not contain sufficient fixed points to permit georeferencing. As well, the lack of fiducial marks, high radial distortion in older photographs (the displacement of image points from their true positions due to lens distortion of unknown magnitude; Slater, 1975) and inconsistent stereo overlap makes it difficult to establish relative and absolute orientation parameters. The 1928 photographs were

therefore mapped by mono-restitution on a standard digitizing tablet. Individual frames were scanned and re-scaled to 50% size, then oriented (best-fit by eye) to produce photo-mosaic mapsheets. Stable locations, such as road intersections that could be identified on more recent mapping, were used to georeference the mosaics (registration error averaged roughly ±50 metres RMS). Since many individual frames in the mosaic did not contain any control points, rubbersheeting was used to reduce displacement errors. The 1938 to 1943 photo sets — the combination of which forms a complete record of channel change between the 1928 and 1949 mapping dates — were registered to 1949 mapping (see below) using control point matching tools in the GIS. Registration accuracy was less than ±10 metres RMS for all points, while the calculated least-squares fit between digitized and true coordinate positions was used to eliminate poor quality control points to improve overall results. These errors are small relative to the size of the channel (average width of 900 metres - see Chapter 4) but nevertheless affect the accuracy by which quantitative comparisons of channel position over time (i.e. bank erosion rates) can be made. For comparison, channel parameters which can be measured from individual years of mapping (i.e. channel width, length) are more reliable, since the photos are correctly scaled.

Table 3-1. Historic airphotos selected for morphologic mapping

Year	Date	Source	Scale[1]	Discharge[2]
1999	March 20	BCB99001	1:40,000	700
1991	Sept 4	BCB91079	1:50,000	4340
1983	July 19 July 22 July 30	BC83007 BC83008,12 BC83017/18,20	1:20,000	6110 5380 4820
1971	March 19	BC5406/7	1:32,000	800
1962	May 7	BC5042	1:32,000	2940
1949	March 23 March 31 April 6	BC717-20 BC720-23 BC730/31	1:12,000	730 730 980
1943	Dec 5	A7077/78	1:15,000	930
1940	July 15	BC204/5	1:32,000	4870
1938	April 7	A5869/70	1:22,500	750
1928	July 15	A288/89,296	1:10,000	5780

1. Scale is approximate only.

2. Mean daily discharge (m^3/s) measured at Hope gauge.

All remaining photo sets were digitized using an analytic stereoplotter, a device which mathematically relates two-dimensional positions on photographs to their real-world three-dimensional equivalents using standard equations for interior, relative and absolute orientation (Slama, 1980). Following these procedures, distortion and displacement errors are minimized, while common scaling is achieved through a statistical fit of digitized control points on the stereo image to coordinates derived from a defined reference system. The stereoplotter also has the advantage of providing a magnified, three-dimensional view of channel topography which aids in the accurate interpretation of channel features. Control points for orientation were obtained from 1:70,000 TRIM (Terrain Resource Information Mapping) diapositive airphotos taken in 1987. The TRIM photos have been used to produce 1:20,000 topographic maps of British Columbia, and are marked with up to seven control points, the locations of which were determined through geodetic field survey and aerotriangulation. The stated accuracy of individual pugged points is ± 0.5 m RMS. Control points were bridged from the TRIM photos to the 1999 photos, yielding absolute orientation errors for individual points of 1-3 metres (calculated as approximately ± 2 m RMS). Images from other years were bridged from the 1999 photography or from successively registered years of photography where common, identifiable control points became less distinct because of development (i.e. there are significant changes in land use patterns from 1949 to 1999, making it difficult to identify common control points). Between successive years, plotting errors are estimated as ± 2.8 metres RMS.

Absolute accuracy is important in this study since mapped imagery is combined with 1952 and 1984 survey data (cf. McLean, 1990) and more recent bathymetric and altimetry data from 1999 to produce complete floodplain-to-floodplain topographic surfaces of the channel (see Section 3.4). Improper alignment of these data will produce erroneous models, hence spurious measures of bed material erosion and deposition volumes along the gravel reach. Absolute mapping errors for the planimetric mapping are consistent with GPS-based positioning errors reported for both (sounding and altimetry) 1999 surveys, and exceed the horizontal accuracy of the 1984 surveys (see McLean, 1990). The horizontal uncertainty of the 1952 surveys is unknown, but is estimated to be 5-10 metres maximum based on the juxtaposition of digitized soundings and contour lines with photogrammetrically mapped banklines.

Channel features on each photo pair were digitized as a series of lines coded by feature type (e.g. banklines). A complete set of mapped channel features includes outer channel banks, islands, exposed channel bars, partly submerged channel bars and backchannels. All digitized data were

subsequently imported into the GIS for further processing, coding and analysis. The initial step involved converting all mapped lines to polygons (enclosed features having the same start and end coordinates) sharing contiguous boundaries. Since mapping did not extend beyond the main outer channel banks, complete channel and floodplain maps were produced by importing the location of bedrock outcrops, Harrison Bay / River and the outer extent of the floodplain. These data were provided by the Provincial Ministry of Environment from proprietary digital files of lower Fraser River gravel reach (data layers for railway lines, flood dykes and bank hardening were also supplied but are not used for producing floodplain maps). Once complete maps of the channel and floodplain were finalized, all polygons were classified by type of morphologic feature and by channel reach, and sequential maps were superimposed. The quantification and interpretation of historic channel characteristics based upon these maps is presented in the following chapter.

3.3 Bathymetric surveys

Repeat topographic surveys of the channel bed and banks are used to measure the spatial distribution of bed material erosion and deposition volumes within common survey boundaries. Individual surveys are analysed to produce topographic models of the channel bed and banks and consecutive models are differenced to determine elevation increases (aggradation) or decreases (degradation) over time. On large, wandering gravel-bed rivers, channel deformation occurs over years to decades with most erosion and deposition occuring in distinct zones. Therefore, bathymetric surveys can be used to adequately describe these patterns provided the temporal and spatial resolution of individual surveys is sufficiently dense. Concerns related to estimating bed material transfer from observations of morphologic change have been reviewed in Chapter 1, while the relation between bed elevation changes and sediment transport is formally established within the context of a sediment budget framework in Chapter 5.

The first complete survey of the river was undertaken in 1898. The survey extended upstream to Hope and included lower reaches of all major tributaries. The final dataset consisted of triangulations, topography, soundings and calculations of discharge, water-surface slope, and flood contours for the 1894 flood (Public Works Canada, 1949). Unfortunately, the original records were stored in New Westminster and subsequently destroyed in a major fire that occured later that same year. Other early records of development in the navigable sections of Fraser River were also lost in the fire (Public Works Canada, 1949). The gravel reach was not resurveyed until 1952. Subsequent bathymetric surveys have been completed in 1984, 1991, 1999 and 2003.

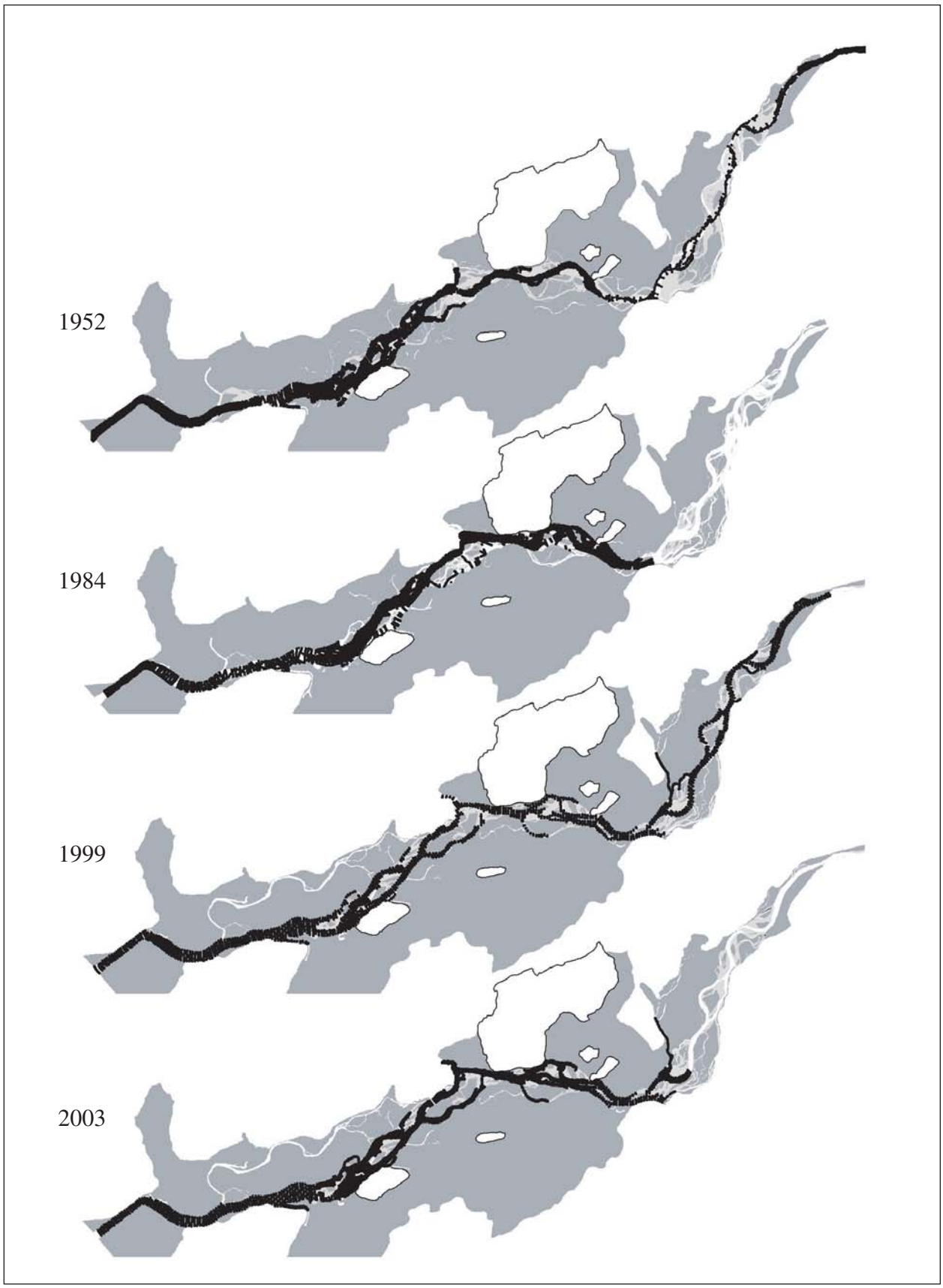

Figure 3-1. Spatial extent of historic bathymetric surveys (black dots).

Various sounding transects have also been taken by government and private consultants for site-specific projects within the gravel reach over the past several decades (including the full channel width between Hopyard Hill and Agassiz in 1962), but the spatial extent of these data are not sufficient for repeat topographic modeling at the reach scale.

Full hydrographic surveys of all study reaches (Mission to Laidlaw) are available for only the years 1952 and 1999. The additional datasets are spatially constrained by comparison — the 1984 survey extends from Mission to Agassiz, the 1991 survey terminates at the confluence with Harrison River, and the 2003 survey ends at lower Herrling Island (Figure 3-1). The 1952 and 1984 data are re-analysed to contrast the methodological approach adopted in this study with results given in McLean (1990) using the same base data. The 1991 data are not used to calculate bed material storage changes, but are incorporated to determine an optimal method of spatial interpolation for bathymetric surveys collected along transect lines (see Section 2.4). The 1999 survey is used to measure the spatial and temporal variability of storage and transport zones within the river more reliably than was possible using a single intersurvey period (cf. McLean, 1990) and allows sediment transport estimates to be extended upstream of Agassiz. The 2003 survey was completed during a smaller than average freshet and no data were collected along elevated bar surfaces, or along major sidechannels where access was limited. However, more recent (March, 2004) acquisition of spatially dense LiDAR data allows these 'data gaps' to be filled in and an accurate 2003 surface constructed. Comparison of 1999 and 2003 modelled surfaces is used to construct a sediment budget in which sites of sediment erosion and deposition are apt to remain distinct.

3.3.1 Compilation of available bathymetric data

The 1952 survey of the gravel reach was undertaken by Public Works Canada and extended from Barnston Island to Yale. River bathymetry was surveyed by fathometer, while exposed (above waterline) surfaces were mapped photogrammetrically (McLean and Church, 1999). Soundings were collected along cross-sections with an average spacing of 140 metres between Mission and Laidlaw. The final dataset was compiled as a series of 1:4800 charts with bed depths given to the nearest 0.1 foot (3 cm) and contours presented at 5 foot (1.52 m) intervals. The data were recovered to digital form by manually digitizing all charts covering the study reaches (approximately 12,000 individual sounding points). In addition, all contour lines from bar and island surfaces within the active channel zone and adjacent floodplain margins were digitized to provide nearly complete spatial coverage of the channel. The data were imported into Arc/Info GIS

(Version 8.3, ©ESRI, 2002) where elevations were converted to metres and positions were adjusted from latitude/longitude to UTM coordinates (NAD83 datum). As depths were given to chart datum (geodetic mean sea level) no additional adjustment for water level was required.

A TIN model (surface of irregular triangles) was created from the data to visually examine the output for coding errors (i.e. points where no elevation value was assigned, or the assigned value was clearly wrong based on neighbouring values) and obvious discrepancies were corrected by hand. The accuracy of contour line elevations was similarly verified, but small positional errors could not be detected (hence corrected) because the dense spacing and thickness of the drawn lines on the charts hindered interpretation in some regions. The TIN model also revealed that contour spacing was commonly too sparse on most of the larger exposed bar surfaces, resulting in an interpolated surface with little or no topographic variability (i.e. many of the modeled bars appeared unrealistically 'flat'). Similarly, contour density was found to be inadequate within several prominant sloughs and most secondary channels, resulting in a modeled surface in which these features appeared either unrealistic in shape, or the model could not distinguish the channels from surrounding topography.

To increase the accuracy with which the 1952 surface could be interpolated, the original survey was amended with photogrammetrically derived elevation data. Large-scale (1:10,000) aerial photographs of the channel from 1949 and small-scale (1:40,000) photographs from 1952 were used to digitize a coarse array of points in regions of insufficient spatial density. Additional points were recorded separately on adjacent island and floodplain surfaces such that relative elevation differences could be calculated. This step was necessary because of the difficulty in establishing absolute vertical accuracy of stereo-model orientation (because the vertical precision of the TRIM points is commonly more than 2 metres) hence the accuracy of recorded elevations. The data were imported into the GIS and relative elevations were calculated locally by comparing surveyed with digitized elevations on the islands and floodplain. Measured differences of at least 0.5 metres were subsequently used to adjust the recorded elevations of nearby points digitized on bars and secondary channels. A total of 1037 photogrammetrically-derived points were added to the original dataset.

The second major survey was completed in 1984 using a combination of automated hydrographic survey, conventional cross-sectional survey, and terrestrial ground mapping (McLean, 1990). The hydrographic data were collected along transects (120 metre average spacing) over 38.5 km of main channel using Environment Canada's HYDAC survey system

(Zrymiak, 1984). A copy of the reduced dataset was obtained on CD-ROM from Environment Canada, Ottawa (UTM coordinates, NAD83 horizontal datum, geodetic vertical datum). The conventional cross-section sounding surveys (average spacing 250 metres) were completed by a UBC crew along 18 km of sidechannels between Chilliwack Mountain and Agassiz and 10 km of main channel between lower Sumas Mountain and Yaalstrick Island. The UBC crew also surveyed exposed bars, islands and channel banks using a terrestrial-based transit level. The UBC data were supplied [from D. McLean] in the same coordinate system as the HYDAC data. The complete 1984 channel survey consisted of 66,600 individual elevation points. The data were imported to the GIS and overlaid on the the 1983 base map to check positional accuracy (i.e. proper alignment with respect to islands and the outer banks). Several sounding lines near Calamity bar were oriented using a different (NAD27) datum, hence were adjusted.

The 1984 survey was found to be more spatially limited than either the 1952 or 1999 surveys between Mission and Agassiz, as relatively low water conditions during the 1984 freshet precluded access to several areas within the channel. This effectively limits the precision with which bed deformation can be detected, as no surface can be interpolated in regions without sufficient topographic data (hence no surface comparison can be made). Rather than exclude these regions (cf. McLean, 1990; McLean and Church, 1999), it was decided to amend the original survey with photogrammetrically derived points, as completed for the 1952 survey. Low-water aerial photographs from 1979 were selected as the large scale (1:10,000) allowed bar and island topography to be clearly discernable and photos were available for the entire gravel reach. Ideally, the selected photos would be nearer to the date of the survey because intervening erosion or accretion of sediment on mapped bar surfaces introduces an unknown bias in elevation measurements. McLean (1990) shows photo mosaics of low-water aerial photographs for 1982 and 1984 that covered much of the gravel reach, but flightline records for those dates could not be recovered. However, a visual comparison of the 1979 photographs with these mosaics shows modest morphologic change, coincident with the lack of major floods during this period. It is therefore assumed that island and floodplain surface elevations would have remained constant, whilst bar surface elevations likely changed by no more than several tens of centimetres on average, based on long-term mean bed-level changes downstream of Agassiz (Church *et al.*, 2001). Elevation changes of this magnitude are equivalent to the precision with which elevations can be measured from aerial photographs using the stereoplotter.

Following initial model orientation of each stereo pair, a point file of coordinates from the 1999 laser altimetry survey was imported into the stereoplotter digitizing program, and positions were displayed on-screen. A replacement set of control points was recorded at these locations (all of which were chosen on stable island / floodplain surfaces), and absolute orientation parameters were re-calculated based on the more accurate altimetry elevations (~15 cm, compared with the 1-5 metre vertical error associated with the TRIM data). This procedure also obviated further vertical datum adjustments in the GIS, as required for the 1952 data. A text file containing coordinates for all 1984 bathymetry data and altimetry data was then imported and displayed to provide simple visual reference on the photographs for identifying locations where elevation data were lacking (and similarly avoided the collection of redundant data within surveyed regions). A total of 13,038 points were digitized from exposed bars and islands and added to the 1984 sounding file.

The 1999 bathymetric survey data were delivered by Public Works and Government Services, Canada in October, 1999. The complete data set consisted of 301,500 sounding points in ASCII format. Although survey lines were spaced roughly 200 metres apart, elevations were obtained at sub-metre spacing along each line, thus accounting for the large total number of points. To reduce the density of the sounding points, a subset of the original data was created using a Fortran program to retain points at 20 metre spacing between the start and end points along each individual survey line (additional data were deemed redundant for the intended bed surface model construction). The edited dataset consists of roughly 12,000 points, comparable with the 1952 survey.

To complete the 1999 dataset, elevation points from exposed bars and floodplain surfaces were incorporated from a laser profiling topographic survey completed in March, 1999. The data were collected using a single-track pulsed laser mounted on a helicopter. Measurements were continuously recorded along 200 metre flightlines across the floodplain (roughly between the flood dykes) along the length of the gravel reach. The raw data were processed by the contractor to calculate ground positions and eliminate outliers, recorded where a signal is returned from buildings or vegetation rather than the true ground surface. The completed dataset consisted of roughly 60,000 points at a spacing of 1 to 10 metres. Initial modeling attempts revealed the presence of remaining outliers (usually isolated single points) that had not been detected. A Fortran program was written to search for adjacent points at least 3 metres higher than their immediate 2 neighbours along each transect line, an experimentally derived value that successfully ‘flagged’ the suspected individual outliers while preserving real topographic variation. The filtered dataset was

then overlaid with the 1999 channel map, so each topographic point could be assigned a channel map classification code (i.e. water, gravel bar, floodplain). Within the GIS, points falling on either the river surface, backchannels, or bar edges were deleted since these points obviously do not represent the actual bed of the river. Following this additional editing, the laser altimetry dataset was reduced to 55,700 points.

The 2003 bathymetric survey data were collected by Public Works and Government Services, Canada during the summer freshet (late June to early July) and delivered in October, 2003. The complete data set consisted of 332,000 sounding points in ASCII format from Mission to lower Herrling Island. The data were collected following the same procedures as in 1999. including near replication of sounding line positions. However, additional lines were collected between the 1999 transects, giving an average line spacing of 100 metres. The modest increase in the total number of recorded points despite the increase in survey density partly reflects the absence of data collection from lower Herrling Island upstream to Laidlaw. More importantly, low water conditions during the data collection period precluded surveying on major bars and bar complexes which were either exposed, or covered by water that was too shallow for navigation. Consequently, the 2003 survey was spatially limited in extent, similar to the 1984 survey.

The 2003 dataset was not completed until June, 2004 when the availability of additional LiDAR data fortuitously became available as part of an independent hydraulic modeling study to update the design flood profile. LiDAR data were collected in April, 2004 across the channel zone extending to the limits of the floodplain (i.e. beyond the flood dykes) from Chilliwack Mountain to lower Herrling Island, and at Matsqui Prairie (the left bank floodplain near the downtream end of the study reach). No data were acquired on the river or floodplain between these locations. Data were collected using a swath-beam system that provided near continuous ground coverage, and were post-processed at 1-metre ground resolution. The complete dataset consisted of approximately 250 million individual 'bare-earth' ground returns. A copy of this survey was obtained in ASCII format (78 separate files) and further edited in the GIS.

Given the physical size of the datafiles, it was first necessary to thin the data to a more manageable survey spacing due to computer memory limitations. A TIN model was created for each of the ASCII files and was converted to a regular grid array using a user-defined spacing (chosen as 5 metres). A second subroutine was used to convert each grid array to points, where each point location is equal to the centroid of a grid cell. This file format is used to store all of the historic bathymetric and terrestrial survey data. Since the LiDAR survey recorded ground returns

on the water surface, these points required deletion or else would conflict with the sounding elevations. The water surface was delimited from 2004 aerial photography (coincidentally taken near the date of the LiDAR survey) and depicts channel conditions at lower flow conditions than during the sounding survey. All points that intersected the mapped water-surface were removed from the point files.

The remaining data gap between Matsqui Prairie and Chilliwack Mountain was closed by amending the 2004 LiDAR survey with points from the 1999 LiDAR survey, as it is assumed that the vertical elevation of the floodplain and islands did not change over this period. Despite these efforts, there remained a paucity of elevation data at lower Yaalstrick bar. However, a comparison of 1999 elevations on the exposed bar surface with several randomly collected photogrammetrically-derived points revealed little or no apparent change in bar elevation. Therefore, 1999 survey data were assumed to adequately represent the true channel topography at this location, though of course no net change will be computed at this location between 1999 and 2003. The final dataset consisted of all sounding points, 4.73 million points from the 2004 LiDAR survey and 7700 points from the 1999 LiDAR survey. The bathymetry data were not thinned, because the 2003 surface is compared only to the 1999 surface, which was also remodeled using the complete set of available data points. Procedures for converting these different sources of elevation data into topographic surfaces that can be directly compared are presented in the remaining sections of this chapter.

3.4 Construction of 3-D surfaces

3.4.1 Introduction

The distribution of elevation behaves reasonably predictably because elevation is not influenced by complex, or unknown, interactions with other variables. Consequently, models that represent topography can usually be constructed with greater fidelity than can models for most other spatial phenomena. Nevertheless, several factors may complicate the accurate portrayal of the earth's surface, including biased or inadequate distributions of data, elevations available only along contour lines, sharp breaks in slope, local low (sink) and high (peak) elevations and the presence of vertical features such as cliffs (ESRI, 1991; Burrough and McDonnell, 1998). Hutchinson (1996) adds that spatially varying surface complexity and anistropic behaviour also preclude a simple analytic approach to interpolation.

Although different interpolation schemes tend to produce similar results given sufficiently dense data, they can produce widely varying surface representations given the presence of one or more complicating factors (Burrough and McDonnell, 1998). For example, a recent study (EGIS, 1997) estimated erosion and deposition volumes for channel islands along a 17 km reach of Brahmaputra River and found differences ranging from -13 million m^3 (net erosion) to +5 million m^3 (net deposition) using two different mathematical functions to interpolate sparse elevation data. Choosing the most appropriate technique for the available data is therefore a key consideration for interpolating sparse data (Isaaks and Srivastava, 1989; Englund, 1990; Bishop and McBratney, 2002) and reducing unwanted artifacts (noise). Despite this, the quantitative comparison of different modeling techniques is rarely considered and does not appear to have been undertaken in the geomorphic literature.

There in no known universally accepted (correct) technique by which to topographically model the bed and banks of a river channel. Indeed, even experts will opt to apply different interpolation approaches to the same dataset based on partly subjective judgements (Englund, 1990). Fluvial researchers have presented diverse approaches including Laplacian and spline interpolation (McLean, 1990), inverse distance weighting (Eaton and Lapointe, 2001) and kriging (Fuller et al., 2003), all of which may be appropriate when the collected data are semi- or fully-distributed. However, most recent studies have suggested that TIN models (specifically Delaunay triangulation) present the most appropriate technique for representing complex river bed topography (Lane *et al.*, 1994; Milne and Sear, 1997; Brasington *et al.*, 2000). Triangulated irregular network models (TINs) are often used to represent a continuous surface because the method preserves known spot elevations and the density of the triangulated mesh can be adjusted during data collection to the complexity of the surface (Burrough and McDonnell, 1998). As well, interpolation can be restricted across breaks of slope (i.e. river banks) to limit topographic distortion (Lane *et al.*, 1994). Delaunay triangulation consistently appears to provide a realistic representation of a channel surface where the data are well distributed (as in the examples cited above). However, the bathymetry data available for lower Fraser River (as is common with available conventional cross-sections on many systems) are heavily biased in the cross-stream direction. Although studies have recognized the weakness of cross-sections for representing distributed channel topography (Lane et al., 1994; Westaway et al., 2000) they have not examined the potential weakness of the TIN model itself for interpolating between cross-sections. Nevertheless, cross-section data continue to be collected because they are convenient for many

other applications (e.g. 1D hydraulic modeling) and because cross-section lines simplify data collection (i.e. river navigation).

One of the major difficulties in choosing the most appropriate interpolation model is that there rarely is an independently acquired true surface with which direct comparisons can be made. As a result, qualitative judgements are commonly applied to reject or accept particular modeling strategies based on the perceived visual representativeness of the output. Because minimum curvature techniques (eg. splines) tend to produce smoother, more realistic appearing surfaces, researchers may be biased in choosing these models without subjecting them to error analysis or verification. A more rigorous approach for model evaluation involves cross-validation, where an estimate is made for a point at a known location by excluding that point and re-estimating its value from remaining data (Isaaks and Srivastava, 1989; Carr, 1995). The difference between actual and estimated values can subsequently be evaluated for the entire datatset to calibrate estimation accuracy (Carr, 1995). Deutsch and Journel (1992) add that different modeling strategies can be compared by examining the distribution of differences (errors) where the best approach produces a symmetrical error distribution centered on zero, minimum variance and no spatial correlation (the errors are independent). Violation of these properties can be used as a guide to adjusting model parameters (eg. sample weight, search radius) until the distribution improves.

Cross-validation is appropriate for evaluating different interpolation schemes, including exact interpolation techniques (i.e. TIN, kriging) where estimates at known data locations are the same as actual data values. However, this procedure is subject to a number of limitations, especially the inability to evaluate model performance where actual data are sparse or absent (Isaaks and Srivastava, 1989). An alternative technique known as jackknifing can be used to overcome this common problem. The term applies to sampling without replacement (Deutsch and Journel, 1992) and refers to separating a dataset into estimation and validation components. Since the 1991 bathymetry data are spatially more dense than in the other years for which soundings were collected, this dataset can best be used for jackknifing, wherein the estimation data can be sampled from sounding lines spaced similarly to the other surveys and the remaining points can represent the validation data.

A modified jackknifing strategy is employed herein, whereby the estimation data are used to produce an estimated surface to compare against a true ‘reference’ surface. The reference surface is derived from both estimation and validation datasets because removal of points between cross-sections may affect the quality of interpolation at retained data locations. As well, the goal

of selecting the most appropriate model is to reproduce the entire channel bed as accurately as possible using the thinned data, rather than simply minimizing estimation errors in regions lacking data. An additional benefit of this approach is that an estimate of model error over the entire channel bed can be provided. The 'best' modeling strategy, therefore, is that which reproduces a continuous surface whose spatial characteristics are most similar to that of the reference surface and which minimizes the absolute difference between the two surfaces. A true reference surface is derived along a morphologically complex 7-km long test reach extending from Queen's Bar to Harrison Bar using the 1991 survey data. The development of this surface, and a comparison of alternate modeling approaches available in the GIS, is presented below.

3.4.2 Reference surface data

Lower Fraser River was surveyed by echo-sounder in 1991 by the Canadian Hydrographic Service (Institute of Ocean Sciences). Soundings were taken along cross-sections spaced 50 metres apart from New Westminster to Foster Bar, and included lower Harrison River. Both instream and off-channel planimetric features (ie. gravel bars, islands, banklines, backchannels) were mapped photogrammetrically from 1:30,000 aerial photographs taken in 1990, but elevations were not recorded. The data were published as a series of 1:10,000 nautical charts, with soundings reduced to water datum (related to geodetic datum by the water-surface slope). A digital copy of the sounding data (15,650 points) was obtained within the study area, with all depths adjusted to geodetic datum, and positions converted to the UTM (NAD83) coordinate system. As the sounding lines were not always perpendicular to the shoreline (the survey also contains longitudinal, oblique and curvilinear cross-sections), the complete survey represents the channel bed as a well-distributed set of sample points, each spaced roughly 30-50 metres apart. This regular distribution is ideal for interpolating spatial phenomena (cf. Burrough and McDonnell, 1998) and is sufficiently dense for capturing the major variability of bed topography within the wetted channel.

Since the purpose of the 1991 survey was to provide updated hydrographic charts within navigable sections of channel, no attempt was made to survey smaller, secondary channels or exposed (above waterline) regions. Upstream of Sumas Mountain (where the channel bifurcates around islands and emergent gravel bars) this results in a significant paucity of data with which to produce a complete topographic surface of the entire channel zone (see Figure 3-2 A). This effectively limits comparison of different interpolation techniques to the morphologically simple channel between Mission and Sumas Mountain. In an attempt to reduce the effect of this restriction, a GIS-based procedure was developed to interpolate elevations in regions of no data,

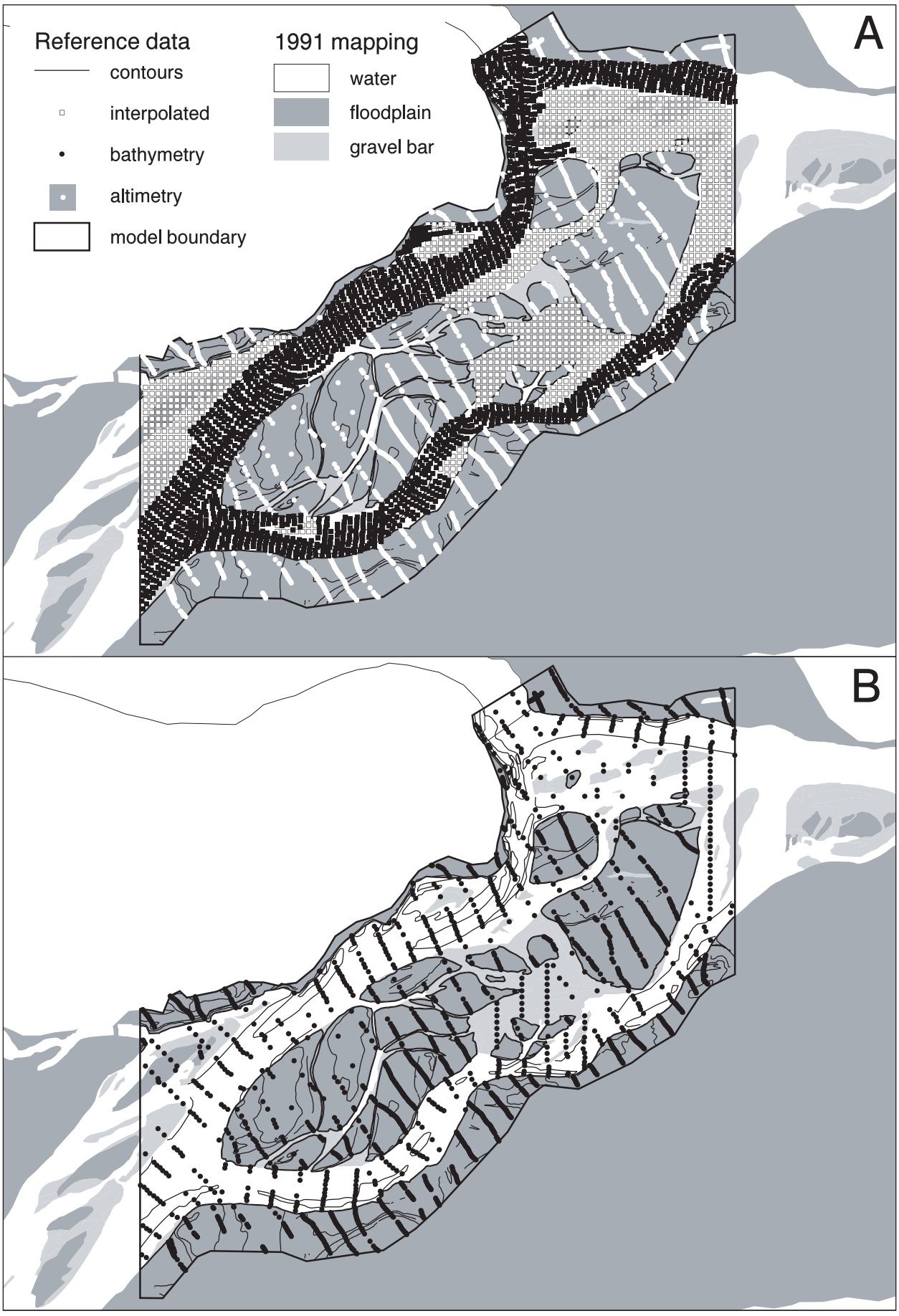

Figure 3-2. (A) The complete testing data for development of the reference grid. A thinned sub-set of data (B) is used to to compare different interpolation schemes (see text).

the boundaries of which were identified in the GIS (there are no low-water photographs near this date from which elevation could be directly measured). The interpolation is based on a difference grid (25 m resolution) calculated from 1984 and 1999 surveys[1]. Since the river is so large and change occurs relatively slowly, it is assumed that there is little compensating scour or fill within this 15 year intersurvey period (i.e. if there was aggradation at a given location between 1984 and 1999, it is likely that there was aggradation in both 1984-91 and 1991-99 intersurvey periods). Absolute errors do not really matter in any case, since this is merely a test dataset for the interpolation methods. This procedure ensures that modeled surfaces appear morphologically (visibly) realistic, which aids in evaluation of interpolator comparison. The change in elevation between these dates was adjusted by 0.5 (eg. half the total bed level change from 1984 to 1999 was assumed to have taken place by 1991), then added to the 1984 surface to produce an estimate of the 1991 elevation. These grid-cell elevations were then converted to a set of equally-spaced points, where each point corresponds to the centre of a grid cell. To make the data spatially comparable to the 1991 bathymetry data, the grid was sub-sampled at a spacing of 50 metres. These equally spaced points were then appended to the bathymetry data.

To complete the point dataset, the 1999 laser altimetry transects were also incorporated into the test dataset, but first were parsed to eliminate points falling on water or bar surfaces and points falling outside the test reach boundary. The complete point dataset consists of 5353 sample points; 2528 from soundings, 1007 from interpolation between 1984 and 1999, and 1818 from laser altimetry. The point records were supplemented with available contour data from the 1952 survey where the contours were coincident with island and floodplain surfaces stable within the 1952-1991 intersurvey period, since contours are known to improve the continuity of a modeled surface. Additional contours were manually interpolated at 5 metre intervals along the channel bed for completeness. A series of breaklines (linear features that define abrupt breaks in surface continuity) mapped as island and floodplain edges from 1991 aerial photography completed the input parameters for model development and comparison. The complete spatial distribution of the input data is shown in Figure 3-2 A.

1. Construction of 3-dimensional surfaces, differencing of surfaces, and the estimation of bed material transport rates have been previously reported using the 1952, 1984 and 1999 survey data in Church *et al*. (2001). A copy of the section of the manuscript detailing computational procedures is given in Appendix B of the thesis.

3.4.3 Reference surface derivation

Although there are a variety of local and global models within the GIS from which interpolated surfaces can be generated, the reference surface was initially constructed using only the TIN and Topogrid modules in Arc/Info since these models have been specifically designed for and tested on elevation data and both models can incorporate the available point and contour data. TIN algorithms are particularly well suited for modeling regular arrays of elevation data provided the point spacing is sufficient to characterize topography in regions of complex terrain (Burrough and McDonnell, 1998). In addition, the inclusion of contours and breaklines reduces the number of invalid triangles (flat triangles across breaks of slope or topographically unrealistic, long, thin triangles). The Topogrid model is based on a "discretized thin plate spline," (i.e., one in which an exact spline surface is replaced by a locally smoothed average). The model replaces the minimum curvature interpolation criterion inherent in the spline model with a minimum profile method that better matches landform processes and preserves drainage structure (Hutchinson, 1996). Effectively, this allows the model to follow abrupt changes in terrain, such as along channel banks, which minimum curvature techniques can not (John E. Hughes Clarke, *pers comm*, 2000). Although elevation contours can be assimilated into the interpolation process, natural breaks in slope can not be explicitly defined except where coincident with a contour or sufficient point data.

The accuracy of both the TIN and Topogrid interpolations was first evaluated by superimposing the original data points on each interpolated surface and comparing the two datasets using the RMSE statistic. For this comparison, the TIN model was first converted to a 10 metre regular raster array (coincident with the resolution of the Topogrid model). This step is neccessary because points can not be directly superimposed onto the TIN data structure in the GIS (similarly, consecutive TINs can not be directly subtracted). The best results (RMSE ± 0.345 m) were produced using a quintic (5th degree polynomial) interpolator to convert the TIN to a raster. For comparison, the best results using the Topogrid model produced a calculated RMSE of ± 0.547 m. The TIN models produce smaller errors, in general, because the interpolation method is exact – the location and value of the original data points is preserved in the model. However, deviations (RMSE) occur during conversion to a regular grid since each grid cell may spatially overlap, hence average, more than one original data value. As the 10 metre grid cell size is small relative to the size of triangle facets (which typically connect 50 metre sounding points) this averaging does not generally lead to large differences between original and modeled elevations.

A scatterplot of the data reveals that only a small number of points display significant deviation between actual and interpolated values in either model (differences are as large as 9 metres near vertical banks - see Figure 3-3 A, B). However, because the RMSE statistic is highly sensitive to outliers, these points account for a large proportion of the total sum of squared deviations. Analysis of these residuals demonstrates that they are slightly skewed for both interpolated grids (more frequently underestimated) while variograms show a pure nugget effect for the TIN, an indication that errors are randomly distributed over the study area (Figure 3-3 C). Errors are similarly random for the Topogrid model, and both variograms exhibits a dip (hole effect) at a distance of 5 km (cf. Figure 3-3 D), indicating noise or a periodic trend in the data (Isaacs and Srivistava, 1989; Burrough and McDonnell, 1998). This trend likely corresponds to channel gradient. However, a simple plot of the residuals in the GIS clearly showed that the largest errors were found along island and bank perimeters, not within the main channel (Figure 3-4). The variogram model likely fails to detect this pattern because island and bank features are well-distributed throughout the study area.

A visual plot of the actual interpolated surfaces illustrates poor interpolation of the TIN model between channel banks and the end of sounding lines and along channel margins between sounding lines, despite the density of available data (Figure 3-5). In comparison, surface continuity in these regions appears more realistic using the Topogrid models (Figure 3-5) even though, statistically, they perform worse overall (larger RMSE). Because statistical measures do not necessarily capture these types of errors (especially when the interpolation is accurate near known data values in the TIN), visual checks are an essential part of the interpolation process (Isaaks and Srivistava, 1989). This problem probably occurs because breaklines were not explicitly defined with elevation values and contours encompass only a fraction of the total bankline length (cf. ESRI, 1991). Since gradient changes are greatest between the channel bed and floodplain, interpolation errors along 400 km of channel margins (i.e. over the entire gravel reach) can cumulatively result in significant total errors that could dominate erosion and deposition measurements, especially given the larger transect spacing of the full surveys. Reducing interpolation error along the bank edges is therefore essential to minimize bias in the entire sediment budget.

To reduce these errors, a method was developed to estimate the elevation along channel margins in an attempt to provide a more reasonable representation of actual topographic variation. The laser altimetry data were isolated and used to create a surface grid model that included island and floodplain surfaces only. Because these surfaces are reasonably flat, the survey line spacing

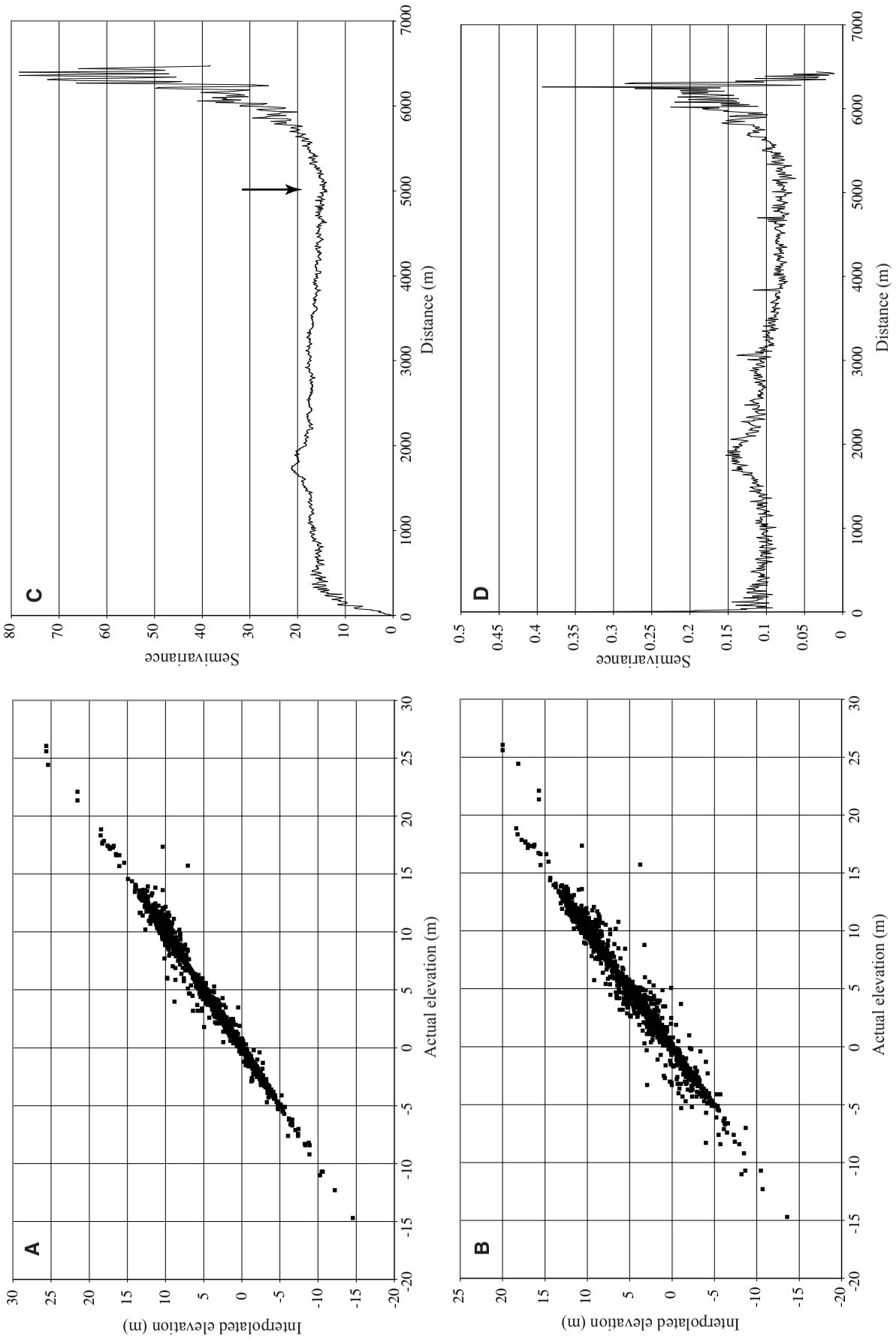

Figure 3-3. Scatterplots showing difference between actual and interpolated values for the reference dataset using A. TIN and B. Topogrid models, and Semivariograms of C. complete reference dataset and residuals from TIN model. Plots for the Topogrid model (not shown) exhibit a similar pattern. Arrow in C indicates a dip in the variogram (see text for discussion).

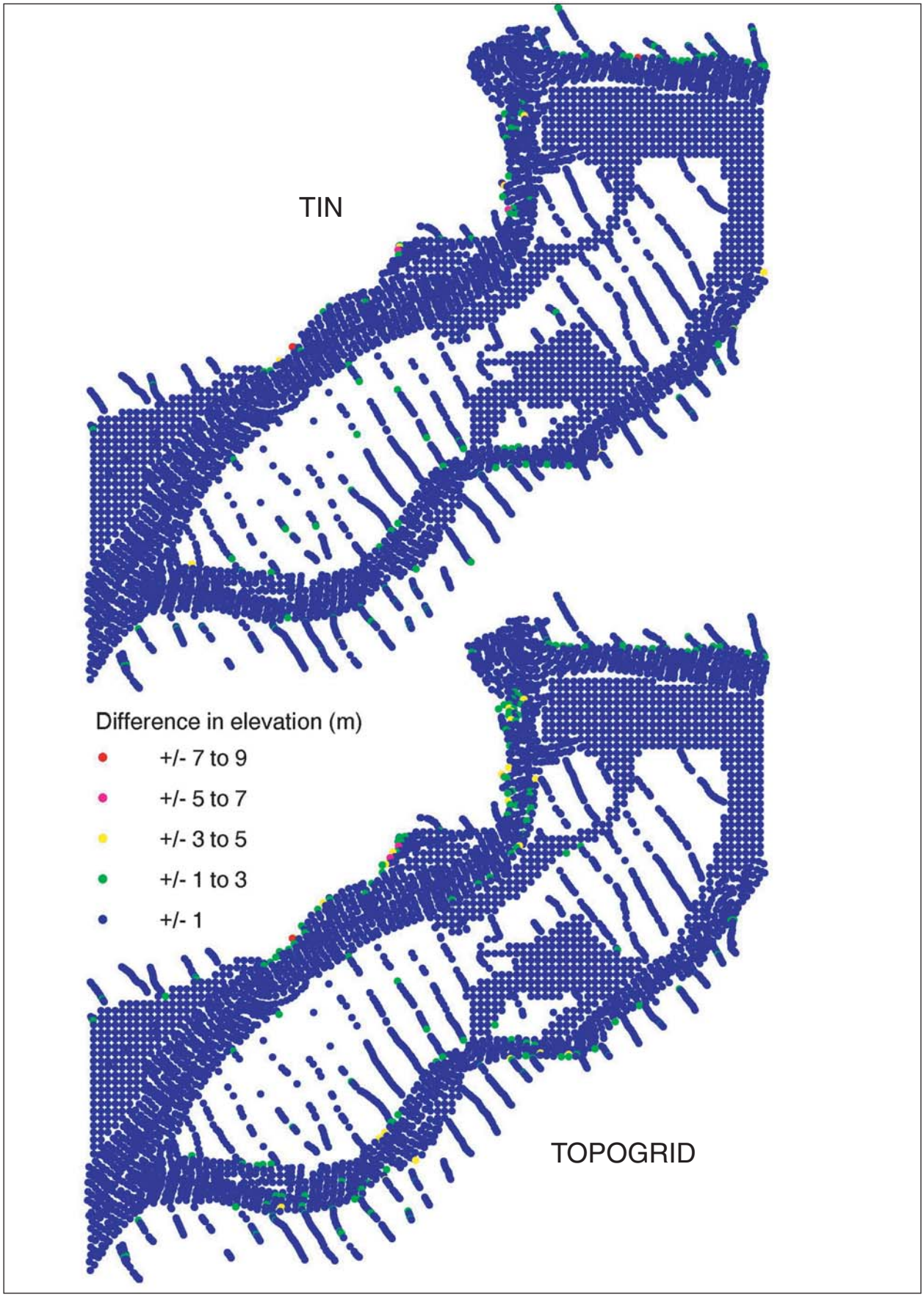

Figure 3-4. Plot of elevation difference between actual and interpolated values for the reference dataset using TIN and Topogrid models.

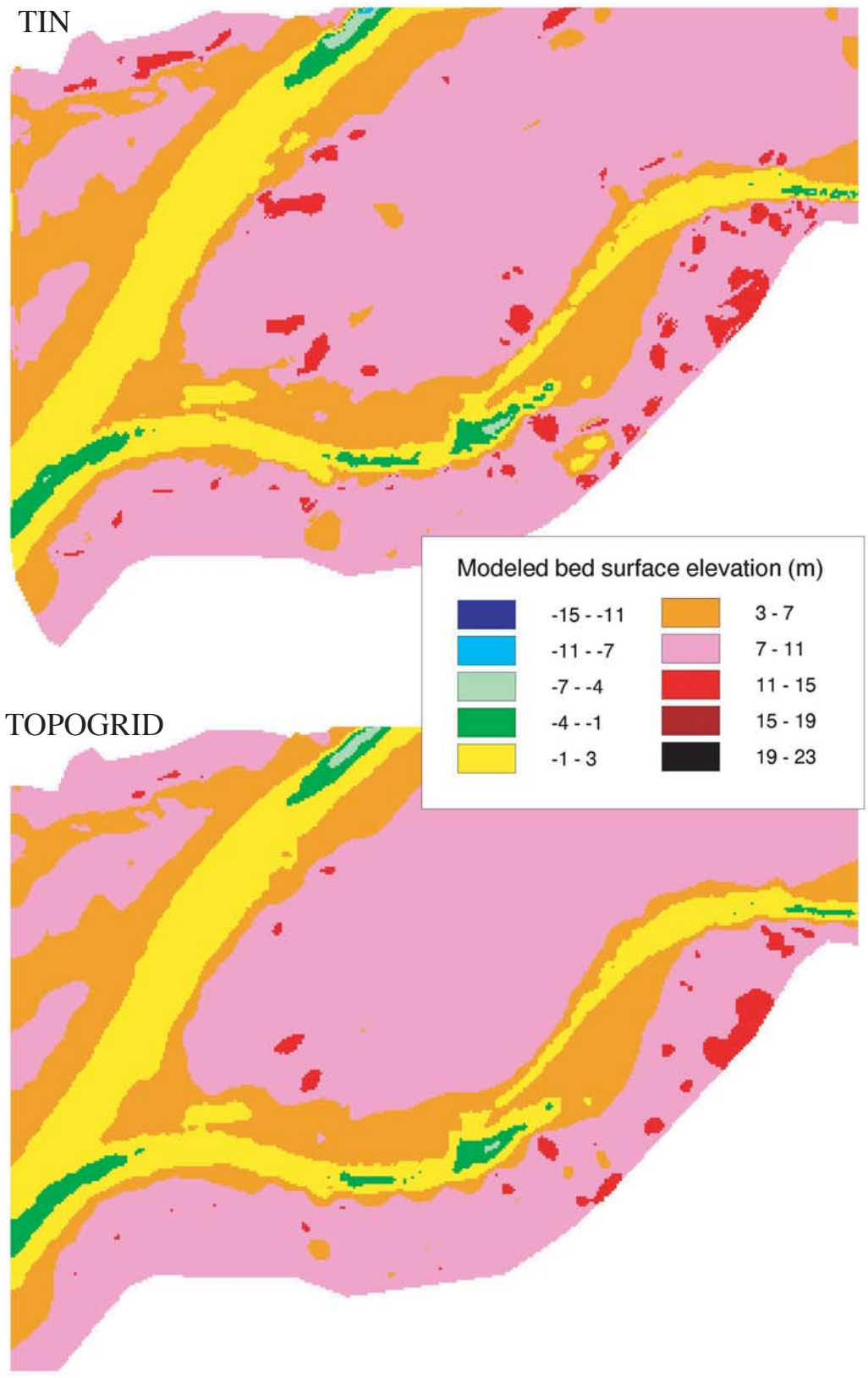

Figure 3-5. Reference surfaces using TIN and Topogrid models with no bankline contours.

does not bias modeled surface continuity. The banklines mapped from airphotos were subsequently overlaid on the floodplain models to produce a set of banktop contour lines (i.e. breaklines with elevation values) that could be incorporated into both models. A second set of parallel contours (with 10 metre offset) was derived for the bottom of the banks using only sounding points. Several TIN and Topogrid models were re-estimated using the test dataset and the bankline contours and altering available input parameters (Topogrid) or trying different combinations of banklines (for example, by eliminating bank bottom contours in TIN). In general, the addition of bankline contours results in visually smoother, more continuous surfaces with a corresponding reduction in RMSE to 0.468 m for the Topogrid model using recommended default input parameters for tolerances that influence data smoothing. By comparison, the TIN models generally showed improved interpolation along the banks, but many invalid triangles remained and obvious interpolation errors were occasionally observed on channel bar and island surfaces. The RMSE actually increased to 0.420 m because the bankline contours frequently overlaid actual survey data, resulting in averaging at those coincident locations. Although the increased RMSE for the TIN model remained smaller than that of the Topogrid interpolator, the Topogrid model is adopted as the reference surface because, visually, it appears to provide a slightly more faithful reproduction of an actual river channel (see Figure 3-6).

3.4.4 Model comparison

In an attempt to test the stability of surface models with reduced information, different interpolation techniques were applied to a thinned subset of the idealized test dataset. The reference dataset was parsed by removing data along sounding transects until the remaining point spacing and density resembled those of the 1952, 1984 and 1999 surveys (i.e., retained points formed a set of parallel sounding lines roughly 200 metres apart). A total of 2864 points (55%) were deleted – however, since all altimetry points were retained, the points removed represent 81% of those within the channel bed (see Figure 3-2 B). A series of tests was then performed by subtracting models based on the thinned dataset (with and without bank contours) from the reference surface. This allows the suite of interpolation tools available in the GIS to be directly compared, and allows the benefits of the bank contouring method to be demonstrated. Since only the TIN and Topogrid modules can incorporate contour lines directly into the modeling routines, all contours were converted to a series of nodes for all other models to provide a comparable set of test data. The optimal modeling strategy is that which minimizes not only the net difference between the model surface and the reference surface, but also the magnitude of the apparent scour and fill, since

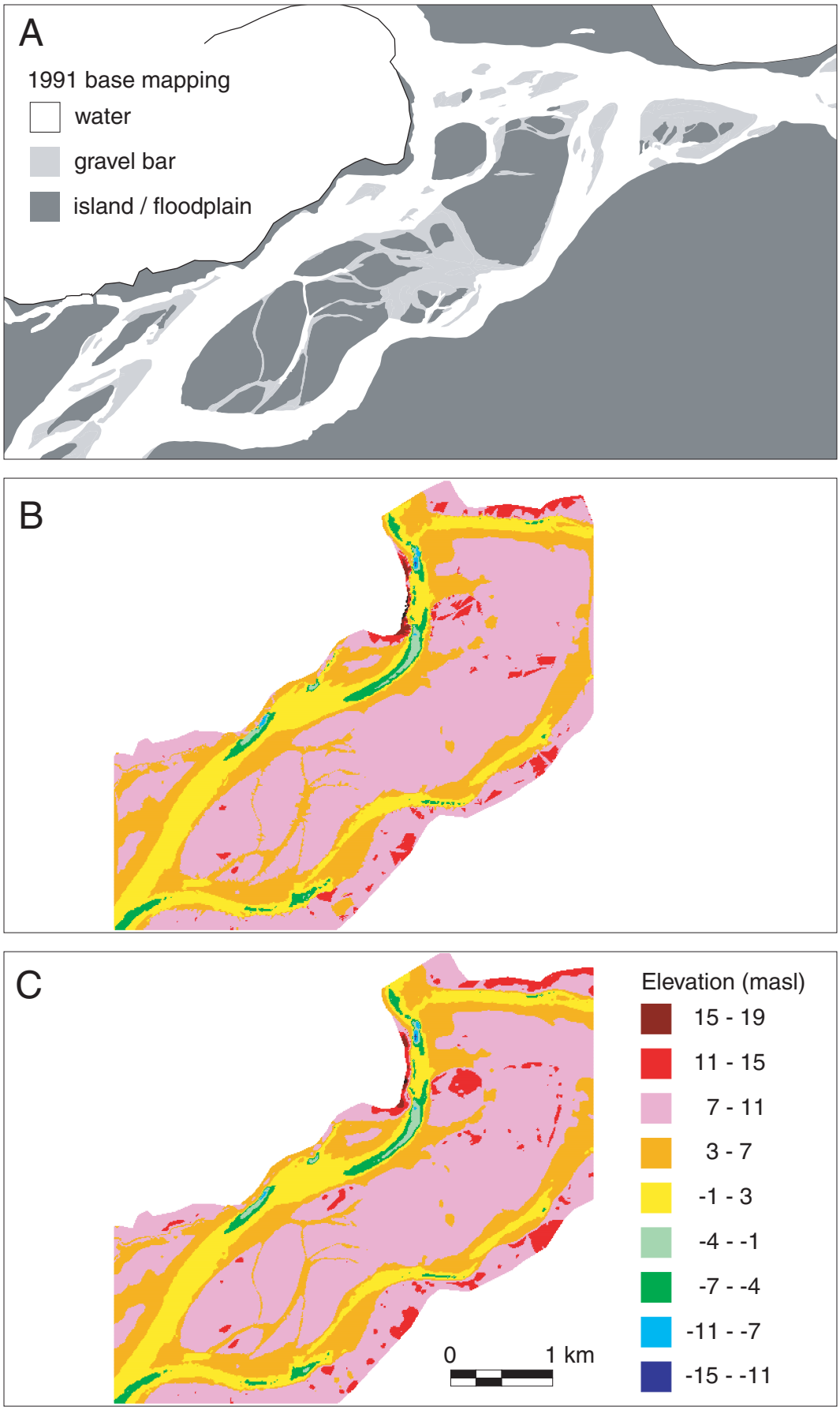

Figure 3-6. Reference surfaces based on TIN (B) and Topogrid (C) models. The mapped channel (A) as interpreted from 1991 aerial photos is shown for comparison.

significant values of either represent interpolation error between survey lines (i.e. both values should be zero). Although there will be no net difference between model and reference surfaces if scour and fill volumes are equal, large values of either measure represent deviation from the reference surface and will produce commensorate changes in the magnitude of the RMSE.

Beyond those models already presented, there exists a wide variety of tools for modeling point data within a GIS. The following presentation is, however, limited to those models commonly applied to interpolating a continuous surface representation of elevation, and includes inverse distance weighting (IDW), splines, and kriging models. While it is recognized that other GIS or modeling programs may have different tools (and may therefore produce very different results) the purpose of this analysis is to compare the models available in a widely-available GIS program.

The use of any model is complicated by the variety of available options (i.e. for sampling weights, search distances, mathematical 'fit' functions) that necessitate some operator knowledge of spatial statistics and the distribution of the phenomenon under study. Each of the tools was used to create a 10-m resolution grid starting with recommended default parameters and this grid was subtracted from the reference surface to calculate apparent scour, fill, and net volumetric change. Default options were then modified within reasonable limits, and each 'modified' 10-m surface was also compared to the reference surface, a process that continued either until no further reduction in apparent scour or fill volumes was observed or until the net volumetric difference became increasingly large. The best results for each model (from a total of 30 trials) are presented in Table 3.2.

The widely varying range of results reflects the appropriateness of the individual interpolators for modeling topographic data. Inverse distance weighting determines cell elevations using a weighted combination of sample points, where weight is a function of distance. As such, it is a local method of interpolation, where it is assumed that the value at unmeasured locations is similar to nearby measured values (Burroughs and McDonnell, 1998). Since the interpolated value for any cell is an average of surrounding values, the method is not able to preserve local maxima or minima, hence can not reproduce ridges and valleys unless these features have been sampled (ESRI, 1992). While the technique may reasonably model densely sampled surfaces, it clearly is not appropriate for complex river topography that is irregulary sampled. Splines are also a local interpolator, but attempt to fit a continuous surface that passes exactly through known data points

while minimizing surface curvature. While this approach results in the relatively small net change observed, smoothing between data points produces unreliable results in general.

Since an underlying trend is the bed surface was previously identified (see Figure 3-4), universal kriging was tested using a linear drift, where drift is defined as a systematic change in elevation over a particular direction (ESRI, 1992). Kriging is a geostatistical interpolator which recognizes that the spatial variation of a continuous attribute may be too irregular to be modeled with a smoth mathematical function and alternatively may be better described by a stochastic surface (Burroughs and McDonnell, 1998). While the technique has been commonly used to create digital elevation models, abrupt local changes in elevation can create discontinuities in surface reproduction that vary with the size of the interpolation neighborhood (Meyer, 2004). In general, the technique is not appropriate for modeling complex river topography because anomalous maxima and minima produce a high degree of variability, which the technique tries to reproduce, resulting in high values of apparent scour and fill. Although these effects could be reduced by stratifying the data into more homogenous regions (ESRI, 1992), this was not done.

Table 3-2. Comparison of different interpolation schemes using thinned dataset with reference dataset

Method	Apparent Erosion (m^3)	Apparent Deposition (m^3)	Net change (m^3)	RMSE
TIN	2,057,405	1,651,979	-405,426	0.444
Topogrid - A	1,508,029	1,438,153	-69,876	0.901
Topogrid - B	3,425,290	3,977,451	+552,161	1.085
IDW	4,844,037	8,991,107	+4,147,070	2.030
Spline	8,245,762	7,986,886	-258,876	2.120
Kriging	24,773,392	22,548,868	-2,224,523	3.522

By comparison, the TIN and Topogrid models produce a much more realistic surface from the thinned data. In particular, these results demonstrate that the Topogrid model [A] replicates the reference surface much more accurately than any of the other available tools. Bishop and McBratney (2002) reached a similar conclusion based on a comparison of elevations modeled using the Topogrid tool with interpolation techniques available in different statistical programs. The 'best' Topogrid results in Table 3.2 incorporate the simulated contours along the bank top and bottom and include a 10 cm vertical error term (equivalent to the reported accuracy of the sounding data). The model was also run without the simulated contours [B] to demonstrate their impacts on

model accuracy. These results show that cut and fill volume errors more than double, and the net volumetric difference increases by a factor of 8. Although the net volumetric difference is small relative to that produced by other interpolation schemes, the individual cut and fill volumes appear large. However, much of the difference occurs in locations where the thinning process resulted in large data gaps – the thinned data are actually less spatially dense than the full bathymetric surveys at several locations. Adding additional contours by hand along the bed would likely reduce the magnitude of cut and fill volumes, but not necessarily the net difference. A visual comparison of the 'thinned' model with the reference model is given in Figure 3-7 and shows that the interpolation appears reasonable given the significant reduction in data. The most obvious modeling discrepancies appear along the channel bed, where the continuity of depth contours is sometimes interupted between sounding lines, and along the transition from the wetted low-flow channel to shallow bars where the modeled surface appears slightly wavy. These differences are more clearly illustrated in a histogram (Figure 3-8). This plot shows a bimodal distribution of elevations, corresponding to the channel bed and bar and island deposits. The jagged interpolation along shallow bar edges is seen in the 0 and 1-metre elevation bins.

In order to test whether the thinned and reference grids are statistically similar, the calculated histograms were subjected to the Kolmogorov-Smirnov goodness-of-fit test for continuous data (Zar, 1984). The K-S test is a non-parametric (distribution-free) method for comparing two independent datasets measured at the ordinal or higher scales of measurement and there are no limitations of the size of the sample or frequencies in categories (Norcliffe, 1982). The test statistic, D, measures the maximum absolute difference between cumulative frequency distributions. The null hypothesis states that the two samples are drawn from populations with the same distribution. Critical values for the K-S test were determined from tables in Zar (1984, after Smirnov, 1939) for large n, as:

$$D(\alpha, n) \cong \sqrt{\frac{-\ln(\alpha/2)}{2n}} - \frac{0.16693}{n}$$

The calculated test statistic, 0.0183, is nearly equivalent to the critical value at $a = 0.05$ (0.0185) but at $a = 0.01$, the critical value increases to 0.0222, so it can be concluded that the two populations are statistically similar.

The net volume difference between scour and fill (70,000 m^3) represents net interpolation error and can be used as a measure of the accuracy in sediment budget calculations provided survey density is similar (Chapter 5). The net difference from the reference surface could actually be

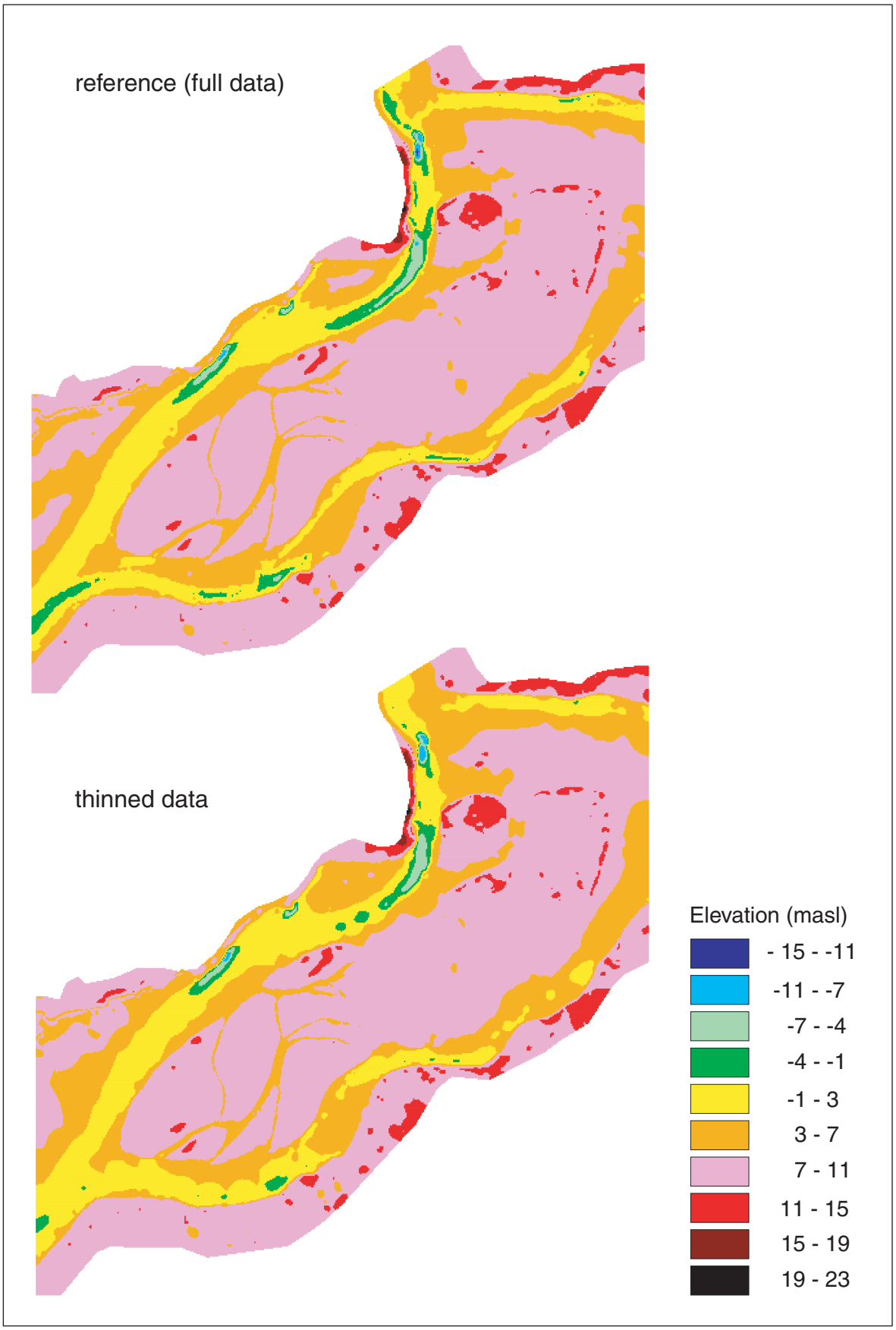

Figure 3-7. Comparison of the reference grid with the modeled grid (Topogrid A) using the thinned dataset.

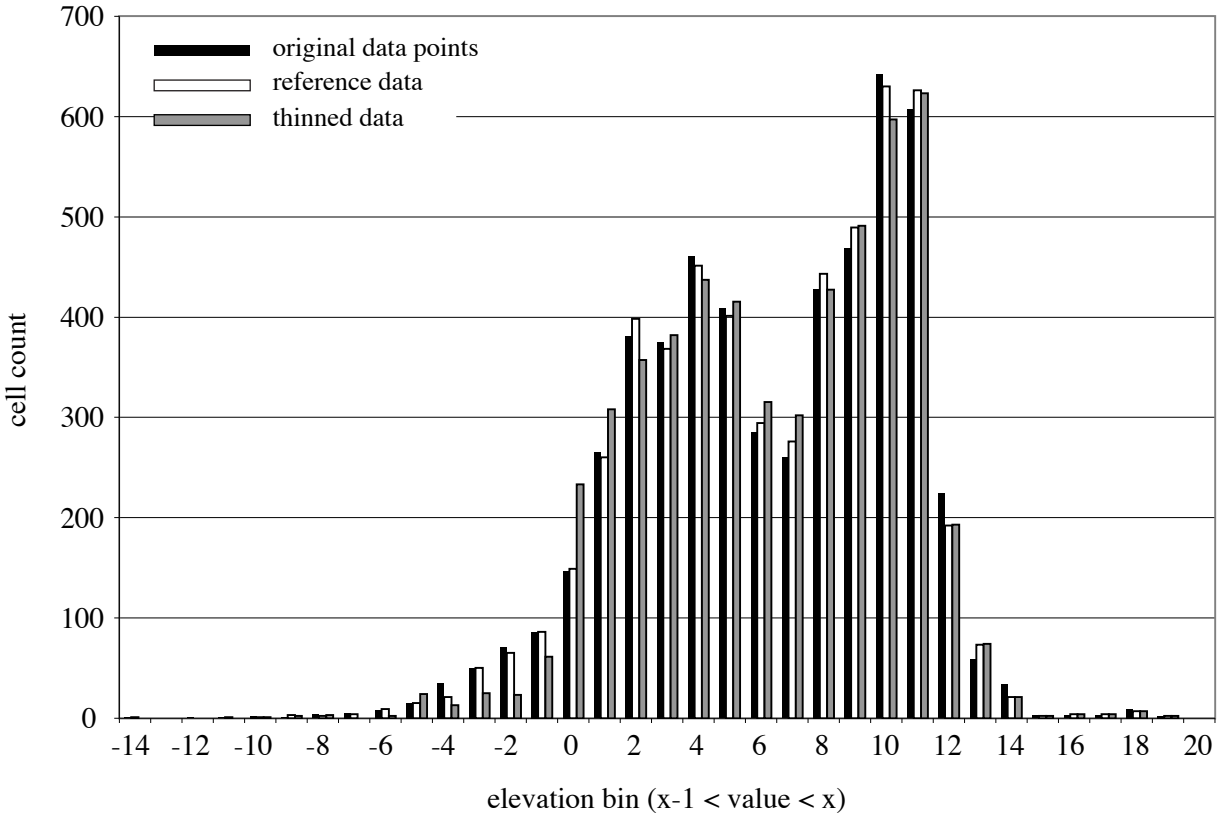

Figure 3-8. Histograms of 1991 elevation data including distributions for the original 5352 points, the reference dataset and the thinned dataset. The reference and test point datasets are extracted from the respective interpolated grid surfaces.

further reduced by increasing the number of model iterations or by decreasing the horizontal error term but, in either case, the magnitude of the individual scour and fill volumes increases. Since these volumes generally lie between sounding lines, and sounding lines are not coincident between surveys, minimizing error in this region is critical to improving the overall accuracy of the sediment budget. This error will be reflected as inflated estimates of the actual volume of scour and fill between consecutive surveys.

Given the apparent success of the Topogrid model with simulated bankline contours for representing the bed and banks of the river, this method is adopted and applied to the individual channel surveys. Comparison of modeled surfaces is used in Chapter 5 to calculate distributed volumes of channel erosion and deposition, hence net storage changes within the context of a reach-scale sediment budget.

Chapter 4: Channel changes

4.1 Introduction

In this chapter, adjustments to channel size, shape and position over the past century on lower Fraser River are investigated. A complete description of channel form must include planform geometry, channel gradient, cross-sectional shape and bed topography. By measuring these characteristics from available planimetric and topographic surveys for different dates, observed spatial and temporal changes can be related to changes in the flow and sediment regimes (the dominant governing factors) and to secondary anthropogenic influences. The magnitude of channel adjustments may provide an indication of the sensitivity of the river to environmental changes that have occured over the past century, and may therefore be used to predict future impacts on the development of channel morphology and complexity.

Lateral migration is a natural, persistent process along alluvial channels that occurs in response to sediment exchange along the system. Channels may widen during periods of persistently above-average flood flows through bank erosion, vegetation removal (stripping) on depositional surfaces, or activation of secondary channels. However, the increase in sediment influx generally associated with higher flows, combined with inputs from bank erosion, will correspondingly cause aggradation on the channel bed and higher water levels if this material is not removed. Consequently, widening may be associated with a change in the shape of the wetted cross-section. In comparison, channel narrowing occurs during periods of persistently below-average flood flows from the establishment and maturation of vegetation on elevated bar deposits, but also because of bar and bank deposition. It is apt to be associated with comparatively modest exchanges of bed material or re-shaping of the cross-section.

Channel width along wandering channels is typically variable over time and irregular along the channel length in response to variations in peak discharge, sediment influx and bank composition. Wide reaches are associated with laterally unstable ‘sedimentation zones’ whilst narrow reaches are associated with quasi-stable ‘transport’ zones (cf. Church and Jones, 1982). Although sedimentation zones are known to migrate over time, narrow reaches of channel may persist where the channel is bounded by erosion resistent materials. While lateral bank shifting and channel width are obviously related, these processes are examined separately since channel width will remain stable if bank erosion and deposition rates match, regardless of magnitude.

4.2 Active channel width

Active channel width is defined as the average width of the water surface and exposed bars between established edges of perennial, terrestrial vegetation. It is calculated in the GIS by summing the total area of digitized water and gravel bar polygons, then dividing by channel thalweg length (measured for each date of mapping to account for thalweg migration). Active channel width represents that part of the channel which experiences active exchange of mobile sediments. Changes in width are related to long-term rates of sediment exchange where width generally increases in response to a greater sediment load (Schumm, 1977, Lyons and Beschta, 1983; Kellerhals and Church, 1989), although the relation is poorly understood (Warburton, 1996). Conversely, narrowing may be indicative of decreased sediment supply, although other factors must be considered (Friedman et al., 1996). Since the active width of the channel further represents the area of potential habitat substrate for fishes and aquatic insects, observed changes in width over time can provide a useful, albeit broad, indicator of changes to potential ecosystem productivity. Historic trends in active channel width between Laidlaw and Mission are shown in Figure 4-1.

Trends in active channel width broadly parallel those of flows, but exhibit less variability. This is partly attributed to inertia in the system since peak flows can be highly disparate from year to year, but changes in channel width occur more gradually on large rivers. For example, many years of below average peak flows are neccessary to allow vegetation to establish and become sufficently dense to be classified as island or floodplain surfaces (i.e. there is a delayed response). Conversely, increases in width can occur more rapidly if channel alignment is conducive to extensive erosion of island or floodplain deposits (so the two trends do not neccessarily balance). This pattern is also influenced by the timing and dates of the photo mapping. The area classified as vegetated may be underestimated during leaf-free periods, while the analysis of only eight mapping dates masks any variability in width trends that might occur over periods shorter than an individual mapping interval, and further, does not always correspond with timing of dates associated with major trends in the flow. Nevertheless, the figure reveals two significant patterns in the long-term development of the river. Overall, the active channel zone has narrowed 22% from 1912 to 1999 betwen Mission and Hope even though flood flows have declined only 5% over the same timeframe (Section 2.2). Since width is generally proportional to the square root of discharge for a wide range of channels (Knighton, 1998), the expected decrease in width can be estimated as $(0.95)^{0.5}$, which is only about 3%. While this relation is approximate only (being subject to variations in boundary conditions, the magnitude of sediment transport and the dominant channel-

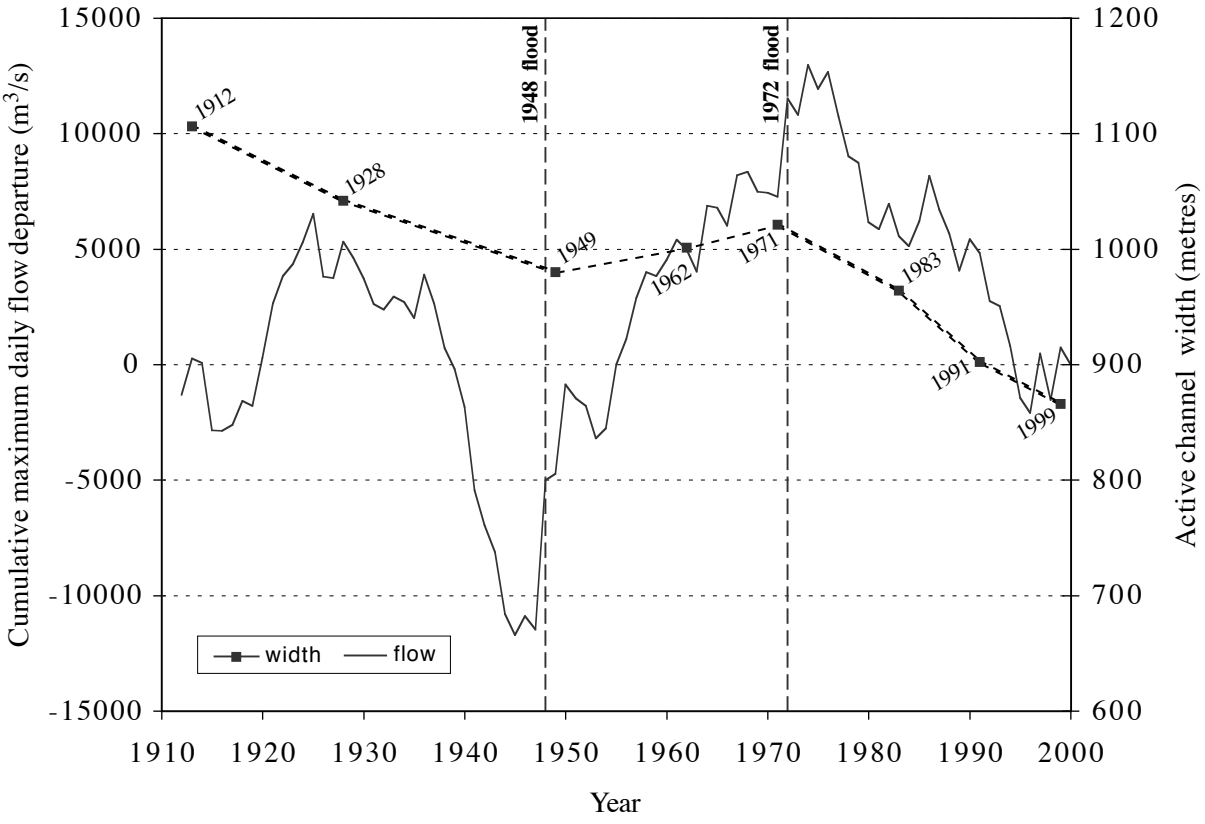

Figure 4-1. Variation of active channel zone width for the entire gravel reach over time shown with long-term trends in annual maximum daily discharge. Major recent floods (1948, 1972) are indicated. The flow trend is calculated as the cumulative departure from the mean annual flood.

forming discharge) the relation does indicate a major loss of potential aquatic habitat. Further, the volume of water through the reach must be flowing at greater depth and / or velocity to compensate for the reduced capacity to maintain conveyance. As well, the rate of channel narrowing (i.e. 1912-1949; 1971-1999) is obviously greater than the rate of channel widening (1949-1971) implying a response to additional forcing unrelated to discharge.

Variations in width changes along the gravel reach were examined by first partitioning the river into 13 individual sub-reaches (Figure 4-2). The sub-reaches delineate the major, wide sedimentation zones which are separated by narrower, stable transport zones. Additional reach breaks were added at channel constrictions (i.e. bedrock outcrops) in an attempt to delineate the river into roughly equal lengths. Changes in width for individual reaches (Figure 4-3) generally follow the trends observed over the entire channel, except that confined reaches (i.e. 1, 2, 13) have changed little over the period of record. These reaches are characterized by modest sand and gravel storage (largely transport zones), no channel islands, and are bounded by erosion resistant terraces. In contrast, alluvial sections of channel have experienced a slightly greater (24%) decrease in average active channel width compared to the entire channel, but there is considerable variability. Channel width actually increased 11% overall since 1912 in reach 5 (adjacent to Chilliwack Mountain) because of the gradual erosion of mid-channel [Yaalstrick] islands, though more recent narrowing is consistent with flow trends. Apart from the rather extraordinary loss of 1.25 km of mean width (54%) in reach 6 from 1912 to 1999, the greatest decrease in width since 1928 (the earliest verifiable mapping) is found along reach 7, where the channel narrowed by 560 m, or 39% by 1999. In fact, significant narrowing has occurred along the entire channel from Chilliwack Mountain to Herrling Island, corresponding to an average decline of roughly one-quarter the active channel zone since 1912, and 19% since 1928.

The observation that increases and decreases in width over time are reasonably uniform amongst the reaches qualitatively suggests that a single process is responsible (cf. Lyons and Beschta, 1983). Significant changes in patterns of sedimentation, for example, would result in greater discontinuity in width trends along a wandering river, since aggradation (or degradation) tends to occur in distinct zones rather than being evenly distributed (sedimentation patterns are discussed in Chapter 5). Further, the mapped area of the water surface for 1949 and 1999 (when flows are similar) is nearly identical, a circumstance that would not occur if width changes were mainly influenced by sedimentation. Instead, most of the loss is directly attributed to the isolation of major sidechannels around island and floodplain deposits through a combination of riprap, flood

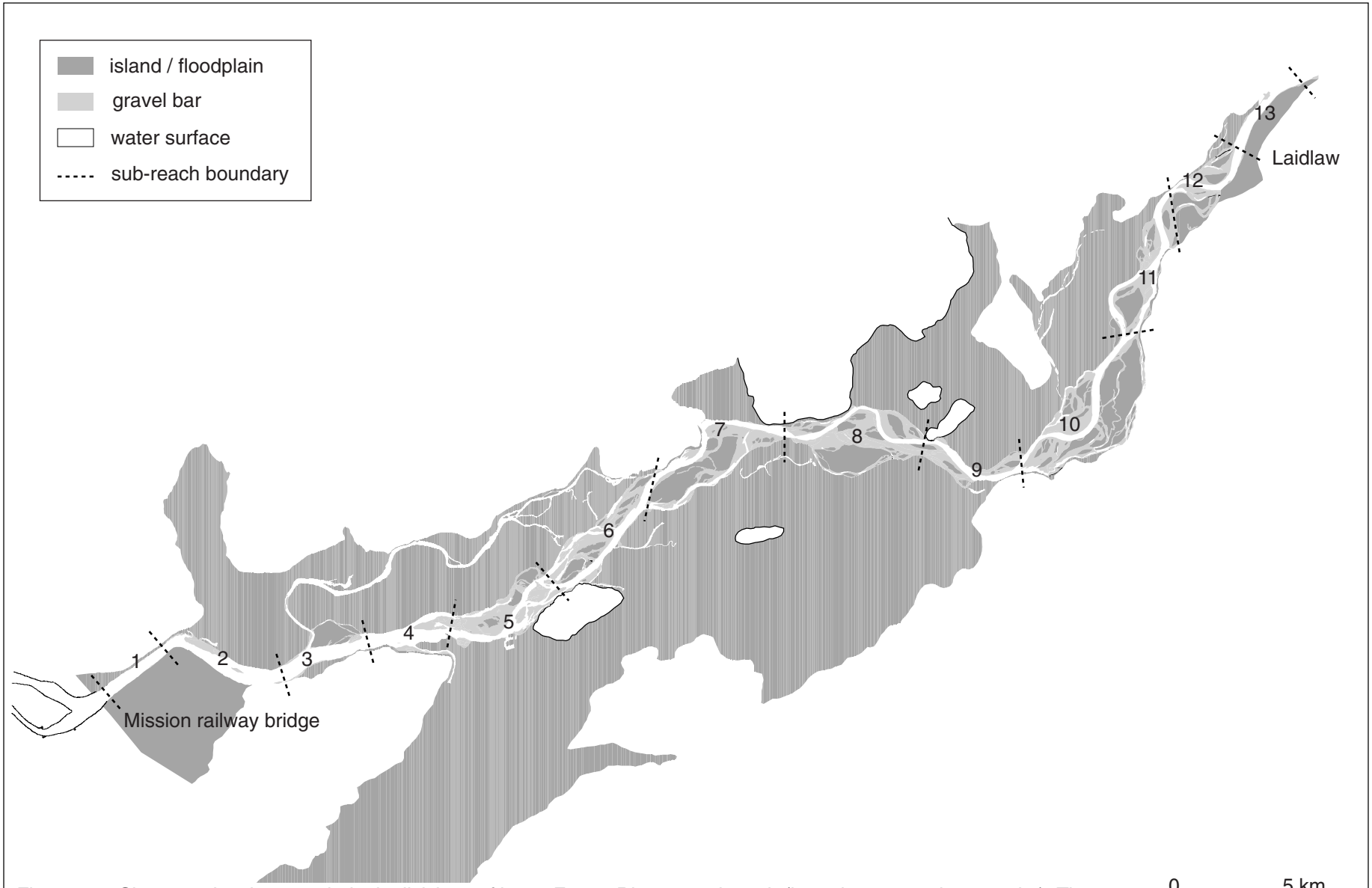

Figure 4-2. Site map showing morphologic divisions of lower Fraser River gravel reach (based on 1999 photography). The river is divided into 13 sub-reaches which correspond to major deposition zones and narrower, stable transport zones.

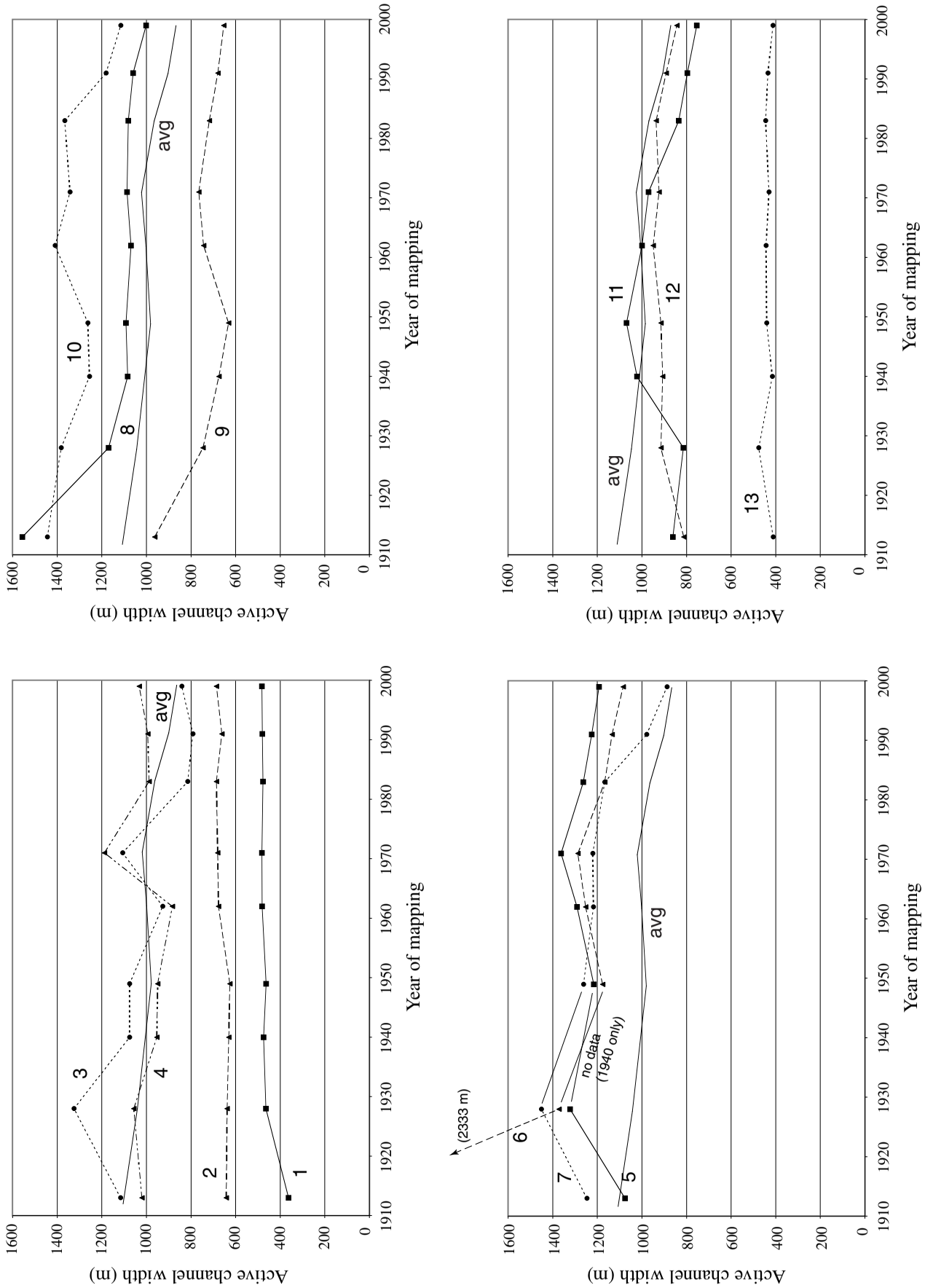

Figure 4-3. Changes in active channel width over time for individual study reaches. Average width (reach mean) is given for comparison.

gate construction, dyking and, eventually, siltation and vegetation growth. These activities are further responsible for the discrepancy between flow changes and width changes over time.

4.2.1 Island evolution

Most of the bank hardening along lower Fraser River has been limited to outer channel banks. In comparison, channel islands remain largely unprotected with the main exception being populated Peters Island. Major adjustments in channel width, therefore, should largely occur as a result of growth or destruction of islands. Changes in island area over time are shown in Figure 4-4. The complete gravel reach including all alluvial reaches shows a dramatic decline in the total area of forested islands during the period 1912 to 1928, with a continued, though reduced decline to 1949 (note that 'missing' 1940 photos do not allow total island area to be computed for that date). This pattern runs counter to the observed decrease in active channel width during a period of mainly below average flood flows. This circumstance could occur if the rate of natural floodplain reconstruction was greater than the loss of island area through erosion, but this explanation seems improbable from a morphologic perspective. In fact, many islands identified on the 1912 map became increasingly isolated from the active channel zone by 1949 because of dyking, flood gate construction and subsequent infilling (siltation), hence re-classification of the islands to floodplain. In effect, artifically high rates of new floodplain generation were created. This process effectively increased the total area of off-channel floodplain, while the dominant cause of channel narrowing was the corresponding loss of side and backchannels around and through the islands.

Island area continued to decline to 1971 (and probably to the late 1970s; see Figure 4.1) but has since increased, consistent with both long-term flow trends and declining active channel width. By 1999, the total surface area of the islands had actually recovered to the 1928 total area, and was greater than during any other year since the 1948 flood, after which the dyking program was expanded. This recovery is particularly noteworthy given that woody debris accumulations — a major nucleus for island formation (Hickin, 1984; Abbe and Montgomery, 1996) — have been mostly eliminated since the debris trap was established in 1979 (see Chapter 2). However, this statement must also be tempered by the possibility that woody debris has never played an important role in island formation on the river. That overall (total area) changes are minor reflects the fact that changes on the river occur slowly, with major sites of erosion and deposition persisting for years to decades because the magnitude of bed material transport is modest relative to the magnitude stored within the channel.

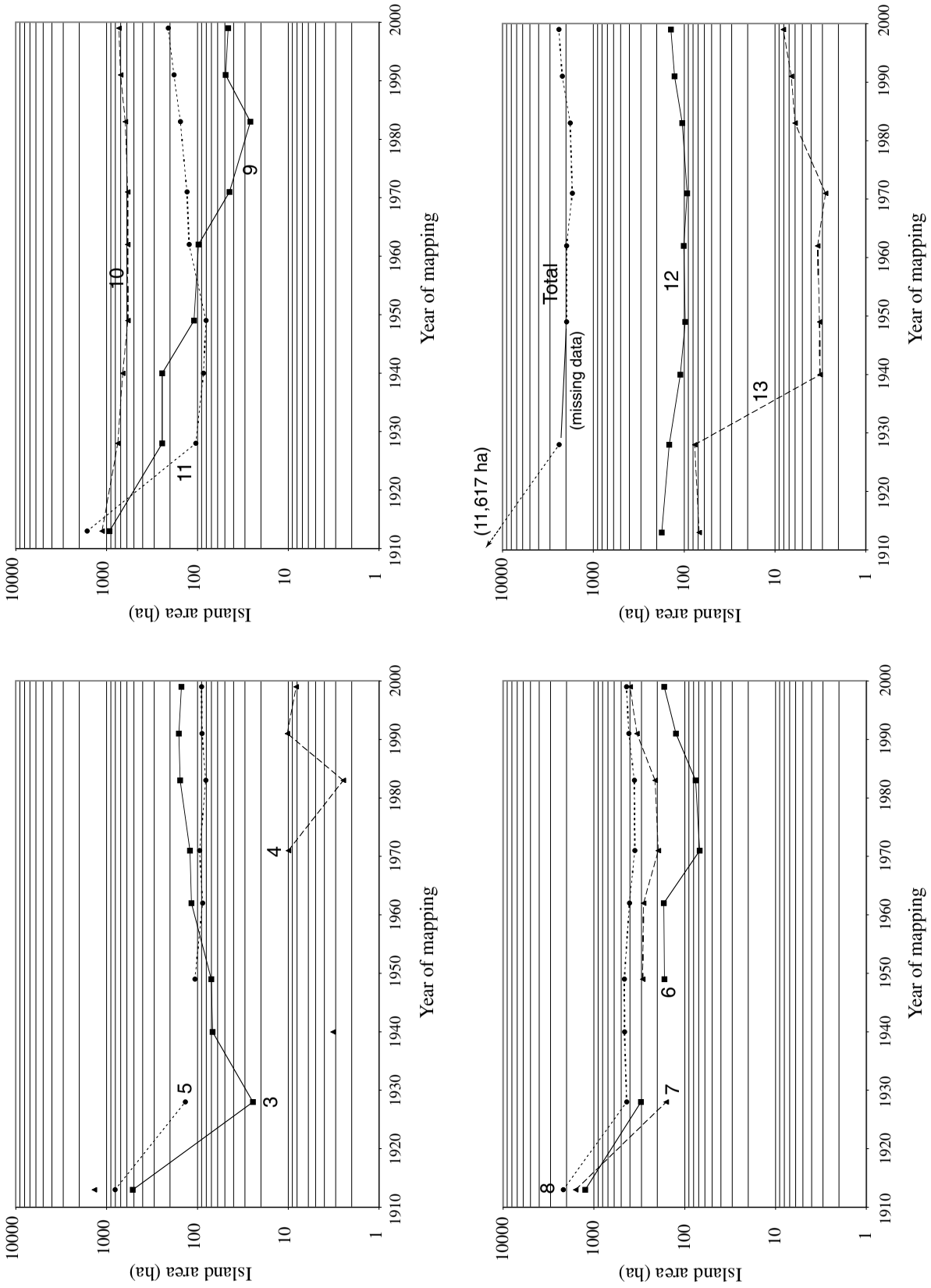

Figure 4-4. Areal changes in island area over time for the sub-reaches. The total area of islands on each date of mapping is given in the last panel. Note logarithmic ordinate.

Although most individual reaches share a markedly similar pattern of island development with the complete channel, others reveal somewhat more dynamic change. Within a reach, the loss of island/floodplain deposits can occur during a single freshet, but re-establishment takes many years so a direct correlation with long-term flood flows is complicated by temporal discontinuities in mapping resolution. The pattern can be particularly erratic where total island area is modest (cf. reach 4) because avulsions or individual floods can influence a high proportion of the surface area (including complete removal of all islands). Reach 3 shows a continuous increase in vegetated area since 1928, though the total area is similarly small and confined to a single island (Strawberry) where mostly sands and fine to medium gravels are deposited. The main exception is found in reach 9, which was characterized by dramatic loss before 1983 as changes in channel alignment related to bar growth caused persistent erosion of large islands up- and downstream of Agassiz-Rosedale Bridge. There are signs of recovery since as new islands have established and grown.

4.2.2 Bank erosion and deposition

Bank erosion and deposition are ubiquitous characteristics of alluvial channels, and can occur even along rivers which exhibit stable equilibrium form (Schumm, 1977). These processes are intimately linked with sediment exchange, with floodplain deposits acting as both a sink for material entrained upstream, and a potential source of erodible material (Meade, 1985; Kelsey et al., 1987). Floodplain surfaces are distinguished from gravel bars in that they are higher in relative elevation and usually well-vegetated, so that sand and silt sized materials (overbank sediments) become included in the process of sediment exchange.

Although the rate of bank erosion depends upon the complex interaction of many variables (Hooke, 1980; Hickin and Nanson, 1986), most bank erosion results from high shear stresses, particularly along the outer apex of bends, that directly entrain material and undercut the banks causing gravitational slumping. The magnitude of bank erosion should therefore be related to the magnitude of flood flows, hence erosional (and depositional) rates should broadly conform to long-term trends in flood flows, though individual large floods may skew averaged short-term rates (Hooke, 1980). Bank erosion was calculated in the GIS by overlaying successive maps and summing the total area of island and floodplain polygons on the early date converted to water on the later date (the reverse situation was used to calculate deposition). These definitions are unaffected by stage since vegetated surfaces are exposed at all flows below bankfull discharge. Normalized bank changes for the gravel reach are given in Figure 4-5. Lateral bank deposition rates exceed erosion rates from 1928[1] to 1949 and since 1983, consistent with channel narrowing during

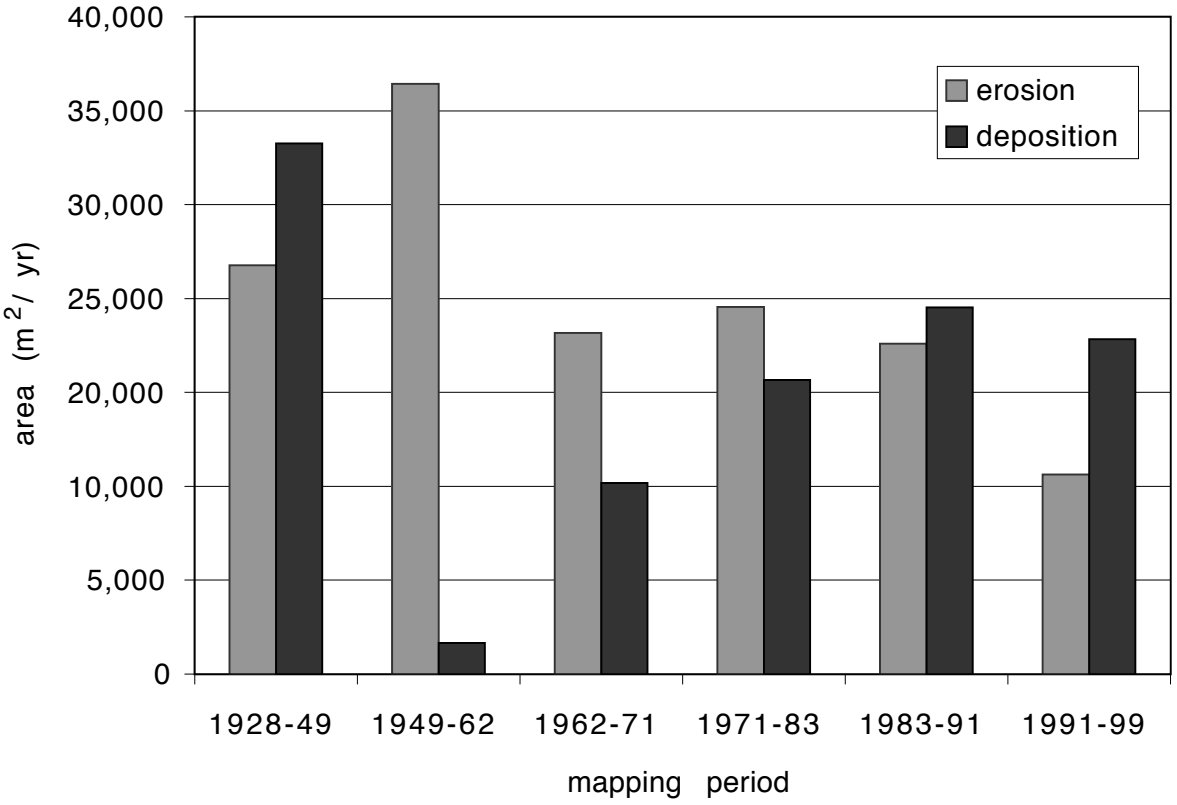

Figure 4-5. Average annual bank erosion and deposition rates for different mapping periods. A rate of 200,000 m^2 per year is equivalent to 1.4 m per year (for each bank) averaged over the 72.5 km length of the gravel reach, but this rate effectively increases to 4.7 m per year if averaged over the total length of unprotected bank (see Figure 2-5).

these periods of mostly below-average floods. The 1928-1949 depositional bias would actually be greater if the potential erosive impact of the large 1948 flood is discounted, but the mapping sequence is not sufficient to isolate its effect on channel morphologic change. Conversely, bank erosion rates were much larger than deposition rates from 1949 to 1971 when channel width increased and flood flows were mainly above-average. However, the modest increase in channel width from 1949 to 1962 is surprising given the rate of bank erosion was much greater than the rate of bank deposition (19:1). This circumstance occured because the major expansion and upgrading of the dyking program narrowed the active channel zone along floodplain margins, countering the effect of erosion along channel islands and unprotected banks. The period 1971 to 1983 also displays an anomalous pattern given that channel width decreased despite the erosional bias. This can be explained by vegetation growth on gravel bars. Although there was a very large flood in 1972, this was a period of predominantly smaller floods conducive to vegetation establishment and expansion.

Bank erosion and deposition rates along individual reaches can obviously be much larger or smaller than the averaged values presented above. The maximum recorded erosion rate was 8.8 metres per year in reach 8 (1949-1962) while maximum deposition averaged 15.2 metres per year in reach 4 from 1971 to 1983. Tables 4-1 and 4-2 summarize these data by reach for the period of mapping. Notwithstanding the complications involved in relating these changes to temporal flow trends, erosion and deposition rates are locally influenced by the amount of bank hardening (cf. inset table, Figure 2-5), the commercial removal of trees, and especially by local alignments in flow caused by bar migration and deposition. Consequently, a detailed examination of temporal trends is not provided.

For comparison with the trends described for the planform mapping, volumetric calculations of bank change were calculated from surfaces of difference modeled from the bathymetric data. Volumes are equivalent to multiplying areal changes by the mean of differences in elevation over the same mapping locations. These calculations reveal that the total volume of sediments lost to bank erosion from 1952 to 1999 was about 10% greater than the total volume deposited, although the total areal gain is actually larger (1.65:1 based on a direct overlay of 1949

1. Bank erosion and deposition rates from 1912 to 1928 are not given because uncertainty in the absolute map orientation for 1912 may inflate rates of actual temporal change. However, since the map was correctly scaled, relative accuracy is preserved, allowing parameters such as channel width and island area to be calculated and presented. Nevertheless, bank shifting appeared to be far more vigorous early in the century compared to the present, with several sites along the gravel reach experiencing apparent lateral erosion up to 500 metres, with a maximum of 1000 metres recorded near Seabird Island (refer to discussion in Appendix C).

Table 4-1. Average annual bank erosion rates. All values expressed in metres per year. Values that exceed the reach mean are shown in bold.

Reach	1928-49	1949-62	1962-71	1971-83	1983-91	1991-99	Average
1	**0.88**	**1.15**	0.11	0.35	0.32	0.57	0.64
2	**1.12**	**2.61**	0.51	0.64	0.36	0.89	1.12
3	**1.97**	1.54	**2.52**	1.57	**2.17**	**2.50**	1.97
4	3.10	1.97	**5.24**	**3.49**	**3.54**	2.71	3.24
5	**4.46**	**7.58**	4.00	3.00	2.85	1.71	4.23
6	**3.09**	2.20	1.93	1.74	**2.41**	1.48	2.29
7	3.50	**6.89**	3.24	**3.76**	1.97	0.76	3.65
8	3.59	**8.78**	4.72	4.76	4.69	3.70	5.02
9	0.95	**3.49**	**4.01**	**2.85**	1.54	0.66	2.16
10	4.68	**7.61**	2.50	**5.20**	**6.39**	2.21	4.94
11	**5.68**	1.94	1.35	2.21	0.70	0.46	2.71
12	2.09	**3.92**	1.74	2.09	1.46	0.90	2.17
13	0.25	**0.96**	0.00	**0.39**	**0.39**	0.00	0.36

Table 4-2. Average annual bank deposition rates. All values expressed in metres per year. Values that exceed the reach mean are shown in bold.

Reach	1928-49	1949-62	1962-71	1971-83	1983-91	1991-99	Average
1	**0.52**	0.01	**0.82**	0.13	**0.93**	**0.52**	0.44
2	**0.87**	0.06	0.32	0.14	**0.98**	**0.65**	0.52
3	**7.68**	0.56	0.36	**11.69**	3.05	1.94	4.96
4	**10.98**	0.16	1.09	**15.15**	1.09	0.72	6.18
5	**4.68**	0.16	0.46	**5.71**	2.34	2.31	2.96
6	**5.00**	0.29	2.40	1.04	**4.24**	**3.77**	2.91
7	**4.55**	0.46	**4.48**	0.32	**6.26**	**5.18**	3.34
8	**4.24**	0.30	0.97	0.64	**2.17**	**3.09**	2.13
9	**2.68**	0.07	2.01	0.48	0.95	1.03	1.36
10	**5.41**	0.33	2.19	0.42	**4.57**	**3.77**	2.95
11	**1.53**	0.11	0.61	0.02	**2.70**	**2.96**	1.19
12	**1.73**	0.30	0.26	0.12	0.83	**1.38**	0.84
13	**1.64**	0.00	0.27	0.09	**1.19**	**0.82**	0.76

and 1999 channel maps). This circumstance occurs since eroded areas include established (mature) deposits that are higher in absolute elevation (i.e. they are thicker sediment bodies) relative to sites of more recent deposition because of vertical aggradation of fines over time. The positive relation between overbank thickness and vegetation age along lower Fraser River has also been demonstrated by Boniface (1985) and McLean (1990). If overbank sediments are removed from the calculations, the deposited volume of gravel and coarse sand is roughly double the eroded volume, a bias that is much greater upstream of Agassiz-Rosedale bridge (3.2 X) than downstream (1.8 X). These results confirm the growth of channel islands over the past half-century, but the mature riparian forests on old islands are increasingly being replaced by young vegetation on new islands, a pattern qualitatively confirmed by visually comparing pre-1950's with recent aerial photography. The transition to lower elevation, immature islands implies a change in the topographic characteristics of the channel. This possibility is investigated by examing changes in the longitudinal profile, cross-sectional area, and distributed water depths over the available period of record.

4.3 Longitudinal profiles

The longitudinal profile of an alluvial channel represents one dimension of adjustment to the prevailing discharge and sediment regimes. The long profile is commonly represented as the elevation of the high water-surface at distances downstream. The water surface parallels the average bed surface at the reach scale, but also masks local variations in bed topography (Richards, 1982; Rice and Church, 2001). These local variations correspond to riffle and pool morphology in alluvial gravel channels. The shape of the bed profile changes over time in correspondence with patterns of bed material erosion and deposition, as the spatial distribution of riffles and pools changes. Persistent bed material aggradation or degradation will further influence the shape of the bed profiles by filling or scouring riffles and pools, and may alter the average slope of the longitudinal profile.

Longitudinal profiles of the channel bed were extracted from 1952, 1984, and 1999 modeled surfaces (see Chapter 3) along the respective channel thalwegs. Thalwegs were defined by digitizing the 'most probable' flow path along the bed between exposed bars and islands. Although well-defined within confined reaches, avulsions that produce isolated pools, the lack of a distinct dominant channel where the flow bifurcates and where flow migrates across shallow riffles neccessitates some qualitative judgements with respect to determining thalweg position.

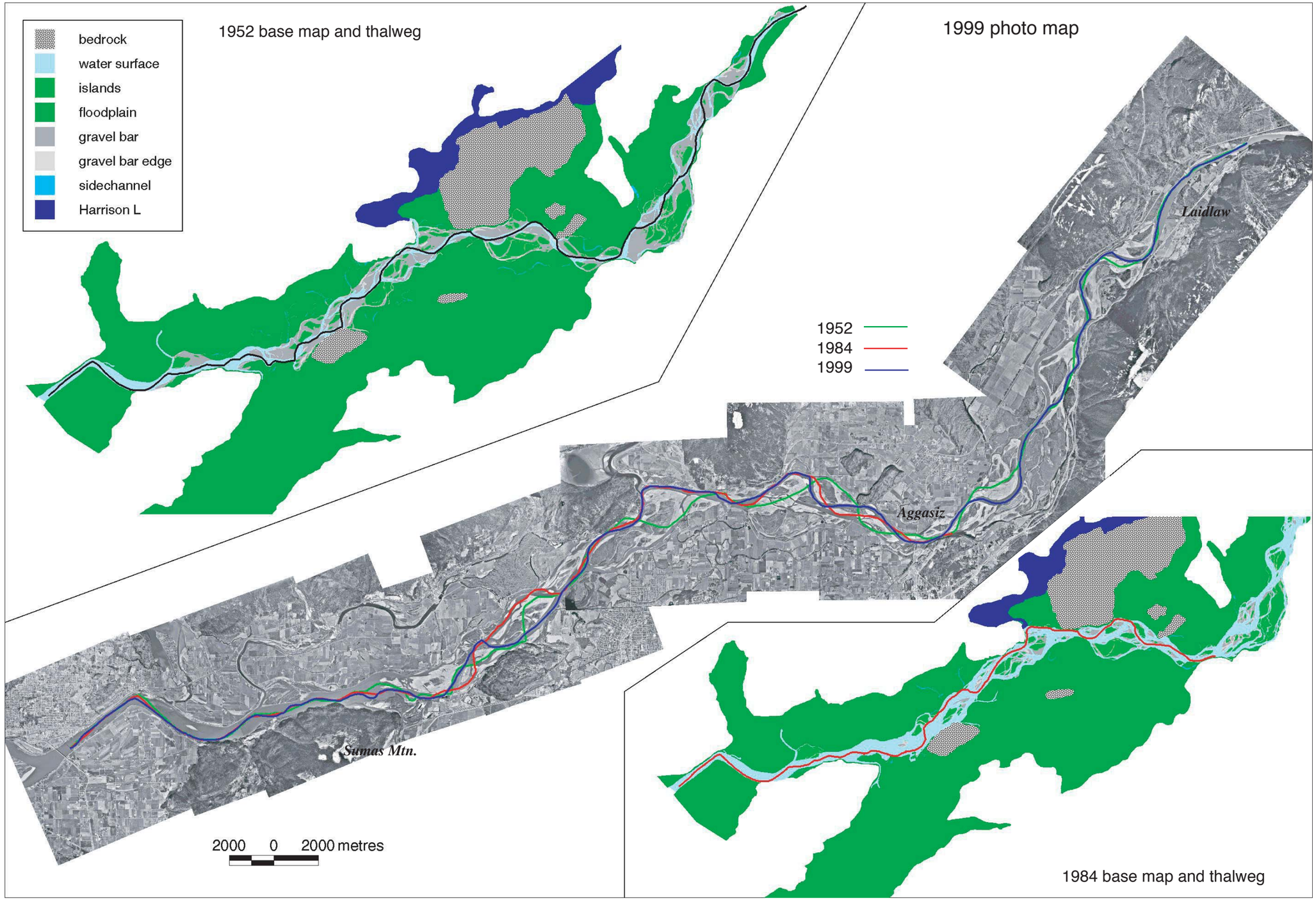

Figure 4-6. Thalweg profiles for 1952, 1984 and 1999 produced from bathymetric data.

However, this approach produces a smoother, more realistic flow path than one which simply connects the lowest-elevation points along successive sounding lines. The plotted profiles (see Figure 4-6) display the 'irregularly sinuous' pattern characteristic of wandering channels (cf. Church, 1983a). Both avulsions and lateral migration are evident between Sumas Mtn. and Laidlaw, where most of the bed material load is deposited. Beyond these limits, modest volumes of mobilisable sediment are stored, channel banks are comparatively stable, and the thalweg has remained remarkably fixed in position.

Bed profiles for each date were sampled in the GIS at regular 100 metre intervals from the interpolated grids between Mission Railway Bridge and the upstream extent of each surface model. However, as the extraction procedure automatically records additional points along the vertices that define each digitized thalweg profile, the average sampling interval decreases to roughly 50 metres. Although this strategy depends on the accuracy of the grid interpolation, it is computationally efficient, produces a much denser profile than could be directly obtained from the sounding points, and avoids sampling difficulties where sounding data are inadequate to represent channel curvature. The geographic coordinates and elevation of each sampled point were written to a spreadsheet to calculate the elevation at cumulative distances upstream. A plot of these data clearly shows a pattern of alternating riffles and pools, several of which exceed 30 metres depth at high discharge (Figure 4-7). The deepest pools are usually found near the outside boundary of sharp bends with erosion-resistant banks. Neill (1973) similarly observed natural deep scour holes at sharp bends on the wandering Athabasca River, Alberta. At such locations, major eddies form and descend, increasing shear stress along the bed (Richards, 1982) and can result in extreme localized bed scour (Mlynarcyzk and Rotnicki, 1989). A water surface profile collected at the time of the 1999 survey is shown for reference, and exhibits a distinct flattening near Sumas Mountain (about 16 km upstream) demarkating the transition zone where sand becomes the dominant bed material.

Although it is clear that several riffles and pools have remained remarkably stable over the period of study, much of the bed is unstable. Most unstable pools are found along the outside edge of sharp bends within sedimentation zones. Pool instability results from migration of the thalweg in response to the downstream staging of bed material stored within transient bars (cf. Church and Jones, 1982). This process fills existing pools and creates new ones through erosional processes that maintain flow conveyance. The stability of the complete pool-bar-riffle sequence, therefore, is related to the supply and mobility of sediments within the active channel zone. Bars develop on the

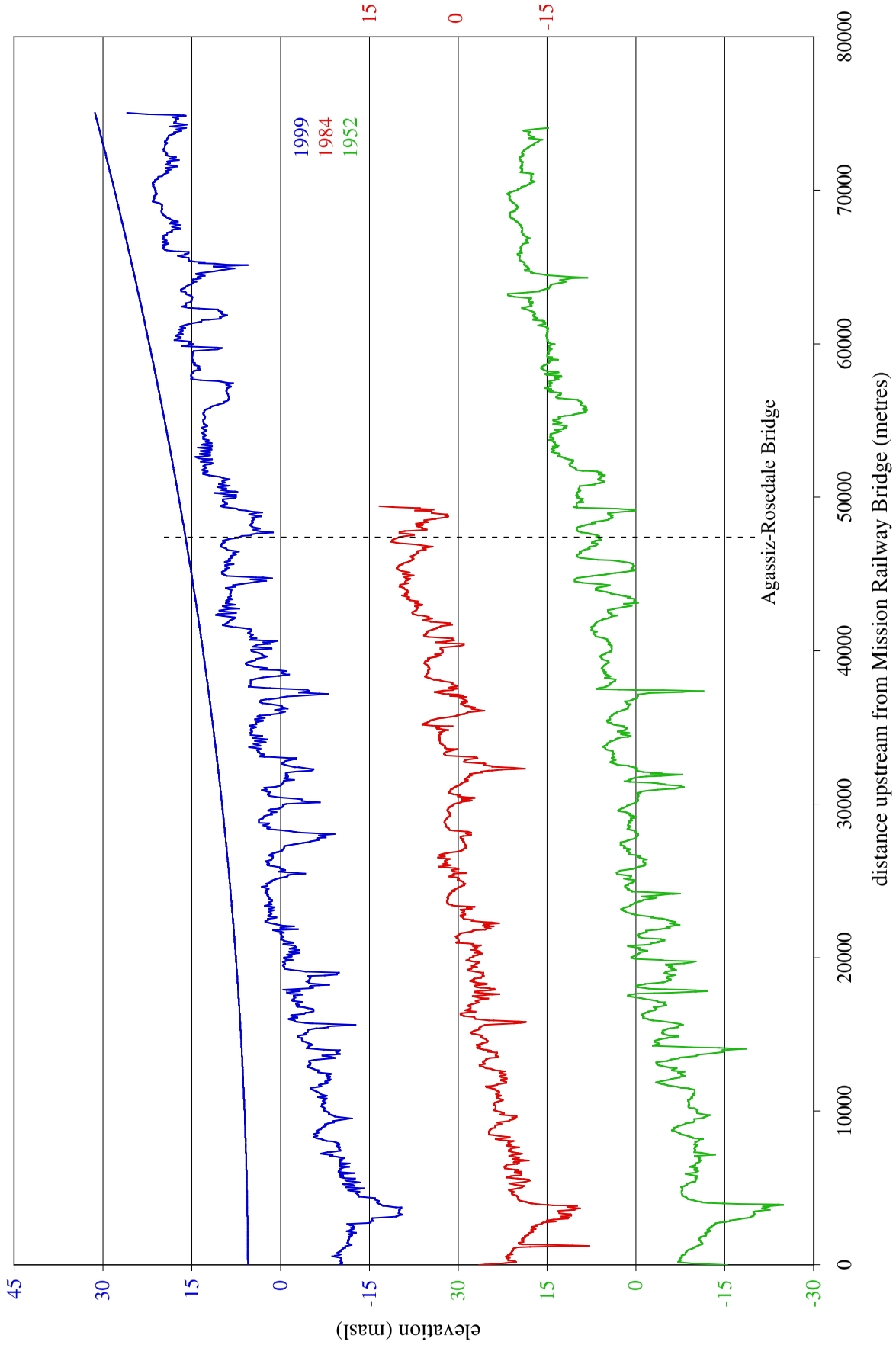

Figure 4-7. Longitudinal bed profiles of lower Fraser River as measured along the channel thalweg for different dates. The profiles clearly show a pattern of alternating pools and riffles. Differences in thalweg length may affect the relative position of features (horizontal distance) providing the illusion of modest up- or downstream movement.

upstream edge of stable riffles, producing an apparently stable morphology that may persist at the temporal scale for river regime stability (Church and Jones, 1982). On Fraser River, this scale corresponds to decades or more at the spatial scale of large bar/island complexes, although local (unit bar scale) changes are common during the annual freshet. Major avulsions can also occur within a freshet, although they are a culminating response to many years of morphologic 'preparation'.

A direct overlay of channel thalwegs (Figure 4-8) suggests an apparent decrease in the number of large pools, an increase in the elevation of several major riffles, and a decline in topographic variability (the range between minimum and maximum channel depths) between 1952 and 1999. Superficially, these characteristics imply that channel morphology has become simplified. However, this conclusion ignores the degree of variability along each profile between major riffles and pools, and that at unsampled flow bifurcations within the channel. Since each profile is a sample of bed topography, the total number of deep pools and riffles on each date remains unknown.

Riffles and pools have been found to exhibit regular downstream spacing in alluvial channels that scales with meander wavelength and channel width (Leopold and Wolman, 1957, Keller and Melhorn, 1978, Church and Jones, 1982). Autoregressive models of bed topography have confirmed cyclic patterns of bedform development (Richards, 1976; Church and Jones, 1982). The well known (and widely accepted) association is that pool spacing averages 5 to 7 channel widths in self-formed channels, although both width and spacing can be highly variable over short distances (Knighton, 1998). An objective and consistent definition of riffles and pools is prerequisite to quantitative description (Madej, 1999). That a wide variety of criteria have been presented to define pools (cf. Montgomery et al., 1995; Madej, 1999) illustrates that this task can be problematic, but two contrasting techniques appear useful. Richards (1976) presents a conceptually simply approach for accomplishing this task whereby a linear trend line is fitted to the bed profile so that riffles (elevations above the trend) become easily distinguished from pools (elevations below the trend). Lisle (1987a) presents an attractive method for defining pools independent of discharge based upon the concept of residual depth. Assuming zero discharge, a pool is defined as the area below a constant line of elevation extending upstream from each riffle crest to the next riffle and residual depth is the maximum depth of each defined pool.

Neither technique seems entirely appropriate along lower Fraser River. Defined 'pools' vary greatly in size, with some sufficiently small to seemingly ignore, while some larger pools

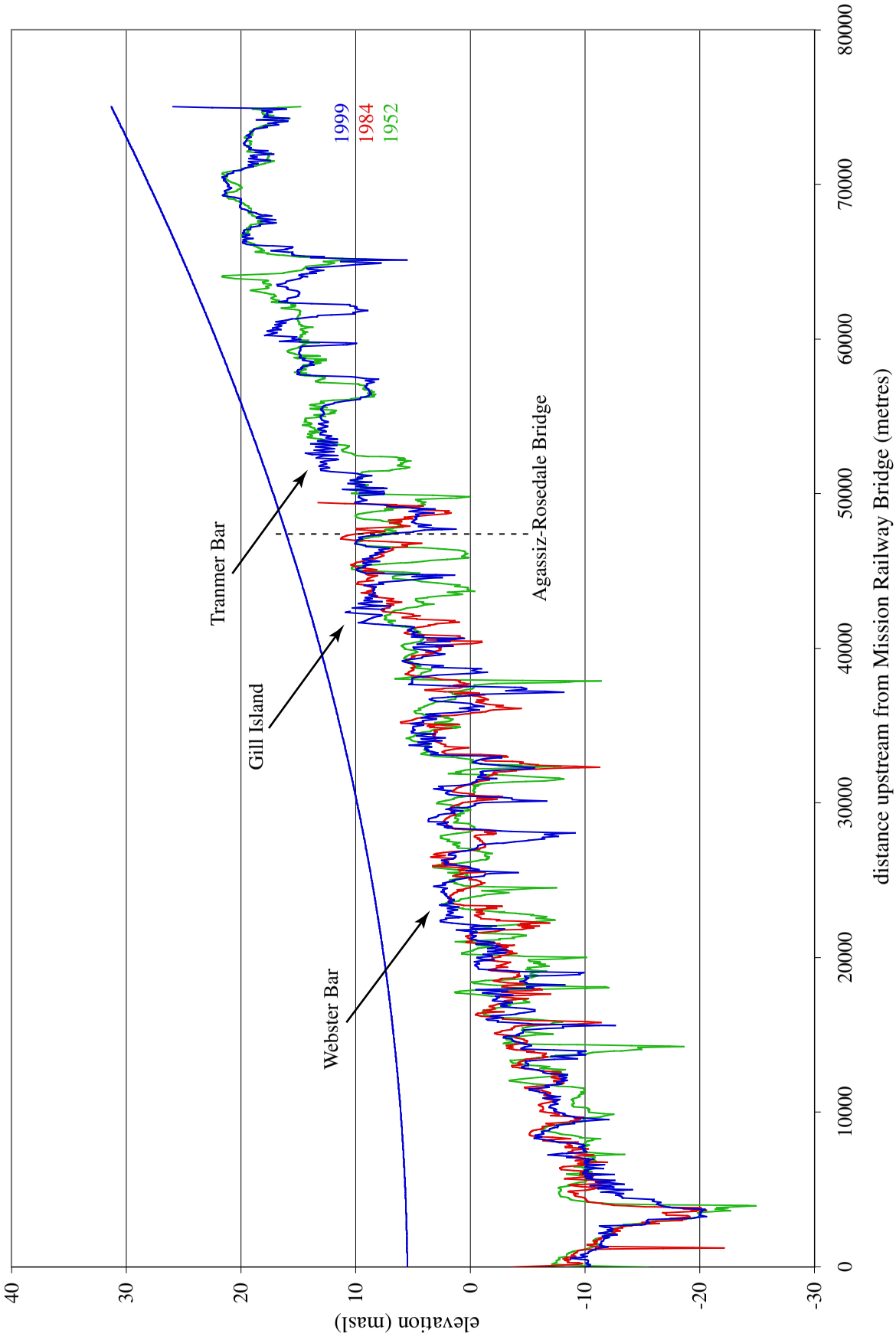

Figure 4-8. Plot of superimposed longitudinal profiles showing variability in the location of riffles and pools over time. The 1952 profile has been 'stretched' to be equivalent with the 1999 profile length to facilitate direct comparison. Note the apparent decrease in the size and frequency of very large pools since 1952. The arrows indicate several prominent riffles that have developed over the past 47 years (approximate locations are noted).

appear to consist of two or more 'sub-pools' having intermediate riffle crest elevations similar to, but less than the downstream riffle crest elevation. Further, it is clear that spatially dense surveys along the long profile will produce higher riffle and pool counts than a more generalized survey because very small riffles and pools are resolved. Therefore, each approach was modified using qualitative judgements to include only reasonable large, distinct pools. Results show that each technique produces a similar count, averaging 27 in both 1952 and 1999, and 20 in the shorter surveyed reach in 1984. Over the length of the gravel reach, pools are spaced every three channel widths for each date, about twice the frequency generally accepted for gravel bed rivers. However, if an equvalent single channel regime width (~ 525 m at Mission and Agassiz gauges) is applied, pool spacing converges towards modal values. Similar results are realized if riffle/pool spacing is normalized by the braid index (roughly 2.0 for lower Fraser River), taken as the average number of flow channels per unit length.

Linear regression lines drawn through the longitudinal profiles also reveal changes in the mean slope of the gravel reach. The slope decreased from 4.59 m / km in 1952 to 4.41 m / km in 1999, corresponding to an increase in thalweg length (by roughly 1 km), hence channel sinuosity (from 1.140 to 1.155). Increasing sinuosity has been associated with a reduced supply of mobile sediments (cf. Schumm, 1977) but such statements must be tempered unless corroborating evidence can be provided. Ham and Church (2002) compared the area beneath each profile (analagous to cross-section plots above a minimum base level) and found a decline in area upstream of Agassiz (signifying degradation) and a downstream increase (signifying aggradation) which is consistent with a lowering of the average profile. More robust investigation of these trends requires an examination of bed level changes that better represents the entire active channel zone. The following sections of this chapter (cross-section and hypsometric analysis) and the following chapter (distributed sediment budget) provide appropriate tools for this inquiry.

4.4 Cross-section morphology

In addition to adjusting channel geometry through changes in channel width, alluvial channels may adjust their depth and velocity to maintain flow conveyance. For any given flow, a reduction in active channel width will generally result in increased flow depth, since this parameter increases proportionately greater than velocity[2]. Along rivers with mobile beds, depth can increase

2. This can be demonstrated, for example, from the Manning and Chezy equations where depth varies with the 1.5th and 2nd power of velocity respectively. Furthermore, the dominant factors influencing flow velocity (flow resistance, bed slope and channel pattern) would remain fairly stable over years to decades on Fraser River.

through degradation of the bed, or by raising water levels for any given flow. As the lower Fraser River gravel reach is known to be aggrading, the latter circumstance must be occuring, although the bed may be degrading locally. Simulations of design flood profiles confirm this general pattern over the past several decades (UMA Engineering, 2001). Specific gauge analysis has also been used to demonstrate persistent bed level changes since gauges are typically sited where channel banks are stable (hence channel width remains fixed). Along wandering channels, however, such sites are typically associated with sediment transport zones, rather than zones of significant erosion or deposition, hence this avenue of study is unlikely to reveal meaningful interpretations.

Adjustments to the shape of the channel can be determined by comparing historic cross-section profiles of the river. These profiles were derived from the bathymetric and topographic surveys completed in 1952, 1984 and 1999. Conventional cross-section comparisons require survey lines that match between survey dates — in practice, this result is achieved by surveying the channel banks and bed between fixed endpoints. However, matching profile lines could not simply be derived from the available data because each survey encompasses a different spatial area of channel, the density of the elevations varies between the surveys, and the transverse survey lines are rarely coincident. To overcome this limitation imposed by the data, a GIS-based technique to derive cross-sections was developed to simulate fixed sections.

A triangulated irregular network (TIN) model of the bed and banks was constructed for each survey date using available bathymetric and altimetric elevations, photogrammetrically-derived elevations, hand-interpolated bed contours and mapped floodplain contours. The models are based on the Delaunay method, wherein each point is connected to its nearest two neighbours to form a series of continuous facets that represent a surface. The main advantages of the TIN versus regular gridded interpolations are that the data structure is based on irregularly spaced point, line and polygon data (ESRI, 1991) and actual elevation values are preserved in the output model (Burrough and McDonnell, 1998). A series of lines representing the location of each desired cross-section was then digitized at roughly 800 metres (four times the spacing of the 1999 survey) from the right-to-left channel banks (see Figure 4-9) to roughly correspond with active channel width. The endpoints of each transect were placed at stable regions beyond the outer extent of active channel margins (between 1949 and 1999) such that areas of intervening erosion or deposition would be captured.

Cross-section profiles were extracted from each TIN by interpolating elevation values at regular (20 metre) intervals along each cross-section. The elevation at each sampling distance is

Figure 4-9. Location of extracted (even-numbered) cross-sections at 800 metre average spacing. Sections that intersect an island in any of the survey periods (1952, 1984 or 1999) are shown as dashed lines. Some islands have eroded by 1999.

estimated from linear interpolation between survey points where the data are not coincident. Since the location of the transects was based on the 1999 tracklines (taking advantage of the regular spacing and spatial completeness of the survey) cross-section profiles extracted from the 1999 TIN more faithfully preserve actual bed elevations than those of the other years. A small subset of cross-sections profiles is plotted in Figure 4-10 to illustrate the magnitude of vertical and lateral instability that occurs along the river, especially within major sedimentation zones. The complete set of extracted profiles is given in Appendix A.

The profiles are each shown with a reference line that approximates the bankfull water-level surface. The region below each line, therefore, represents the active channel zone cross-section area, while the region above represents island or floodplain cross-section area. The reference line corresponds to the average elevation of young island surfaces along the channel. Although the vegetation trim line can be identified for each survey from airphoto mapping, the young island elevations are a convenient surrogate because the high water mark along outer channel banks is not always easily defined, especially along confined sections bounded by high terraces or bedrock (e.g. RB of XS 4, Figure 4-10). High bar surfaces recently stripped of vegetation, steep unvegetated banks, and natural variation in the age (hence elevation) of vegetated surfaces also introduces considerable variability in the elevation of the trim line across most cross-sections. This makes it difficult to establish a mean bankfull elevation for an individual section, to compare areas above and below the water surface between survey dates, and creates an unrealistic downstream elevation profile.

The reference elevations were derived from the laser-altimetry survey data collected in 1999. Channel maps produced from 1949, 1971 and 1999 low-water aerial photography were superimposed to identify three surface types: old bars (polygons mapped as gravel bars on all dates); mature islands (polygons mapped as island or floodplain on the all dates); and young islands (polygons mapped as bars in 1971 and island or floodplain in 1999). The overlay map was subsequently divided into 1-km computing cells and overlaid with the altimetry data such that elevations could be averaged for each surface type and plotted by distance along the channel (Figure 4-11). A best-fit polynomial line was computed for each surface class to smooth scatter or anomalies due to deposit age differences (some island surfaces are older than 50 years) or to insufficient data (some 1-km cells have no islands or bars). The difference in elevation between old bar and young island surfaces represents the thickness of recent overbank (fine sand and silt) deposition, whilst the difference in surface elevation between young and mature islands represents

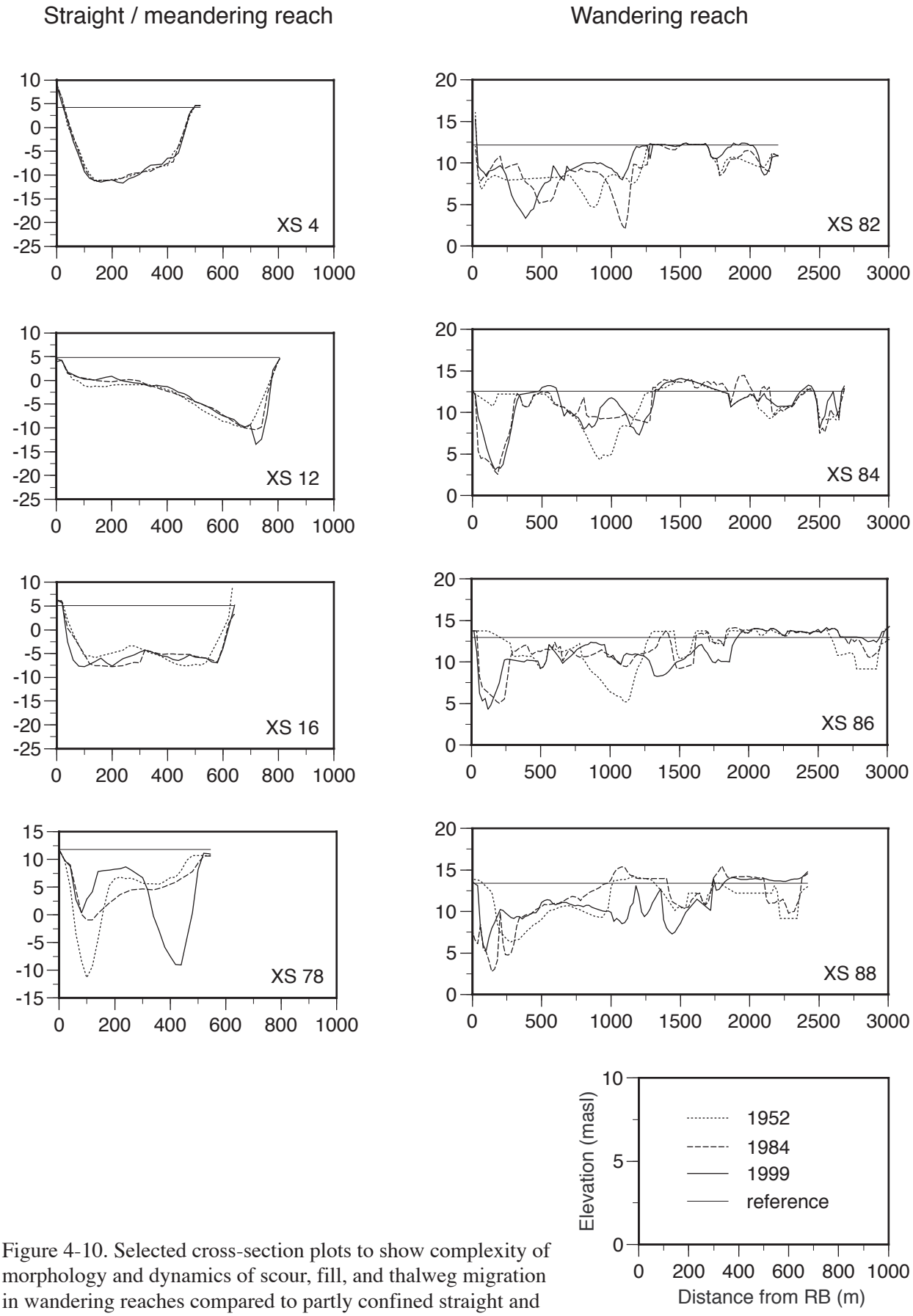

Figure 4-10. Selected cross-section plots to show complexity of morphology and dynamics of scour, fill, and thalweg migration in wandering reaches compared to partly confined straight and meandering reaches.

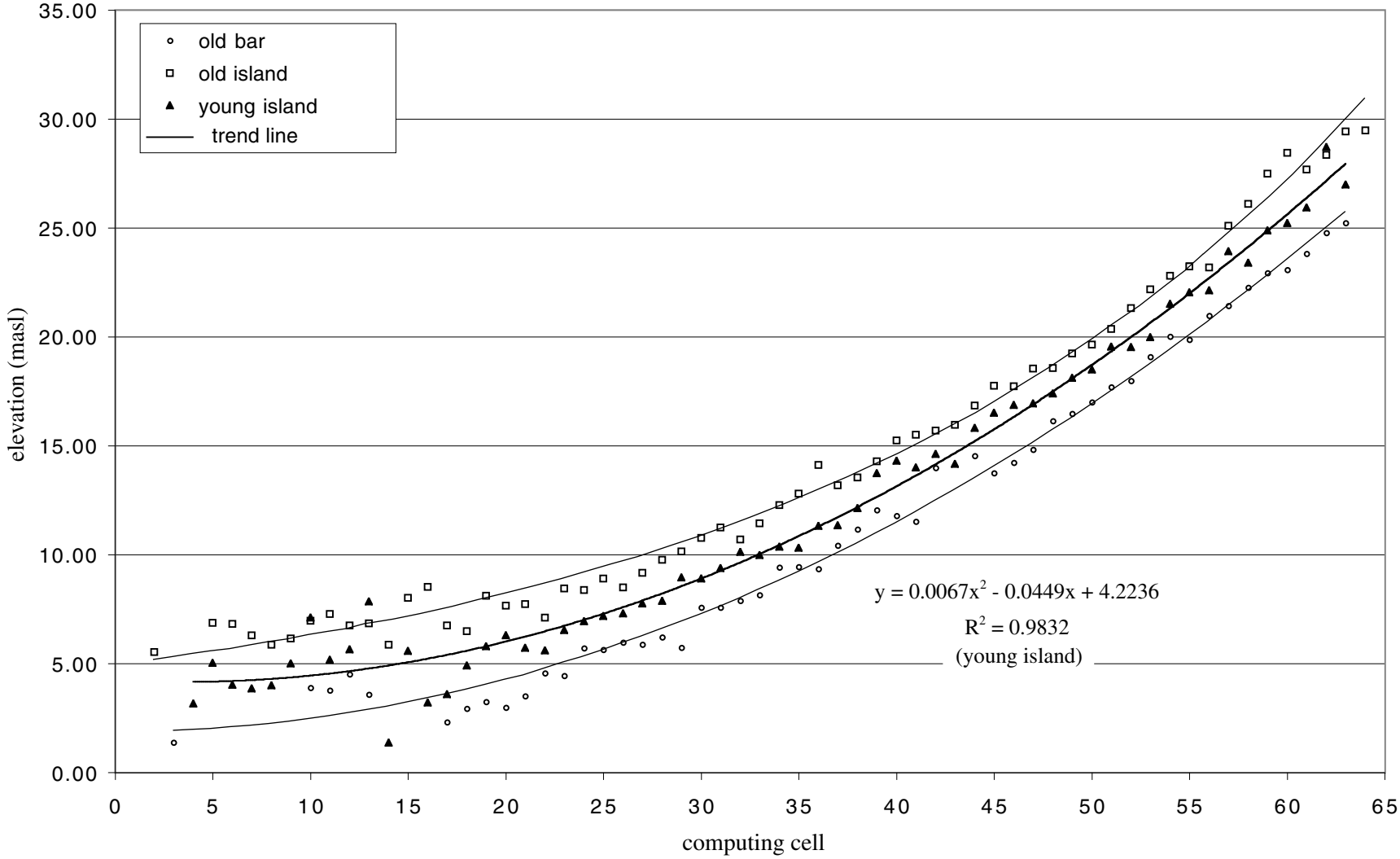

Figure 4-11. Relation between surface age and surface elevation for old bars, young islands and old (mature) islands between Mission (km 0) and Laidlaw (km 65).

the thickness of erodible overbank deposits (adopted for sediment budget calculations - see Chapter 5). These thicknesses (1 and 3 metres respectively) closely correspond with limited field measurements made by McLean (1990, p. 74).

Active cross-section area was calculated for all 78 profiles, and subdivided into forested (island) and unvegetated (bar) groups. A further division was made for profiles located up- and downstream of Agassiz-Rosedale Bridge for comparison with the observed decrease in channel slope (Section 4.3). Since it is known that vegetation is associated with greater bank stability (cf. Millar, 2000) and influences channel morphology (cf. Hickin, 1984; Murray and Paola, 2003), differences in area (and shape) are expected between the two groups. Forested profiles were identified from areal photography because defining islands based strictly on the reference elevation was found to exclude some cross-sections where the elevation of immature islands was equal to or less than the interpolated bankfull elevation. It is assumed that a gain in active channel area over time indicates bank erosion if width at that location also increases, and a deepening of the channel if width is stable or declines. A gain in area above the reference water-level is associated with overbank fine deposition and island growth. The data are summarized in Figure 4-12 and Table 4-3.

The significance of changes in cross-sectional area over time was examined through a statistical comparison of section mean and variance values. Clearly, any channel with a labile bed and banks will exhibit sufficient variability in cross-sectional form that half the sections will be larger than the mean area, on average, with the remainder smaller. Along morphologically complex channels, however, it is expected that the range of size deviations from the mean is much greater than in a channel with a comparatively simple morphology. Therefore, if the complexity of channel morphology is changing over time, both the mean and variance of cross-section area should be altered. Changes in these properties are tested using the t-test for means, and the F-test for variance. Results for cross-section area below the bankfull reference level are summarized in Table 4-4.

Mean active channel area between Mission and Agassiz increased from 1952 to 1984 for both forested and unvegetated sections, although the change is not statistically significant. However, as the active channel width was slightly narrower in 1984 compared to 1952, there must have been some deepening of the channel to maintain flow conveyance. The area above the reference surface also increased despite an overall (albeit modest) decline in island area. While the change is not statistically significant, growth is consistent with the known trend of generally above-average flood flows, a neccessary prerequisite for vertical aggradation. From 1984 to 1999, mean

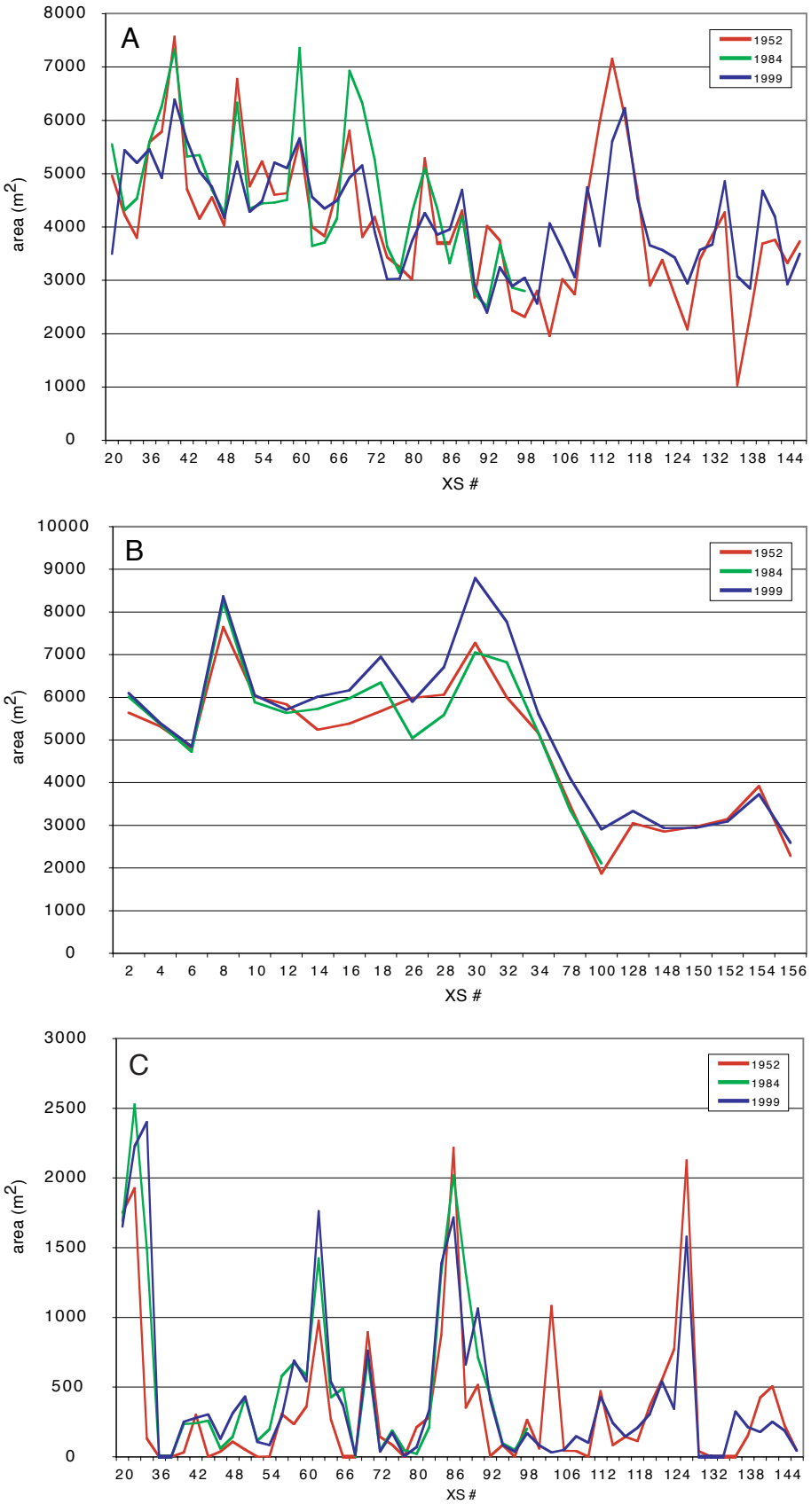

Figure 4-12. Active channel cross-section area (a) below reference line along x-sections with islands, (b) below reference line along unvegetated x-sections, and (c) above the reference line (solid area). Refer to Figure 4-9 for location (ordering is sequential, but not continuous).

cross-section area declined amongst vegetated sections. This change is consistent with the observed increase in island area within the same period on most reaches. However, since the area above the reference water level did not also increase, island and floodplain growth must be associated with younger, low elevation surfaces. Lack of growth on mature, higher elevation surfaces is coincident with the general lack of large floods since the late 1970s. During the same period, there was an areal increase amongst unvegetated sections, the magnitude of which was sufficient to produce an overall balance in the mean area of all cross-sections.

There is also weak evidence to suggest that the variability of vegetated cross-section area has been in decline downstream of Agassiz. This finding implies that individual islands have become larger in total area, but that they have correspondingly declined in number. In-filling and vegetation growth along sidechannels separating adjacent islands may be partly responsible for this pattern. Overall, channel width has declined by 82 metres (8%) since 1949, but channel area has not. This provides clear evidence that the channel has become deeper, on average, over the past half-century. Dividing mean active channel area by mean active channel width illustrates these changes. Average depth is estimated as 4.84 metres in 1952, 5.07 metres in 1984, and increased to 5.50 metres by 1999.

Upstream of Agassiz, mean active channel area below the bankfull datum increased along both vegetated and non-vegetated cross-sections between 1952 and 1999. Although the change is not statistically significant, an increasing area and corresponding narrowing along most upper reaches (18% overall) indicates a deepening channel overall. As calculated above, estimated mean channel depth increased from 3.53 to 4.55 metres. That the channel appears to be degrading more rapidly upstream than downtream of Agassiz is consistent with the overall decline in channel profile (Section 4.2). There is also a distinct pattern of decreased area variability amongst upstream reaches that is statistically significant overall. The decline is also statistically significant for vegetated cross-sections. The overall increase in island area implies a morphologic development toward fewer, larger islands, paralleling the pattern downstream. A significant decrease in variability above the high water mark provides additional evidence to support this claim. At present, the channel is narrower and deeper with reduced ecotone habitat as smaller island clusters have coalesced into larger island complexes.

Table 4-3. Summary statistics for total active cross-section area below the reference datum along the extracted cross-sections.

MISSION-AGASSIZ	***1952***	***1984***	***1999***
All cross-sections	n = 50 $\bar{x}$ = 4730 m^2 s.d. = 1298 m^2	n = 50 $\bar{x}$ = 4924 m^2 s.d. = 1390 m^2	n = 50 $\bar{x}$ = 4923 m^2 s.d. = 1398 m^2
Vegetated sections	n = 34 $\bar{x}$ = 4387 m^2 s.d. = 1143 m^2	n = 34 $\bar{x}$ = 4623 m^2 s.d. = 1293 m^2	n = 34 $\bar{x}$ = 4376 m^2 s.d. = 969 m^2
Unvegetated sections	n = 16 $\bar{x}$ = 5460 m^2 s.d. = 1340 m^2	n = 16 $\bar{x}$ = 5563 m^2 s.d. = 1412 m^2	n = 16 $\bar{x}$ = 6085 m^2 s.d. = 1482 m^2
AGASSIZ-LAIDLAW	**1952**	**1984**	**1999**
All cross-sections	n = 28 $\bar{x}$ = 3485 m^2 s.d. = 1310 m^2	no data	n = 28 $\bar{x}$ = 3695 m^2 s.d. = 894 m^2
Vegetated sections	n = 22 $\bar{x}$ = 3608 m^2 s.d. = 1437 m^2	no data	n = 22 $\bar{x}$ = 3858 m^2 s.d. = 928 m^2
Unvegetated sections	n = 6 $\bar{x}$ = 3033 m^2 s.d. = 528 m^2	no data	n = 6 $\bar{x}$ = 3100 m^2 s.d. = 392 m^2

Table 4-4. Tests for significant differences between mean (t) and variance (f) of active cross-section area below the reference datum. P is the probability that the test statistic is less than the critical value (shown in bold type).

MISSION-AGASSIZ	***1952 - 1984***		***1984 - 1999***		***1952 - 1999***	
All x-sections	F = 1.15 p = 0.32	t = 0.72 p = 0.47	F = 1.01 p = 0.48	t = 0.002 p = 0.999	F = 1.16 p = 0.30	t = 0.72 p = 0.48
Vegetated sections	F = 1.28 p = 0.24	t = 0.80 p = 0.43	F = 1.78 **p = 0.05**	t = 0.89 p = 0.38	F = 1.39 p = 0.17	t = 0.04 p = 0.97
Unvegetated sections	F = 1.11 p = 0.42	t = 0.21 p = 0.83	F = 1.10 p = 0.43	t = 1.02 p = 0.32	F = 1.22 p = 0.35	t = 1.25 p = 0.22
AGASSIZ-LAIDLAW	***All x-sections***		***Vegetated***		***Unvegetated***	
1952 - 1999	F = 2.15 **p = 0.03**	t = 0.70 p = 0.49	F = 2.40 **p = 0.03**	t = 0.68 p = 0.50	F = 1.82 p = 0.26	t = 0.25 p = 0.81

4.5 Hypsometry

The ecological productivity and diversity of river channels is directly related to the extent and variety of available physical habitats (Kondolf and Wilcock, 1996). Indeed, most channel restoration efforts emphasize increasing morphologic complexity by excavating pools and adding large roughness elements to create aquatic habitats (Kellerhals and Miles, 1996; Kondolf, 1998). The wandering planform in particular provides excellent habitat for fishes and aquatic insects because the complexity of characteristic channel forms provides a variety of depth and velocity conditions over the full range of discharge (Payne and Lapointe, 1997; Church, 2002).

Long-term mensuration of changes to the physical habitat can provide a surrogate means for evaluating potential habitat loss. While the isolation of backchannels and ecotone habitats from the river corridor is apparent, changes within the active channel zone are not as easily recorded because they are three-dimensional in nature. Hypsometry provides a convenient means for summarizing the cumulative distribution of elevations for a defined landscape above a reference plane. A hypsometric plot can reveal details of the evolutionary [morphologic] history of a geomorphic surface (cf. Strahler, 1952) and is particularly valuable for comparing landform development over time. In recent years, landscape evolution modelers have begun to adopt the technique for comparing the evolution of simulated to real landscapes (Willgoose and Hancock, 1998), a task made increasingly facile by the availability of elevation data in digital form.

The distribution of active channel area for different depth intervals can reveal information about the nature of morphologic complexity within a given river, while temporal comparisons should provide a means for illustrating the response of a river to changes in natural (scour and fill) or anthropogenic (gravel removals and bank hardening) impacts. In the simplest case of a rectangular canal with fixed banks and no bed material transport, the entire bed would be covered by water of constant depth for any given discharge. The presence of mobile sediments and deformable banks provides increasingly complex channel morphologies with a broader distribution of area-depth classes for a given discharge. It is therefore supposed that channels with highly complex morphologies (i.e. braided and wandering reaches) exhibit a higher degree of spatial complexity than simpler morphologies (straight or meandering reaches).

For this investigation, the total area for different depth bins is calculated for bankfull discharge, a procedure that is analogous to the representation of ocean depths (cf. Harrison, 1998). A GIS coverage containing water surface elevations was constructed by adding a new database

field, surface elevation, to an existing coverage depicting 1-km long computing cells. For each 1-km cell, the water-surface elevation, Zs, was estimated using the polynomial equation fitted to the young island elevations. The 1952 and 1999 interpolated grids were then converted to coverages and combined with the water surface coverage, and morphologic maps produced from the airphotos. The composite GIS layer, therefore, gives the bed surface elevation for each computed grid cell, and a single water-surface elevation for all grid cells within each 1-km computing cell. Bankfull depths were then calculated as Zs - Zbed for all grid cells defining the active channel zone, including channel islands because some immature islands may be inundated at bankfull flow.

A histogram showing changes in the area-depth distribution of the gravel reach from 1952 to 1999 is shown in Figure 4-13. This plot demonstrates a loss of shallow-water habitats at high flow (less than 4 metres total depth) and a corresponding increase in deep-water habitats, a pattern that is consistent with evidence of channel degradation presented in section 4-3. It should be realized, however, that this assertion is complicated by a lack of knowlege with respect to actual water levels in 1952. Water levels would have been somewhat lower, on average, in 1952 because of aggradation that has since occurred. Changes in flow alignment will also have affected water levels. Therefore, the loss of shallow-water area may be exaggerated. Correspondingly, the observed increase in deeper water environments over this same period may be over-estimated, but it provides further evidence of a trend towards a narrower, deeper, channel.

To examine the differences in hypsometry that are expected for distinct morphologies, confined and wandering sub-reaches were partitioned from the complete dataset. The single-thread meandering section includes 10 km of channel upstream from Mission, plus 4 km downstream from Laidlaw. A continuous 25 km long stretch from lower Yaalstrick Island to Big Bar near the Agassiz-Rosedale Bridge was used to represent the wandering planform. Most artificial training works and gravel mining activities have been undertaken in this reach of channel (see Figure 2-5). The confined reaches actually exhibit a wider range of depth classes than the wandering reaches because they include the deepest pools along the lower river. Roughly 80-85% of the active channel lies at depths between 4 and 16 metres in both periods, while the area of shallow (0-4 m) areas increased by half from 11% in 1952 to 16% by 1999. Overall, there is no clear trend in channel depth changes in these reaches, reflecting their relatively small total area, and the dominance of sandy bed-material transport and deposition, especially near Mission. Although the available data do not permit direct mensuration, changes in the frequency distibution of some channel depth intervals possibly occur every few years in response to sediment transfer.

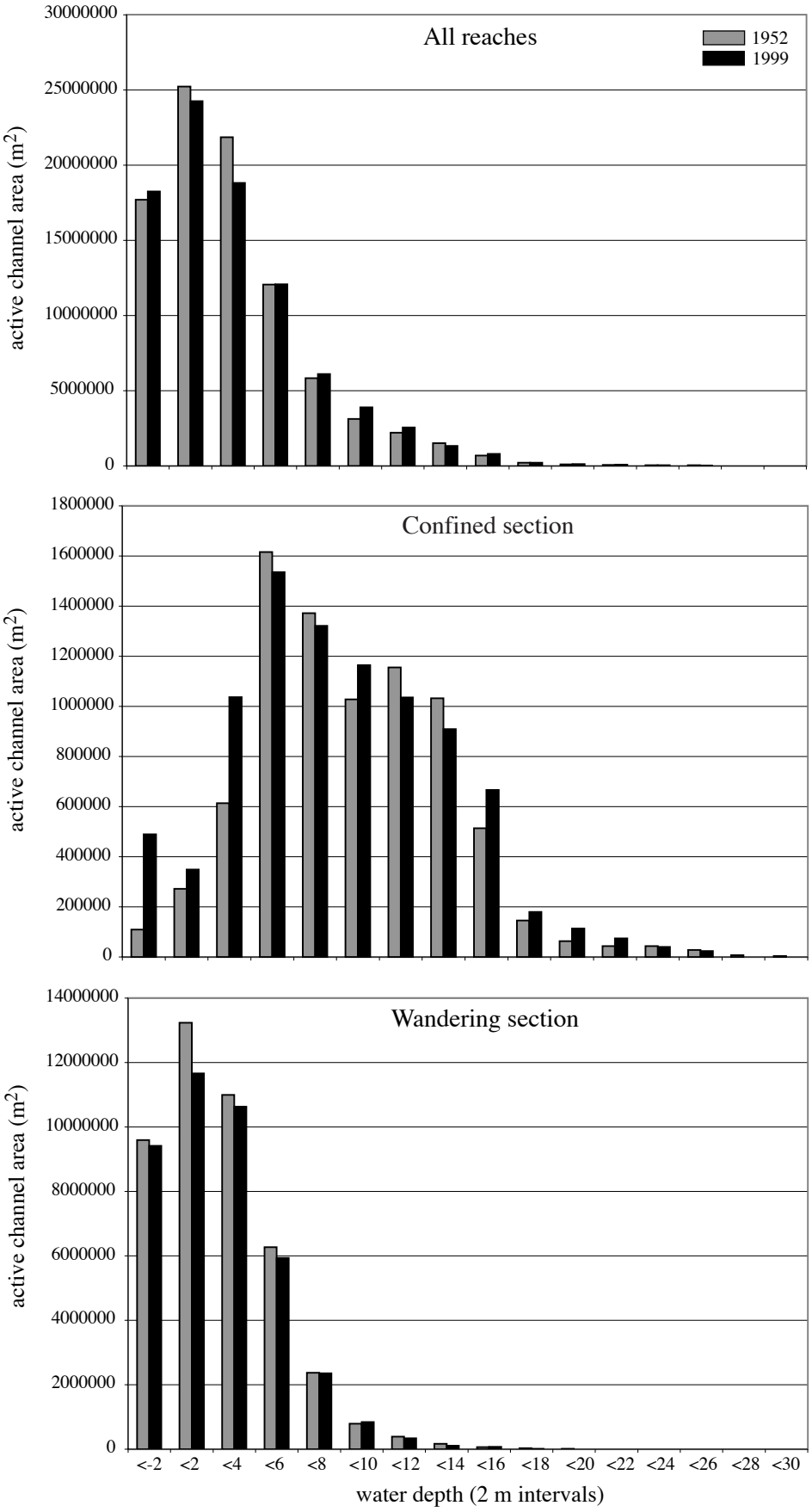

Figure 4-13. Histograms of flow depths (relative to 1999 bankfull discharge) within the active channel zone. Confined and wandering sections do not represent a complete inventory of total active channel area but illustrate comparative differences due to morphology.

The wandering sub-section displays a similar overall pattern to that of the entire gravel reach because this is the dominant morphology. Roughly 96% of the active channel lies at depths less than 8 metres in both periods. Very deep pools (>8 metres depth) occupy the remaining 4% of the active channel, and appear to be a minor component of morphologic complexity in wandering reaches. Shallow (0-4 m) areas show a similar decline in proportion compared to the entire gravel reach, but changes are mainly pronounced in the 0 to 2 metre depth class (which is the most sensitive to bar aggradation). Similarly, the apparent loss of area from 2 to 6 metres may be influenced by bed aggradation since the actual change is fairly modest. The differences in morphologic complexity between the two channel typologies is further emphasized using a hypsogram plot (Figure 4-14). The dominance of shallow depths as a percentage of total active channel area on the wandering planform is clearly shown.

4.6 Summary

There are several lines of evidence which indicate that the morphologic complexity of the gravel reach has become reduced over the past century in response to the cumulative effects of anthropogenic influences. The channel has narrowed more quickly than can be explained by a corresponding decline in bankfull discharge over the period of record, hence must be responding to other forces. Since changes in width are fairly uniform amongst the different study reaches, a single process dominates, though the impacts of individual factors are difficult to isolate. However, it is known that much of the loss in active channel area early in the century is the direct consequence of dams and flood gate construction that isolated prominent sloughs and secondary channels, which have since silted up over time and become vegetated.

As many of the secondary channels encompassed large islands, this isolation also led to a dramatic loss of island area early in the century, as these deposits were effectively converted to floodplain. The loss of island area continued to the 1970s, consistent with generally above-average flood flows, but their total area has since recovered to levels not seen since before the dyking program was expanded. Superficially, this pattern implies that dyking, bank hardening and woody debris removal have had no significant impact on the morphologic development of channel islands, but available evidence indicates that mature, riparian forests are becoming replaced by young vegetation on newly established islands. This has been accompanied by a trend towards fewer, but larger islands, resulting in a loss of ecotone habitat.

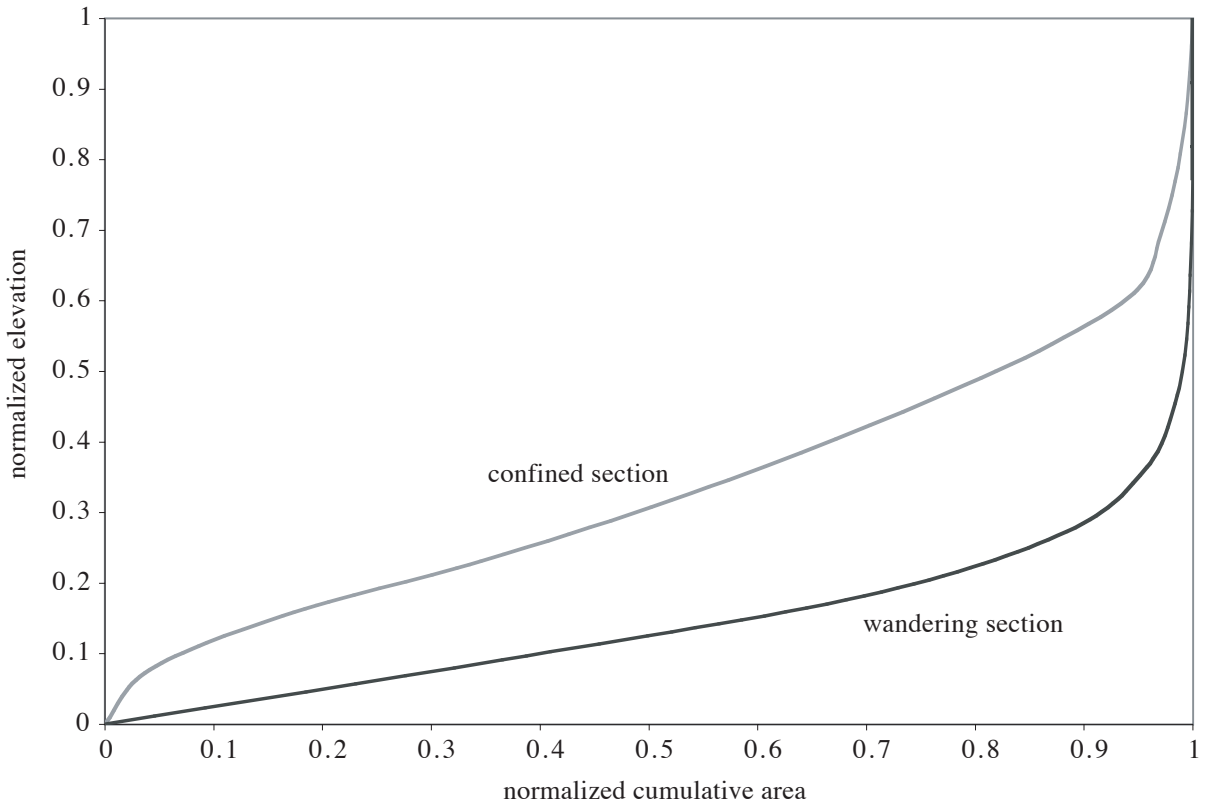

Figure 4-14. Hypsogram for a confined and wandering section of channel from 1999. Confined sections have depths ranging from 0 to 26 metres, while wandering sections range from 0 to 22 metres.

Channel narrowing and changes in island morphology have also modified the topographic characteristics of the channel. The gravel reach has become less steep, with degradation upstream of Agassiz-Rosedale and corresponding aggradation in downtream reaches. Analysis of extracted cross-section profiles demonstrates that the channel has actually degraded in these reaches, but the rate is more modest than observed upstream. Hypsometric analysis reveals that sedimentation in lower reaches has become concentrated on higher bar surfaces, reducing the area of shallow habitats at bankfull discharge. However, given the absence of a bankfull water-surface profile for 1952, it is not possible to definitively state that aggradation since has reduced channel capacity, or that gravel mining and bank hardening have reduced morphologic complexity. The seemingly remarkable resilience of the river to respond markedly to environmental and anthropogenic changes since 1952 may primarily reflect inertia given its large size. If the volume of material stored within the active channel zone is far greater than the average annual influx of bed material, or of sand and gravel removals, the morphology may alternatively be dominated by internal modifications over periods of decades. A sediment budget is presented in the following chapter and is used to investigate this supposition more fully.

Chapter 5: Bed material transport

5.1 Introduction

In this chapter, an estimate of the bed material transport rate along the lower Fraser River is provided over the past half-century. Sediment transfer and deposition dominate the morphologic development of the gravel reach and present a number of engineering and management challenges because of development on the floodplain. The primary response to combat river morphologic development has been to harden outer channel banks and selectively remove gravels. Establishing the relation between the nature and magnitude of these channel modifications and the sediment transport regime provides a means for evaluating the sensitivity of the channel to environmental changes, and provides a tool for predicting the response to additional forcing. Given the large size of the river, many decades may be required to resolve the impacts, if observable, of these activities on the rates and volumes of sediment input and transfer, and hence channel stability. Assuming these activities will continue, it is important to understand the past effectiveness (or failure) of these applied management strategies for protecting developed areas while maintaining the quality of available aquatic habitat. Establishing a detailed bed material sediment budget provides a means to pursue this line of inquiry and establish guidelines for future management decisions.

Measured morphologic changes are related directly to sediment transport rates within the sediment budget framework. This technique is suitable for large gravel-bedded channels in which significant channel changes occur over years to decades. Estimates of bed material transport for the lower Fraser River are provided for 1952 to 1984, 1984 to 1999, and 1999 to 2003, and are used to illustrate the dynamics of sedimentation over periods commensurate with timescales for management practices. The availability of recent (1999 and 2003) bathymetry and altimetry data further provides a means for investigating the linkages between channel deformation and sediment transport at a resolution that may be unique for such a large river system.

The sediment budget estimates are subject to a number of limitations, including the reliability of historic channel and floodplain topographic surveys, the accuracy with which these data can be converted to interpolated surfaces that reflect actual topographic variability and the reliability of assumptions required to parse complete topographic models of the bed and banks into channel and bank sediments, and hence to estimates of the total load distributed into washload, coarse sand and gravel components. These problems are addressed in a discussion of sediment

budget errors at the end of the chapter. The validity of the estimates is further examined by comparing results presented herein with those of past studies.

5.2 Sediment budgets from morphologic change

5.2.1 General approach

The basis for relating changes in channel morphology to sediment transport is the morphologic sediment budget, essentially an accounting procedure for tabulating net sediment exchanges within a defined reach of channel. The approach is most suitable for describing the movement of bed material, since this is the material that determines channel morphology and governs stability. An estimate of washload can be made under certain conditions (Church et al., 1987; Ashmore and Church, 1998) although none is provided in this thesis. On the gravel reach of lower Fraser River, exchanges of bed material include sediments entrained upstream of Laidlaw and transported downstream, channel scour and fill, erosion and construction of island and floodplain deposits and output at the downstream limit of the study area. To complete the budget, sediment evacuations through dredging (documented in Chapter 2) are added back to the reach from which they were removed as a depositional volume. The incomplete knowledge of all past gravel removal volumes represents a negative bias in the sediment budget (meaning transport estimates represent a minimum) although the magnitude of this bias remains unknown. Nominally, the contribution from major tributaries must also be accounted for. However, as neither of the two major tributaries that enter the gravel reach (Chilliwack-Vedder and Harrison Rivers) contributes material larger than sand which mainly travels through the reach in suspension (McLean et al., 1999), this volume is ignored.

The sediment budget can be summarily expressed as:

$$V_o = V_i - (1-p)\,\Delta V - V_d$$

where V_o is the volumetric sediment output, V_i is volumetric sediment input to the reach during some specified time period, and V_d is the volume removed from dredging. The storage term, ΔV, is measured as the net difference between scour and fill of the channel bed and banks, and is estimated from differences in modeled bathymetry surfaces over the period between surveys. The equation can be reduced to a mean transport rate by dividing all terms by the time between successive surveys. An additional adjustment for sediment porosity ($1-p$) or unit weight (t/m^3) is conventionally included to express all terms as mineral volumes. Finally, total volumetric changes can be converted to bed material volumes by adjusting for Φ, the proportion of material finer than

medium [wash material] sand (<0.177 mm). Within the active channel zone, the adjustment is negligible, but considerable volumes of fines can be stored overbank on island and floodplain surfaces where they become trapped or settle at high discharge due to lower flow velocities.

McLean (1990) assumed that the transport of gravel past Mission was negligible, noting that material >2 mm comprises less than 5% of channel bed material below Mission, and coarse gravels are nearly absent downstream. Given this assumption, the transport rate of bed material at Mission was assigned a value of zero, and calculations of sediment influx were propagated upstream. However, it is not clear that the assumption is entirely valid because some gravel has been found in sand dune troughs downstream of Mission. Although this material could be derived locally (i.e. from erosion of terrace deposits), the possibility remains that gravel is actually transported past Mission. Bed material particle-size analysis data published by the Water Survey of Canada will be examined to revisit this question. Nevertheless, the zero transport assumption remains desirable because it implies that all material that enters the gravel reach is trapped, hence there is no practical upper limit for the temporal interval between successive surveys. Further, the requirement to estimate a reference transport rate is eliminated. In channels with no defined 'zero' boundary condition, the possibility for unmeasured throughput increases with the length of the survey interval, and only a lower bound estimate of transport can be made (Carson and Griffiths, 1989; Ham and Church, 2000). Nevertheless, details on sediment transfer and channel deformation within lengthy intersurvey intervals are, of course, limited by compensating scour and fill.

The complete sediment budget expressed as a mean transport rate is:

$$Q_i = Q_o + Q_d + (1\text{-}p)\,\Delta V_c / \Delta t + (1\text{-}p)(1\text{-}\Phi)\,\Delta V_f / \Delta t$$

where Q represents the mean flux rate, while V_c and V_f define channel and floodplain changes respectively. If the value of Q_i exceeds Q_o at any location, the channel is locally aggrading. The sediment budget can further be defined for any arbitrary length of channel smaller than the total study reach length. In this thesis, the channel is divided into 65 computing cells of approximately 1-km in length, allowing the transport rate to be estimated at any location within the study reach (Figure 5-1). This approach is useful for illustrating the variability in transport that can occur downstream and provides a means to relate the displacement and storage of sediment to channel stability, details of which are provided in the following chapter.

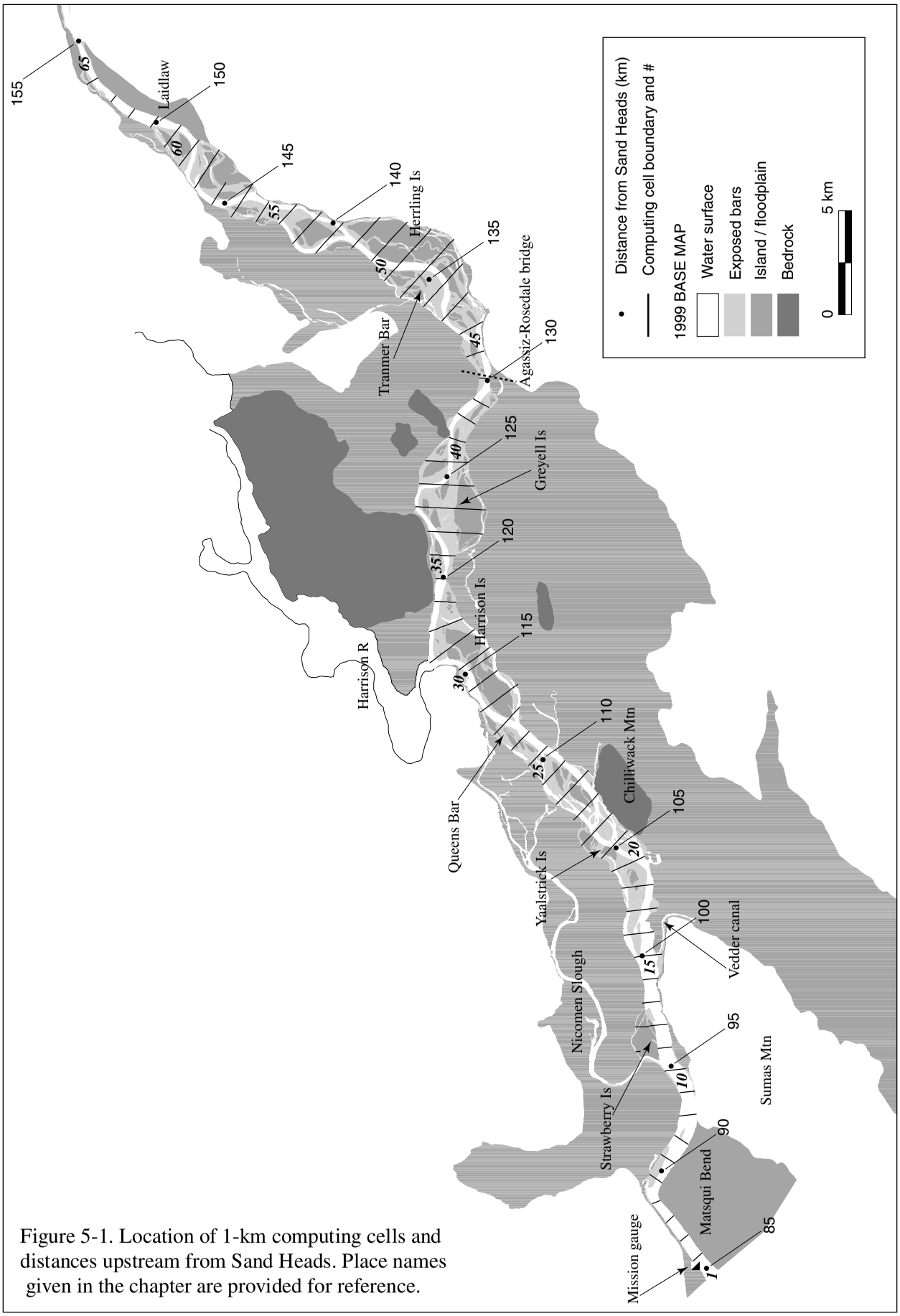

Figure 5-1. Location of 1-km computing cells and distances upstream from Sand Heads. Place names given in the chapter are provided for reference.

5.2.2 Sediment budget construction

The construction of period sediment budgets for lower Fraser River is based on a sequence of computing steps that have been refined and adjusted to minimize error margins within the constraints of available information (cf. Ham and Church, 2003). Topographic models of the bed and adjacent floodplain were constructed for 1952, 1984 and 1999 following the conventions described in Chapter 3. As the 1999 data were collected at higher spatial density along individual sounding lines than in previous surveys, they were thinned to be compatible with the 20-metre spacing of the earlier surveys. Individual datasets should have similar spatial density to ensure self-consistent comparisons between modeled surfaces over time. However, as the 2003 soundings were collected at roughly the same density as in 1999 (although sounding line spacing was reduced from 200 to 100 metres) no data thinning was required for the 1999-2003 intersurvey comparison. In addition, the availability of 1-metre ground resolution LiDAR data on stable islands and floodplains enabled construction of topographic surfaces for both 1999 and 2003 that are more accurate than for the older datasets. Therefore, the sediment budget results presented herein are based on modeled surfaces computed at higher (10-metre) spatial resolution. This change preserves more of the actual topographic variability that exists on bars and islands, such as ridges and chute channels, that is otherwise‘smoothed out’ at lower resolution.

The net of bed level changes for each intersurvey period is calculated by subtracting consecutive modeled surfaces using GIS tools. These ‘surfaces of difference’ illustrate the complex patterns of channel scour and fill that occur in response to the downstream staging of bed material (Figure 5-2). Each was then superimposed with a masking layer to replace interpolated differences with a ‘no-data’ value in regions where the interpolation was known to be weak due to insufficient data, outside the margins of known channel change (i.e. on large islands and floodplain) or where the modeled region extended beyond the area of principal interest (i.e. Vedder Canal, major sloughs). The same mask was applied to the 1952-84, 1984-99 and 1952-99 surfaces to ensure all computing areas were identical and contain the actual active channel zone over the past 50 years. The masked surfaces were also overlaid with morphologic maps produced from available airphotos nearest to the date of the soundings. The morphologic maps permit each 20-metre grid cell to be associated with a particular type of channel transition, including:

- channel scour and fill (polygons coded as water or gravel bar on both mapping dates)
- bank erosion (island or floodplain on early date, water or gravel bar on later date
- bank deposition (water or gravel bar on early date, island or floodplain on later date)

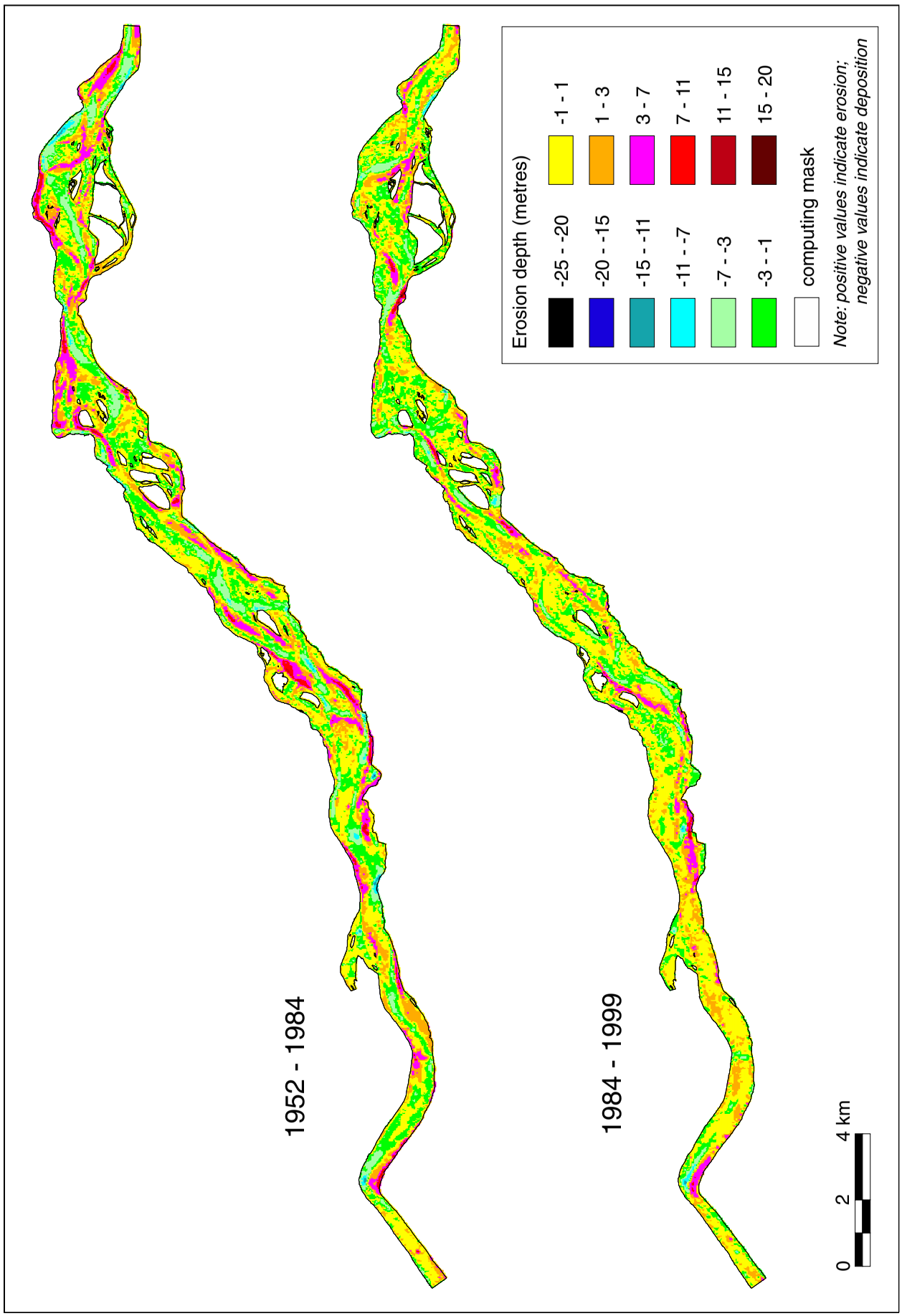

Figure 5-2. Surfaces of difference from individual topographic models between Mission and Agassiz showing complex patterns of scour and fill.

- no change (island or floodplain on both dates; assumed that these are stable surfaces)

It is assumed that a 'no change' polygon has a constant surface elevation over the study period, so these may be ignored (although some surface compaction or overbank sedimentation could technically occur). The remaining cells, therefore, define common regions of channel scour and fill, bank erosion, and bank deposition: the constituent components of morphological change. Cells divided by more than one transition type are assigned separate transition codes for each cell 'piece'. Since the dates of the airphotos and bathymetry surveys do not correspond exactly, some codification error is possible. Two additional processes, vegetation stripping (island or floodplain to gravel bar) and recovery (gravel bar to island or floodplain) were also identified, but are collapsed into the bank erosion and deposition categories respectively since the data are reduced in an identical manner. Data reduction refers to the process of converting gross volumetric changes into estimates of bed material (sand and gravel) and wash material (which is eliminated from the calculations). Procedural details vary somewhat by transition type and are described below.

The volumetric calculations for channel scour and fill are reasonably straightforward. The total volume change for an individual grid cell is simply the product of the elevation change and the cell (or cell piece) area. For each of the 65 1-km reaches, individual channel grid cell volumes are summed, giving the net of scour or fill over the intersurvey interval. This total volume consists of bed material only — material finer than medium sand is not deposited on the active bed. Although silt lenses have been observed on some exposed bars at low flows, the small size, and accordingly volume, of these deposits can be considered negligible compared to the volume of mobilized bed material in any computing reach. Grain size data were collected in 1983 along bar heads and flanks throughout the entire gravel reach (McLean, 1990) while suites of 9 20-kg bulk samples were collected from upper-, mid-, and lower-bar sites along the reach in 2000, then combined to yield 3 measurements for each bar. Church et al. (2001) found no systematic difference between the data collected in the different years, allowing all 70 samples to be pooled and plotted as grain size versus distance upstream (Figure 5-3). An additional division of bed material into sand and gravel fractions is also presented based on the estimated proportion of sand along the gravel reach as determined from each field sample. A fitted trend line is used to estimate the sand fraction for different reaches because of considerable scatter, which increases linearly from 17% at Laidlaw to 27% at lower Sumas Mountain (Figure 5-4). The given equation is used to interpolate the sand fraction for each 1-km computing reach between these locations (computing

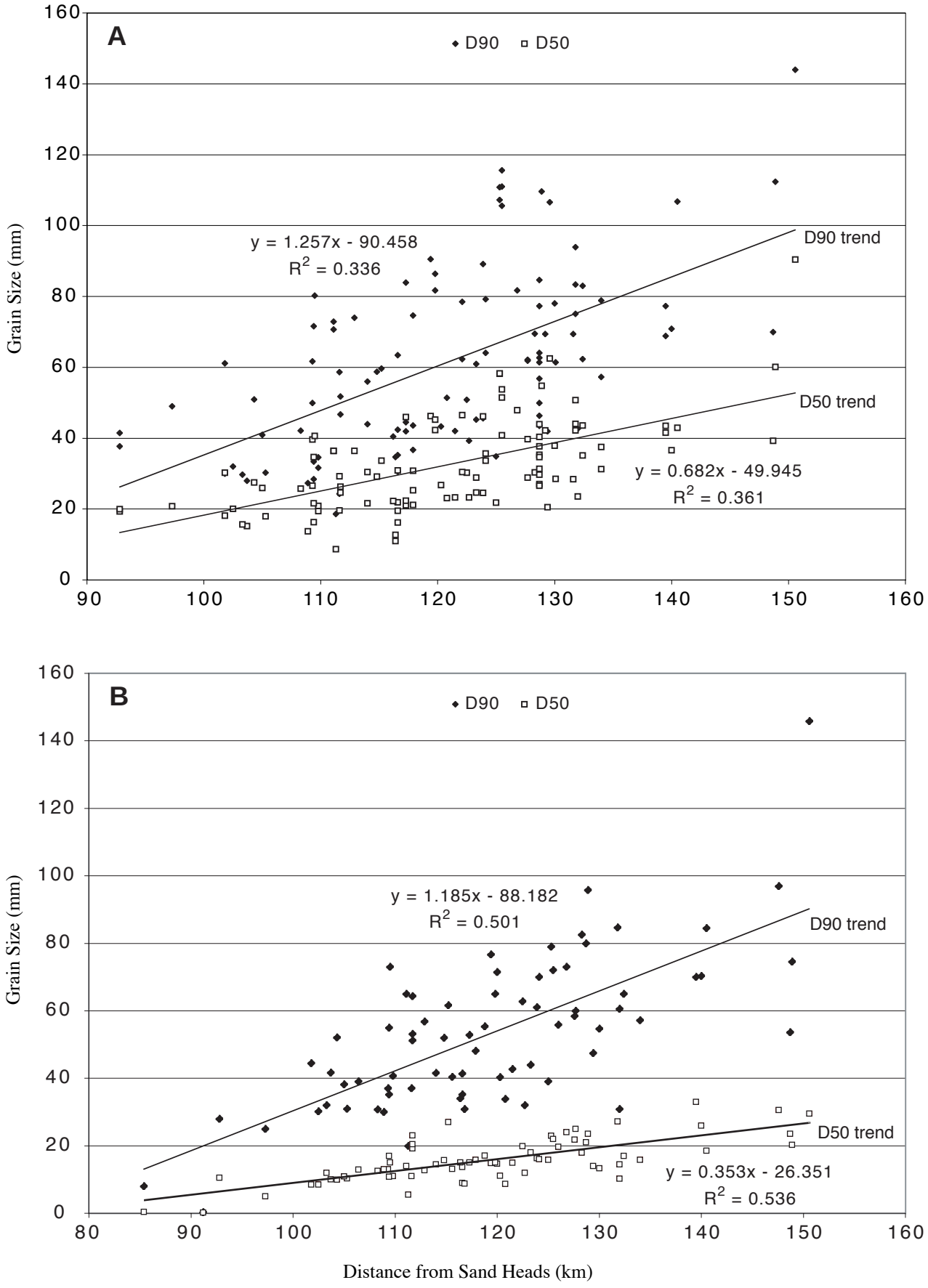

Figure 5-3. (A) Surface and (B) subsurface grain size versus distance upstream from Sand Heads. Data are based on pooled samples collected in 1983/84 and 2000.

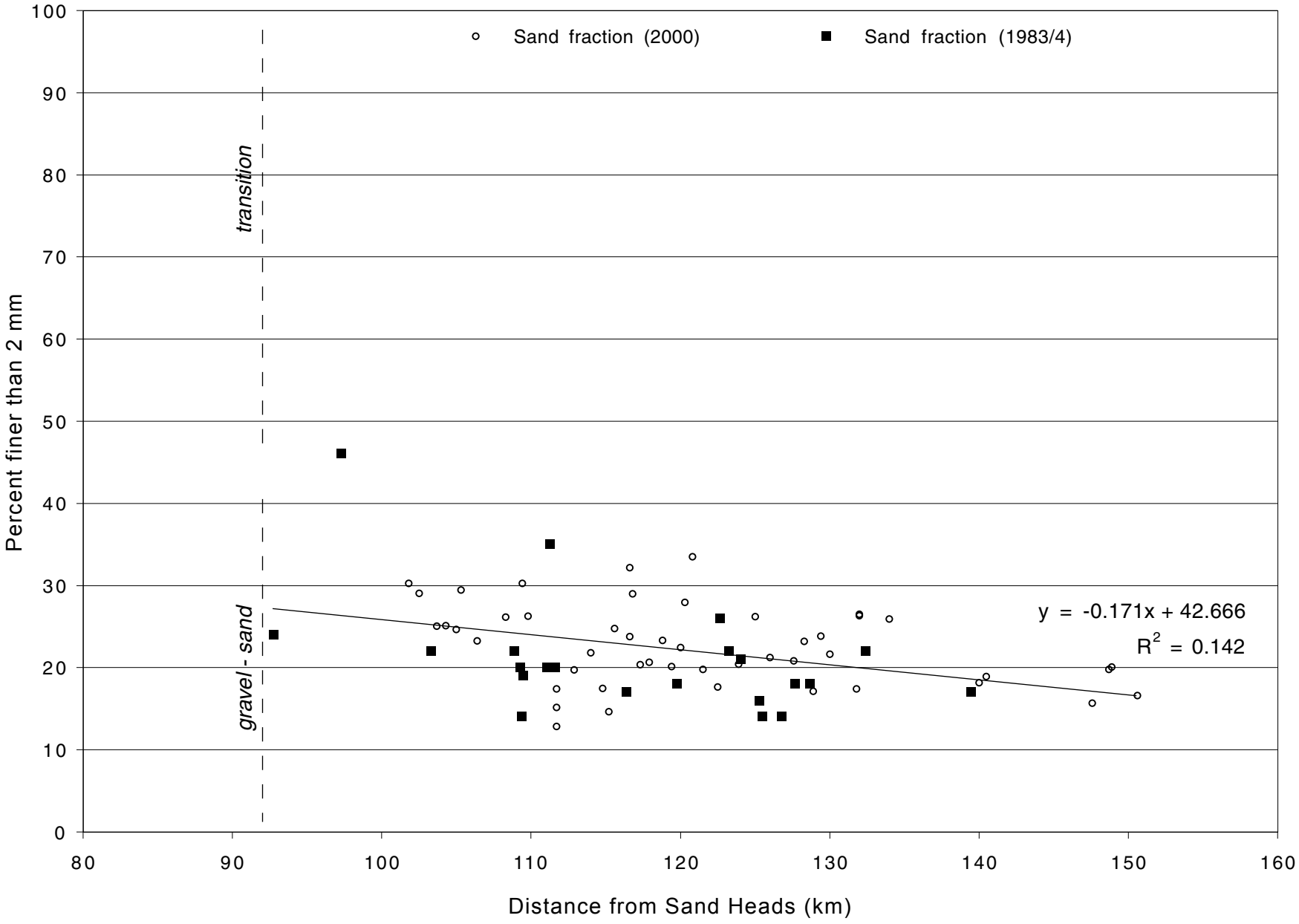

Figure 5-4. Subsurface sand fraction (%) plotted against distance upstream from Sand Heads.

cells 9 to 65). Information on grain-size distributions below Sumas Mountain is nearly absent because of sampling limitations. The sand fraction was arbitrarily increased to 30% and 40% in the following two cells downtream. This ratio of sand to gravel is apt to completely fill all pore spaces and minimal gravel transport would continue downstream. The remaining cells were all assigned a value of 95% following values reported by McLean (1990). The adopted values are also given in the sediment budget tables (Tables 5-5 to 5-8).

The calculations for bank erosion and deposition volumes are considerably more complex because of a 1 to 3 metre layer of fine sand and silt that overlies the basal layer sand and gravels. Variations in the thickness of this material have been correlated to the age of overlying vegetation at different sites (Boniface, 1985; McLean, 1990). McLean (1990) estimated bank erosion and deposition volumes by multiplying eroded areas by the thickness of the basal gravels based on direct field measurement at each site, although extrapolation was necessary where former islands were completely eroded. An alternative GIS-based approach is adopted that relates site surface elevation to the deposit age (rather than the vegetation age) and the estimated overbank volume is subtracted from the total volumetric change at eroded and deposited island and floodplain sites. Combinations of morphologic maps from low-water airphotos taken in 1949, 1971 and 1999 were used to define young island, old bar and old island surfaces, given as:

- *young island*: bar surface in 1971, vegetated by 1999
- *old bar*: bar surface in both 1949 and 1999
- *old island*: island (or floodplain) in both 1949 and 1999

The polygons corresponding to these surface types were intersected with the 1999 LiDAR data, and the elevations of individual spot heights were spatially averaged by each computing reach. These data are plotted as average surface elevations relative to the distance upstream from Mission (cf. Figure 4-11). Best-fit exponential lines are fitted to average scatter or anomalies that may exist because of insufficient elevation data (i.e. several reaches have few or no spot heights on young islands). It is assumed that the difference in elevation between old bar and young island surfaces represents the thickness of recent overbank deposition, while the difference between old bar and old islands represents the thickness of eroded overbank deposits. A value of 0.84 metres, or half the maximum deposited thickness, is adopted as these surfaces will be in various stages of development. The maximum thickness of the overbank sediments on eroded surfaces is 3 metres, considerably larger than the deposited value, but consistent with the previously cited thickness /

vegetation age relation. The same values are applied to all 1-km computing reaches since the best-fit lines are very nearly parallel.

Although these conventions appear straightforward, they do not always lead to a simple adjustment for erosion and deposition volumes. The possibility exists for apparently mature surfaces to actually be former (1949) islands that have been eroded and replaced with initially bare bar surfaces that have re-vegetated within the following 50 years. Similarly, some eroded islands may have considerably less than 3 metres of overbank deposits. Following these examples, removing 3 metres of sand along an eroded polygon, multiplied by its erosional area, may result in a volume of overbank material to be subtracted that is larger than the total eroded sand and gravel volume calculated by the GIS. In such cases, the total (GIS) erosional volume is simply assigned to sand. Where the product of the stripping area and the 3 m overbank thickness was found to be smaller than the total volume recorded by the GIS, gravel was also assumed to have been eroded. Similarly, measured revegetation volumes in excess of 0.84 m times the revegetated area were assumed to have also resulted from additional gravel deposition. These gravel volumes are separated to gravel and coarse sand volumes using the same proportions described for channel scour and fill. While it is recognized that assigning different adjustments for erosional and depositional volumes based on the relative age of different surfaces (which can be estimated from available mapping) is theoretically feasible, the technical details of managing such a large database make such an exercise practically onerous.

A final calculation is required to adjust the volume of removed overbank fines by Φ, the proportion of material finer than 0.177 mm. From direct sampling, this is estimated as 70% of the overbank deposit volume. This proportion is considered wash material and is eliminated from the computations. The remaining 30% is combined with the sand fraction associated with erosion and deposition within the basal gravel layer and with the volume of sand removed by mining. The total sand sum is reported in the sediment budget tables. The gravel sum includes the total volume of gravel eroded or deposited within the channel bed and lower banks and the volume removed by mining. A more detailed description of the calculations for sand and gravel volumes for individual computing cells is given in Church et al. (2001) and is repeated in Appendix B. The total sand and gravel sum deposited within each computing cell is also given in the tables. This quantity, divided by the computing cell area, gives the relative change in the average elevation of the bed over the intersurvey period. The final budget is as complete as possible given imperfect knowledge of sand distribution throughout the study reach. This includes not only the thickness of overbank sands, but

also the proportion found within the bed and banks. It should be recognized that this limits the precision of both sand and gravel budget estimates.

5.3 Sediment transport

5.3.1 Summary sediment budgets

A strict summation of all positive and negative elevation changes for modeled surfaces demonstrates the magnitude of total sediment flux (including overbank deposits) over time within the gravel reach (see Table 5-1). Up to 53 million m^3 of sediment was eroded (with 49 million m^3 deposited) between 1952 and 1984, giving a net loss of 4.3 million m^3. An additional 33 million m^3 was eroded between 1984 and 1999, but a larger volume (39 million m^3) was deposited, resulting in 5.6 million m^3 net aggradation. Adding the net changes from the intersurvey periods (1952-1984 + 1984-1999) produces the same result as the direct difference from 1952 to 1999, consistent with the basic continuity equation for mass flux. In contrast, the sum of cut and fill volumes for the intersurvey periods do not equate to the direct difference from 1952 to 1999. This discrepancy occurs because compensating scour and fill masks the full range of channel changes, the magnitude of which increases with the survey interval. Conversely, shorter survey intervals should display increasingly large volumes of sediment scour and fill (although the net difference would remain constant). This is demonstrated by the 1999-2003 surveys that show up to 22 million m^3 eroded and 30 million m^3 material deposited within the gravel reach over 4 years, a far greater average annual rate than is observed between 1952 and 1999, since scour and fill areas remain largely distinct. These numbers illustrate the magnitude of sediment exchange that occurs as bars and islands are eroded and migrate downstream. The actual volume of 'new' material that is transported into the reach (i.e. net volume) is, however, comparatively modest.

Table 5-1. Gross volumetric changes between Mission and Agassiz

Survey Period	Cut Volume (m^3)	Fill Volume (m^3)	Net Volume (m^3)
1952-1984	53,150,000	48,809,000	- 4,341,000
1984-1999	32,991,000	38,598,000	+ 5,607,000
1952-1999	56,277,000	57,543,000	+ 1,266,000
1999-2003	22,289,000	29,933,000	+ 7,644,000

Any discussion of total sediment flux is complicated by both the entrainment and deposition of fine sediments on islands and floodplain, and by the suspended fraction of the sand load. The movement of this material inflates the magnitude of apparent morphologic change in the reach. By removing these components of the total load according to the conventions described

earlier, the bed material fraction can be isolated. A summary of bed material exchanges in the gravel reach is given in Table 5-2. All values correspond to the influx past Agassiz-Rosedale Bridge. Reported totals including values for individual 1-km reaches are given in the sediment budget tables.

Table 5-2. Summary of bed material sediment budget calculations. All values are bulk in millions of m^3.

Period	Sediment	Channel bed	Channel banks	Mining	*Total*
1952 - 1984	gravel	4.918	-0.999	1.554	**5.473**
	sand	2.208	-3.519	0.463	**-0.848**
	Total	**7.126**	**-4.518**	**2.017**	**4.625**
1984 - 1999	gravel	3.576	-0.118	0.951	**4.409**
	sand	1.079	-0.005	0.288	**1.362**
	Total	**4.655**	**-0.123**	**1.239**	**5.771**
1952 - 1999	gravel	2.831	3.075	2.505	**8.412**
	sand	1.806	-1.723	0.751	**0.834**
	Total	**4.638**	**1.352**	**3.256**	**9.246**
1999 - 2003	gravel	3.404	-0.473	0.135	**3.067**
	sand	1.734	-0.585	0.038	**1.188**
	Total	**5.139**	**-1.058**	**0.174**	**4.254**

The summary sediment budget shows that the net influx of gravel exceeds the input of sand in all periods, with most of the material deposited on the channel bed and bars. Channel banks represent a negative net flux (erosion exceeds deposition) for all periods except for the full 1952-99 intersurvey comparison. This occurs because banks and islands can be significantly eroded by a few floods depending on local channel alignment, but many decades are required to establish large areas of new floodplain. From 1952 to 1984, there was a net gain of 145,000 m^3/yr of bed material to the gravel reach. The influx of gravels was actually larger, 171,000 m^3/yr, because of an apparent sand deficit. From 1984 to 1999, the total bed material influx rate increased to 385,000 m^3/yr, 76% or 294,000 m^3/yr of which was gravel, and to 1,292,000 m^3/yr from 1999 to 2003 (59% or 767,000 m^3/yr gravel). Average annual transport volumes are summarized in Table 5-3. The bulk volumes can be converted to weight using a bulk density of 1770 kg m^{-3} ± 110 m^{-3}. This conversion is based on six 100 kg field measurements along the gravel reach (with a 2 standard deviation range).

Table 5-3. Average annual transport rates (m^3 / yr) for sand, gravel and total bed material load. Rates are equivalent to tthe influx past Agassiz-Rosedale Bridge.

Period	Gravel	Sand	Total bed material
1952 - 1984	171,000	-27,000	145,000
1984 - 1999	294,000	91,000	385,000
1999 - 2003	767,000	297,000	1,292,000
1952 - 1999 (Direct)	179,000	18,000	197,000
1952 - 1999 (Sum)	210,000	11,000	221,000

The direct difference of the 1952 and 1999 surveys yields a total bed material influx rate of 197,000 m^3/yr, or 179,000 m^3/yr of gravel (91%). For comparison, the direct sum of the intersurvey budgets gives 221,000 m^3/yr (total bed material) and 210,000 m^3/yr (gravel). These figures are respectively larger by a factor of 1.12 and 1.17 times and represent a negative bias associated with the direct 1952-1999 budget. While reasonably close to unity, the sediment budgets should express mass continuity since the intersurvey budgets are simply intermediate sub-components of the full computing period. Although sand certainly is transported past Mission, it is assumed that all gravels are 'trapped' and there should be no negative bias in the gravel budgets. Although there is a small possibility that a large volume of gravel actually does move past Mission which could account for the bias, the problem likely relates to uncertainty in the actual sand to gravel proportion downstream of Sumas Mountain. Since large volumes of mainly sand are mobilized in this region, small errors in the sand fraction could produce large errors in the gravel fraction. Amplifying this problem is the possibility that gravels may be prograding downstream over a former sand bed and the gravel estimates may be negatively biased as a consequence. As there are no bed samples available from 1952, and few since, there is insufficient information to fully resolve this problem.

Upstream of Agassiz-Rosedale Bridge, direct difference of the 1952 and 1999 modeled surfaces reveals a modest net loss of bed material (3300 m^3/yr) because of a sand deficit. In contrast, there has been a minor gain of 2400 m^3/yr of gravel (see Table 5-7). Adding these figures to the transport rate at the bridge gives the bed material influx at Laidlaw, estimated as 193,000 m^3 (94% gravel). The positive net flux of sand and gravel along channel banks is consistent with the pattern observed downstream over this same period, but the channel bed and bars show substantial degradation. Although interpretation of these figures must be viewed cautiously because of limited

spatial resolution associated with the 1952 survey data between the bridge and Laidlaw, a degrading channel zone is consistent with a lowering of the thalweg (Chapter 4).

The summary sediment budget data imply that average annual transport rates have been increasing over time. In particular, the most recent (1999-2003) transport rate is considerably greater than during the longer term from 1952 to 1999 (Table 5-2). The total influx of bed material between 1984 and 1999 exceeds that recorded from 1952 to 1984 despite the shorter computing period and generally smaller flood flows. The estimate of gravel from 1952 to 1984 is, however, reasonably consistent with a value of 4.012 million m^3 reported by McLean and Church (1999) using a similar morphologic study approach (no estimate of sand was given). Further, those authors estimated the gravel influx past Agassiz to be 4.54 million m^3 from Water Survey of Canada measurements. Nevertheless, the limited spatial extent of the 1984 survey means that potential errors associated with the surface model could account for the discrepancy between the sub-periods. For example, a modeled 1984 surface that was too low, on average, would inflate the 1984-1999 transport rate (while the 1952-1984 estimate would correspondingly decline).

Although the 1999 to 2003 figure appears anomalously large, the topographic data upon which the estimates are based produces a more accurate surface of difference than is possible for the earlier intersurvey periods. The high influx of bed material derives in part from 1.5 kilometres of bank erosion (up to 130 m lateral shifting) on mid-Herrling Island across from Tranmer Bar and scouring of the adjacent bed. This eroded volume does not, however, account for the total sediment influx. Lateral erosion at this site has been on-going since the 1940s, when Tranmer Bar was initially established (Church and Ham, 2004). High rates of sediment influx past Agassiz-Rosedale Bridge are likely to continue for several more years until the island is bissected, whence rates are likely to decline significantly. Additional discussion of the progression of these events is given in Appendix C.

Although the estimated influx rates at Agassiz-Rosedale Bridge for the different computing periods appear reasonable, the above discussion also acknowledges that summary sediment budgets may be sensitive to a variety of factors that influence reliability of the results. These include compensating scour and fill that masks the magnitude of channel changes when converting gross bed changes into component values of sand and gravel and uncertainty in the ratio of sand to gravel, especially in lower computing cells. These factors are related to, or are amplified by, the time interval between successive surveys, suggesting the potential for systematic time-dependent bias that negatively influences the results. This potential is reviewed below.

5.3.2 Time-integrated bias

A major assumption of the sediment budget approach is that there is no compensating scour and fill between successive surveys. While major sites of erosion and deposition remain distinct over short intersurvey periods, the possibility for undetected changes increases over time. For example, a cell may experience 2 metres aggradation from 1952 to 1984, followed by degradation of 2 metres to 1999. In such a case, there is no apparent change in elevation, hence storage, over the full computing period. While any sequence over the three dates that is persistent (erosion, deposition or no change) will not produce any bias, any succession from scour to fill will introduce this complication. The morphologic coding of individual 20 metre grid cells permits such circumstances to be identified. Over the period 1952-1999, 23.2% of the total surface of difference area was found to exhibit non-persistent transitions. Nonetheless, continuity suggests that the gravel component of the bed material load should still be located within the gravel reach regardless of potential displacement between 1952 and 1999 (because sand may truly be transported past Mission, the same assertion does not necessarily hold). There are, however, transition sequences where mass continuity fails because wash material is discarded from the calculations. A simple case involves the transition island > bar > island which, for an individual grid cell, is equivalent to a net loss of 2.16 metres elevation (overbank erosion minus deposition thickness) over the intersurvey calculations, but the same cell is regarded as stable (no net change) between the end-member dates. Since many transitions involve either non-persistent bank erosion or deposition, the appearance of bias is introduced. A more detailed review of this problem is given in Appendix B.

The sediment budgets also present an apparently remarkable circumstance whereby the transport rate of gravel decreases in proportion to the length of the intersurvey interval. The sand fraction (hence total bed material load) displays a similar pattern (Figure 5-5). This occurrence could be the outcome of some time-dependent bias, of which undetected transport (compensating scour and fill) is the most likely source. If this negative bias is real, then extrapolating back to an even shorter period than 4 years may be a necessary means for estimating an unbiased transport rate (i.e. when there is little or no compensating scour and fill). However, it is not known what this interval actually is. Using the equation from a best-fit logarithmic trend-line for this adjustment, the annual influx of gravel is estimated as 1,064,000 m^3 per annum, a far greater influx rate than is estimated from the intersurvey budgets or from direct measurements.

There are, however, several reasons not to accept this result as being credible. First, the inverse relation between the transport rate and intersurvey interval may be spurious given that there

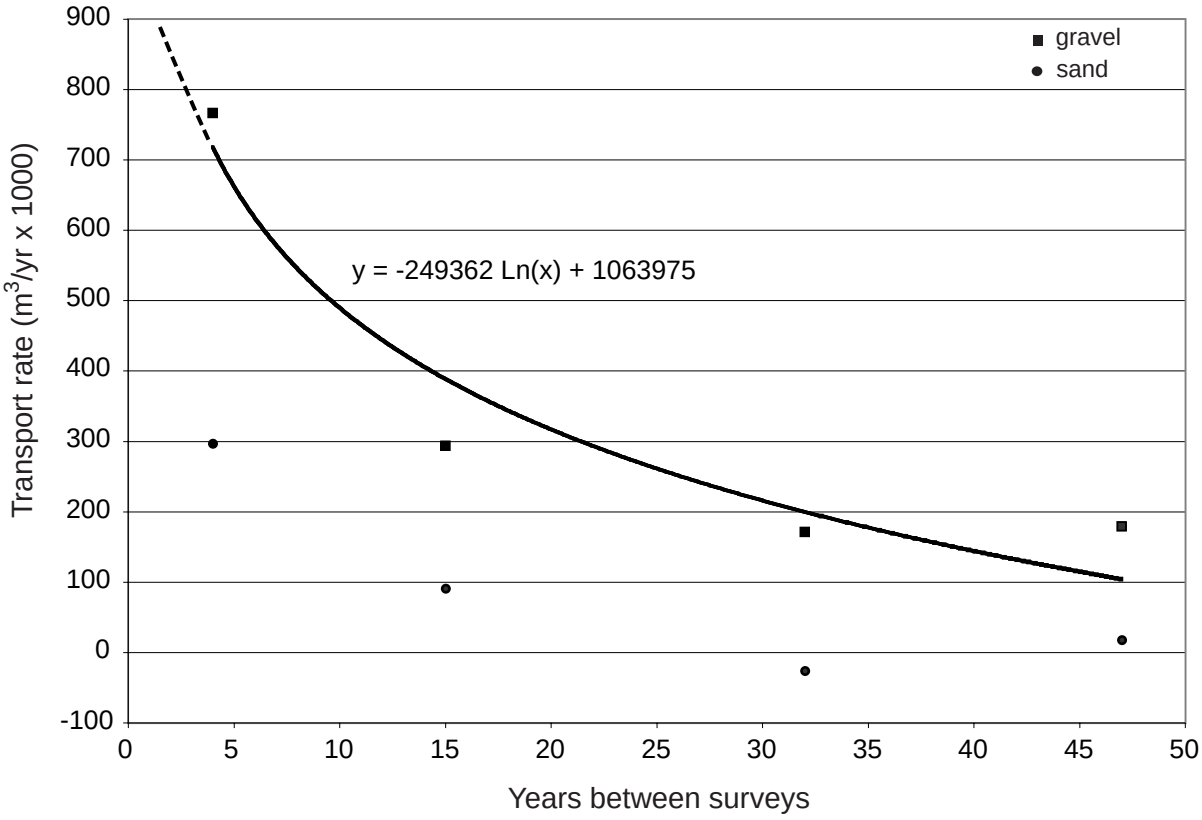

Figure 5-5. Net apparent influx of sand and gravel as a function of the intersurvey period. A best-fit (logarithmic) trend line is given for gravel.

are only 4 data points upon which the analysis is based. Second, the 1999-2003 surface of difference shows a number of very distinct erosional sites and it is not likely that large volumes of intervening compensating scour and fill could have occurred within only 4 years. Finally, extrapolating the unbiased estimates for gravel transport over 47 years (assuming this material does not exit the study reach) yields a total gravel deposition of 50 million m^3 between Mission and Agassiz. This volume works out to an average deposited depth of 1.25 metres over the entire active channel zone, or 2.5 metres over the main 500 metre wide thalweg zone. The total volume of dredged bed material (3.3 million m^3) is insufficient to compensate for this deposition (although this is lower bound estimate given undocumented mining). As well, the actual survey data (either gross volumetric changes or extracted cross-sections - see Chapter 4) simply do not support this quantity of aggradation. Such a large quantity of deposition would also create morphologic changes including a transition to a dominantly braided channel, yet there is no evidence of this. Nevertheless, the possibility for unmeasured sediment flux remains and is further examined in the discussion of sediment budget errors.

5.3.3 Distributed sediment budgets

Details on the distributed pattern or magnitude of erosion and deposition within the gravel reach are desirable for many direct management concerns, including where erosion might threaten local infrastructure or where deposition increases the local flood risk. Stored volume changes for the bed material load and for gravels are summarized on a cell-by-cell basis for the period 1952-99 in Figure 5-6. The volume changes summarize the constituent components of the sediment budget and display an alternating pattern of erosional and depositional lengths of channel. However, since displayed values are net changes, local details of complex scour and fill patterns within each computing cell are not revealed (refer to Figure 5-2). Eroding areas are typically associated with partly confined lengths of channel but are also common where the channel is shifting laterally, while depositing areas correspond to major bar/island complexes. Over shorter comparative intervals, the association between erosional and downstream depositional zones becomes more distinct and can be linked with changes to channel morphology (see Chapter 6). These relations are largely obscured over the full study interval.

Upstream of the Agassiz-Rosedale Bridge, most computing cells degraded from 1952 to 1999, although there is significant storage 5 to 6 km upstream on Tranmer Bar. In comparison, downstream cells are dominantly aggradational with major storage zones near Greyell, Harrison, and Yaalstrick Islands. Most lateral instability occurs in these areas because deposited sediments

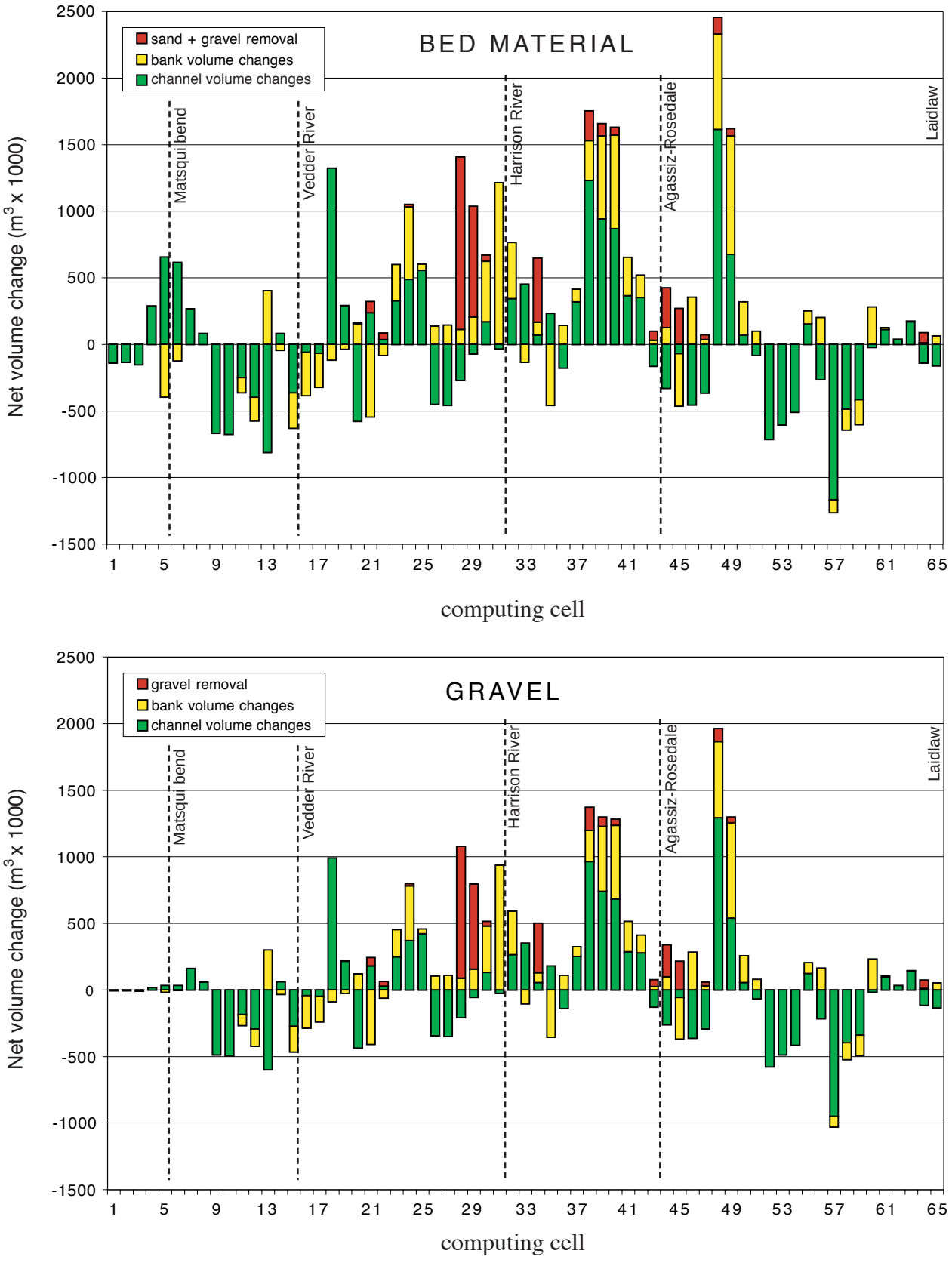

Figure 5-6. Cell-by-cell volumetric changes of bed material (top) and gravel (bottom) computed for the period 1952 to 1999 by direct difference of surveys.

force the channel to flow around them to maintain conveyance. Upstream of Vedder River, net stored gravel volumes are a scaled (74-80%) fraction of the total bed material load. Below Vedder River, the rapidly increasing sand fraction begins to dominate channel changes and there is a major zone of degradation with a corresponding (albeit more modest) downstream zone of deposition at Matsqui bend. In contrast, there is a major zone of gravel degradation, but no downstream storage of this material. It is reasonable that the sand fraction in the computing cells immediately downstream of Vedder may be underestimated and the [apparent] degradation of gravel is actually a loss of sand. This circumstance could also occur if the assumption of zero gravel transport past Mission is violated. The magnitude of this potential problem can be better illustrated by assuming the sand and gravel input to a cell is equal to the output from the next cell upstream and extending calculations on a cell-by-cell basis.

5.3.4 Accumulated sediment budgets

By accumulating stored volumes of coarse sand and gravel along each 1-km computing cell upstream from Mission, transport rates can be estimated at different locations within the gravel reach. The accumulated transport plots more clearly delineate the major storage and transport zones along the gravel-bed reach. Figure 5-7 plots the higher transport rate of bed material and gravel for 1999-2003 on a separate scale than for the other periods so trends in transport are more clearly discernible than when all data are plotted at equivalent scaling. The 1952-99 plot shows that the transport rate increases between Laidlaw and mid-Herrling Island because the channel is degrading, while all plots show that the transport rate generally declines downstream to Mission as sand and gravels become deposited. In the 1952 to 1984 period, there are three major and 2 minor deposition zones that match reasonably in location (and magnitude) with those identified by McLean and Church (1999). From 1984 to 1999 the transport rate declines fairly steadily from Agassiz-Rosedale bridge to Queens Bar and a second major deposition zone extends downstream to Sumas Mountain. The direct 1952 to 1999 comparison shows a fairly consistent decline in bed material transport that extends from Agassiz-Rosedale to Vedder River though several distinct depositional zones can be identified. Downstream of Vedder River, the transport rate generally increases to Mission, reflecting a net loss of bed material sands. The 1999-2003 sediment budget extends upstream to lower Herrling Island and reveals a consistent decline in the transport rate to Chilliwack Mountain (cell 21) though there is only modest storage between Agassiz-Rosedale and Gill Island (cell 37) and downstream of Harrison River. Below Chilliwack Mountain, the transport rate increases to cell 18, then declines to zero at Mission, paralleling the pattern in 1952-84.

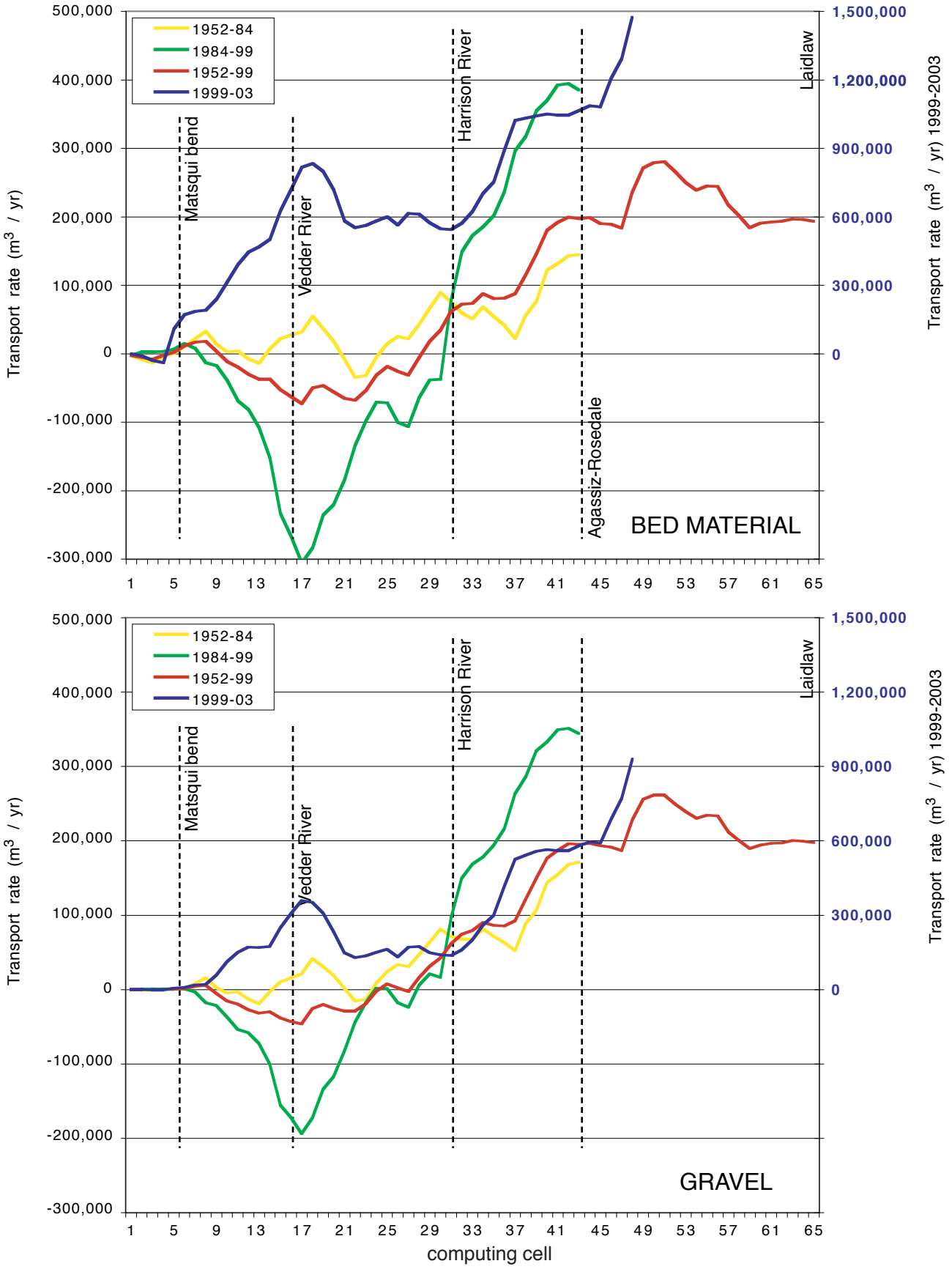

Figure 5-7. Downstream trends in bed material (top) and gravel (bottom) transport rates estimated from the sediment budget calculations. A falling plot (downstream direction) indicates a deposition zone, while a rising plot indicates an erosional zone.

With the exception of the most recent (1999-2003) results, the period gravel budgets present a troubling aspect whereby the calculated transport rate is negative for some computing cells (Figure 5-8). Assuming no gravel transport past Mission, negative transport implies that gravel is moving in an upstream direction, which is not physically reasonable. Since sands are mobilized past Mission, the bed material load may legitimately be negative if the magnitude of sand erosion exceeds that of deposition. Martin and Church (1995) encountered the problem of negative gravel transport on Vedder River and attributed the result to a violation of the zero downstream transport assumption. From 1952 to 1984, the rate of gravel 'loss' is equivalent to 10% of the gravel load entering the reach past Agassiz-Rosedale. The actual volume is relatively modest and could remain undetected if it remained along the channel bed downstream of Mission. However, the apparent losses in 1984-99 and 1952-99 represent respective losses of 64% and 25% of the total gravel influx. The magnitude of these volumes over many years should be manifested in the formation of gravelly barforms downstream, though none exist, at least on the surface. There exists the possibility that gravel lenses are transported along the bed in the active thalweg (where they can not be seen) or that gravels are buried by sand as the freshet wanes, but there is no simple means to sample the bed in this location to validate this supposition.

A second troubling aspect of the budgets is that the large negative transport rate near Vedder River (1984-1999 and 1952-1999) corresponds with a large positive transport rate at the same location (1999-2003). The sediment budget tables reveal mainly large negative bed changes in downstream cells for the early computing periods, and mainly large positive bed changes in the most recent computing period. Such a circumstance could occur if the 1999 bed elevations for these cells were too low, on average. The 1999 soundings were collected over a period of 11 days, with soundings collected on the second day of the survey covering cells 11 through 20 – the cells with the potential bed error. Although there is no reason to suspect any systematic bias in the 1999 survey, some human or computing error introduced during data collection, or post-processing, may have affected the accuracy of those survey points.

There are additional potential problems that could also lead to, or at least amplify, the magnitude of the negative transport rates. The major factors include unreported sand and gravel mining and uncertainty in the ratio of sand to gravel, especially among computing cells below Vedder River. The magnitude of each source of error, and an adjustment to correct for its effects, is examined below in a discussion of sediment budget errors.

5.4 Sediment budget errors: Negative transport rates

5.4.1 Violation of the zero transport assumption

Although previous attempts to calculate the sediment budget of lower Fraser River have assumed the gravel transport rate at Mission is zero, or at least negligible (McLean, 1990; McLean and Church, 1999; Church et al., 2001), sediment budget results presented herein show a potential conflict with this assertion. While there are no contemporary records, the WSC analysed particle size for 74 bedload and 124 bed material samples collected at Mission between 1966 and 1986. A brief review of these data shows clasts up to 32 mm collected in some samples, so it is reasonable that the percentage of smaller sized gravels moving along the bed may be significant.

Analysis of all bed material samples reveals that, over a range of flows up to 13,000 m^3/s, a consistent 15% of the bed material sampled at Mission is greater than 2 mm. For flows above 5000 m^3/s, the data reveal that 10% of the bedload is greater than 2 mm. This is the preferred figure for adjustment because bed material moves in intermittent suspension near Mission (McLean et al., 1999). The mean annual bedload transport rate at Mission (1966 - 1986) was reported by McLean et al. (1999) to be 154,000 tonnes / year, so the adjustment to the budget becomes 15,400 tonnes or 8800 m^3 per annum. This value, multiplied by the length of each survey interval, is added to the first cell of each accumulated sediment budget. As the unaccounted sum is modest in relation to the size of the gravel and bed material deficits for the periods 1984-1999 and 1952-1999, this adjustment has a minimal impact on eliminating the negative transport rates, but it is sufficiently important to reduce the bed material deficit for 1952-1984 by 25% and the gravel deficit by half. To fully eliminate negative transport rates from 1952 to 1984, 40% of the mean bedload transport measured at Mission would have to be added, but even this amount would not eliminate negative transport rates for the other periods. Consequently, there must be additional sources of error remaining.

5.4.2 Sounding errors

As reported, the possibility of data collection or processing errors for computing cells 11 through 20 may explain the anomalously large negative transport rates near Vedder River. A simple means to explore this issue is to ignore the 1999 survey and compute a sediment budget directly from the 1984 and 2003 surveys. This comparison yields a total bed material influx rate of 470,000 m^3/yr, or 350,000 m^3/yr of gravel (74%) - see Figure 5-8; Table 5-10. The transport rate declines rapidly to Harrison Bar as sediment is deposited, while a second, smaller, sedimentation zone extends from Wellington Bar to lower Yaalstrick Bar. Negative transport rates — the

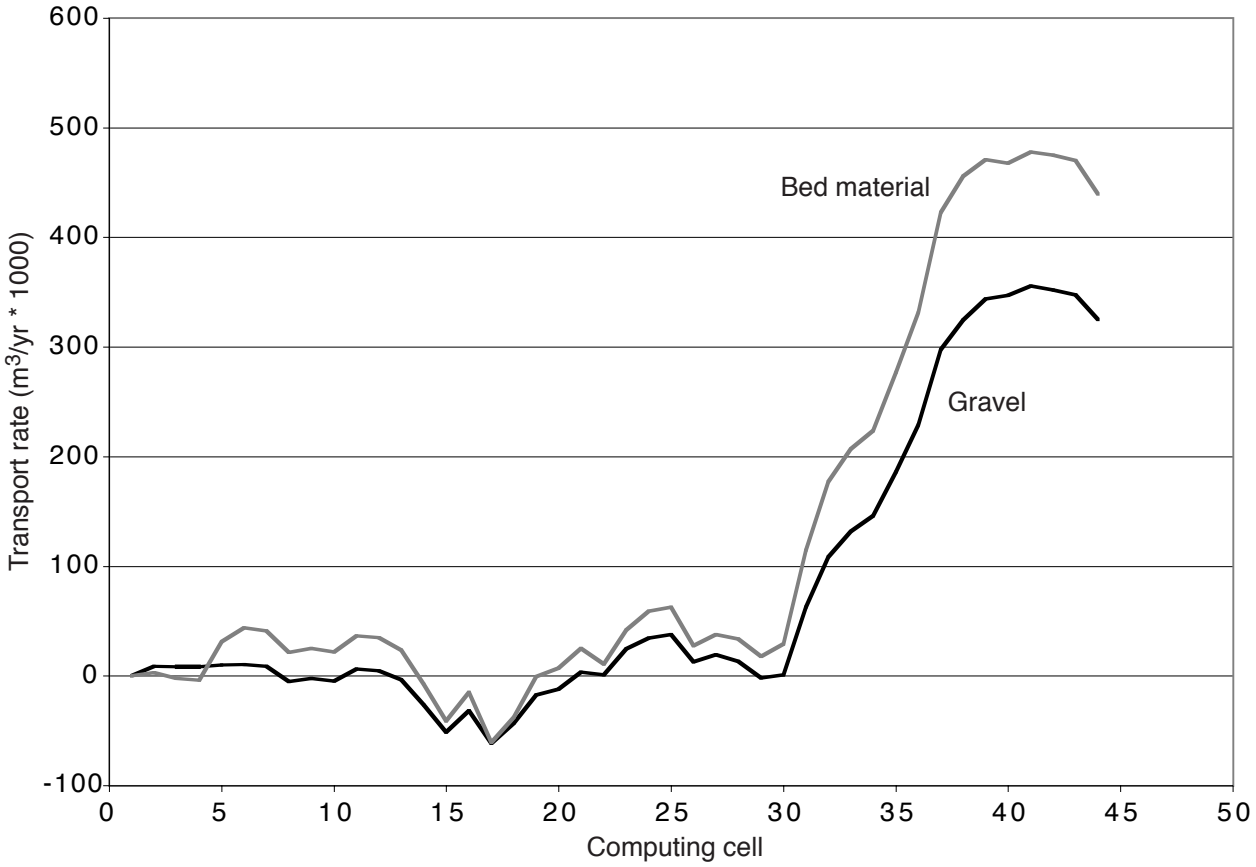

Figure 5-8. Downstream trends in bed material and gravel transport rates, 1984 to 2003. The plots include the correction factor for bedload transport past Mission.

consequence of accumulated sand and gravel deficits on the bed within cells 11 through 20 — remain, but are strongly abated. The net (total bed material) change in these cells is -279,000 m^3, compared with -1.11 million m^3 calculated for the sum of the 1984-1999 and 1999-2003 intersurvey budgets. These findings indicate that an error in the 1999 survey remains likely, but additional sources of error must also be considered since the comparison does not satisfy mass continuity. These are reviewed in the following sections of the chapter.

If the 1999 survey is in error, then it is necessary to estimate the magnitude of the error by increasing (adding sediment to) the 1984-1999 budget and decreasing (removing sediment from) the1999-2003 budget by some volume. Sediment must also be added to the 1952-1999 budget for consistency. This approach is considerably more efficient than changing the sounding elevations and recomputing topographic models of the bed. Since there is no obvious way to estimate this adjustment, an iterative procedure was developed whereby a fixed volume was added or subtracted from cells 11 to 20, and the effects were reviewed by examining the updated sediment budget plots (cf. Figure 5-7). To adjust the gravel budgets, the fixed volume was multiplied by 0.75 to correct for the sand fraction.

The largest accumulated negative transport rate for all budgets is roughly 4.5 million m^3 between 1984 and 1999. Distributing this volume over the 10 cells (11 to 20) reduces the magnitude of the annual bed material transport rate from -300,000 to -87,000 m^3/yr, and gravel transport from -220,000 to -63,000 m^3/yr. The running sum remains negative because there was more sand and gravel erosion than deposition in the first 10 computing cells. The adjustment also eliminates negative transport rates for both bed material and gravel for the 1952-1999 computing period. However, subtracting the same volume from cells 11 to 20 for the 1999-2003 budget creates such a large sediment 'deficit' that the accumulated transport rate for bed material and gravel attains a maximum of -564,000 and -520,000 m^3/yr respectively in cell 22, and the transport rate remains negative for all cells upstream to Agassiz-Rosedale Bridge. This adjustment is obviously too great, so was incrementally reduced by 50,000 m^3 to 150,000 m^3 per cell for the bed material budgets (and correspondingly, 112,500 m^3 for gravel budgets). Dividing 150,000 m^3 by the average cell area yields an estimated elevation adjustment of 15 cm. This value provides the best compromise between reducing the size of the negative transport rates and maintaining positive transport rates for the 1999-2003 computing period. The budget modifications also result in a minor reduction of the negative bias (from 1.12 to 1.10 times) between the direct sum of the intersurvey budgets and the direct difference of the 1952 and 1999 surveys. Updated transport rates

for sand and gravel are summarized in Table 5-4, and accumulated transport plots are shown in Figure 5-9.

Table 5-4. Average annual transport rates (m^3/yr) for sand, gravel and total bed material load incorporating adjustments for bedload transport at Mission and possible sounding errors in cells 11-20. Rates are equivalent to the influx past Agassiz-Rosedale Bridge.

Period	Gravel	Sand	Total bed material
1952 - 1984	180,000	-27,000	153,000 ± 16,000
1984 - 1999	378,000	116,000	494,000 ± 33,000
1999 - 2003	494,000	203,000	697,000 ± 41,000
1952 - 1999 (Direct)	212,000	25,000	237,000 ± 11,000
1952 - 1999 (Sum)	243,000	19,000	262,000 ± 15,000

The persistence of negative transport rates in lower computing cells remains a concern, especially from 1984 to 1999. The possibility of systematic sampling bias in 1984 must also be considered. Cells 10 to 17 were surveyed by a UBC crew using a much smaller, lighter boat than was used elsewhere along the main channel in 1984 (McLean, 1990) or in 1999 and 2003. This circumstance could yield measurements of the bed elevation that were too high on average relative to the mapping datum. Terrestrial surveying was additionally used near the mouth of Sumas River (cell 15) which is coincident with the largest sand and gravel deficit of any single computing cell. Although there is no available means to confirm that topographic points measured in 1984 may have been consistently biased, the precision of individual points was certainly lower relative to more recent measurements given contemporary survey techniques and available ground control. Indeed, McLean (1990, Table A3) shows that vertical closure errors in survey traverses were much larger between Sumas Mtn. and Chilliwack Mtn. than for the remainder of the channel. Given the very real likelihood that the large bed material deficit in this region from 1984 to 1999 is merely an artefact of survey imprecision, the local transport rate must be considered unreliable relative to that estimated between Agassiz-Rosedale and Chilliwack Mtn. Likely errors associated with the 1999 survey in this same region only compound the uncertainty, but there are also remaining possible sources of error.

5.4.3 Unreported dredging

An additional explanation for negative transport rates is that dredged gravel volumes have been underestimated. Removal volumes are known to be negatively biased before 1974 because of undocumented removals (Chapter 2). Adding an additional 800,000 cubic metres of unreported

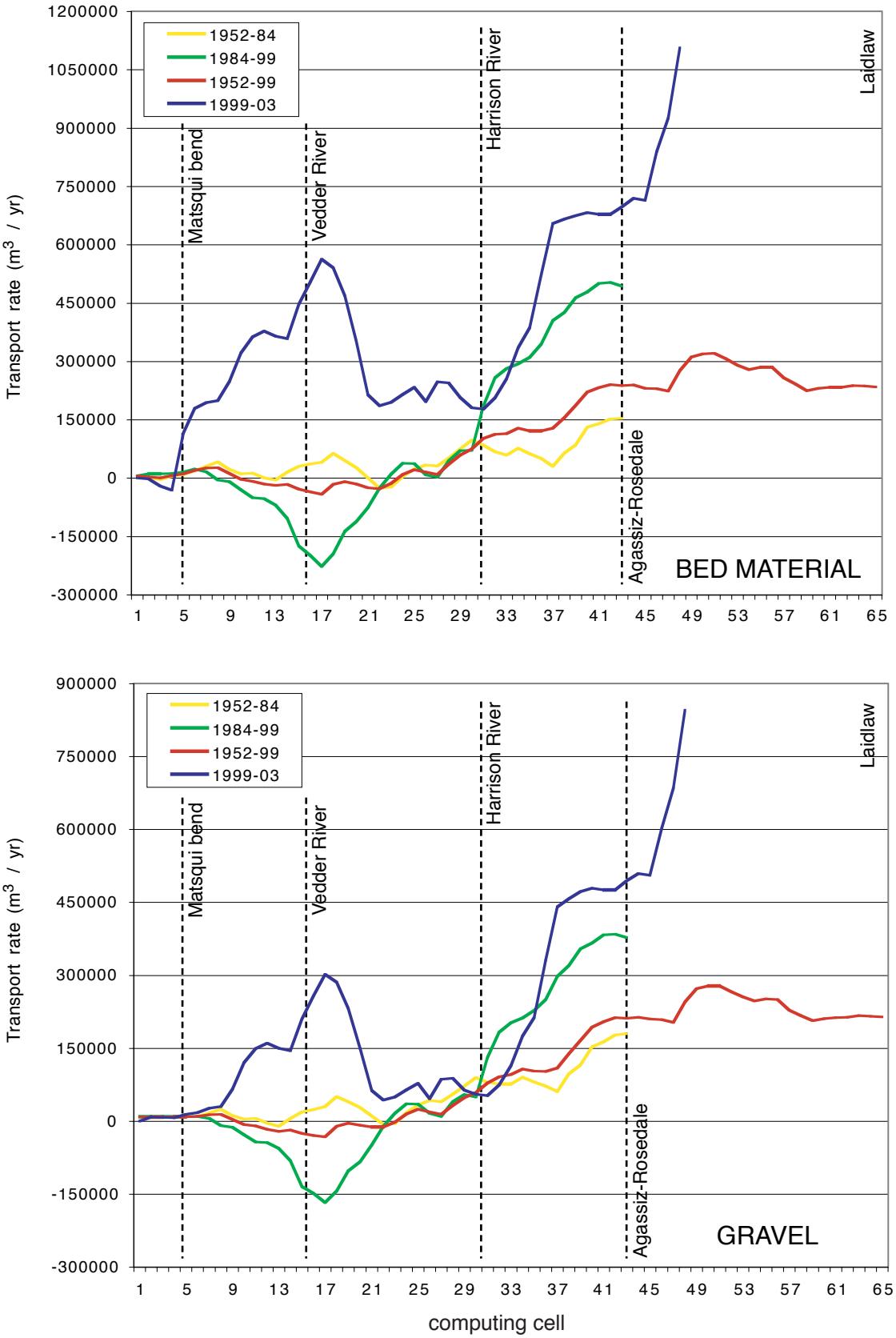

Figure 5-9. Downstream trends in bed material (top) and gravel (bottom) transport rates estimated from the adjusted sediment budget calculations. A falling plot indicates a deposition zone, while a rising plot indicates an erosional zone. Note the change of ordinate scaling.

gravel to the 1952-84 budget would eliminate the negative transport rate. This volume is comparable with that removed from a single removal site near lower Minto channel, hence appears credible. A similar adjustment would also correct the 1952-99 budget, but the required volume (2 million m^3) is considerably larger and more difficult to justify given available evidence. The remaining deficit is sufficiently large from 1984 to 1999 (3.4 million m^3) that unreported volumes of this magnitude are not believable given that permitting requirements were in place during this period. Therefore, an alternative consideration that could negatively bias the transport rate must also be examined.

5.4.4 Sand and gravel fractions

Perhaps the main factor that could produce negative transport rates is uncertainty in the actual sand and gravel fractions for individual computing cells, since this could inflate the volume change of sand or gravel, while suppressing the other. From 1952 to 1984, there is a loss of 1.8 million m^3 of gravel in cells 19-22 (near modern Wellington Bar) that likely accumulated in downstream cells (mainly 14 to 18). If this was assumed the true zero boundary of gravel transport — given that the proportion of sand in the deposits become increasingly large downstream — the accumulated transport rate upstream would remain positive and the influx at Agassiz-Rosedale would increase to 186,000 m^3/yr. While some modest amount of gravel probably is deposited below cell 14, the accumulation of a large gravel deficit in these cells produces a negative upstream transport rate. If most of this deficit actually reflected the erosion of bed material sands, the gravel budget would again remain positive. Conversely, an underestimate of the gravel fraction in cells which show apparent large stored volumes of sand would also correct budget problems. As discussed earlier, there has been minimal bed material sampling in the lower end of the reach because there are few emergent bars and no islands so the assigned sand / gravel fractions are imprecise.

Similar arguments obviously apply to the 1984-99 and 1952-99 budgets, but problem cells are more difficulty to identify. In 1952-99, there is a gravel deficit of 700,000 m^3 in cells 15 to 17, yet no obvious downstream storage of this material since there is a further sand and gravel deficit of 2.2 million m^3 in cells 9 to 14 with no corresponding zone of accumulation. A combination of uncertainty in the actual sand to gravel fraction and unrecorded gravel removals may explain most of the deficit. There is a further possibility that gravels have been prograding downstream over a former sand bed which would result in a negative bias of the gravel estimates. However, there are no bed samples for any date near 1952 that could resolve this question. From 1984 to 1999, a very

large (3.8 million m^3) deficit of both sands and gravel in cells 7 to 17 produces correspondingly large negative transport rates. While these cells are consistent in location with the transition to a sand-dominated bed, the possibility of sounding errors remains a significant concern.

5.5 Sediment budget errors: uncertainty of the estimates

5.5.1 Introduction

The development of the sediment budget approach is also subject to a number of errors and assumptions that produce uncertainty in the estimates. The main source of error relates to imprecision associated with the channel bed and banks modeling from available bathymetry and topographic data, since all following computations are based upon manipulations of these modeled surfaces. Errors in individual models can result in apparent erosion or deposition when none has actually occurred, inflating the magnitude of actual change. The budgeting approach to parse gross volumetric changes into estimates of sand, gravel and wash material introduces additional error since there is insufficient field sampling to confirm the actual proportions of these sediments as they vary along the gravel reach. While field samples collected in 1983 and 2000 show no significant difference in the sand fraction, there is considerable local scatter that could affect the precision by which the sand / gravel ratio is proportioned for any 1-km cell. The possibility that these ratios change over time must be recognized, but there is no physical means to consider this problem. The following discussion of different sources of error provides estimates of the error margins associated with the budgets, hence the probable range of sand and gravel transport influx for each computing period.

5.5.2 Survey error

Surveying and mapping errors limit the accuracy by which individual modeled surfaces can be represented (Chandler, 1999) and can be introduced at any stage from initial observation to presentation of results (Burrough and McDonnell, 1998). Lane et al. (1994) point out that individual points may be subject to random, gross, or systematic errors. Random errors refer to the precision within which repeat measurements yield the same result, gross errors relate to equipment or operator blunders and systematic errors (bias) refer to a persistent measurement problem, such as an incorrect datum. Since conventional approaches such as ground truthing for checking the quality of individual points are neither practical over such a large area nor feasible for historic data, it is difficult to quantify these errors. However, the vertical precision of the 1999 and 2003 sounding data is reported by PWGSC to be roughly ±10 cm, reflecting the accuracy with which the sounder can measure the bed depth relative to the water surface, and to relate the water surface

elevation to the geodetic datum. Horizontal positioning errors are larger (up to 2 metres) and are caused by imprecision in the GPS measurements. The altimetry data collected in 1999 by Terra Surveys Ltd. are reported to have the same vertical and horizontal precision as the sounding data. For comparison, McLean (1990) estimated maximum vertical errors for the 1984 survey at several tens of centimetres, while horizontal errors ranged from 2 to 5 metres at most locations. The precision of the 1952 soundings is unknown, but the error of photogrammetrically derived contour elevations is conventionally estimated as half the contour interval, or ±75 cm. Photogrammetric points appended to both the 1952 and 1984 surveys have similar errors, estimated as ±50 cm based on stereoplotter parameters and operator experience.

While the potential error associated with the surveys is substantial, it is reasonable to assume that the errors are random. Therefore, the effect of individual points is reduced as these errors become compensating or are averaged out by the Topogrid modeling procedure (Chapter 3). The possibility for gross errors was examined by producing TIN models from the bathymetry data and visually checking for anomalous values. The utility of this exercise is limited for the 1984 and 1999 datasets, but several digitizing and coding blunders were discovered, then corrected, for the 1952 dataset. Additional discussion of survey errors is pursued indirectly by examining the accuracy of the individual surface models into which the survey errors are incorporated, which may introduce bias into the final sediment budget results. Several different approaches for estimating modeling error are considered, following results presented in Ham and Church (2003).

5.5.3 Floodplain error

An empirical test of modeling bias was made by comparing interpolation errors on stable floodplain areas between survey dates. The surface models extend beyond the active channel zone (which includes channel scour and fill, bank erosion and bank deposition) to the floodplain. If it is assumed that the surface elevation of these areas has remained constant (although some amount of compaction or overbank deposition could technically occur) then any computed volumetric differences on these areas should correspond to model interpolation error. Extending this error over the entire active channel zone can therefore provide an indication of the volumetric error included in the sediment budget calculations. These errors are calculated by dividing computed volumetric changes over the stable floodplain by the corresponding area over which the measurements are made. These differences are -3 cm from 1952 to 1984, +12 cm from 1984 to 1999 and +3 cm between 1952 and 1999 (positive numbers indicate net aggradation). The 1999-2004 surface of difference shares common 2004 Lidar data on much of the stable floodplain so the floodplain error

is reduced overall to -0.4 cm. Most of the error occurs along modeled surface boundaries or where 1999 Lidar data overlap — elevation differences between the 2 floodplain surfaces is otherwise typically less than 1 mm (the maximum resolution of the models). The 1984-99 errors are significantly larger than for the remaining computing periods, but most of the error is limited to three adjacent computing cells. These cells are characterized by a paucity of elevation data near the edge of the floodplain and the channel bed, so model interpolation is poor in this region. Eliminating these three cells decreases the average floodplain error to 4 cm.

An approximation of the potential effect of these errors on the sediment budget calculations can be made by pooling the volumetric precision in bed elevation changes for individual computing cells. Each cell has an average area of the order 1,000,000 m^2, so the corresponding volumetric precision is roughly 30,000 - 40,000 m^3. From 1952 to 1984 and 1952 to 1999, the pooled error is estimated as 197,000 m^3, rising to 262,000 m^3 from 1984 to 1999. These figures represent roughly 5% of a sediment budget. The pooled error from 1999 to 2003 is reduced by a factor of 10x from the 1952-84 and 1952-99 periods. In general, floodplain modeling errors are probably smaller than bed modeling errors because a relatively flat surface can be modeled by a GIS with greater fidelity than a more complex topography. This is especially relevant for the 1999-2003 comparative period since the spatial density of the 2004 LiDAR data (even thinned from 1 m to 5 m) produces a much more accurate model of the floodplain than is possible for any previous comparative period, and is certainly more accurate than bed topography interpolated from spaced sounding lines. The reliability of individual bed models may therefore provide a better indication of survey error.

5.5.4 Channel Error

The comparison of different interpolation schemes in Chapter 3 provides a direct means to empirically examine modeling bias in the channel. It was demonstrated that the adopted Topogrid model yielded the smallest net difference between a reference surface and one derived from a thinned subset of the data used to create the reference surface. The calculated difference was 70,000 m^3 over a 7-km long test reach between Queen's Bar and the mouth of Harrison River (indicating an erosional bias). This test reach was selected because it is morphologically complex, hence should provide an indication of the maximum expected modeling error. By pooling this area by the number (9) of morphologic reaches between Mission and Agassiz, a total pooled error of 210,000 m^3 is estimated for an individual survey. Between successive surveys, the combined error becomes 297,000 m^3, similar to the pooled floodplain error. These results show that the volume

bias associated with the selected modeling procedure is actually not large relative to the volume of sediment that is mobilized within the gravel reach, hence does not appear to be a major factor limiting the reliability of the sediment budgets.

A further analysis of channel modeling error can be pursued by validating the precision of the actual channel models, or the difference in elevation between the modeled surface elevations and the survey elevations at corresponding locations. The bathymetry, altimetry and photogrammetric spot elevations were overlaid on the grids interpolated from these same data and the root mean square error was calculated for each survey. This measure actually quantifies accuracy in addition to precision unless the mean error of the data is zero (Lane et al., 2003). However, to calculate accuracy independently requires comparison to a true model, but none exists. The magnitude of RMS errors is partly dependent on the size of the modeled grid cells. As cell size increases, the possibility for multiple survey elevations to overlap the cell also increases. Consequently, large RMS values can occur where these points have disparate elevations, since the grid cell represents a single, spatially averaged elevation. Lowering cell size reduces this possibility, and also increases the total number of computing cells, further suppressing RMS values. However, cell sizes smaller than the average spatial density of the survey data can not reliably reproduce any real variability in channel morphologic complexity at the same spatial resolution.

The RMS error is calculated as ±0.97 m in 1952, ±0.85 m in 1984, ±0.79 m in 1999 for the 20 m grids. Errors are reduced to ±0.63 m in 1999 and ±0.56 m in 2003 using 10 m grids. The reduction in error occurs despite the use of original (non-thinned) bathymetry data so individual grid cells may spatially overlap more than 20 bathymetry points. The estimated precision between surveys is $E_{diff} = (E_1^2 + E_2^2)^{0.5}$ where E is the RMS of the successive surveys. This produces an estimate of ±1.29 m from 1952 to 1984, ±1.16 m from 1984 to 1999, ±1.25 m from 1952 to 1999 and ±0.84 m from 1999 to 2003. The RMS error of the mean difference in elevation is given as $E_{diff} / (n)^{0.5}$ where n is the number of independently determined points in each surface of difference. Since interpolated cell elevations are estimated from the value of surrounding points centered around each grid cell, n must be divided by 9 (the assumed number of points in a computing array). From 1952 to 1984, there are 13,410 independent cells, yielding a pooled error of ± 517,000 m^3, or ± 4.1 cm over the entire reach. This result is slightly better than the RMS error of ± 4.7 cm estimated by McLean (1990) and probably reflects the inclusion of bed and bank contours in the modeling procedure (see Chapter 3). Corresponding values for the period 1984 to

1999 are ± 491,000 m^3 (± 3.9 cm), ± 524,000 m^3 (± 4.1 cm) from 1952 to 1999 and ± 163,000 m^3 (± 1.3 cm) from 1999 to 2003. These values are also reported in Table 5-4. Although these errors are small relative to the total bed material influx for each period (5 to 10%) it is recognized that not all potential sources of error have been considered. Consequently, the total *actual* uncertainty is almost certainly larger than these *reported* values, but there is no obvious (and perhaps possible) manner by which all error terms can be calculated and propogated.

5.6 Comparison with other studies

Several previous attempts have been made to establish bedload influx to the lower gravel reach. Most of these efforts have been associated with the program of direct sediment sampling undertaken by the Water Survey of Canada from 1965 to 1987 in support of various river management concerns. Initial results were presented by Tywoniuk (1973) who found that coarse sediments aggraded in the Mission to Agassiz reach, but there was a much greater loss of sand and finer sediments. Tamburi (1979) made no attempt to compute annual loads for bedload transport, but demonstrated a highly non-linear relation between discharge and transport for material coarser than 6 mm at Agassiz. The first comprehensive review of the entire sampling program was given by McLean and Church (1986), while McLean and Tassone (1987) examined the precision of the WSC sampling procedures. McLean et al. (1999) also provided an overall assessment of the program in an attempt to make the results more accessible. The authors reported that 62 bedload measurements were collected at the Agassiz-Rosedale Bridge during freshet from 1968 to 1976. Adjustments were made to correct for sampler inefficiency and the proportion of fine (<6 mm) gravel that was not trapped, while annual loads were estimated from a rating curve based on daily measurements. McLean et al. (1999) estimated the average annual influx of bedload past Agassiz to be 227,000 tonnes per year, or 130,000 m^3 (adopting a gravel unit weight of 1.75 t/m^3). The bedload and bed material load can be considered equivalent at Agassiz, since few particles < 2 mm are trapped within the bed and these move in suspension once entrained (McLean et al., 1999).

Church (2001a) related estimated annual loads (reported in McLean et al., 1999) to the annual maximum daily flow, assumed to be the most relevant flow index given the highly nonlinear nature of sediment transport on Fraser River. The results yielded a smaller standard error of estimate because the annual rating curve exhibits less scatter. Church's back-transformed equation is given as:

$$G_a = 2.231x10^{-19}Q_{max}^{6.037}$$

where G_a is given in tonnes per year, and Q_{max} is given in m^3/s, measured at Hope gauge. Using this relation, annual loads at Agassiz can conveniently be calculated for different periods, and thus can be compared with the sediment budget estimates (see Table 5-5).

Table 5-5. Comparison of WSC transport estimates with sediment budget estimates for gravel. The budget estimates include the adjustment for bedload transport at Mission and the possible sounding errors in cells 11-20.

Period	WSC (total m^3)	WSC (m^3 / yr)	Budget (total m^3)	Budget (m^3 / yr)
1952 - 1984[1]	4,334,000	134,000	5,473,000	180,000
1984 - 1999[1]	1,668,000	97,000	4,409,000	378,000
1952 - 1999[1]	6,002,000	123,000	8,412,000	212,000
1999 - 2003[2]	670,000	168,000	3,067,000	494,000
1984 - 2003	2,338,000	186,000	6,604,000	350,000

1. Values reported in Church et al., (2001) using a unit weight of 1.75 t / m^3
2. Calculated from Hope flow records using relation given in Church (2002) and unit weight of 1.75 t / m^3

These results show that sediment budget estimates of gravel transport are consistently greater than the sediment transport estimates, although there is reasonably good correspondence from 1952 to 1984. Since sediment traps are known to underestimate total load because of sampling difficulties and trap inefficiencies, McLean et al. (1999) adjusted annual loads based on sampler calibrations and assigned an error bound of 40% around the annual estimates. Church et al. (2001) calculated pooled errors from these annual estimates to be 1.77 million m^3 over the 1952-1999 period. Incorporating this result, the upper bound estimate from the sediment transport data becomes 7.77 million m^3, which is close to the sediment budget estimate for the same period and almost certainly overlaps the lower bound estimate of the sediment budget error margins (these margins are presented in the following section of this chapter). However, the annual transport rate does not necessarily correlate with the size of the peak annual flow since the river is often transporting less material than its hydraulic capacity. Consequently, the transport rate can vary considerably for a given flow (McLean and Church, 1999). Certain channel configurations may therefore yield large volumes of available sediment and produce correspondingly high transport rates, at least for short durations. The present channel alignment whereby Tranmer Bar forces the current directly towards an eroding Herrling Island provides an example of this, and appears to explain the relatively high,

recent (1999-2003) transport rate. Regardless, the 1984 to 1999 sediment budget estimate remains suspiciously large.

The most comprehensive attempt to estimate sediment transport on the river was by McLean (1990) who contrasted the WSC measurements with a number of bedload formulae and morphologic estimates based on the 1952 and 1984 bathymetric surveys. Estimates for gravel influx at Agassiz-Rosedale were found to vary from a low of 70,000 m^3/yr using the Meyer-Peter and Muller equation, to a high of 150,000 m^3/yr following Neill's approach based on bank erosion. Some of the differences were attributed to the unequal time periods considered by each method. McLean and Church (1999) presented a re-examination of these methods and concluded that the long-term average annual inflow of gravel is 200,000 t/yr, or 114,000 m^3/yr (equivalent to the bulk volumetric rate of gravel input from the sediment budget). The figure of 180,000 m^3/yr presented herein is not unreasonable given this range of estimates. Although this number is larger than that given by McLean and Church (1999) using the same bathymetric data, the discrepancy can be attributed to several factors incorporated into this study, including a less restrictive computing mask, additional topographic data on bar surfaces, a larger adjustment for eroded overbank deposits and a different modeling algorithm.

A distributed gravel budget has also been computed by Li and Millar (2004) based on a depth-averaged 2-D numerical model. Five runs at different discharges were executed until equilibrium transport conditions were achieved. An annual transport rate based on 1999 river topography was calculated by integrating a discharge-transport rating curve with the flow duration histogram at boundaries that discriminate aggradational and degradational zones. The analysis yielded an estimate of 206,000 m^3/yr at Agassiz-Rosedale, which the authors suggested would be most directly comparable with the 1999-2003 morphologic budget estimates because of similar channel configuration. The underestimate of actual transport over this same period (compared to the sediment budget) occurs because the transport rate was effectively calculated as a function of discharge. However, the transport rate does not necessarily correlate with discharge, and is largely dependent on sediment availability, hence estimates of bed material transport may be accordingly over- or under-estimated during computing periods of several years or less. It is expected that these aberrations are averaged over periods of decades.

Given the issue of short-term variability, and uncertainty in the accuracy of the 1984 survey, the long-term sum (1952-1984 + 1984-1999) rate of 243,000 m^3/yr appears to be the best,

or at least most conservative, estimate of gravel influx for river management purposes. Construction of period sediment budgets is a complex task, and the numbers should not be considered as final. There are a variety of assumptions and errors that affect the reliability of the estimates, and there is no means at present to fully resolve all of the issues presented in this chapter. It does appear, however, that sediment influx has been much larger since 1984 than before that date, with corresponding implications for gravel and flood management. Additional surveys at fairly regular intervals will be required in the future to appraise this observation.

Table 5-6: Sediment budget - 1952 to 1984

		bed changes				bank changes												
Cell	bed area (m^2)	channel change	% sand	channel gravel	channel sand	erosion (sub 3m)	deposition (sub 0.84m)	bank total	bank gravel	bank sand	O/B sand (>0.177 mm)	gravel removal	sand removal	gravel sum (m^3)	sand sum (m^3)	total s+g (m^3)	Cell
1	105,543	-86,440	95	-4,322	-82,118	0	48	48	2	46	-526	0	0	-4,320	-82,599	-86,918	1
2	483,895	-195,763	95	-9,788	-185,975	0	1,792	1,792	90	1,702	-816	0	0	-9,699	-185,088	-194,787	2
3	437,985	-142,856	95	-7,143	-135,713	0	0	0	0	0	467	0	0	-7,143	-135,246	-142,389	3
4	372,880	286,127	95	14,306	271,820	0	75	75	4	72	-318	0	0	14,310	271,574	285,884	4
5	544,760	445,859	95	22,293	423,566	-293,103	47,011	-246,092	-12,305	-233,787	-50,632	0	0	9,988	139,148	149,136	5
6	629,784	419,511	95	20,976	398,535	-64,199	1,187	-63,012	-3,151	-59,861	-46,883	0	0	17,825	291,791	309,616	6
7	721,734	377,450	40	226,470	150,980	0	0	0	0	0	-9,435	0	0	226,470	141,545	368,015	7
8	800,881	372,310	30	260,617	111,693	0	0	0	0	0	-21,098	0	0	260,617	90,595	351,212	8
9	631,219	-584,136	27	-428,104	-156,031	0	0	0	0	0	-23,659	0	0	-428,104	-179,691	-607,795	9
10	760,305	-324,778	27	-238,580	-86,198	0	0	0	0	0	-33,927	0	0	-238,580	-120,124	-358,704	10
11	722,515	121,628	26	89,556	32,073	-62,691	0	-62,691	-46,160	-16,531	-20,948	0	0	43,396	-5,407	37,989	11
12	607,124	-338,891	26	-250,106	-88,784	-64,738	0	-64,738	-47,778	-16,961	35,131	0	0	-297,884	-70,613	-368,498	12
13	722,274	-415,525	26	-307,374	-108,151	0	134,272	134,272	99,325	34,948	93,377	0	0	-208,049	20,174	-187,875	13
14	545,692	751,176	26	556,948	194,228	-75,744	22,793	-52,952	-39,260	-13,691	-40,806	0	0	517,688	139,730	657,419	14
15	856,885	869,463	26	646,137	223,326	-308,990	3,618	-305,372	-226,936	-78,436	-88,685	0	0	419,202	56,205	475,407	15
16	982,603	273,600	26	203,793	69,808	-48,014	0	-48,014	-35,763	-12,250	-40,160	0	0	168,029	17,398	185,427	16
17	996,985	345,853	25	258,202	87,651	-100,725	0	-100,725	-75,197	-25,527	-113,206	597	203	183,602	-50,879	132,722	17
18	1,217,050	1,145,592	25	857,218	288,374	-270,619	0	-270,619	-202,498	-68,122	-133,464	0	0	654,720	86,789	741,509	18
19	1,344,434	-353,017	25	-264,757	-88,259	-95,730	0	-95,730	-71,796	-23,934	-128,480	1,725	575	-334,828	-240,098	-574,926	19
20	1,424,141	-569,560	25	-428,135	-141,425	0	60,385	60,385	45,391	14,994	-92,360	4,585	1,515	-378,159	-217,276	-595,435	20
21	1,140,624	-364,005	25	-274,243	-89,762	-486,929	38,258	-448,671	-338,031	-110,640	-108,529	57,259	18,741	-555,015	-290,190	-845,205	21
22	1,146,263	-607,697	24	-458,881	-148,816	-114,689	0	-114,689	-86,604	-28,086	-127,688	0	0	-545,485	-304,589	-850,074	22
23	1,248,533	-27,135	24	-20,536	-6,599	0	98,790	98,790	74,767	24,023	29,460	0	0	54,231	46,885	101,116	23
24	1,528,863	794,661	24	602,778	191,883	-34,266	168,602	134,336	101,898	32,437	-81,406	0	0	704,677	142,914	847,591	24
25	1,221,580	654,204	24	497,356	156,849	-10,342	7,954	-2,389	-1,816	-573	-25,353	0	0	495,539	130,923	626,462	25
26	1,036,854	403,807	24	307,683	96,124	0	146	146	112	35	-62,021	0	0	307,794	34,138	341,932	26
27	1,174,899	-166,094	24	-126,840	-39,254	0	54,609	54,609	41,703	12,906	13,472	0	0	-85,137	-12,876	-98,013	27
28	1,187,079	-61,051	23	-46,727	-14,324	0	60,500	60,500	46,305	14,195	6,195	499,790	153,210	499,368	159,276	658,644	28
29	1,119,470	126,516	23	97,049	29,468	0	43,566	43,566	33,419	10,147	42,086	415,453	126,147	545,921	207,848	753,769	29
30	1,498,734	565,829	23	435,006	130,822	0	113,526	113,526	87,278	26,248	4,281	35,365	10,635	557,649	171,986	729,636	30
31	1,463,718	-293,513	23	-226,153	-67,360	-110,569	0	-110,569	-85,194	-25,375	-29,857	0	0	-311,347	-122,592	-433,939	31
32	1,117,674	-97,404	23	-75,217	-22,187	-102,583	48,247	-54,336	-41,959	-12,377	-377,856	0	0	-117,176	-412,420	-529,597	32
33	844,961	218,083	23	168,780	49,303	-267,230	45,469	-221,762	-171,627	-50,135	-258,049	0	0	-2,847	-258,881	-261,728	33
34	643,393	171,437	22	132,973	38,464	0	92,866	92,866	72,030	20,836	-6,732	237,344	68,656	442,347	121,224	563,571	34
35	665,710	-242,543	22	-188,540	-54,003	-156,736	0	-156,736	-121,838	-34,898	-53,061	0	0	-310,377	-141,962	-452,339	35
36	1,428,674	-354,184	22	-275,929	-78,255	0	0	0	0	0	-48,563	0	0	-275,929	-126,818	-402,747	36
37	1,127,393	-435,767	22	-340,231	-95,535	0	0	0	0	0	-204,953	0	0	-340,231	-300,488	-640,719	37
38	1,118,303	1,260,010	22	985,926	274,084	0	0	0	0	0	-393,468	173,709	48,291	1,159,636	-71,094	1,088,542	38
39	931,040	346,121	22	271,423	74,698	0	289,629	289,629	227,123	62,506	-51,488	72,145	19,855	570,691	105,571	676,262	39
40	1,037,152	1,404,870	21	1,104,080	300,790	0	102,922	102,922	80,886	22,036	-60,991	2,986	814	1,187,953	262,648	1,450,601	40
41	797,303	417,917	21	329,154	88,764	-17,588	34,643	17,055	13,433	3,622	-139,679	0	0	342,587	-47,293	295,293	41
42	546,391	964,026	21	760,920	203,106	-417,213	18,865	-398,348	-314,422	-83,926	-193,422	0	0	446,498	-74,243	372,256	42
43	537,182	50,556	21	39,991	10,565	0	0	0	0	0	-60,585	52,999	14,001	92,989	-36,019	56,971	43
R1-43	39,470,480	7,126,250		4,918,025	2,208,224	-3,102,699	1,489,775	-1,612,924	-998,567	-614,357	-2,904,634	1,553,958	462,642	5,473,416	-848,124	4,625,292	R1-43

Table 5-7: Sediment budget - 1984 to 1999

		bed changes				bank changes											
Cell	area (m^2)	channel change	% sand	channel gravel	channel sand	erosion (sub 3m)	deposition (sub 0.84m)	bank total	bank gravel	bank sand	O/B sand (>0.177 mm)	gravel removal	sand removal	gravel sum (m^3)	sand sum (m^3)	total s+g (m^3)	Cell
1	106,741	-48,635	95	-2,432	-46,203	0	0	0	0	0	147	0	0	-2,432	-46,056	-48,487	1
2	494,455	82,881	95	4,144	78,736	0	0	0	0	0	779	0	0	4,144	79,515	83,659	2
3	447,283	-328	95	-16	-312	0	0	0	0	0	638	0	0	-16	327	310	3
4	375,795	5,144	95	257	4,886	0	0	0	0	0	982	0	0	257	5,868	6,125	4
5	604,410	52,096	95	2,605	49,491	0	19	19	1	18	147	0	0	2,606	49,656	52,262	5
6	677,044	124,390	95	6,220	118,171	0	216	216	11	205	1,225	0	0	6,230	119,600	125,831	6
7	747,773	-105,554	40	-63,333	-42,222	0	0	0	0	0	-23	0	0	-63,333	-42,244	-105,577	7
8	829,248	-314,575	30	-220,202	-94,372	0	1,275	1,275	892	382	-1,972	0	0	-219,310	-95,962	-315,272	8
9	658,920	-69,325	27	-50,807	-18,518	0	628	628	460	168	-259	0	0	-50,347	-18,609	-68,955	9
10	806,125	-315,853	27	-232,024	-83,829	0	0	0	0	0	643	0	0	-232,024	-83,186	-315,210	10
11	740,098	-449,745	26	-331,150	-118,596	0	0	0	0	0	-2,049	0	0	-331,150	-120,644	-451,794	11
12	655,217	-188,703	26	-139,266	-49,437	0	0	0	0	0	-4,301	0	0	-139,266	-53,738	-193,004	12
13	715,199	-395,300	26	-292,413	-102,887	0	177	177	131	46	-763	0	0	-292,282	-103,603	-395,886	13
14	589,780	-656,839	26	-487,003	-169,836	0	0	0	0	0	-3,854	0	0	-487,003	-173,689	-660,693	14
15	954,076	-1,222,480	26	-908,480	-314,000	0	0	0	0	0	4,397	0	0	-908,480	-309,603	-1,218,083	15
16	1,040,531	-35,765	26	-26,640	-9,125	-394,081	0	-394,081	-293,533	-100,548	-82,736	0	0	-320,173	-192,409	-512,582	16
17	1,117,195	-481,197	25	-359,245	-121,952	-60,835	108	-60,726	-45,336	-15,390	-32,325	0	0	-404,581	-169,668	-574,249	17
18	1,329,174	294,607	25	220,447	74,160	0	30,596	30,596	22,894	7,702	9,094	0	0	243,341	90,956	334,297	18
19	1,297,617	451,885	25	338,907	112,978	0	225,284	225,284	168,959	56,324	45,200	0	0	507,867	214,503	722,370	19
20	1,586,769	228,709	25	171,920	56,790	0	166	166	125	41	-3,087	0	0	172,044	53,744	225,789	20
21	1,289,589	655,965	25	494,207	161,758	-1,241	23,015	21,774	16,405	5,369	-140,869	5,123	1,677	515,735	27,935	543,669	21
22	1,256,391	726,596	24	548,664	177,933	-8,051	6,910	-1,140	-861	-279	-25,560	35,868	11,632	583,671	163,725	747,396	22
23	1,173,212	450,744	24	341,135	109,610	0	72,693	72,693	55,016	17,677	17,581	0	0	396,150	144,868	541,018	23
24	1,344,348	363,750	24	275,917	87,833	0	0	0	0	0	26,447	15,171	4,829	291,088	119,110	410,198	24
25	1,163,611	-6,992	24	-5,315	-1,676	0	0	0	0	0	-4,885	0	0	-5,315	-6,561	-11,877	25
26	957,233	-377,085	24	-287,322	-89,763	0	0	0	0	0	-49,465	0	0	-287,322	-139,228	-426,550	26
27	1,040,860	-118,270	24	-90,319	-27,951	0	0	0	0	0	22,919	0	0	-90,319	-5,033	-95,352	27
28	965,073	-60,949	23	-46,649	-14,300	0	0	0	0	0	50,195	491,371	150,629	444,722	186,524	631,246	28
29	731,208	4,898	23	3,757	1,141	0	0	0	0	0	92,803	223,644	67,906	227,401	161,850	389,251	29
30	1,037,948	-50,577	23	-38,884	-11,694	-41,540	0	-41,540	-31,936	-9,604	109,714	0	0	-70,820	88,416	17,597	30
31	973,838	1,349,104	23	1,039,491	309,613	0	228,058	228,058	175,720	52,338	136,171	0	0	1,215,211	498,122	1,713,333	31
32	1,285,608	1,012,155	23	781,601	230,554	0	0	0	0	0	69,581	0	0	781,601	300,134	1,081,736	32
33	1,084,795	370,701	23	286,895	83,806	0	0	0	0	0	-16,870	0	0	286,895	66,936	353,831	33
34	648,575	12,637	22	9,802	2,835	0	0	0	0	0	-1,608	135,736	39,264	145,538	40,491	186,029	34
35	614,565	587,388	22	456,603	130,785	-392,494	104,001	-288,493	-224,259	-64,234	-50,300	0	0	232,345	16,251	248,596	35
36	1,187,823	386,391	22	301,020	85,371	0	50,283	50,283	39,173	11,110	80,212	0	0	340,193	176,692	516,885	36
37	1,215,904	907,498	22	708,543	198,955	0	0	0	0	0	-3,437	0	0	708,543	195,518	904,061	37
38	1,380,573	432,158	22	338,153	94,005	0	0	0	0	0	-117,066	0	0	338,153	-23,061	315,092	38
39	1,299,809	663,833	22	520,568	143,265	-3,839	0	-3,839	-3,010	-828	-93,159	0	0	517,558	49,278	566,836	39
40	1,033,797	176,544	21	138,745	37,799	0	0	0	0	0	-11,020	44,167	12,033	182,912	38,812	221,724	40
41	871,156	317,871	21	250,357	67,514	0	0	0	0	0	15,335	0	0	250,357	82,850	333,207	41
42	631,587	28,691	21	22,646	6,045	0	0	0	0	0	9,400	0	0	22,646	15,445	38,091	42
43	594,330	-133,434	21	-105,549	-27,884	0	1,494	1,494	1,182	312	-14,153	0	0	-104,367	-41,725	-146,092	43
R1-43	39,555,284	4,655,031		3,575,554	1,079,477	-902,081	744,922	-157,159	-117,967	-39,192	33,849	951,080	287,970	4,408,667	1,362,104	5,770,771	R1-43

Table 5-8: Sediment budget - 1952 to 1999

		bed changes				bank changes											
Cell	area (m^2)	channel change	% sand	channel gravel	channel sand	erosion (sub 3m)	deposition (sub 0.84m)	bank total	bank gravel	bank sand	O/B sand (>0.177 mm)	gravel removal	sand removal	gravel sum (m^3)	sand sum (m^3)	total s+g (m^3)	Cell
1	105,179	-138,245	95	-6,912	-131,333	0	362	362	18	344	357	0	0	-6,894	-130,632	-137,526	1
2	482,079	-133,395	95	-6,670	-126,725	0	5,033	5,033	252	4,782	2,997	0	0	-6,418	-118,947	-125,365	2
3	437,314	-152,327	95	-7,616	-144,710	0	0	0	0	0	3,460	0	0	-7,616	-141,251	-148,867	3
4	372,511	288,660	95	14,433	274,227	0	0	0	0	0	604	0	0	14,433	274,831	289,264	4
5	549,284	653,942	95	32,697	621,245	-437,146	38,676	-398,471	-19,924	-378,547	-51,877	0	0	12,774	190,821	203,594	5
6	626,766	615,558	95	30,778	584,780	-138,008	12,586	-125,422	-6,271	-119,151	-47,189	0	0	24,507	418,440	442,946	6
7	721,655	267,010	40	160,206	106,804	0	0	0	0	0	-6,169	0	0	160,206	100,634	260,840	7
8	800,690	80,037	30	56,026	24,011	0	0	0	0	0	-26,482	0	0	56,026	-2,471	53,555	8
9	631,089	-667,285	27	-489,043	-178,242	0	0	0	0	0	-19,264	0	0	-489,043	-197,506	-686,549	9
10	762,666	-676,335	27	-496,832	-179,503	0	0	0	0	0	-23,936	0	0	-496,832	-203,439	-700,271	10
11	728,274	-250,859	26	-184,709	-66,150	-114,824	0	-114,824	-84,545	-30,279	-24,663	0	0	-269,254	-121,092	-390,346	11
12	631,705	-398,307	26	-293,957	-104,351	-178,084	0	-178,084	-131,428	-46,655	74,279	0	0	-425,385	-76,727	-502,112	12
13	742,715	-811,601	26	-600,362	-211,240	0	402,615	402,615	297,824	104,791	88,196	0	0	-302,537	-18,253	-320,790	13
14	545,030	80,091	26	59,383	20,709	-89,838	42,748	-47,090	-34,914	-12,176	-42,283	0	0	24,468	-33,750	-9,282	14
15	854,257	-365,873	26	-271,897	-93,976	-273,476	7,598	-265,878	-197,586	-68,292	-92,728	0	0	-469,483	-254,996	-724,479	15
16	1,026,199	-59,995	26	-44,688	-15,308	-327,978	0	-327,978	-244,296	-83,682	-91,902	0	0	-288,984	-190,892	-479,876	16
17	995,226	-67,842	25	-50,648	-17,193	-257,748	334	-257,414	-192,176	-65,238	-143,026	597	203	-242,227	-225,254	-467,481	17
18	1,188,927	1,321,780	25	989,055	332,725	-170,964	51,362	-119,601	-89,495	-30,107	-121,921	0	0	899,561	180,698	1,080,258	18
19	1,158,355	286,897	25	215,168	71,728	-172,074	133,496	-38,578	-28,933	-9,645	-83,801	1,725	575	187,960	-21,142	166,818	19
20	1,427,735	-578,662	25	-434,978	-143,685	0	152,844	152,844	114,892	37,952	-28,992	4,585	1,515	-315,500	-133,210	-448,711	20
21	1,179,466	237,332	25	178,807	58,525	-614,685	66,853	-547,833	-412,740	-135,093	-202,085	62,382	20,418	-171,551	-258,235	-429,786	21
22	1,129,061	35,236	24	26,607	8,629	-84,805	0	-84,805	-64,038	-20,768	-121,170	35,868	11,632	-1,563	-121,677	-123,240	22
23	1,157,396	326,782	24	247,317	79,465	0	270,708	270,708	204,879	65,829	62,544	0	0	452,195	207,838	660,034	23
24	1,248,368	485,807	24	368,502	117,305	0	543,646	543,646	412,374	131,271	9,514	15,171	4,829	796,047	262,921	1,058,968	24
25	1,133,537	553,252	24	420,607	132,645	0	46,689	46,689	35,495	11,194	-12,477	0	0	456,101	131,362	587,463	25
26	888,176	-450,143	24	-342,988	-107,154	0	136,274	136,274	103,835	32,439	-10,166	0	0	-239,154	-84,880	-324,034	26
27	1,030,108	-458,164	24	-349,884	-108,280	0	142,569	142,569	108,875	33,694	50,044	0	0	-241,009	-24,542	-265,551	27
28	933,607	-269,375	23	-206,173	-63,202	0	111,441	111,441	85,294	26,147	76,867	991,161	303,839	870,282	343,651	1,213,932	28
29	712,461	-71,976	23	-55,212	-16,764	0	202,241	202,241	155,136	47,105	146,111	639,097	194,053	739,021	370,505	1,109,526	29
30	999,054	168,167	23	129,286	38,881	-27,921	483,400	455,479	350,170	105,309	98,877	35,365	10,635	514,820	253,703	768,523	30
31	908,136	-34,189	23	-26,343	-7,846	-37,459	1,250,371	1,212,912	934,555	278,357	106,593	0	0	908,212	377,104	1,285,316	31
32	835,266	341,712	23	263,875	77,837	0	421,512	421,512	325,498	96,014	-269,286	0	0	589,373	-95,436	493,937	32
33	800,935	452,340	23	350,077	102,263	-257,198	119,982	-137,216	-106,195	-31,021	-271,073	0	0	243,882	-199,831	44,051	33
34	607,604	67,822	22	52,605	15,217	0	97,186	97,186	75,381	21,805	15,886	373,080	107,920	501,067	160,828	661,894	34
35	559,180	230,080	22	178,851	51,228	-690,342	229,582	-460,760	-358,170	-102,591	-95,859	0	0	-179,318	-147,221	-326,540	35
36	1,128,482	-178,097	22	-138,747	-39,350	0	139,705	139,705	108,838	30,867	69,308	0	0	-29,910	60,825	30,915	36
37	1,016,240	318,709	22	248,837	69,872	0	93,815	93,815	73,248	20,568	-113,993	0	0	322,084	-23,553	298,531	37
38	976,715	1,229,069	22	961,716	267,353	0	300,319	300,319	234,992	65,327	-457,680	173,709	48,291	1,370,418	-76,709	1,293,708	38
39	840,067	941,589	22	738,380	203,209	0	621,529	621,529	487,394	134,135	-173,830	72,145	19,855	1,297,919	183,369	1,481,288	39
40	849,411	868,125	21	682,255	185,870	0	701,568	701,568	551,359	150,209	-44,032	47,154	12,846	1,280,768	304,894	1,585,662	40
41	718,940	363,007	21	285,906	77,101	0	290,024	290,024	228,424	61,600	-101,746	0	0	514,330	36,955	551,285	41
42	414,306	350,150	21	276,379	73,771	-266,617	436,348	169,730	133,971	35,760	-158,053	0	0	410,350	-48,522	361,828	42
43	528,159	-162,769	21	-128,755	-34,015	0	29,395	29,395	23,252	6,143	-60,948	52,999	14,001	-52,503	-74,819	-127,322	43
44	615,997	-328,943	21	-260,765	-68,178	0	124,287	124,287	98,527	25,760	-1,591	237,939	62,211	75,701	18,202	93,903	44
45	623,688	-72,173	21	-57,337	-14,835	-399,468	4,389	-395,079	-313,869	-81,210	-221,394	214,500	55,500	-156,706	-261,941	-418,646	45
46	1,248,249	-455,036	20	-362,279	-92,757	0	353,111	353,111	281,131	71,980	61,213	0	0	-81,148	40,436	-40,712	46
47	1,568,237	-365,144	20	-291,335	-73,808	0	35,122	35,122	28,022	7,099	20,753	27,127	6,873	-236,185	-39,083	-275,269	47
48	1,238,489	1,614,182	20	1,290,659	323,522	0	715,238	715,238	571,886	143,352	-1,201	98,348	24,652	1,960,893	490,325	2,451,218	48
49	1,012,703	672,998	20	539,263	133,735	0	891,794	891,794	714,581	177,213	50,526	43,269	10,731	1,297,113	372,204	1,669,318	49
50	706,241	68,228	20	54,787	13,441	0	248,302	248,302	199,386	48,917	59,129	0	0	254,172	121,488	375,660	50
51	509,400	-82,218	20	-66,162	-16,057	0	98,617	98,617	79,358	19,259	65,822	0	0	13,196	69,025	82,221	51
52	1,021,036	-714,512	19	-576,193	-138,319	0	0	0	0	0	44,796	0	0	-576,193	-93,523	-669,716	52
53	939,529	-603,867	19	-488,000	-115,867	0	0	0	0	0	-178,383	0	0	-488,000	-294,250	-782,250	53
54	1,031,268	-510,143	19	-413,132	-97,011	0	0	0	0	0	-14,535	0	0	-413,132	-111,547	-524,678	54
55	896,256	151,451	19	122,909	28,542	0	98,604	98,604	80,022	18,582	29,866	0	0	202,931	76,990	279,920	55
56	951,185	-263,733	19	-214,482	-49,251	0	200,793	200,793	163,296	37,497	53,428	0	0	-51,186	41,675	-9,511	56
57	931,581	-1,166,805	19	-950,905	-215,900	-173,299	75,134	-98,165	-80,001	-18,164	-9,632	0	0	-1,030,906	-243,696	-1,274,602	57
58	740,250	-487,900	18	-398,455	-89,444	-157,520	0	-157,520	-128,642	-28,877	-100,507	0	0	-527,098	-218,829	-745,926	58
59	1,213,784	-417,360	18	-341,561	-75,799	-289,219	101,404	-187,815	-153,705	-34,110	-201,362	0	0	-495,266	-311,271	-806,537	59
60	847,341	-21,851	18	-17,920	-3,931	0	279,595	279,595	229,294	50,300	32,430	0	0	211,374	78,800	290,174	60
61	681,076	110,517	18	90,824	19,694	0	15,025	15,025	12,348	2,677	-28,009	0	0	103,171	-5,638	97,534	61
62	484,233	37,618	18	30,979	6,639	0	446	446	367	79	-6,476	0	0	31,346	242	31,588	62
63	409,336	168,848	17	139,338	29,510	0	4,508	4,508	3,720	788	-715	0	0	143,058	29,583	172,641	63
64	478,153	-138,399	17	-114,447	-23,952	0	11,012	11,012	9,107	1,906	4,635	62,847	13,153	-42,493	-4,258	-46,751	64
65	549,080	-161,714	17	-134,004	-27,711	-15,530	76,710	61,180	50,696	10,483	-5,653	0	0	-83,307	-22,880	-106,187	65
1-43	35,382,330	4,637,713		2,831,340	1,806,373	-4,139,168	7,582,810	3,443,643	3,075,244	368,398	-2,090,994	2,505,037	750,613	8,411,621	834,390	9,246,012	1-43
44-65	18,697,111	-2,965,956		-2,418,219	-547,737	-1,035,036	3,334,090	2,299,054	1,845,523	453,532	-346,860	684,031	173,119	111,335	-267,946	-156,612	44-65
1-65	54,079,441	1,671,757		413,121	1,258,636	-5,174,203	10,916,900	5,742,697	4,920,767	821,930	-2,437,854	3,189,069	923,731	8,522,956	566,444	9,089,400	1-65

Table 5-9: Sediment budget - 1999 to 2003

		bed changes				bank changes											
Cell	area (m^2)	channel change	% sand	channel gravel	channel sand	erosion (sub 3m)	deposition (sub 0.84m)	bank total	bank gravel	bank sand	O/B sand (>0.177 mm)	gravel removal	sand removal	gravel sum (m^3)	sand sum (m^3)	total s+g (m^3)	Cell
1			95	0	0	0	0	0	0	0	0	0	0	0	0	0	1
2	491,616	-47042	95	-2,352	-44,690	0	0	0	0	0	1,326	0	0	-2,352	-43,364	-45,716	2
3	446,169	-71264	95	-3,563	-67,701	0	0	0	0	0	-1,538	0	0	-3,563	-69,238	-72,801	3
4	378,771	-40512	95	-2,026	-38,486	0	0	0	0	0	0	0	0	-2,026	-38,486	-40,512	4
5	614,312	586443	95	29,322	557,121	0	0	0	0	0	112	0	0	29,322	557,233	586,555	5
6	681,529	254728	95	12,736	241,991	0	0	0	0	0	-419	0	0	12,736	241,572	254,308	6
7	753,194	59711	40	35,827	23,884	0	0	0	0	0	0	0	0	35,827	23,884	59,711	7
8	839,439	20336	30	14,235	6,101	0	0	0	0	0	0	0	0	14,235	6,101	20,336	8
9	663,649	196513	27	144,022	52,492	0	0	0	0	0	0	0	0	144,022	52,492	196,513	9
10	816,715	294716	27	216,497	78,219	0	0	0	0	0	0	0	0	216,497	78,219	294,716	10
11	764,404	311400	26	229,285	82,115	0	0	0	0	0	64	0	0	229,285	82,179	311,465	11
12	632,324	210799	26	155,573	55,226	0	0	0	0	0	59	0	0	155,573	55,285	210,858	12
13	706,619	95971	26	70,992	24,979	0	0	0	0	0	633	0	0	70,992	25,612	96,605	13
14	598,314	127275	26	94,366	32,909	0	0	0	0	0	0	0	0	94,366	32,909	127,275	14
15	963,466	501633	26	372,786	128,847	0	0	0	0	0	0	0	0	372,786	128,847	501,633	15
16	1,144,653	520425	26	387,641	132,784	-114,065	0	-114,065	-84,962	-29,103	-24,414	0	0	302,679	79,267	381,946	16
17	1,157,859	387661	25	289,414	98,247	0	0	0	0	0	-4,729	0	0	289,414	93,518	382,932	17
18	1,329,963	63429	25	47,462	15,967	0	0	0	0	0	-615	0	0	47,462	15,351	62,814	18
19	1,291,600	-135751	25	-101,812	-33,940	0	0	0	0	0	-2,844	0	0	-101,812	-36,783	-138,595	19
20	1,604,463	-164659	25	-123,774	-40,886	-127,421	0	-127,421	-95,782	-31,639	-29,819	0	0	-219,556	-102,344	-321,900	20
21	1,445,963	-199022	25	-149,944	-49,078	-258,849	0	-258,849	-195,018	-63,831	-88,930	0	0	-344,962	-201,838	-546,800	21
22	1,256,428	-102606	24	-77,479	-25,127	0	0	0	0	0	-10,981	0	0	-77,479	-36,108	-113,587	22
23	1,151,379	16364	24	12,385	3,979	0	17,986	17,986	13,612	4,374	1,747	0	0	25,996	10,099	36,096	23
24	1,310,159	76255	24	57,842	18,413	0	0	0	0	0	5,364	0	0	57,842	23,777	81,619	24
25	1,190,207	68563	24	52,125	16,438	0	0	0	0	0	3,113	0	0	52,125	19,551	71,676	25
26	898,045	-199884	24	-152,303	-47,581	0	34,516	34,516	26,300	8,216	19,028	0	0	-126,003	-20,337	-146,340	26
27	1,025,285	208647	24	159,336	49,311	0	0	0	0	0	-5,428	0	0	159,336	43,882	203,218	27
28	941,042	11689	23	8,947	2,743	0	0	0	0	0	-22,327	0	0	8,947	-19,584	-10,638	28
29	719,021	-118451	23	-90,862	-27,589	-8,457	0	-8,457	-6,487	-1,970	-22,511	0	0	-97,349	-52,070	-149,420	29
30	952,625	24915	23	19,154	5,760	-70,512	0	-70,512	-54,209	-16,303	-60,755	0	0	-35,055	-71,297	-106,352	30
31	958,261	-13697	23	-10,554	-3,143	0	0	0	0	0	852	0	0	-10,554	-2,291	-12,845	31
32	1,282,512	42005	23	32,437	9,568	0	0	0	0	0	1,304	54,055	15,945	86,492	26,817	113,309	32
33	1,113,235	208650	23	161,480	47,171	0	0	0	0	0	-9,952	0	0	161,480	37,219	198,698	33
34	640,218	313052	22	242,814	70,238	0	0	0	0	0	5,077	0	0	242,814	75,315	318,129	34
35	674,793	195437	22	151,922	43,515	0	0	0	0	0	10,856	0	0	151,922	54,371	206,293	35
36	1,160,741	705856	22	549,901	155,955	-97,947	0	-97,947	-76,306	-21,641	-61,701	0	0	473,595	72,614	546,209	36
37	1,290,229	508391	22	396,934	111,457	0	0	0	0	0	-32,068	39,038	10,962	435,972	90,351	526,323	37
38	1,546,355	75451	22	59,038	16,412	0	0	0	0	0	-41,957	7,825	2,175	66,863	-23,369	43,494	38
39	1,360,952	75738	22	59,393	16,345	0	0	0	0	0	-38,813	0	0	59,393	-22,468	36,925	39
40	1,003,890	-8805	21	-6,920	-1,885	0	0	0	0	0	-3,008	34,422	9,378	27,503	4,484	31,987	40
41	874,886	-16168	21	-12,734	-3,434	0	0	0	0	0	-1,103	0	0	-12,734	-4,537	-17,272	41
42	625,426	-1014	21	-801	-214	0	0	0	0	0	464	0	0	-801	250	-550	42
43	636,681	95532	21	75,568	19,964	0	0	0	0	0	-19,397	0	0	75,568	566	76,135	43
44	613,024	70609	21	55,974	14,635	0	5,670	5,670	4,495	1,175	10,353	0	0	60,468	26,163	86,631	44
45	562,427	-18864	21	-14,987	-3,878	0	0	0	0	0	148	0	0	-14,987	-3,729	-18,716	45
46	1,302,627	488956	20	389,285	99,671	0	0	0	0	0	10,251	0	0	389,285	109,923	499,207	46
47	1,658,056	409337	20	326,596	82,741	0	0	0	0	0	-63,284	0	0	326,596	19,457	346,053	47
48	1,389,520	803477	20	642,440	161,037	0	0	0	0	0	-79,457	0	0	642,440	81,579	724,019	48
R1-43	39,937,390	5,138,710		3,404,312	1,734,398	-677,251	52,502	-624,749	-472,852	-151,897	-433,310	135,340	38,460	3,066,800	1,187,651	4,254,451	R1-43
R1-48	45,463,045	6,892,224		4,803,619	2,088,604	-677,251	58,171	-619,079	-468,358	-150,721	-555,299	135,340	38,460	4,470,602	1,421,044	5,891,645	R1-48

Table 5-10: Sediment budget - 1984 to 2003

		bed changes				bank changes											
Cell	area (m^2)	channel change	% sand	channel gravel	channel sand	erosion (sub 3m)	deposition (sub 0.84m)	bank total	bank gravel	bank sand	O/B sand (>0.177 mm)	gravel removal	sand removal	gravel sum (m^3)	sand sum (m^3)	total s+g (m^3)	Cell
1			95									0	0	0	0	0	1
2	495,016	-122,019	95	-6,101	-115,918	0	7,711	7,711	386	7,326	3,072	0	0	-5,715	-105,520	-111,235	2
3	447,149	-99,298	95	-4,965	-94,333	0	0	0	0	0	811	0	0	-4,965	-93,523	-98,487	3
4	378,188	-48,484	95	-2,424	-46,060	0	11,736	11,736	587	11,149	1,836	0	0	-1,837	-33,075	-34,912	4
5	601,015	640,624	95	32,031	608,593	0	25,773	25,773	1,289	24,485	1,441	0	0	33,320	634,518	667,838	5
6	675,940	229,344	95	11,467	217,877	0	3,282	3,282	164	3,118	7,669	0	0	11,631	228,664	240,295	6
7	749,909	-67,701	40	-40,621	-27,080	0	9,537	9,537	5,722	3,815	5,090	0	0	-34,898	-18,176	-53,074	7
8	829,823	-396,496	30	-277,547	-118,949	0	22,375	22,375	15,663	6,713	3,281	0	0	-261,884	-108,955	-370,840	8
9	660,646	67,836	27	49,716	18,120	0	5,489	5,489	4,023	1,466	-4,261	0	0	53,739	15,326	69,065	9
10	807,174	-67,105	27	-49,295	-17,810	0	1,594	1,594	1,171	423	806	0	0	-48,124	-16,581	-64,705	10
11	871,884	275,579	26	202,910	72,669	0	6,145	6,145	4,525	1,620	2,226	0	0	207,435	76,515	283,950	11
12	649,052	-37,432	26	-27,626	-9,807	0	1,731	1,731	1,277	453	2,989	0	0	-26,348	-6,364	-32,713	12
13	716,355	-216,284	26	-159,991	-56,293	0	5,145	5,145	3,806	1,339	-4,746	0	0	-156,185	-59,700	-215,885	13
14	591,070	-589,955	26	-437,413	-152,542	0	0	0	0	0	-2,208	0	0	-437,413	-154,749	-592,163	14
15	932,700	-637,458	26	-473,724	-163,734	0	0	0	0	0	-2,675	0	0	-473,724	-166,410	-640,133	15
16	1,025,857	499,096	26	371,754	127,342	0	0	0	0	0	1,310	0	0	371,754	128,652	500,407	16
17	1,119,585	-65,407	25	-48,831	-16,576	-687,766	637	-687,129	-512,987	-174,143	-113,621	0	0	-561,817	-304,341	-866,158	17
18	1,327,000	532,135	25	398,183	133,952	-111,593	43,234	-68,359	-51,151	-17,208	-32,600	0	0	347,032	84,144	431,176	18
19	1,284,070	424,101	25	318,069	106,032	0	231,748	231,748	173,807	57,940	52,912	0	0	491,876	216,884	708,760	19
20	1,583,828	92,988	25	69,899	23,089	0	41,044	41,044	30,853	10,191	9,628	0	0	100,752	42,909	143,660	20
21	1,300,340	521,957	25	393,245	128,712	-138,344	9,451	-128,893	-97,109	-31,784	-50,559	0	0	296,137	46,369	342,506	21
22	1,228,679	490,486	24	370,373	120,113	-561,580	0	-561,580	-424,057	-137,522	-200,969	0	0	-53,684	-218,379	-272,063	22
23	1,149,185	509,914	24	385,915	123,998	-84,135	169,302	85,167	64,457	20,711	-4,213	0	0	450,372	140,496	590,868	23
24	1,284,732	237,273	24	179,980	57,293	-11,541	25,137	13,596	10,313	3,283	74,049	0	0	190,293	134,625	324,918	24
25	1,173,560	72,851	24	55,385	17,466	0	9,629	9,629	7,321	2,309	-13,182	0	0	62,705	6,593	69,299	25
26	896,570	-622,933	24	-474,647	-148,286	-640	0	-640	-487	-152	-38,730	0	0	-475,135	-187,169	-662,303	26
27	1,047,038	159,590	24	121,874	37,717	0	0	0	0	0	28,364	0	0	121,874	66,081	187,954	27
28	961,557	-216,235	23	-165,501	-50,734	0	71,320	71,320	54,587	16,734	68,122	0	0	-110,914	34,121	-76,793	28
29	728,103	-380,656	23	-291,996	-88,661	0	0	0	0	0	80,428	0	0	-291,996	-8,233	-300,228	29
30	969,842	-116,562	23	-89,612	-26,950	0	193,708	193,708	148,922	44,786	138,328	0	0	59,310	156,164	215,474	30
31	954,302	1,336,949	23	1,030,126	306,823	-227,078	412,144	185,066	142,594	42,472	99,371	0	0	1,172,721	448,666	1,621,387	31
32	1,285,752	889,377	23	686,790	202,587	0	164,300	164,300	126,875	37,425	64,051	49,000	21,000	862,665	325,062	1,187,727	32
33	1,092,650	569,422	23	440,690	128,732	0	2,519	2,519	1,949	569	-586	0	0	442,639	128,716	571,355	33
34	670,750	347,087	22	269,213	77,874	0	4,794	4,794	3,719	1,076	-36,516	0	0	272,932	42,434	315,366	34
35	626,578	744,567	22	578,785	165,781	0	233,864	233,864	181,793	52,071	31,811	0	0	760,578	249,663	1,010,242	35
36	1,227,774	863,156	22	672,446	190,710	-287,109	476,437	189,328	147,497	41,831	-8,726	0	0	819,943	223,815	1,043,758	36
37	1,226,747	1,381,635	22	1,078,732	302,903	0	241,049	241,049	188,203	52,846	56,957	35,000	15,000	1,301,935	427,707	1,729,642	37
38	1,403,832	502,022	22	392,820	109,202	0	147,869	147,869	115,704	32,165	-29,195	7,000	3,000	515,524	115,173	630,697	38
39	1,275,311	480,729	22	376,980	103,748	-47,758	29,555	-18,203	-14,275	-3,929	-180,951	0	0	362,705	-81,132	281,574	39
40	1,005,632	95,991	21	75,439	20,552	-58,208	0	-58,208	-45,745	-12,463	-141,088	30,660	13,140	60,354	-119,859	-59,505	40
41	874,516	206,996	21	163,031	43,965	0	0	0	0	0	-10,071	0	0	163,031	33,894	196,925	41
42	629,436	-103,536	21	-81,723	-21,813	0	12,548	12,548	9,905	2,644	36,916	0	0	-71,818	17,747	-54,071	42
43	621,895	-105,472	21	-83,431	-22,041	0	4,718	4,718	3,732	986	3,453	0	0	-79,698	-17,602	-97,300	43
44	622,971	-541,758	21	-429,470	-112,287	0	0	0	0	0	-36,489	0	0	-429,470	-148,776	-578,246	44
R1-48	39,381,038	7,736,914		5,580,938	2,155,975	-2,215,750	2,625,528	409,777	305,031	104,746	-136,466	121,660	52,140	6,007,630	2,176,395	8,184,025	R1-48

Chapter 6: Channel deformation and sediment transport

6.1 Introduction

In this chapter, spatial and temporal patterns of channel development are examined, and a direct connection is made to the underlying processes that influence the erosion, transport and deposition of coarse sediments. Over time, the morphology of the gravel reach has evolved in accordance with the annual volume of water and sediment supplied from upstream but, over the past century, has also been conditioned by bank hardening, blockage of secondary channels and sand and gravel removals. The most geomorphically active locations are associated with large accumulations of gravel and large channel islands. In these 'sedimentation zones', the deposition of gravel bars alters local flow alignment, eroding adjacent deposits and propagating instability downstream where entrained material becomes redistributed. In the long-term, fluctuations in the supply of bed material may be associated with a variety of channel evolution processes acting at various timescales.

Between Vedder River and Agassiz-Rosedale Bridge, variation in the position and number of sedimentation zones is related to changes in channel morphology over time. Major accumulations occur where channel alignment reduces current velocity, encouraging deposition (and compensating erosion). These zones may persist for periods of years to decades in accordance with the magnitude of local transport rates. Indeed, historic airphoto sequences reveal that major bar and island groups have remained within the same computing cells over the period of record, although the morphology of the deposits has evolved as bars migrate and island and floodplain sediments are eroded. These developments indicate that transport rates are not consistent over time. Significant changes may occur within relatively short periods when bed material accumulations force the main channel to migrate. McLean and Church (1999) identified a 1972 avulsion near Harrison mouth as an example of this process. Change in sediment transport rate, both downstream and over time, is analogous to the passage of sediment in waves or slugs (Meade, 1985; Nicholas et al., 1995). This pattern of sediment transport appears to be characteristic of supply-limited rivers, although other processes can also produce pulses (Hoey, 1992).

The next section of the chapter briefly reviews common examples of channel and floodplain formation on wandering channels to provide context for the types of processes and corresponding channel deformation observed on lower Fraser River. This is followed by a discussion on the how sediment is displaced on the river between major morphologic features to

investigate spatial (length) scales of sediment transfer, then by a more detailed analysis of the direct relation between channel bar growth and channel deformation for a major deposition zone extending from Agassiz-Rosedale Bridge to Carey Point using a series of low water photographs taken between 1943 and 1999. By elucidating the association between the spatial and temporal variability of sediment transfer and morphodynamic change, locations and rates of future instability may be predicted. A model of channel evolutionary development is proposed, and validated by comparing expected changes with actual changes documented by additional low water photography collected in 2003. Model results from the qualitative analyses will be contrasted to a GIS-based probabilistic approach developed from transition-state analysis.

6.2 Channel and floodplain formation on wandering channels

The characteristic morphology of wandering channels is a product of the underlying mechanisms that establish and modify channel bar, island, and floodplain elements as sediment is transferred through the system. We can therefore improve our understanding of channel morphodynamics by examining the erosional and depositional processes that maintain channel pattern (Dykaar and Wigington, 2000). Wolman and Leopold (1957) presented a generic model of floodplain development consisting of lateral accretion by point bars on convex bends with corresponding bank erosion on the opposite concave bend. Although typically associated with meandering rivers, the authors stated that the process is common to all channel typologies, but only rivers that transport significant quantities of bed material sediment actually conform with this style of lateral instability. Rivers that transport mainly wash material or fine to medium sand build their floodplains vertically, and are relatively less active laterally although meander migration remains important. More recently, Nanson and Knighton (1996) have suggested that avulsion and accretion-based process are fundamental formative mechanisms on all types of anabranching channels. Sediments deposited as point or complex medial bar forms dominate the depositional environment. In addition to forcing compensating erosion, growth of these bars also creates instream and floodplain channel avulsions (cf. discussion in Chapter 1).

Neill (1973) observed that channel shifting and deposition of point bars and islands were dominant channel processes on the wandering Athabasca River, Alberta, although the progression was more erratic than described by Wolman and Leopold (1957). A cursory examination of maps and photographs of the planform channel reveals a more complex channel and floodplain morphology than could be created by the simple point bar model, indicating that additional

processes must be involved. Church and Jones (1982) discussed the accumulation of extensive bar assemblages in wandering channels, which they termed sedimentation zones. These preferred zones of deposition are found at discrete locations along the channel as pulses of bed material propagate downstream. Although they may be spaced at regular intervals, tributary inputs, alluvial fans, and erosion resistant boundaries can introduce deviations. Each assemblage comprises a complex variety of barforms produced by channel migration and cutoffs, and its presence is associated with local channel instability. However, no details of the association between channel and floodplain deposits were given.

Church (1983a) examined historic maps and airphotos of Bella Coola River, British Columbia, allowing a descriptive analysis of erosional and depositional development to be constructed. It was found that most sedimentation zones generally persisted over time because they were anchored by alluvial fan constrictions, but extensive local modifications occurred in response to changes in sediment supply. For some sedimentation zones, continued bar accumulations forced avulsions and reoccupation of old flood channels. Correspondingly, others became stabilized where the upstream supply was reduced and much of the deposit was subsequently incorporated into the existing floodplain. In contrast to the dominant island and medial bar complexes found in the sedimentation zones, stable reaches contained mainly bank-attached lateral bars (Desloges and Church, 1987).

Ferguson and Werrity (1983) examined bar and channel development over a period of 5 years on the River Feshie, Scotland, concluding that progradation of alternate diagonal bars was the dominant process driving morphologic evolution. Flow divergence and convergence around migrating bars was found to cause erosion on the outer banks opposite accreting bar margins. However, avulsions, initiated from chute channels across elongated bars or into the floodplain, were found to interrupt the process. Based on these observations, the authors concluded that channel evolution on wandering rivers is neither simple nor follows regular cycles of development. A similar review of morphologic development over a period of 60 years on Willamette River, Oregon is given by Dykaar and Wigington (2000). It was found that a combination of erosional and depositional processes was responsible for maintaining the multi-channel planform. The establishment of point and medial bars produced proximal lateral bank erosion and scalloping, driving overall channel migration. Accretionary processes which constrict flows in secondary channels and promote infilling, or which force migration of the channel thalweg, provide the nucleus for incipient floodplain formation and maturation. Similarly, bar deposition maintains

multiple channels by splitting the flow, forcing new cut channels across point bars and enlarging secondary channels where accumulations block the main channel flow (Dykaar and Wigington, 2000).

Woody debris has also been recognized as providing an important feedback mechanism linking channel and floodplain changes on wandering rivers. Channel migration promotes a significant influx of woody debris that affects channel process and form (Desloges and Church, 1989; Gottesfeld and Gottesfeld, 1990). Wood plugs at the head of sidechannels can force their eventual abandonment and establishment of new floodplain, while large jams can cause main channel avulsions through former channels and through stable floodplain, generating further wood inputs (Gottesfeld and Gottesfeld, 1990). Ice buildup can play a similar role in northern climes. Woody debris accumulations have also been associated with island and floodplain formation. Jams that establish on bar tops may create conditions favorable for the establishment of vegetation, hence growth into islands, while jam development on meander bends can lead to the creation of new floodplain elements (Hickin, 1984; Abbe and Montgomery, 1996). The importance of wood in maintaining multi-channel morphologies was demonstrated by Sedell and Froggatt (1984) and by Collins et al. (2002) who found that woody debris removals since the mid-1800s have reduced both instream channel complexity and interaction with the floodplain on large Pacific Northwest rivers. However, a paucity of wood on Fraser River bars relative to these examples suggests that large jams are not a ubiquitous formative mechanism of the wandering planform – indeed, wandering channels have been identified in the Arctic tundra (cf. Forbes, 1983). Nevertheless, the possibility remains that the role of wood in influencing island and floodplain formation may have been greater in the past when it was not removed for navigational safety.

Several studies have directly examined erosional and depositional processes on lower Fraser River. Morningstar (1987) reviewed mechanisms of floodplain formation near Chilliwack, summarized as the consequence of island formation in the main channel followed by attachment of islands to the floodplain by chute infilling. He found that vertical accretion of sands in the lee of grounded woody debris on a deposited gravel platform creates suitable conditions for vegetation establishment, while depressions in the bar become chute channels as flow becomes concentrated with increasing discharge. The chute channels separate islands from each other or from the adjacent floodplain (Roberts and Morningstar, 1989). Sediment blockage at a chute head decreases flow intensity and frequency of inundation downstream, allowing fines to be deposited in the chute tail because of the backwater effect (Morningstar, 1987). The infilling and abandonment of chutes

separating islands from the main channel banks was argued to be the main mechanism for floodplain accretion.

Wooldridge (2002) used a combination of bathymetric soundings, historic aerial photography and ground penetrating radar signatures to examine the evolution of bank-attached, partially bank-attached and mid-channel macroforms. The prominence of sub-horizontal reflections in the GPR surveys was interpreted as the vertical and lateral stratification of migrating bedload sheets 2 to 3 grains thick, while the widespread occurrence of slipface accretions, formed where the current is aligned directly with the emergent bar, was found to distinguish wandering rivers from braided and meandering deposits. Wooldridge (2002) also noted that large floods initiate channel changes that are completed by successive floods, but do not cause immediate channel changes, suggesting that this is a characteristic feature of wandering channels. McLean and Church (1999) make a similar claim, but submit that in Fraser River, the rate of change is tempered by the modest transport rate relative to the size of the channel and stored sediment volume.

McLean (1990) was the first to describe channel morphodynamics on lower Fraser River, associating bar and island developments at major storage zones to morphologic changes immediately downstream. Eroded sediments are transferred downstream, creating or adding to existing bar deposits which affect local flow alignment. McLean and Church (1999) suggested that these local disturbances propagate down the river as a wave-like phenomenon that travels faster than the rate of sediment transport. McLean (1990) and McLean and Church (1999) noted that erosion and deposition sites change over roughly a decade as channel realignment alters the pattern of erosional attack, while migrating zones of instability can be traced for several decades.

The next section of the chapter examines the processes by which sediment is routed downstream and is followed by a review of the genesis of bar and island formation in a major sedimentation zone to examine whether distinct repeating cycles of depositional and erosional patterns exist.

6.3 Sediment transfer length

While the movement of individual clasts has been demonstrated to be fundamentally stochastic, particles tend to aggregate into major accumulations where bars act as sediment traps (Hassan and Church, 1992). Despite this association, most efforts to measure particle movement have focussed on channel hydraulics, while neglecting potential morphologic controls (Pyrce and

Ashmore, 2003). On many gravel channels, bars establish on stable riffles which have a somewhat regular sequence that scales to channel dimensions (Richards, 1976; Church and Jones, 1982). On regularly meandering channels, sediment transfer proceeds in a reasonably orderly manner, with erosion on concave bends and deposition on point bars at downstream convex bends. Neill (1971) recognized that the downvalley migration of a channel meander belt associated with this development could be used to provide an estimate of sediment transport at an arbitrary cross-section if the average travel distance of the sediment could be estimated. Neill (1987) stated that the travel distance during flood was equal to one-half the meander wavelength on rivers with regular meanders, but recognized that this distance may need to be modified for different morphologies.

Church et al. (1987) presented a generalization of this approach applicable for more complex channel patterns, where sediment step lengths were assumed equivalent to riffle spacing. Investigations on braided channels have demonstrated similar results (cf. Goff and Ashmore, 1994) but other studies have adopted the distance between distinct erosion and deposition zones (Carson and Griffiths, 1989; Ferguson and Ashworth, 1992), although these can be difficult to identify (Goff and Ashmore, 1994). On the wandering gravel reach of lower Fraser River, the links between major erosion and deposition zones are more clearly distinct because of the large size of the channel (Desloges and Church, 1989). Since changes to channel morphology are largely governed by the rate and magnitude with which bars develop and migrate, the distribution of primary morphologic features may provide a means to investigate the length scales of sediment transfer. Several approaches are presented below.

The relation between meander wavelength and sediment transport over the past half-century on Fraser River is first investigated by defining successive meander bends, and measuring their respective lengths from Laidlaw to Mission Bend, roughly 4 km upstream of Mission railway bridge. These locations do not correspond exactly with the linear extent of the gravel reach, but clearly demarcate start and end points of the meandering sequence[1]. The channel has developed a more regular sinuous planform since 1949 that has been propagating downstream (Church and Ham, 2004; also see Appendix B), but meanders on the river are not well-developed. Consequently, it is difficult to identify meanders definitively and hence the interpretation remains partly subjective. A total of 13 meanders were delineated in both 1949 and 1999 (Figures 6-1, 6-

1. A single meander is defined as a complete sine wave, or twice the distance between successive points of inflection on the meandering wavelength path (after Leopold and Wolman, 1957).

2). Mean meander wavelength for both dates is 5.1 km since the thalweg lengths are nearly equal. Summary statistics for defined meanders are given in Table 6-1. Following Neill's (1987) assumption, the characteristic step length on the river (assumed during the annual freshet) should average roughly 2.5 km, and ranges from 1.6 to 3.4 km where variations in meander wavelength are associated with changes in local morphology.

Table 6-1. Summary statistics for delineated meanders, 1949 and 1999.

Statistic	1949	1999
n	13	13
mean (m)	5123	5115
S.D. (m)	799	1097
range (m)	3900 - 6400	3200 - 6700
total length (m)	66,600	66,500

Although wavelength variability has increased, the change is not signficant ($F=1.88$, $p=0.14$). In 1949, the shortest wavelengths were all associated with major bar / island complexes upstream of Agassiz-Rosedale Bridge, but this pattern was partly interupted by 1999 with the development of a more regularly sinuous thalweg near Herrling Island and re-organization of downstream deposits at Greyell complex and Queens Bar. Although mean meander wavelength remained unchanged, the change in wavelength variability may be accomodated by changes in other morphologic parameters.

Meander wavelength has been shown to scale with the square root of dominant discharge, hence channel width, as this parameter displays a similar geometric association (Leopold et al., 1964). Since the active channel zone has been narrowing over the past half-century, the meander wavelength, hence sediment step length, should be declining. Although there were 3 meanders in 1999 shorter than the smallest 1949 meander, this pattern does not hold for the entire gravel reach, but the ratio of meander wavelength to main channel width has remained within the expected range of 10 to 14. Neill (1987) added that smaller values of meander wavelength are associated with greater values of bank material thickness or bank erosion rates to maintain sediment continuity. However, the known pattern of decreased bank erosion from 1949 to 1999 (Chapter 4) is not consistent with Neill's statement. Indeed, it appears possible that the combined effects of channel narrowing and decreased bank erosion are compensating such that meander wavelength has not changed over the past half-century.

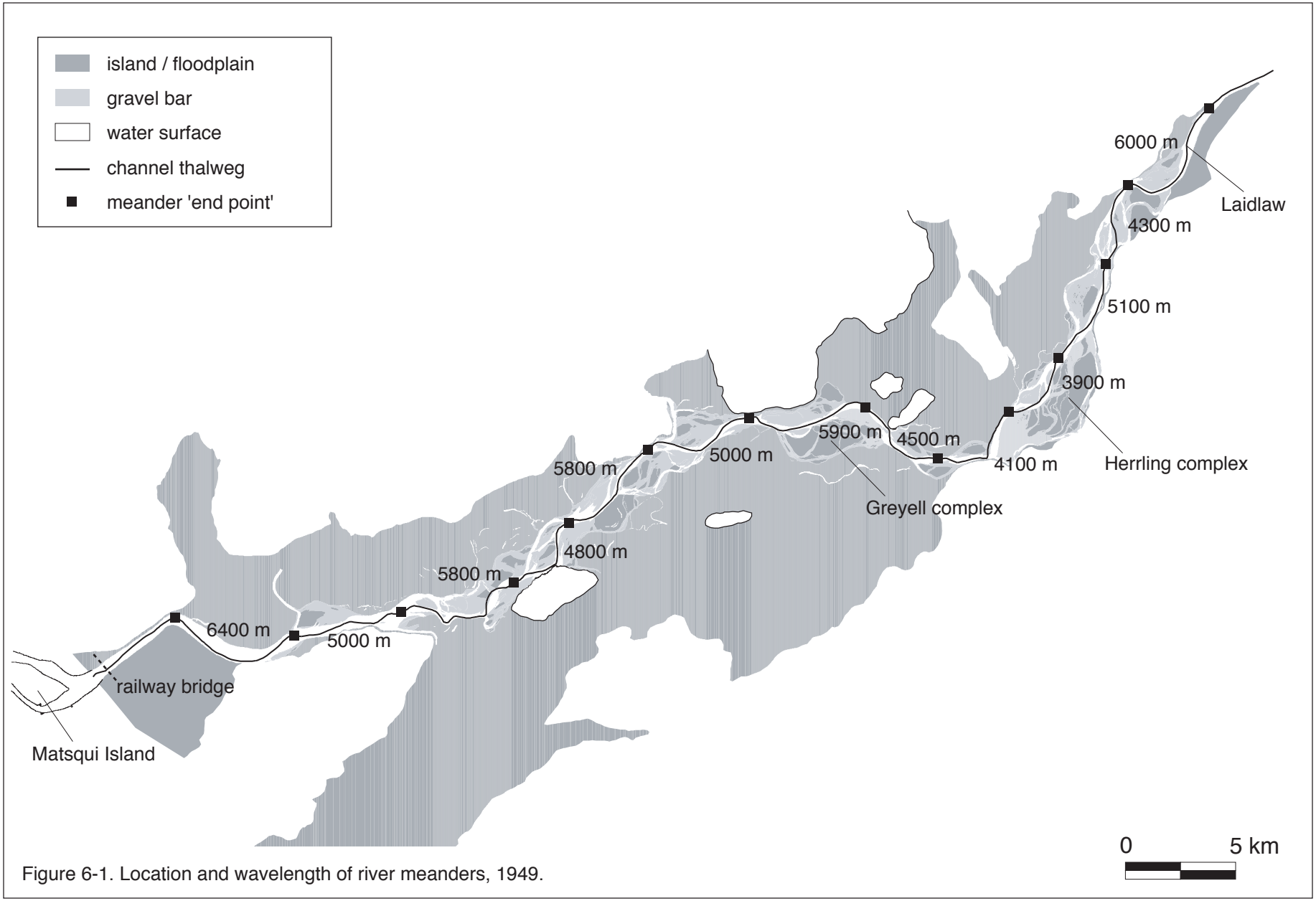

Figure 6-1. Location and wavelength of river meanders, 1949.

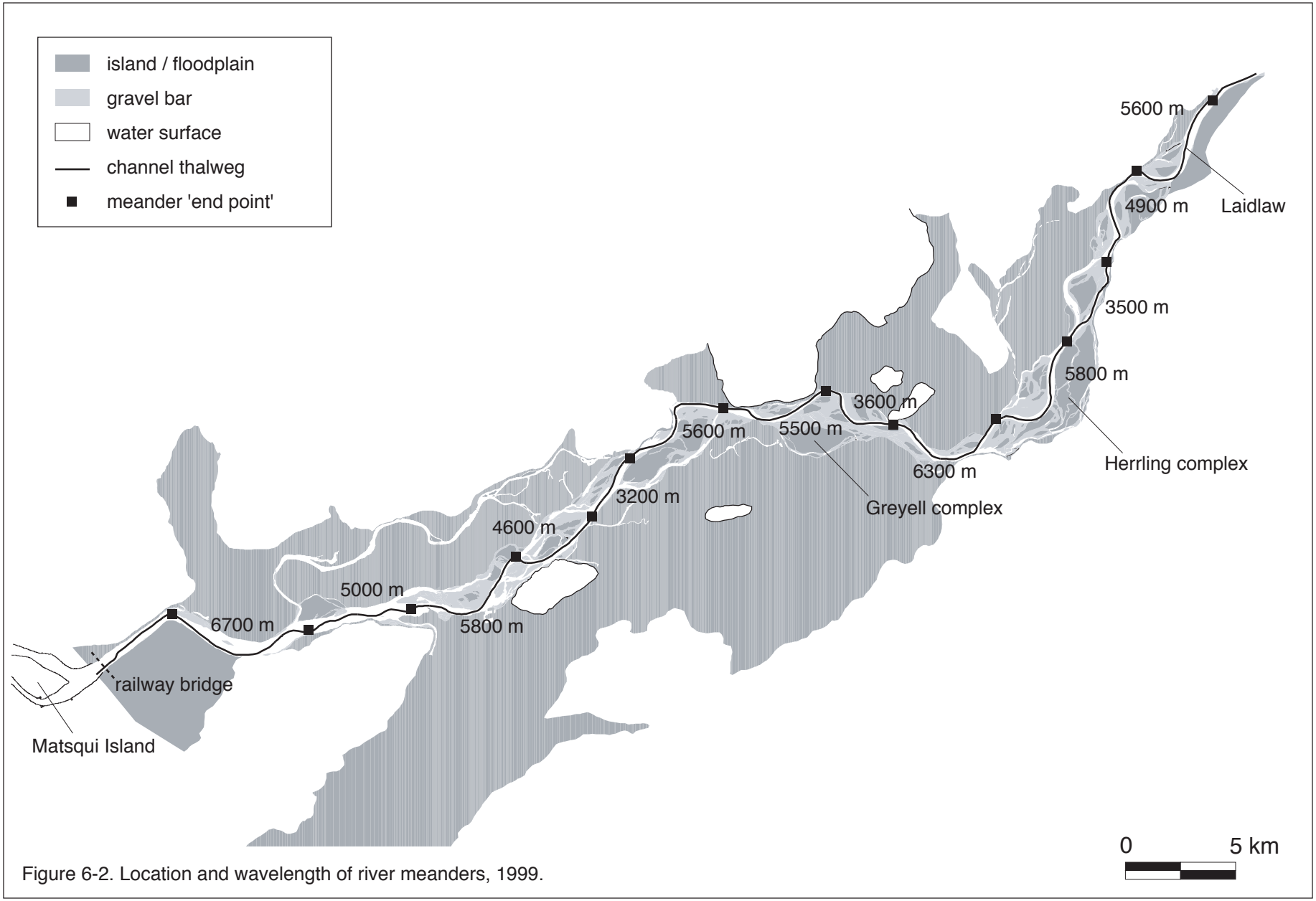

Figure 6-2. Location and wavelength of river meanders, 1999.

The spacing of major riffles and pools provides an alternative means to investigate average step lengths. Leopold and Wolman (1957) found that the distance between successive riffles scales to one-half the meander wavelength. It is expected that a similar relation holds for pools, which are sequentially opposed forms along the thalweg and represent discrete erosion zones. In Chapter 4, it was shown that there were 27 major pools in both 1952 and 1999, giving an average pool spacing of 2.7 km for each date. This result is close to 3 bankfull widths, but increases to 6 channel widths if scaled to the average width of the dominant main channel, or normalized by the braiding index. This is within the expected range (5 to 7 widths) for self-formed channels and matches the findings of Church and Jones (1982) for the wandering Bella Coola and Peace rivers. It is also consistent with the expected spacing based on meander wavelength.

The spacing of major deposition zones is another obvious candidate for estimating path lengths, since these features are clearly preferential sites of clast accumulation because of increased flow resistence. Hassan and Church (1992) note that bar spacing is potentially a significant transport length scale on gravel channels, especially in large floods. In 1949, there were 26 major bars within the gravel reach, giving an average bar spacing of 2.7 km, increasing to 3.1 km by 1999 when there were 3 fewer bars. Although river meander lengths did not correspondingly change, the increase in bar spacing is assuredly modest. Similarly, McLean (1990) measured the distance between major zones of deposition along the river (identified as accretions on existing bars and the creation of new unit bars) and found mean separations of 2.75 km from Agassiz-Rosedale to Carey Point, increasing to 5 km downstream to Mission. The seemingly close correspondence between bar and riffle/pool frequencies provides an indication that bar location is associated with, and likely conditioned by, riffle location on wandering rivers. This relation is explored in further detail in the following section of the chapter.

Based on the preceding results and the assumptions about clast movement, typical sediment step lengths on the river would fall consistently within the range of 2.5 to 3.1 km, with modal values near 2.8 km. These lengths are equivalent to the spacing of major morphologic features on the river. Pyrce and Ashmore (2003) point out that path length is also controlled by flow hydraulics, but add that there is significant evidence linking this distance to the length scale of channel morphology on low-gradient rivers with large (or long duration) floods. Sediment transport rates might therefore be estimated by multiplying this value by the volume of sediment eroded, or deposited, along the channel. McLean and Church (1999) investigated this possibility at the downstream end of Herrling Island, and found reasonable correspondence between bank

erosion and sediment transport rates (compared to sediment budget estimates at Agassiz-Rosedale Bridge) except during periods when channel curvature was reduced. Consequently, the technique may under-predict the true transport rate over longer time periods, and may not be adequate for situations where there are multiple modes of transport (McLean, 1990). Indeed, since many studies have indicated that most bed material transport occurs in the form of unit bar construction and migration, mensuration of the size and spacing of these features may provide a more reliable means for estimating spatial variations in the local transport rate. Such an approach also recognizes that sediment transport may be the product of different volumes, distances and rates of transfer (Nicholas et al., 1985; Gaeuman et al., 2003). This possibility is explored further in the following section of the chapter.

6.4 Sedimentation and morphology of bar complexes

The availability of a sequence of low-water aerial photographs at fairly regular frequency (5 to 8 years - see Table 6-2) provides an opportunity to examine in detail the direct association between styles of bar deposition and channel deformation in a major sedimentation zone extending from Agassiz-Rosedale bridge downstream to Carey point, a distance of 10 km. The study area is comprised of a large island complex (Greyell Island) that has been developing since at least the mid 1800s, and several large bar complexes that have undergone extensive reorganization over the period of study, although the nucleus of contemporary Gill and Carey bars had established by the date (1943) of the earliest photographs in the sequence.

Before discussing bar and channel development, it is necessary to clarify terminology related to morphologic classification, since a wide array of terms has been presented in the literature. Crowley (1983) pointed out that fluvial scientists recognize a large number of distinct bar types based on external morphology or position in the channel but there is no definitive classification of these features. Different classification schemes have also been criticized because planform morphology is largely stage dependent (Jackson, 1978; Smith, 1978; Bridge, 1993). This can lead to interpretive confusion since bedform size, frequency and geometry will vary with discharge. Most definitions of islands (vegetated bars) are less ambiguous because these deposits remain exposed except at extreme flows, although as Bridge (1993) points out, it is difficult to determine exactly when bars become islands.

With the exception of 1986 photography, flows on all dates fall within a reasonably small range, so the area, and morphology, of exposed bar forms is sufficiently uniform to permit

Table 6-2. Selected low-water photography

Date of photography	Flow at Hope (m^3/s)	Water surface area (m^2)
Mar 20, 1999	701	4,182,379
Feb 24, 1993	581	3,268,080
Sept 4/5, 1986	2500	6,317,756
Mar 22, 1979	1010	4,679,129
Mar 19, 1971	799	4,914,108
Apr 6, 1964	1110	4,854,138
?, 1959	1172*	4,450,243
May 7, 1954	1170	4,462,750
Mar 23, 1949	733	3,809,258
Dec 5, 1943	929	4,510,484

* Estimated from ratio of discharge to water surface area between 1954 and 1964 because exact date of photography is not known

consistent classification and discussion. Nevertheless, to account for small variations in bar exposure produced by differences in discharge, a morphologic feature termed 'bar edge' was additionally mapped from the photography (see Figure 6-3). Bar edge defines submerged bars, which are either partly or fully inundated by shallow water and are visible because water clarity in the river is highest during winter and early spring periods (when most of the low-water photo sets were flown) as suspended sediment concentrations are lowest. Incorporating the bar edge and exposed bar polygons makes the extent of total bar area similar for all dates, thus minimizing complications of channel and bar classifications which change with discharge.

In the following discussion, a hierarchical classification of bed forms is adopted, where 3rd order unit bars refer to individual bedload sheets, crescents, or plugs deposited by a single flow event onto an existing (2nd order) bar that itself forms a major sedimentary body. Following the nomenclature of Church and Jones (1982), medial, point, and diagonal bars appear most prominent in the wandering reach. A bar complex (1st order) is a collection or group of individual bars and is separated from other bar complexes by open water at low discharge. Bar complexes may include immature vegetation, but mature islands are considered a separate depositional unit for purposes of discussion. Examples of migrating gravel sheets are provided in Figure 6-4, while Figure 6-5 illustrates the hierarchical identification and coding of the different depositional units.

These features correspond to macroforms (3rd order) and megaforms (1st and 2nd order) which scale to the size of the channel on gravel bed rivers (Church and Jones, 1982). Similar

Figure 6-3. Examples of bar edge delineation. Photos from 1949 (Q = 733 m^3/s).

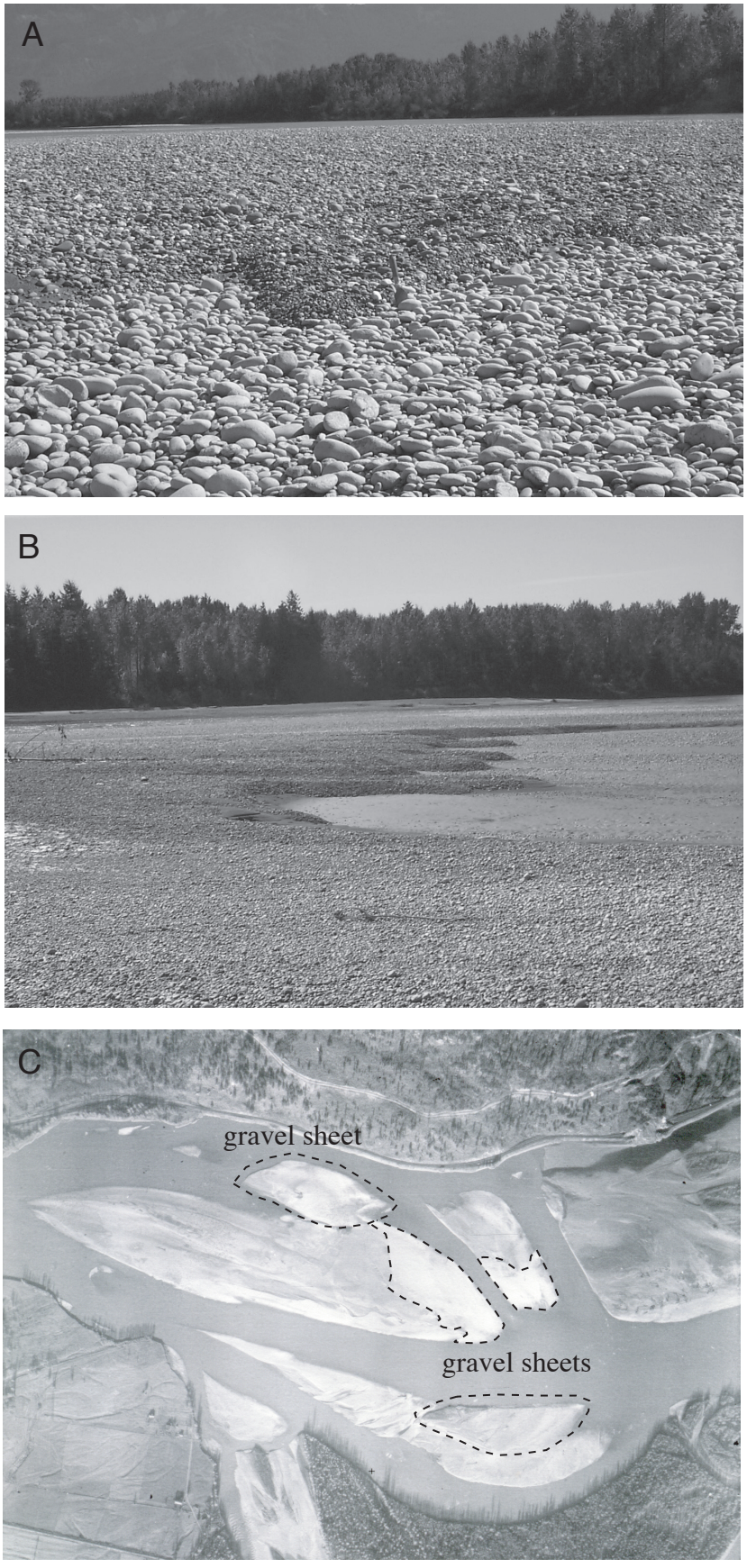

Figure 6-4. Close range (A) and distal (B) views of gravel sheets prograding on existing bar surfaces at Queens Bar complex. (C) Annotated 1943 photo near lower Carey Bar complex showing example delineation of gravel sheets based on tone and morphology.

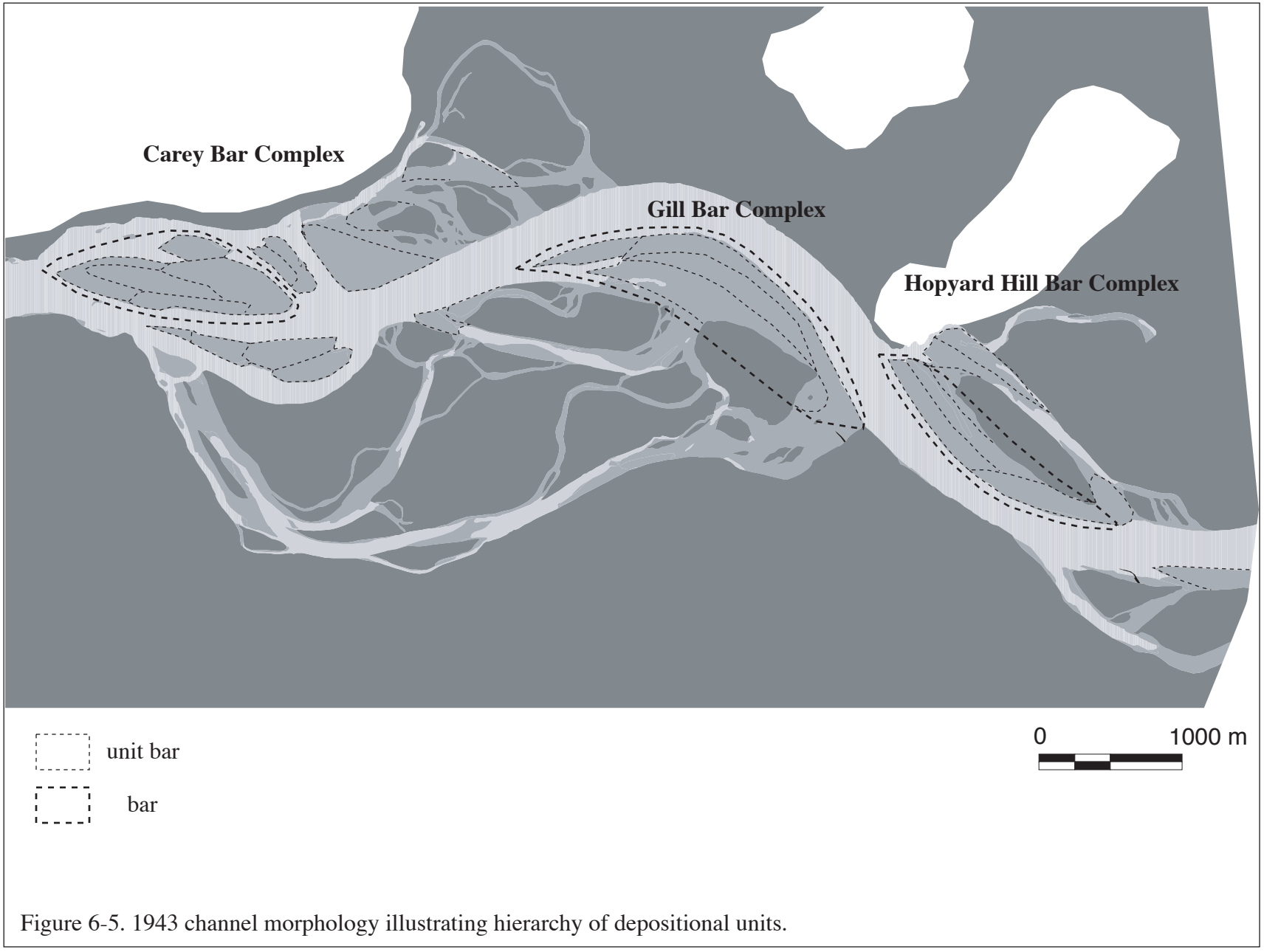

Figure 6-5. 1943 channel morphology illustrating hierarchy of depositional units.

ordering schemes have been presented by Williams and Rust (1969) and Bristow (1987). They have also been associated with temporal scales of development, with macroforms having a duration of formation from days to years, and megaforms from weeks to millennia (after Jackson, 1975). Hierarchical schemes may therefore provide a template for explaining form-process relations at a range of scales (cf. Brierley, 1996). Primary bedform accumulations, termed microforms and mesoforms (cf. Church and Jones, 1982) are not discussed as these features are rarely visible on aerial photographs (Kellerhals et al., 1976) and their longevity is too brief to be examined over periods of several years.

The relation between bar and channel morphologic development is specifically concerned with the following major questions, the scope of which is limited by the information that can be derived from planform analysis. The major questions include:

- what are the dominant unit bar types characteristic of each date;
- can their movement and development into bars and bar complexes be tracked;
- what is the magnitude of a unit bar deposition event;
- is their rate of transit related to the development of islands, avulsions and cutoffs; and
- are repeating patterns of morphologic evolution observed which could be used to predict short-term channel changes

It should also be realized that the following discussion is based upon an interpretation from the historic photo sequence and there is no direct confirmation that any of the erosion / deposition sequences discussed are definitively correct.

The 1943 map (Figure 6-5) shows extensive, partially bank-attached sediment deposits at Gill and Carey bar complexes. A third, smaller, bar complex is found upstream of Hopyard Hill while several medial bars are found near the downstream end of the study reach. Prominent channel islands with mature trees are found at all three sites, indicating that these surfaces have remained stable for decades. At least part of the large islands near the left bank at the Gill complex are more than a century and a-half old given their appearance on the 1859 sketch map. Secondary channels between large islands and major sloughs adjacent to outer channel banks preserve evidence of small migrating sheets and plugs. Minor accumulations of sandy mesoforms (dunes) are observed at a few sites. Smaller, immature islands are also common, growing on elevated bar deposits. The persistence of these features throughout the historic photo record (see Appendix C photomaps)

demonstrates that sediment exchange within the reach does not encompass the entire active channel zone.

There is evidence of recent unit bar deposits along wetted channel margins at all sites. Here, migrating gravel sheets a few grains thick are stacked upon existing major bar assemblages, and appear to dominate the depositional environment (refer to Figures 6-4, 6-5). These elongated features are oriented both parallel and obliquely to the main flow, and have typical lengths of several hundred metres, and stored volumes in the range of 10^3 to 10^4 m^3. Some of these bar units have a detached tail that extends into the main channel, giving the distinct appearance of a 'claw'. Miall (1977) suggests that gravel sheets are the primary depositional units of medial bars, deposited where the current wanes. Church and Jones (1982) add that all common bar types in actively changing gravel-bed channels appear to be formed from sheets. Research by Wooldridge (2002) has confirmed the prominence of stratified bedload sheets on lower Fraser River macroforms. Unit bar typology away from active channel margins becomes less distinct. Although remnant sheets, plugs and crescents can be partly distinguished, repeat cycles of washing, erosion and deposition produce a more homogenous bar surface. Dissection of these deposits by numerous chute channels and scour holes during waning flood flows compounds the difficulty in identifying individual bar units.

By 1949, there was lateral accretion on existing bar margins at all three bar complexes, but the basic morphology of the reach was maintained despite the magnitude of the 1948 flood (Figure 6-6 A). There was only a single additional flood (in 1946) larger than the mean annual flood during this intersurvey period. Near Hopyard Hill, two new gravel sheets (1: see figure for site numbers) extended the existing bar both laterally and downstream, directing the main flow towards the upstream end of Gill bar complex which experienced compensating erosion. Sedimentation on a large diagonal riffle (amplified by the lower flow stage) connected this feature to Gill Bar across the low flow channel (2). This sediment probably derived from a unit bar that became fully detached from the upstream bar and was subsequently modified (dissected) by the flow. There was more extensive lateral and downstream extension by new unit bar deposits on the convex bend at Gill Bar (3) which forced the flow into the right bank, eroding up to 100 metres of floodplain and trimming bar and island deposits at the head of the Carey complex. However, minor expansion of existing islands here provides evidence that this deposition did not significantly increase flows through the minor chute channels separating the islands (4). At Carey Bar, sediment deposition in existing chute channels (5) coalesced existing smaller bars into a single bar complex, while at least

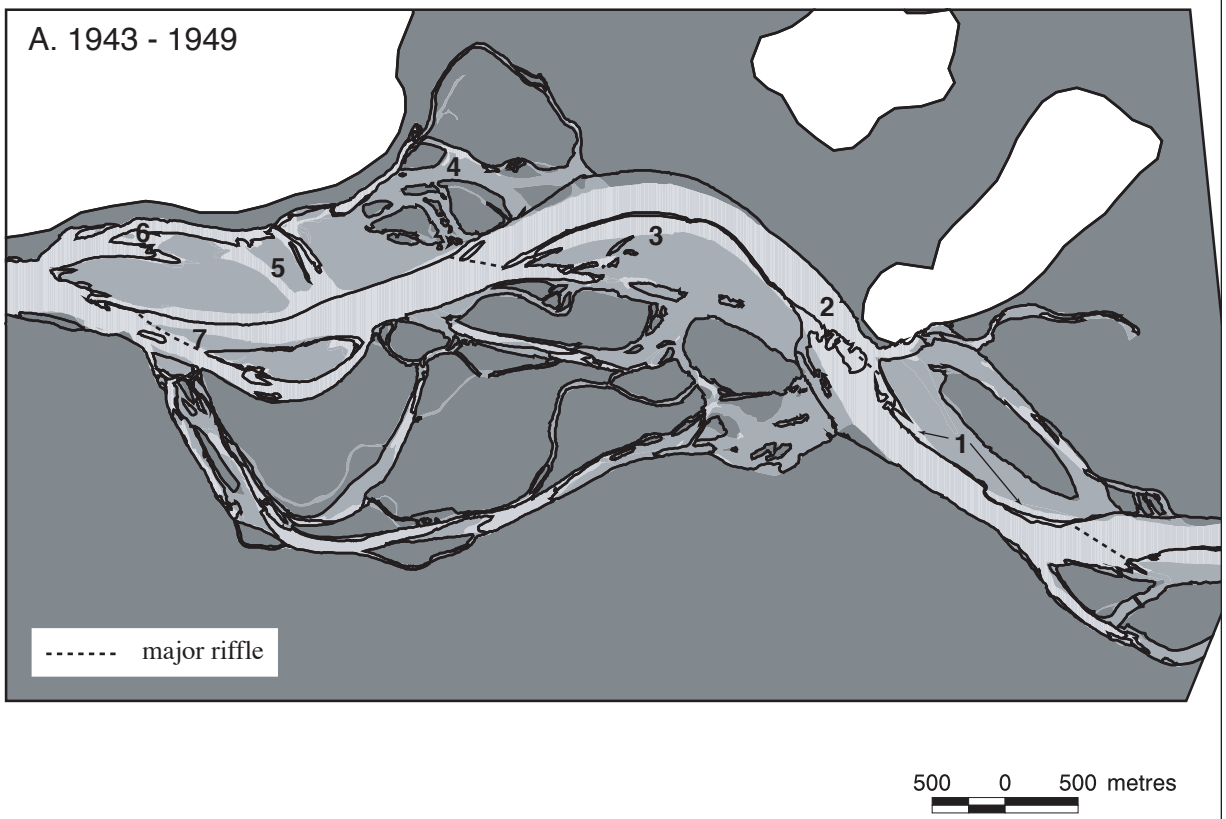

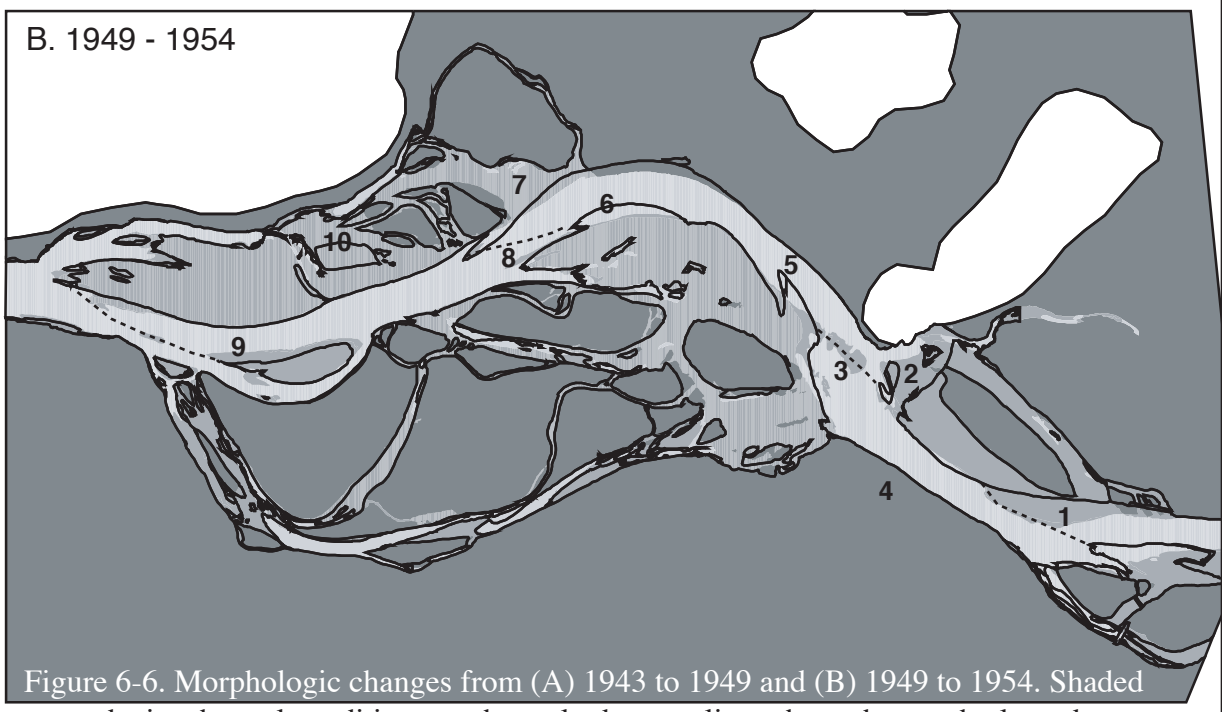

Figure 6-6. Morphologic changes from (A) 1943 to 1949 and (B) 1949 to 1954. Shaded maps depict channel conditions on the early date; outlines show changes by later date. Numbers denote features in the text. Dashed lines indicate diagonal riffles.

one unit bar was deposited downstream, extending the north side of the bar (6) and reducing the size of the secondary channel. The reduction of flow through the chute channels and lateral extension of lower Carey Bar complex forced the thalweg south, eroding the tail of a medial bar (7) to maintain conveyance, though minor unit bars were also deposited on the east and south sides of this feature.

By 1954, lateral extension of a bar at Ferry Island forced the flow north, partly eroding two small islands and removing 14 ha (est. 290,000 m^3) from the Hopyard bar complex (1; Figure 6-6 B). Most of this erosion likely occurred during the large 1950 flood; freshets for all other years were at or below the long-term average. This development must have increased flow through the prominent right bank secondary channel, because there was significant erosion at the bar tail near Hopyard Hill (2) where the current is forced to take a hard turn left. The diagonal riffle (3) appears reduced in size by the main current (although the feature may simply be underwater) which deflects north off the hardened left bank (4). These eroded sediments were transported downstream and deposited as new unit bars that further extended existing bars at Gill complex (5, 6). Deposition at lower Gill Bar (6) forced further compensating erosion on the right bank and increased flow through the head of the Carey complex, trimming the edge of a large island (7). A new unit bar at Carey (8) was formed from the material eroded just upstream, and directed flows towards the left bank. Downstream, the medial bar at (9) was further eroded. This alignment also reduced flows across lower Carey Bar, providing suitable conditions for vegetation extension (10). As the location of the new unit bars (5, 6, 8) is coincident with the location of older bar tails, these sites appear conducive for trapping and accumulating migrating bedload sheets. Wooldridge (2002) found that sheet-like deposition dominates topographically low areas that grade into the main channel at Queens Bar, suggesting that these features form at falling stage. It is expected that further accumulations and compensating erosion will be observed by 1959 at these same sites.

There were in fact a number of significant modifications to reach morphology by 1959 (Figure 6-7 A) with annual flood flows greater than the mean annual flood in all years. The Ferry Island bar migrated downstream, and a distinct crescentic-shaped unit bar (1) developed in mid channel. This event marks the origin of contemporary Big Bar (see Appendix C, Figure 1). This caused extensive compensating erosion at Hopyard Bar / Island, but the eroded material rebuilt the point bar that had been removed in the previous period (2), while a small medial bar (3) was deposited at the site of an existing bar tail on the diagonal riffle. Consequently, the flow was increasingly forced toward the left bank, removing unit bars on the upstream end of Gill Bar.

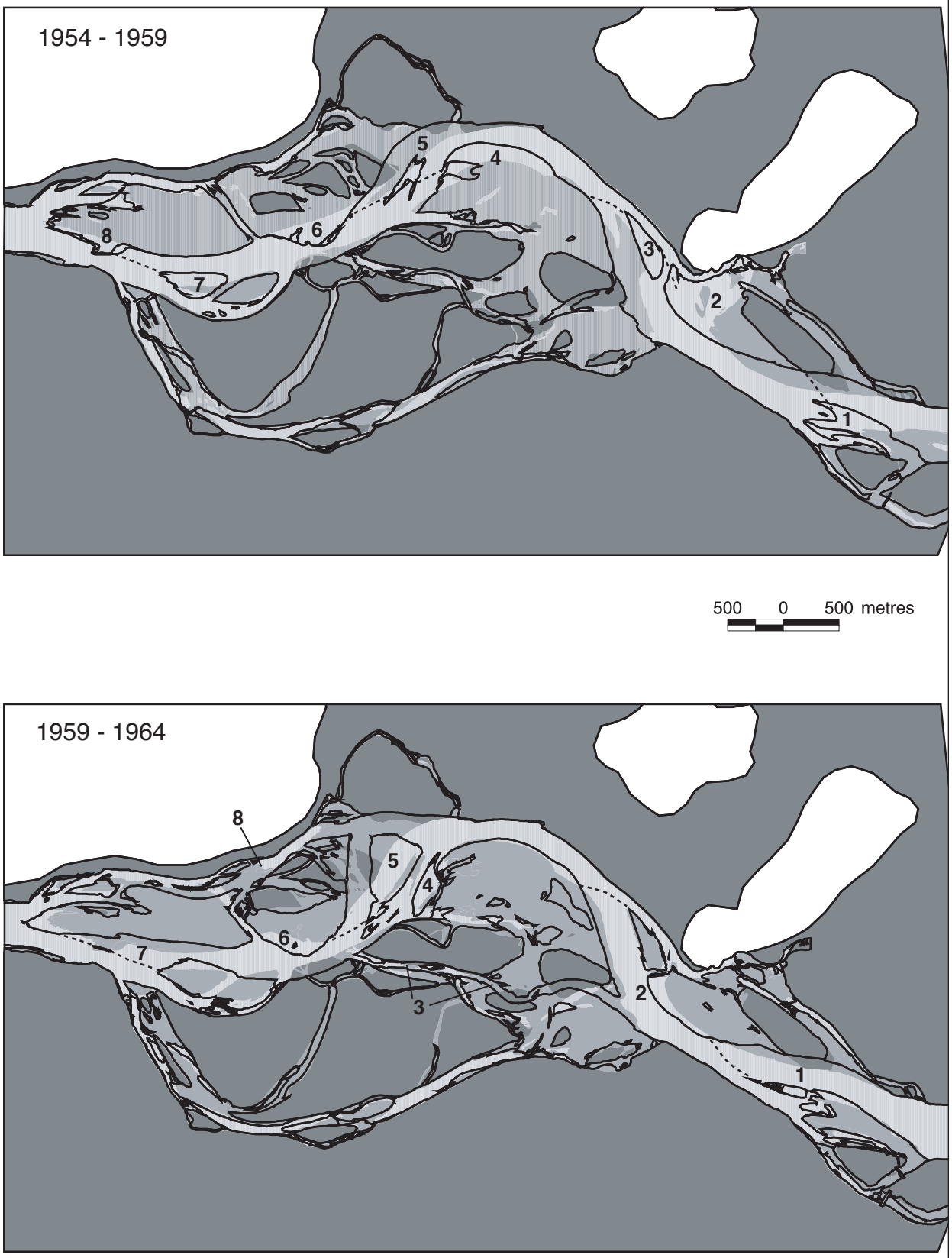

Figure 6-7. Morphologic changes from (A) 1954 to 1959 and (B) 1959 to 1964. Shaded maps depict channel conditions on the early date; outlines show changes by later date.

Hardening of the right bank to protect the flood dyke helped direct the current away from the right bank. The material from these unit bars became trapped at the Gill Bar tail, also the upstream end of the major diagonal riffle (4) and more directly aligned the current towards the head of Carey Bar complex, which was extensively eroded (5). This resulted in a considerable widening of the low-flow channel, creating an area of flow expansion where a new cresentric unit bar formed on the riffle. Sediment eroded from upper Carey was deposited at mid Carey Bar (6), extending the bar more than 200 metres laterally and causing erosion at Gill Island. Unit bars were also attached to existing deposits at the mid-channel bar downstream (7) and the tail of Carey Bar (8). Overall, the pattern of increased sedimentation between Carey and Gill bar complexes indicates that flow conveyance through the main channel had become reduced. As a result, a partial avulsion is in prospect in order to maintain flow conveyance.

The morphologic developments described to this point present an emerging picture of a reasonably orderly pattern of channel change directly associated with the location of persistent diagonal riffles. These features appear to be stable 'framework' riffles (sensu Church and Jones, 1982) rather than transient ones associated with migrating bar fronts, although they do migrate and develop over decades. Unit bars develop on the convex edge of existing bars at the downstream limit of the riffles, where their progression becomes stalled. This deposition forces compensating erosion in pools on the opposite bank, providing source material to the next downstream riffle. Less common variations of this progression include medial deposition on a riffle crest (e.g. '2' on 1943-49 map) and unit bar deposition on the upstream limit of the riffle (e.g. '6' on 1949-54 map). The features probably become trapped at falling stage when shear stress falls below critical values.

The major riffles are established at a fairly regular interval of 1500 metres, or one-half the average step-length estimated in Section 6.3. Therefore, the average annual volume of sediment influx to the reach is apt to be represented by the volume stored in 'recent' unit bars at four consecutive riffles (which essentially define a complete meander unit). For the periods discussed, this volume falls within the range of 100,000 to 300,000 m^3 per year, consistent with estimates from the long-term sediment budget. However, because sedimentation in the reach is focussed at the same loci for many years, the channel must eventually become too constricted to maintain an orderly development. Growth of the medial bar between Carey and Gill complexes (1954-59) portends such a change.

By 1964, additional sedimentation at developing Big Bar (1) caused further compensating erosion at Hopyard and extension of the existing point bar (2), continuing the pattern observed in

the previous mapping period (Figure 6-7 B). This growth, combined with the downstream migration of the riffle, forced sufficient flow into Gill/Greyell complex to create a small erosional channel separating them at low flow (3). The new current channel alignment favoured additional unit bar accumulations at the riffle tail and increased flow, hence erosion, through the island complexes. Downstream, the previous pattern of unit bar accretion on the convex bank of Gill Bar effectively stopped, but a new unit bar was deposited at the tail of Gill Bar (4). The sequence of morphologic developments near the head of Carey Bar is fairly complex. Sediments continued to accumulate on the existing medial bar in the area of flow expansion (5) which was maintained by erosion of upper Carey Bar. New unit bars, constructed from this material, were deposited at the downstream end of the migrating riffle (6) and the upstream end of the next riffle (7). Compensating erosion occurred at both locations. However, the gradual westward erosion at the head of Carey Bar also resulted in the expected partial avulsion by 1964. This created a prominent secondary channel along the right bank extending the length of Carey Bar complex (8). These events further developed a tortuous 90^{o} bend that reduced conveyance through the main channel. As a result, amalgamation of the medial bar to Carey bar is a probable future development because of the reduced flows, while the right bank channel along Carey Bar is therefore likely to increase in prominence. Overall, the changes in reach morphology were fairly dramatic given the absence of significant floods. This provides further evidence that sediment transport is not strongly correlated with the size of the freshet, rather that the alignment of major morphologic features influences the rate and magnitude of future channel development.

Changes to 1971 were less dramatic overall than in the previous reporting period despite two major floods, but there were several important developments (Figure 6-8 A). Accretion of additional unit bars became amalgamated on the downtream end of Big Bar (1) causing extensive compensating erosion at Hopyard complex (est. 600,000 m^3). The resulting channel re-alignment also created a new secondary channel along the right bank (2) which uncoupled the complex from the floodplain. Material eroded from Hopyard was deposited on the riffle tail (3), reducing downstream (northward) flow conveyance, but increasing the flow between Gill and Greyell complexes. This altered the shape of the existing secondary channel and excavated a new one (4), providing sediment for unit bars at the channel egress, and downtream on the riffle tail at Carey Bar (5). Compensating erosion of a bar across the channel provided material for several unit bars deposited along the existing riffle downstream (6). Material was also deposited on the north and west banks of the large medial bar at the upstream end of Carey, respectively causing compensating

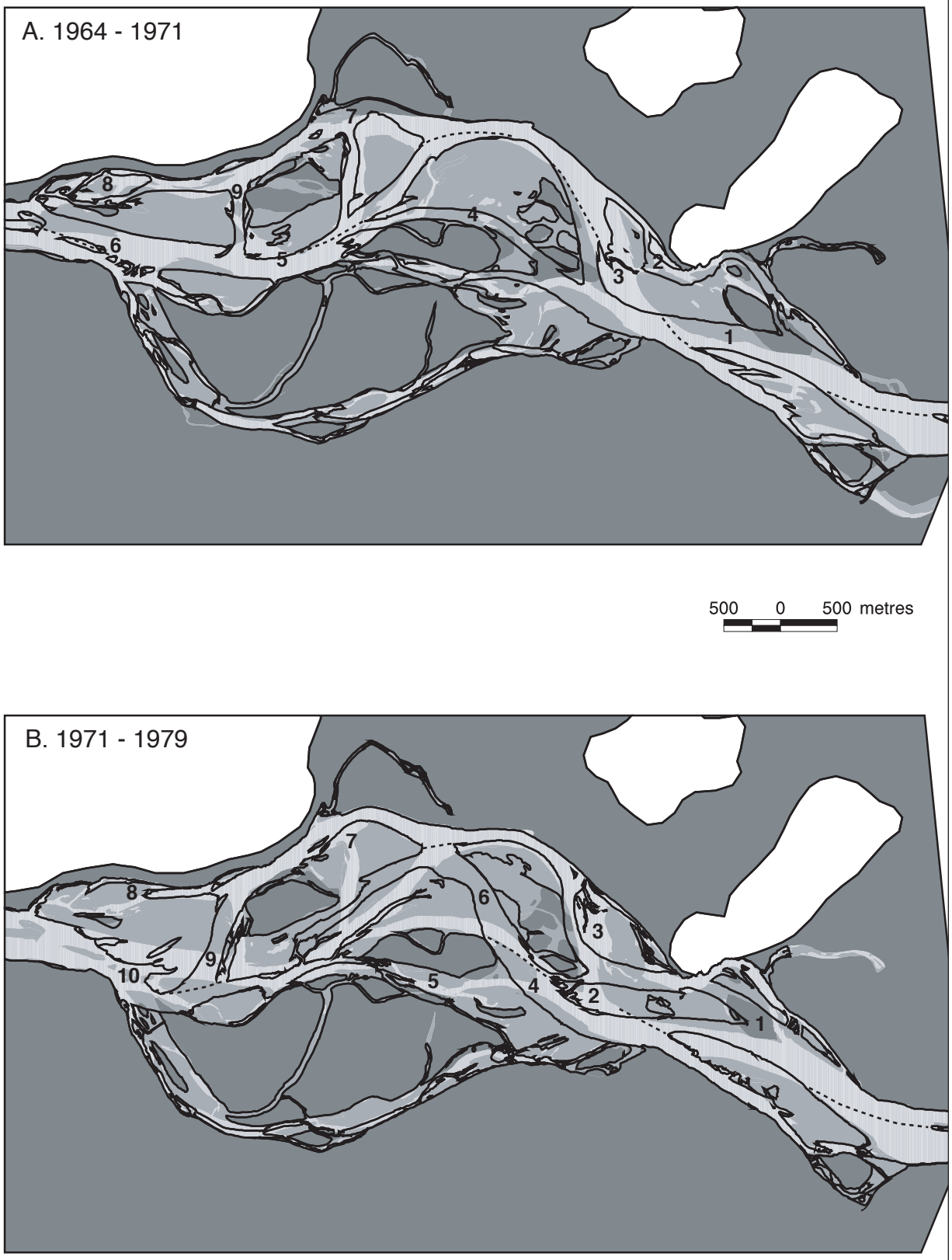

Figure 6-8. Morphologic changes from (A) 1964 to 1971 and (B) 1971 to 1979. Shaded maps depict channel conditions on the early date; outlines show changes by later date.

right bank floodplain erosion and channel narrowing, given the tortuous entrance approach (7). Eroded floodplain sediments formed new unit bars at the lower end of Carey Bar complex, effectively blocking the secondary channel and partly attaching the existing bar to the right bank floodplain (8). This appears to have created sufficient backwater effect to direct the secondary channel's flow directly south, re-aligning the existing chute channel (9).

The period 1971 to 1979 reflects changes following the second largest flood (1972) within the period of the photo record and two subsequent freshets larger than the mean annual flood (Figure 6-8 B). Changes to reach morphology are substantial in comparison to the fairly modest modifications observed after the 1948 flood. Several new unit bars were deposited on Big Bar, increasing flow towards the right bank. This trimmed existing bar material and removed remnants of Hopyard Island that was well-established by 1943 (1), effectively splitting the flow and forming an elongated medial bar (contemporary Hopyard Bar/Island). Eroded material was deposited as a new unit bar on the downstream riffle tail, conjoining the upstream bar (2), and on a large point bar — an early stage of contemporary Hamilton Bar (3). Removal of Hopyard Island further aligned the right bank channel towards a bedrock knob (Hopyard Hill), forcing a hard turn west through the middle of the bar complex, then rejoining the former main channel. Overall, these developments created a more regularly sinuous thalweg along the right bank, but it was no longer the dominant channel. Sedimentation at the riffle tail (2) caused compensating erosion at upper Greyell Island (4) but, surprisingly, did not force additional flow through the existing chute channel (5), possibly because the channel entrance was blocked by wood or a sediment plug. Instead, the thalweg was directed to the northwest, eroding a large (250 metre wide) channel directly through Gill Bar (6) before re-connecting with the main channel near the head of Carey complex.

This erosion initiated a number of significant developments downstream. Most of the eroded material was deposited in the former main channel that separated Carey from Gill and Greyell complexes, nearly reducing it to a summer channel only, while the right bank channel at Carey complex was enlarged and had become dominant. A prominent chute channel was also infilled, creating a larger, single bar complex (7). Downstream, continued sedimentation in the minor right bank channel (8) directed flow from the right bank channel through the second chute channel, which had become an extension of the main channel thalweg by 1979 (9). This alignment promoted extensive unit bar deposition on the convex edge of lower Carey Bar, but also caused considerable erosion of established bar deposits at lower Greyell Island (10). Overall, the re-

organization of channel elements appears to be related to the migration of major stabilizing riffles as persistent sedimentation eventually inundates them. This sediment congestion forces flow into, hence enlarges, existing erosional channels or initiates a channel avulsion. Consequently, entire channel bars can be displaced downstream as these features become separated from outer channel banks, or from one another. Despite the rather chaotic changes that occurred during this period, however, there is an emerging appearance of a return to a more regularly sinuous thalweg. If this assertion is correct, changes in the following period should be comparatively modest, with consolidation of major bars as secondary channels become sedimented, similar to the reach configuration of previous decades.

There were three floods in excess of the mean annual flood between 1979 and 1986, the largest of which had a return period of roughly 5 years. Two chute channels developed across Big Bar (1), but they may be an artefact of the relatively high discharge when the 1986 photography was taken (Figure 6-9 A). Similarly, the apparent removal of small unit bars and minor trimming of larger medial bars throughout the reach may not assuredly be real (e.g. site 2). There was neither sedimentation nor erosion near Hamilton Bar (3) and the establishment of vegetation is an indication that this area was becoming increasingly stable. However, lowering of the riffle connecting Hopyard Bar with the downstream bar (4) indicates that the right bank channel was becoming more active. Eroded sediments were deposited on outer Hamilton Bar (5) causing compensating erosion with downstream deposition at the head of Gill Bar (6). Headward extension of Hopyard Bar drove sufficient flow towards Greyell Island that the old chute channel was re-activated (7) and enough material was removed to separate Greyell from Gill Bar complex. The large unit bar at Gill (6) caused compensating erosion at lower Hamilton Bar and directed the thalweg towards the right bank. Consequently, flow through the chute channel that once separated upper Carey Bar from Gill Bar was reduced, while sedimentation increasingly consolidated both features. Minor extension of vegetation on Gill bar complex illustrates that this site, much like Hamilton Bar, was largely inactive. Overall, these patterns of morphologic development imply that the reach was becoming increasingly stable, likely the consequence of reduced sediment influx. The thalweg remained hard against the right bank towards the head of Carey Bar, partly re-activating the minor secondary channel (8) but most of the flow was maintained in the existing channel. However, unit bar deposition at the outlet of the eroded chute channel between Greyell and Gill (9) forced the thalweg to migrate 300 metres westward, removing nearly one-third the

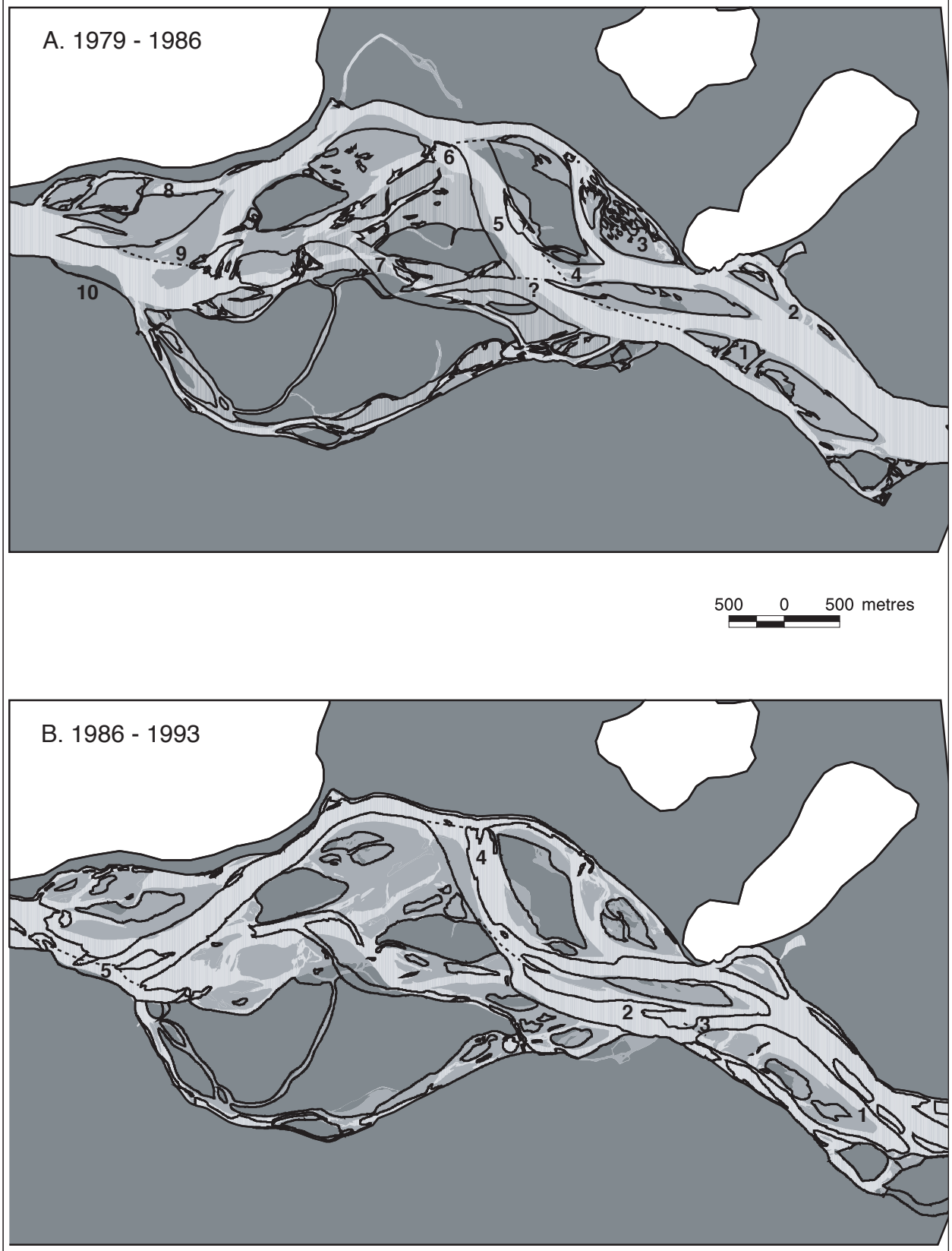

Figure 6-9. Morphologic changes from (A) 1979 to 1986 and (B) 1986 to 1993. Shaded maps depict channel conditions on the early date; outlines show changes by later date.

surface area of Carey Bar and directing flow toward Carey Point (left bank) where major erosion occurred (10).

There were several small freshets from 1986 to 1993, with only the 1990 freshet exceeding the mean annual flood. Not surprisingly, there was considerable extension and consolidation of establishing vegetation throughout the reach as a result (Figure 6-9 B). There is also the appearance of substantial sedimentation, but the actual magnitude is tempered by a decrease in discharge from 2500 m^3/s to 580 m^3/s on the respective dates of photography. There was extensive deposition on the right margin of Big Bar (1), but this did not cause compensating erosion because of extensive right bank armouring. Similar sedimentation appears at the head and left margin of Hopyard Island (2), but the absence of compensating erosion at the unprotected Greyell complex suggests that these sediments were more likely exposed than deposited as new unit bars. In fact, much of the flow had become focussed in the right bank channel, as a riffle between Hopyard and Big Bars reduced flow into the left bank channel. This development promoted siltation within the channel between Greyell and Gill complex, effectively rejoining these two features. However, because the chute channel was only partly infilled (a smaller, but topographically distinct, channel remained along much of the right bank of Greyell Island), re-activation during a large flood remains probable. Vegetation growth also continued at Hamilton Bar, while the former main channel and several smaller chute channels that once dissected this feature (refer to Figure 6-8) were increasingly infilled. There was extensive lateral extension on [newly formed] Hamilton bar complex, trimming up to 150 metres of Gill Bar (4), but the flow was becoming quite restricted with a sharp turn towards the west. Erosion at Gill appears to be the primary source of material for new unit bars deposited near Carey Point (5). These deposits have effectively formed a major riffle that highly restricts local flow, so lower Carey Bar is likely to become eroded to increase flow conveyance. Although protected by bank hardening, some erosion may also occur at Carey Point because the channel is sufficiently deep (~12 metres) to undermine existing bank protection.

Flows from 1993 to 1999 were also modest, with only the 1997 freshet larger than the mean annual flood. Further consolidation of vegetation occurred throughout the reach and major channel changes were subdued (Figure 6-10 A). Several small medial unit bars along Big Bar were removed (1) and deposited on the riffle between Big Bar and Hopyard Island, nearly amalgamating the two deposits (2). A larger medial bar near Hopyard Hill was also nearly destroyed (3) as the thalweg was maintained along the right bank, hence directly aligned towards the bedrock. This continued to maintain the current westward though the established channel, removing several unit

bars (4) which were deposited on outer Hamilton bar complex (5) and more directly aligning the channel with Gill complex. The combination of these sequences produced up to 150 metres of lateral erosion over a length of 100 metres on outer Gill bar complex. A new unit bar was also established on the tail of Hopyard Island (6) which more directly aligned the smaller left bank channel towards the head of the chute channel separating Gill and Greyell. This portends a partial avulsion if the left bank channel captures sufficient flow. Indeed, enlargement of the channel entrance, and re-connection of the chute channel with the main channel near Carey Bar, provide evidence that this development was already in progress. It is also a shorter, steeper route than the sinuous current main channel. The final major change over this period was extensive erosion of lower Carey Bar as the channel continued to migrate westward, removing several small unit bars, and left bank erosion near Carey Point as the channel was forced to increase conveyance (7). The now widened area of flow expansion is likely to become a significant depositional site in the future, and may increasingly force the thalweg north towards Carey Bar, removing much of this feature.

Figure 6-10 B shows low water channel conditions in December, 2003, following large freshets in 1999 and 2002 (return periods between 5 and 10 years). The thalweg was maintained in the right side of the channel by Big Bar and Hopyard Bar, while the chute channel separating them was nearly infilled, joining both features (1). Deposition is likely to continue at this site for several more years because it coincides with the tail of a large cross-over riffle that has established. Further upstream, incision at the head of Big Bar (2) increased flow into the left bank channel, and there was modest widening to increase conveyance. Because of the riffle on the downstream end of Hopyard Island, the left channel continued to be aligned directly towards the channel separating Greyell and Gill Islands. The increased flow (abetted by spillover across the riffle at high discharge) was sufficient to complete a partial channel avulsion through both complexes, clearly separating them for the first time since 1971. Erosion at the head of Gill Island (3) has increased the spillover volume, and the left bank channel is likely to become dominant within the next several years. Material derived from the erosion at Gill was deposited on the convex bend of Gill Island downstream, with compensating erosion at lower Hamilton Bar complex creating a more tortuous flow path (4). Over time, this may increase deposition in the channel between Gill and Hamilton bar complexes, possibly even joining them. Near lower Greyell Island, several new unit bars — comprised of material eroded during the partial avulsion — were deposited in the area of flow expansion (5). As expected, this forced the thalweg north, and up to 200 metres of lower Carey Bar complex was eroded (6).

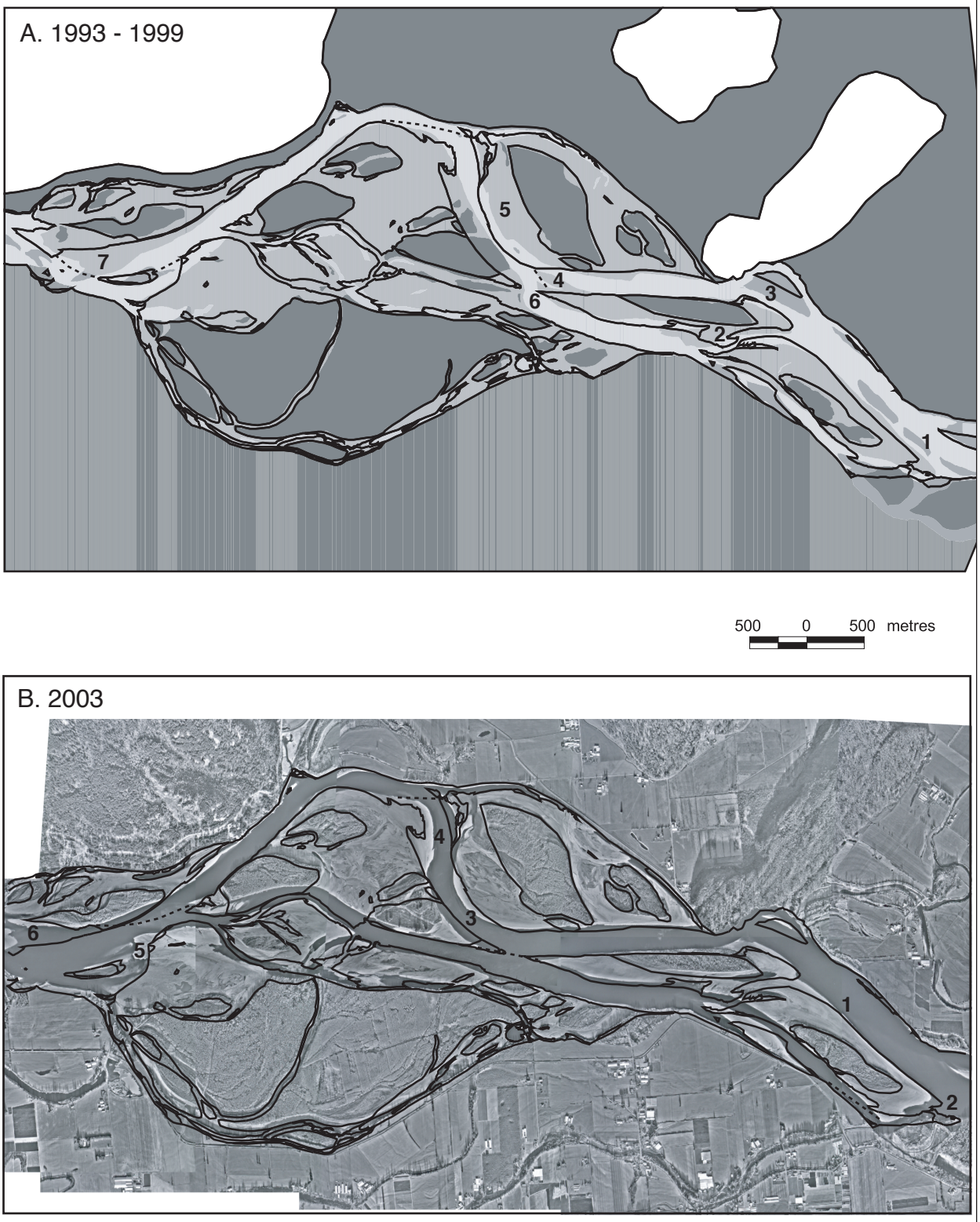

Figure 6-10. Morphologic changes from (A) 1993 to 1999. Shaded map depicts channel conditions on the early date; outlines show changes by later date. (B) Photo mosaic from low water photography taken December, 2003 with superimposed 1999 outlines (reverse convention for all other maps).

The reach has undergone a number of significant changes over the past 60 years but, fundamentally, the basic wandering morphology (an alternating riffle-pool-bar sequence) has been maintained despite long-term fluctuations in discharge and sediment supply, and increasing anthropogenic constraints. Changes have usually, though not invariably, proceeded in a fairly predictable manner for periods of several years to several decades. Sediment transported into the reach is deposited as unit bars on convex bends, traveling across major riffles. The accretion of these features produces compensating erosion across the channel, thereby providing source material for new unit bars downstream. This manner of point bar deposition and compensating erosion follows an orderly pattern usually ascribed to meandering channels. However, wandering channels, by virtue of proportionately greater sediment loads, disrupt this sequence when sedimentation overwhelms the riffles and the channel becomes constricted. Deposition of medial unit bars in areas of flow expansion or on riffle crests produces a similar effect. This can initiate partial avulsions along existing chute channels where resistence to erosion is reduced, and correspondingly leads to stabilization and amalgamation of existing bars where the dominant flow channel becomes abandoned.

A higher order pattern is also evident over the complete mapping sequence, visible when successive maps are overlaid and viewed in quick succession (as if animated). Downstream of Hopyard Hill, reach morphology has been developing in a counter-clockwise fashion as the main channel thalweg has migrated both northward and westward. This occurs as entire bars and bar complexes slowly migrate downstream after they develop in mid-channel, or become isolated from outer channel banks. Conversely, compound forms that remain attached or partly attached to the floodplain are far more stable, and may be able to persist for hundreds of years. Greyell Island, initially buffered by the prevailing channel alignment, and recently by a crest protection structure in Greyell (Jesperson) Slough, has maintained its general form over the past 60 years, while all other bars and bar complexes have evolved and migrated downstream about its outer margins. Given that both Big Bar/Hopyard Island and Gill Island complexes are no longer attached, both features are expected to become completely reworked in coming decades. The evolution of these features is complex, but identifying distinct temporal patterns or trends could reveal further details on long-term sediment transport and channel evolution. It is a line of inquiry suitable for analysis by computer-based techniques.

6.5 GIS-based spatial analysis: channel transitions

Since all of the low-water mapping is in digital form, combinations of successive maps can be made in the GIS to examine channel transitions, or the probability that a classified morphologic surface (i.e. gravel bar) retains that state over time. The re-classification of bar-edge to bar polygons (see Section 6.4) is critical for this type of analysis, as it provides a reasonable analogue of steady-state conditions – fluctuating water levels would produce multiple cases of false transitions (cf. Brabets, 1997). Transition state analysis provides a quantitative means for examining spatial patterns of channel instability, can be used to infer whether the underlying mechanisms that control channel morphology have changed, and further serves to highlight the dynamics of the fluvial system. The approach does not, however, reveal any details of the actual processes that cause channel changes, such as bar erosion and deposition, so the analysis is complementary with the preceding chronological account. Several variations of transition state analysis are also presented below that provide information on the probability that a given state will be encountered, and of the expected longevity of depositional forms, thereby illustrating the dynamics of channel evolution on the river.

Transition matrices are calculated for successive mapping periods by tabulating the proportional area of water surface, channel bar, and floodplain polygons on the early date that retain these respective states, or are succeeded by a new feature class because of intervening erosion and deposition (yielding 9 possible transitions). Dividing each area in the matrix by its row total gives the conditional probability, or the likelihood that a particular feature will occur given the current morphology (Davis, 1986). An example of these calculations is given in Table 6-3 below, and transition probabilities for water surface and gravel bar polygons for all mapping periods are given in Figure 6-11.

. The graph demonstrates two interesting properties of channel change. First, there is a far greater tendency for the system to retain its original state than to change to another. This is directly related to the small volume of sediment transfer within the 5 to 8 year interval of the comparison periods relative to the total volume of sediment stored within the study reach. However, the plots for successive mapping periods suggest that the persistence of this tendency is in decline. The decrease in water to water transitions is mirrored by an increase in water to bar transitions (although neither trend is strong) providing some evidence that the channel is becoming less stable, supporting the same assertion presented in Chapter 4. Bar transitions show a similar pattern, but also demonstrate that the vegetation growth is increasing over time (in effect, islands are

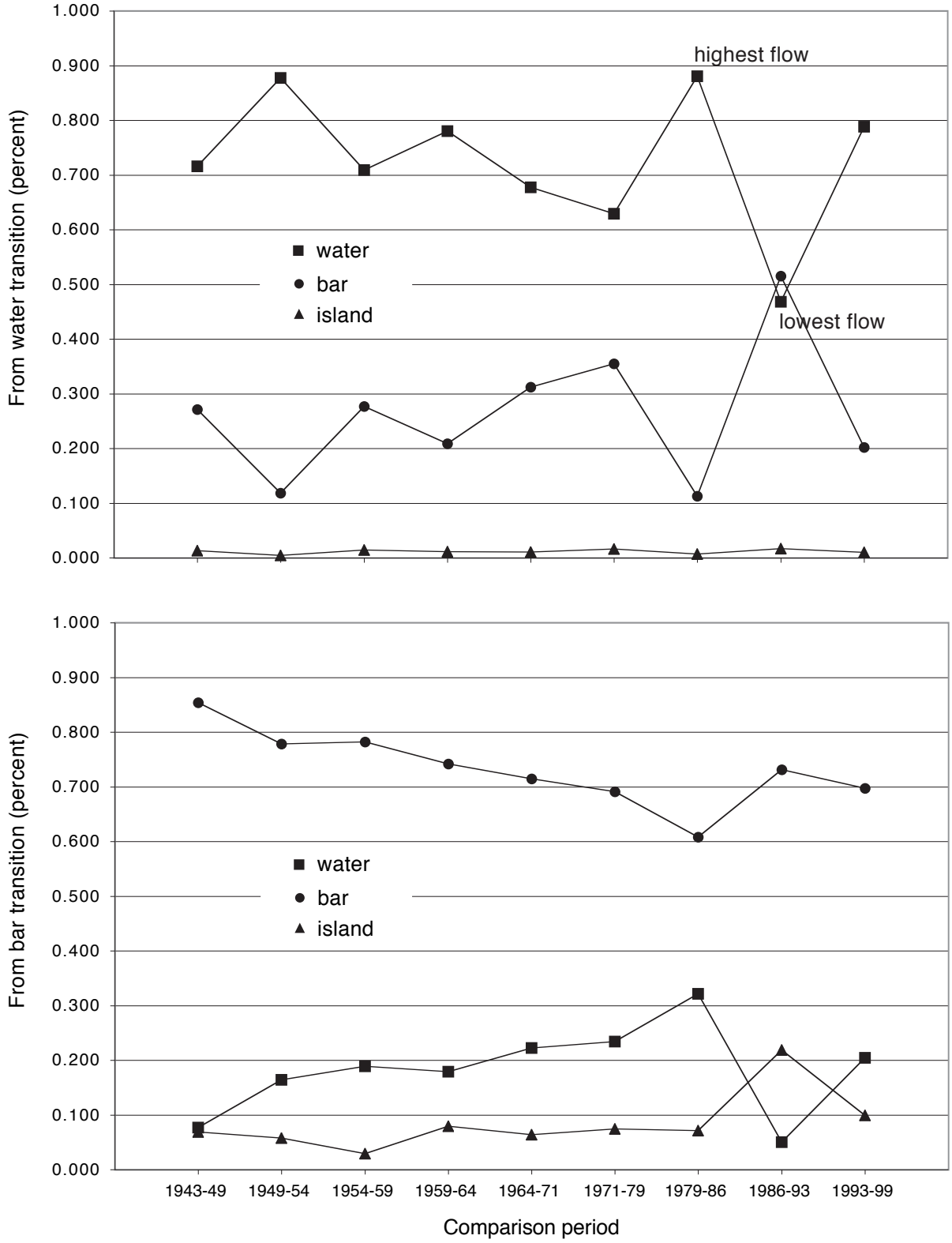

Figure 6-11. Transition state probabilities for water surface and gravel bar polygons throughout the low-water mapping series. Island to island transitions (not shown) range from 0.84 to 0.91 and do not exhibit any temporal structure because the mapping interval is too brief to effect significant change in island area.

'replacing' bars). Since island and bar deposits constitute the majority of mapped surface area on each date, this pattern demonstrates that the channel is actually becoming increasingly stable. It is a quantitative signal of the gradual development of 'mega-islands' (Chapter 4). Although the trends of bar 'loss' and island 'gain' indicate a modest reduction in the area of exposed transient deposits, the total area of exposed bars has not changed appreciably over the period of record. This circumstance occurs because of the modest increasing trend in water to bar transitions.

Table 6-3. Transition area and probability matrices for the period 1943 to 1949. 'FROM' states are given in the first column, while 'TO' states are given in the first row.

AREA	Water surface (m^2)	Gravel bars (m^2)	Islands[1] (m^2)	Total (m^2)
Water surface	3,227,264	1,221,591	59,565	4,508,240
Gravel bars	382,881	4,248,557	343,062	5,567,612
Islands[1]	198,422	281,273	5,087,917	4,974,500
PROBABILITY	Water surface	Gravel bars	Islands[1]	Total
Water surface	0.716	0.271	0.013	1.00
Gravel bars	0.077	0.854	0.069	1.00
Islands[1]	0.036	0.051	0.914	1.00

1. All transitions include the area of eroded and deposited floodplain but not the area of stable floodplain. This defines the outer boundary within which channel changes are expected to occur. Extending the analysis to include the complete area of mapped floodplain would be meaningless since most of this area does not change.

A channel transition can be desribed as intermediate between purely deterministic and random events. Given a particular morphology for some arbitrary date, the future morphology can not be predicted with any certainty. However, channel evolution is not completely random, but is partly dependent upon the preceding state or states and can be analysed as a Markov chain (Davis, 1986). Clearly, there is a temporal influence on the strength of the association between states over time. Over increasingly long survey intervals, it is reasonable to assume that persistence probabilities trend towards zero. This can be investigated by a method of analysis termed a 'similarity matrix' which examines whether conformity in channel pattern is associated with the length of survey measurement. Details of the development of individual bars and islands are not preserved. Each date of mapping is considered to be an independent snapshot of channel conditions, and is superimposed with every other map to tabulate the areal proportions of water, bars, and islands that have been identically classified on both dates. By testing for the possibility

that mapped channel sequences corresponding to specific time intervals (e.g. 20 years) are more or less similar to sequences at various other intervals, it is intended that a tool for predicting channel evolution can be developed. This approach should provide further insight into the dynamics of channel change on the river. An example for gravel bar transitions is given in Figure 6-12.

The plot shows that the likelihood of the river retaining its current state gradually declines as the survey interval increases. Although not shown on the graph, the trend actually stabilizes by the fifth interval (corresponding to mapping comparisons separated by 30 years on average) with roughly 40% to 50% of original bar surface remaining. Within this timeframe, the similarity matrix shows that the channel remained closer in form to the original morphology (e.g. 1943 to 1971) than for the same temporal spacing starting later in the mapping sequence (e.g. 1971 to 1999). This separation of the time series allows the impacts of the 1948 and 1972 floods to be demonstrated. Between 1943 and 1949, 85% of the mapped bar area retained that state, while an additional 7% became vegetated. Although the 1972 flood was smaller, only 70% of bar area remained stable (7.5% became vegetated) reflecting the avulsion through Gill Bar complex and subsequent re-organization of channel elements downstream (see Section 6.4). This event was significant enough to dominate the similarity matrices from 1971 to 1999, giving the appearance of decreasing channel stability in recent decades. Similarly, the lack of major changes following passage of the 1948 flood gives the impression that the channel was much more stable in the past. In fact, the transitions from bar to island are larger since 1971, and reflect an increasingly stable morphology. Although the plot does not clearly demonstrate any mapping interval where the similarity index reverts to a higher value (which would indicate that a pre-existing morphologic state was re-forming), the stabilizing trend at 30 years provides an indication that this is the temporal scale at which major bar and bar assemblages develop. As such, this timescale provides a template for forecasting future channel evolution.

Repeating sequences of mapped aerial photography have also been used to graphically illustrate the most common configuration of a channel over some mapping period, hence by extension, to illustrate the likely future position of channel elements (Tiegs and Pohl, in press). The location probability model (cf. Graf, 2000) can be constructed for the entire channel, or for individual morphologic surfaces. For this exercise, bar and water polygons for each mapping date are superimposed, and are assigned a weight proportional to the number of years represented in the mapping sequence. Following the method of Graf (2000), weights are calculated as:

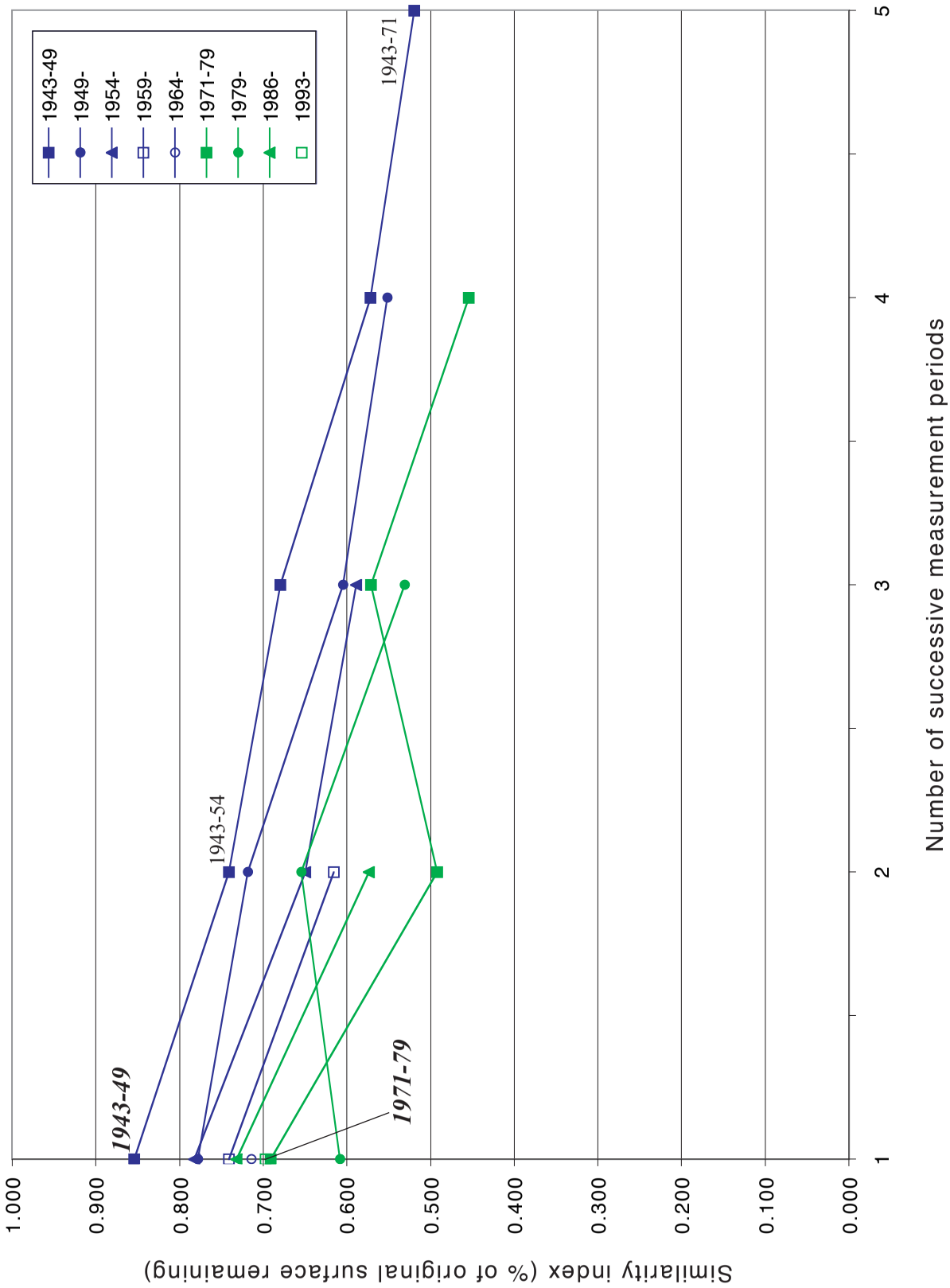

Figure 6-12. Similarity matrix values of gravel bar transitions for low-water mapping periods. The colour coding separates the mapping into the period 1949-71 and 1971-99 to isolate the impacts of the very large floods in 1948 and 1972.

$$W_n = t_n / m$$

where W_n is the weight assigned to each morphologic unit on a map, t_n is the number of years the feature was present (equivalent to the temporal spacing of photographs), and m is the length of the complete record. For simplicity, t_n was estimated to be 6 years for all periods, and the actual record length (54 years) was rounded up to 60 years, assuming that bar and water surface polygons in 1943 could reasonably be 3 years old at the time of photography, and that these same features in 1999 were maintained for a following three years (until the next major freshet). This means that if a feature is present on any individual mapping date, it is assigned a weight of 0.1. Over the complete sequence of mapping, the locational probability then becomes:

$$p = (W_{1943} + W_{1949} + ... W_{1999})$$

where *p* is the locational probability that any position in the active channel zone was occupied by either a bar or by water over the period of record. The value ranges from 0 (never occupied) to 1 (always occupied) in increments of 0.1. Calculated in this manner, probability is not a continuous value, but more correctly is a relative frequency.

Visual examination of the locational probability maps (Figure 6-13) reinforces the observation that the channel has a stronger tendency to retain its existing morphologic configuration than to change. The top plot (bar) clearly shows that higher counts are associated with the location of the major bar/island assemblages within the reach but, over the period of record, much of the active channel zone has been occupied because of unit bar and bar migration. Lower counts are associated with frequent occupation by water and roughly define the sinuous average thalweg (bottom plot). The most persistent locations are narrow constrictions at the up- and downstream mapping boundaries where bed material is not deposited. The generally contiguous pattern of higher frequency counts demonstrates that thalweg location is quite stable, restricted by the more dominant morphologic evolution of channel bars. Breaks in this pattern (near the upstream end of Hamilton and Greyell complexes) are locations of past channel avulsions. Areas with zero probability are typically locations of stable islands, but include a few locations of persistent flow paths (top plot) and stable bars (bottom plot). Overall, the morphology of the reach has been sufficiently modified that few remnants of very stable bars (i.e. counts of 9 or 10) remain. With the exception of stable bars on the left bank near Greyell Island, most are likely to be destroyed within the next few decades.

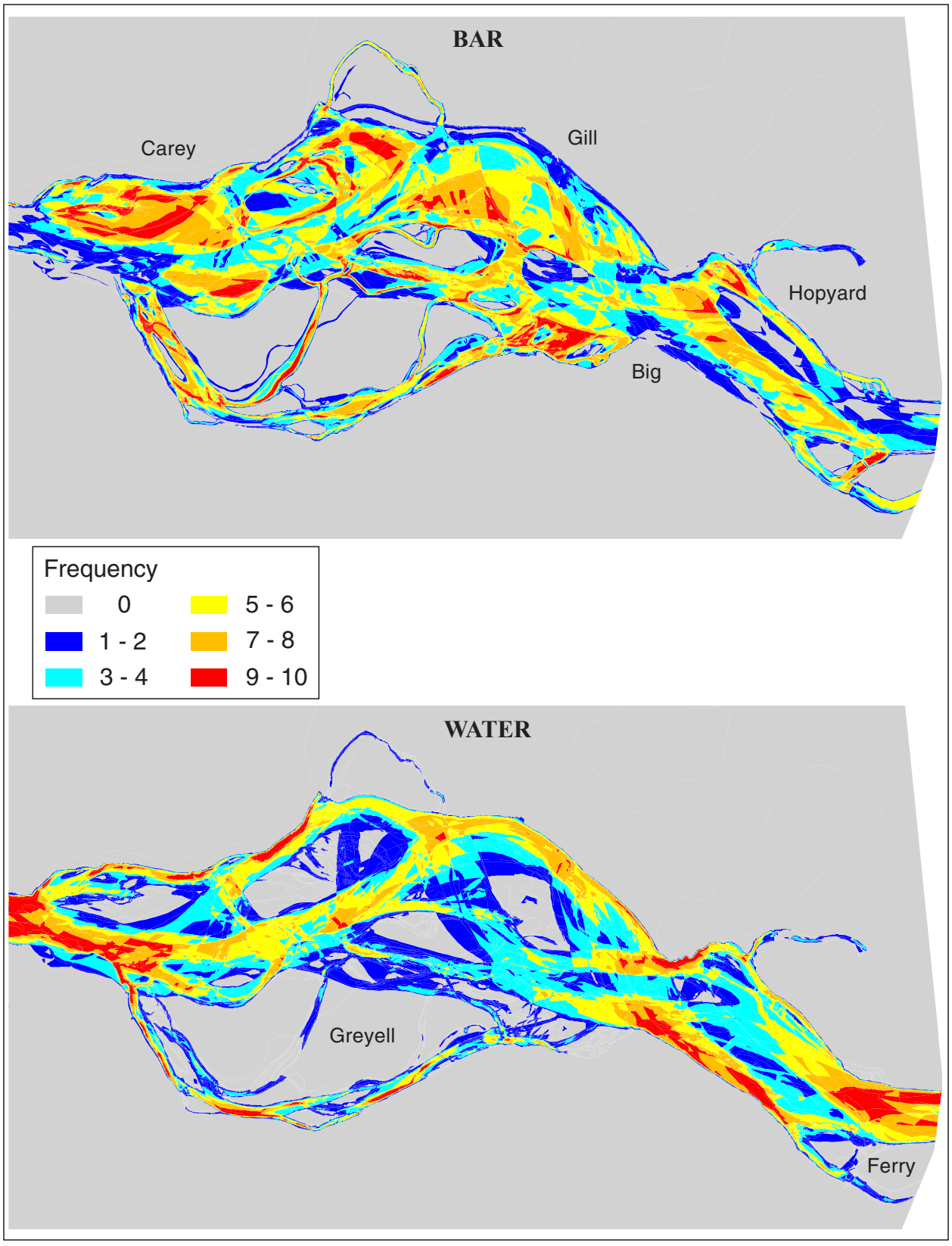

Figure 6-13. Locational frequency of channel bars and water surface. Probability is expressed as the frequency of occurence (count) for the 10 mapping periods.

The actual time required to rework the remaining stable bars (and islands), added to the length of the mapping period, is equivalent to the length of time required to entirely remove a stored volume of sediment from the reach. Dividing the volume of sediment stored in the channel by this turn-over (or residence) period, yields a long-term estimate of the sediment volume transported through the sedimentation zone. The procedure is equivalent to reservoir theory but is simplified because the age of different storage zones does not have to be estimated. Decay curves were developed from the composite low-water mapping series by calculating the areal percentage of the original (1943) water surface, bar and island features that remained in the same position over successive mapping dates. The decay of bar and island surfaces can be modeled with an exponential function which can be linearized by plotting the abscissa (percent remaining) on a logarithmic axis. The turnover rate can then be extrapolated by graphically estimating the intercept with the x-axis (Figure 6-14). The bar deposits have a turnover rate of roughly 90 years, while the island deposits are estimated to be removed every 270 years. A small fraction of island deposits may in fact be much older but this can not be accurately determined by this method.

Long-term sediment transfer rates were determined by dividing the stored (1943) sediment volumes of bar and island deposits by the turnover rates, then summing the averaged annual volumes. Volumes were calculated as the product of feature surface area and the mean thickness of the deposits (excluding overbank fines), estimated by Martin and Ham (*in press*) to be 3.2 metres.[2] This yields an estimated average annual transfer rate of 64,000 m^3/yr for islands and 177,000 m^3/yr for bars, or 241,000 m^3/yr total bed material transport. For comparison, the rate of bed material transport at Agassiz-Rosedale bridge was estimated as 197,000 m^3/yr based on the direct comparison of the 1952 and 1999 channel surveys (Table 5-3), but the result is nearly identical to the error-adjusted rate of 237,000 m^3/yr, though smaller than the 262,000 m^3/yr sum of the period sediment budgets (Table 5-4). The transport rate from the decay-curve approach is sensitive to the correct turnover rates, but dating to establish the true age distribution of sediment is difficult (Lisle, 1987b). Nevertheless, the similarity of these results from two independent techniques is encouraging and warrants further investigation.

2. For this exercise, the width and area of each extracted cross-section (see Chapter 4, also Appendix A) were first calculated. The intersection of the bed profile and the line representing the high-water surface was used to create each cross-section polygon for calculating area. For each morphologic sub-reach, the sum of total cross-section area was then divided by total width to provide an estimate of mean bankfull depth.

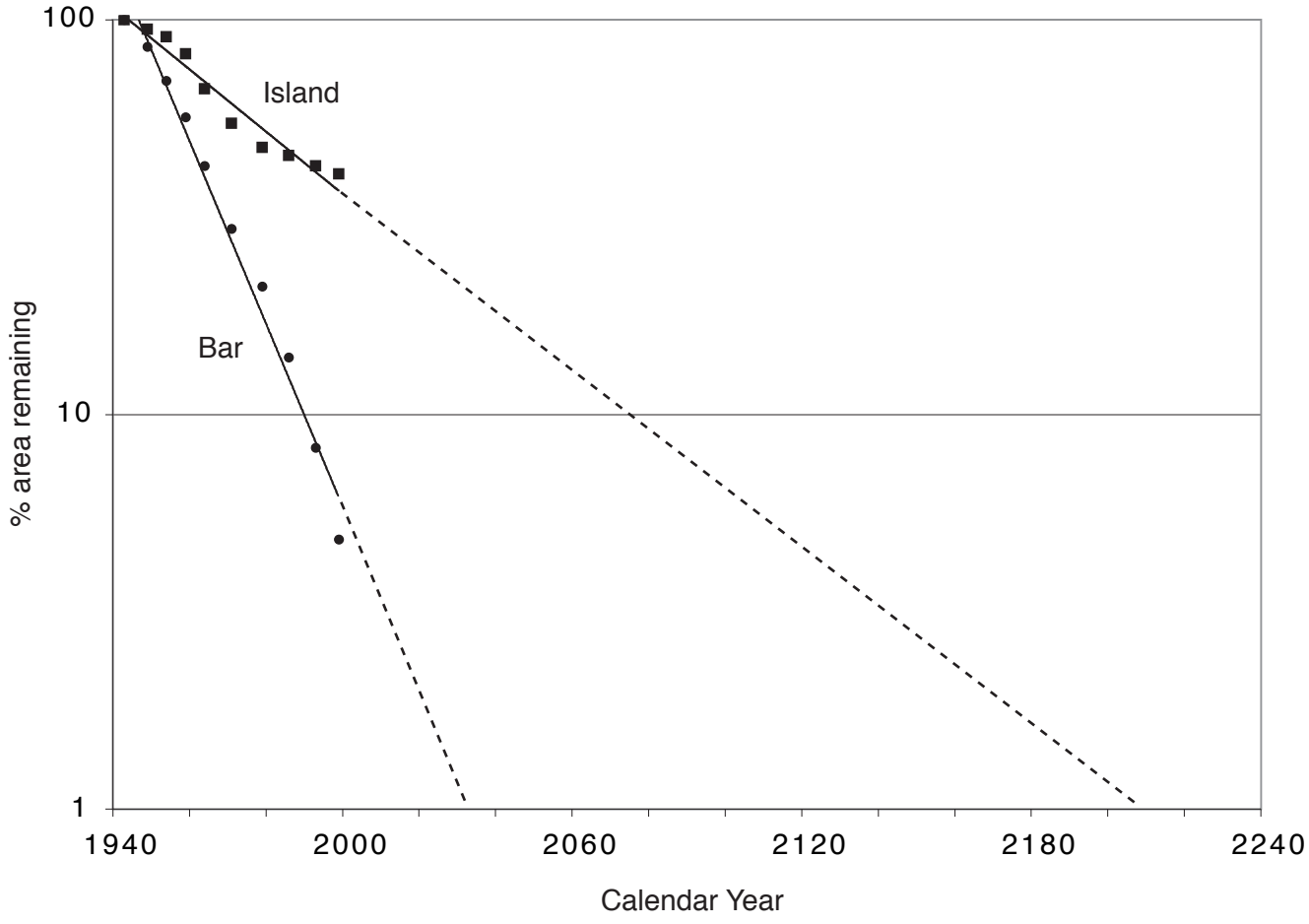

Figure 6-14. Decay curves showing loss of bar and island surfaces since 1943

Results from the transition state analysis demonstrate important trends in channel development over the past 60 years. Over the scale of several years to a decade, the channel exhibits a strong tendency to retain its original morphologic state, regardless of the magnitude or frequency of intervening flood flows. This occurs because the magnitude of sediment transport is small relative to the volume stored, so many years, even decades, are required to effect significant change. This timescale corresponds to the development of major bars and bar assemblages on the gravel reach. Although the technique is useful for quantifying the rate of channel change, it does not reveal information on the underlying process that cause the change. It has also been shown that channel instability has been increasing in recent decades, although this analysis does not provide a direct reference to the underlying causes. While the channel may have become increasingly unstable after the 1940s in response to extensive bank hardening, gravel removals and the passage of several large floods, these effects appear to be waning.

Chapter 7: Conclusions

7.1 Summary

A combination of historic maps, aerial photographs and bathymetric surveys has been used to investigate the rate and magnitude of distributed three-dimensional morphologic changes on the wandering gravel-bed reach of lower Fraser River over the past century. The main objective of this thesis has been to elucidate the association between the staging of sediment and the style of channel deformation by examining the variables that directly influence the entrainment, transport and deposition of bed material, since this controls the morphology, hence stability, of alluvial channels. Measuring channel adjustments over time further provides a means to monitor and evaluate the sensitivity of the river to environmental changes, hence to predict channel response to disturbance. It is intended that this research will provide tools for effectively managing erosion and flooding concerns while preserving ecosystem diversity if the impacts of decisions on channel development are better understood.

Channel morphology in the gravel-bed reach is dominated by the downstream transfer of coarse alluvial sediments, but because the transport rate is small relative to the volume of bed material stored within the reach, changes to morphology usually occur slowly. Most bed material tends to accumulate in wider 'sedimentation zones' where migrating bedload sheets are accreted to larger mid-channel and point bars associated with the location of prominant diagonal riffles. Lateral instability is greatest where deposition of these unit bars forces compensating erosion to maintain flow conveyance, hence propagating instability downstream. The average spacing of major riffles controls the location of major morphologic features on the river. Major changes are associated with the downstream migration of the riffles, or where sedimentation overwhelms the riffles, forcing migration of the thalweg. Consequently, there is a tendency for the channel to retain its general morphology for several years or more, regardless of the magnitude or frequency of large floods. Large bar and island complexes may persist for decades to centuries as the capacity of the channel to completely re-mobilize these deposits is limited over shorter timescales.

Channel changes in the reach were pronounced early in the century following initial settlement of lower Fraser Valley. After a series of devastating floods in the late 1800s, several prominent floodplain channels were isolated from the main channel by small dams and flood gates. This effectively reduced the width of the active channel zone, and many large islands were incorporated into the floodplain as the secondary channels silted up and became vegetated. Bank

hardening to reduce shoreline erosion and protect railway lines was also an important early development in influencing channel morphologic development. An expansion of the dyking program following the devastating 1948 flood moderated further width increases to the mid 1970s despite the coincidence with generally above-average flood flows, while the channel has since continued to narrow, a consequence of mainly below-average floods.

At present, the area of channel islands has recovered to 1949 totals, but available evidence indicates that mature, riparian forests are being increasingly replaced by younger vegetation on newly established islands, and that variability in cross-sectional area amongst these islands is in decline. Overall, these modifications portend a gradual change from a multi-thread wandering to a single-thread meandering channel, as has been demonstrated on several European rivers modified for navigation and flood protection purposes (Decamps et al., 1989; Steiger et al., 2001; Surian and Rinaldi, 2003). This evolution has resulted in numerous detrimental impacts, including local bank erosion and bed scour, downstream aggradation and widening, loss of riparian ecotones and a consequent reduction in the availability and quality of aquatic habitat. Corresponding with this transition is a gradual flattening of the channel as reaches upstream of Agassiz-Rosedale Bridge are degrading, with entrained sediments deposited downstream on higher bar surfaces, reducing the extent of shallow water habitats during flood. In general, channel narrowing and deepening are associated with greater shear stresses, and hence an increased capacity to transport bed material farther downstream, although this circumstance is partly tempered by the reduction in channel gradient and armouring. Aggradation over the past half-century is, however, apparent, and appears to have accelerated in recent decades (although 'true' transport rates have proven difficult to calculate). It is not clear that this pattern is strongly related to channel confinement, since local channel alignment also appears key in initiating and maintaining sites of persistent erosion that drive downstream transport.

In recent years, the passage of several large floods has begun to focus the attention of both the public and river managers on the effects of this aggradation in raising water levels. Although constrictions in channel alignment are known to be locally significant, recent studies (UMA, 2004) have clearly demonstrated an increase in the design flood profile since 1952, prompting renewed action. While there are several options for mitigating flood levels, lowering the bed of the river through targeted gravel removals appears the most favorable option because it is far more cost-effective that any other consideration. Some dyke reconstruction also remains likely, however, especially where they remain below standard (Church, 2001). Additional riprap is apt to be placed

on channel banks to protect them, where necessary. Understanding the past impacts of these activities on patterns of sedimentation, and morphologic development along the gravel reach is pre-requisite to ensuring that future decisions are able to maintain a balance between sound engineering practice and habitat maintenance.

7.2 Evaluation of research hypotheses

The association between sediment transport and channel deformation developed in this thesis has been reviewed by examining channel morphodynamics over decadal timescales. The pursuit of this relation led to the initial development of several research hypotheses, which were investigated thorough a systematic analysis of available historic data. Through these efforts, the scientific understanding of the long-term behaviour of wandering channels has been improved, with several aspects of channel change having been quantified for the first time. Although the investigation of the hypotheses has been largely successful, there are remaining questions that could not be fully addressed. A summary discussion of the major findings is presented below.

1. Spatial and temporal variability in sediment transport on lower Fraser River can be directly related to observable sequences of channel morphodynamics. This thesis has shown that wandering rivers exhibit a fairly regular sequence of development similar to that observed on meandering channels. Most bed material transport occurs as migrating unit bars (gravel sheets) with length scales to several hundred metres, thicknesses of one or a few grain sizes, and volumes of the order 10^4 to 10^5 m^3. Unit bars travel across major riffles and are accreted to existing point and mid-channel bars, forcing compensating erosion to maintain conveyance. Eroded sediments provide source material for new unit bars as the pattern propagates downstream. This orderly sequence may persist for several decades and is not strongly related to the magnitude or frequency of large floods, since the volume of material that is transported is small relative to that stored within the active channel zone. Sediment transport rates are highly variable over space and time in accordance with local channel alignment. The highest transport rates occur when the thalweg is forced into existing bar and island deposits, causing extensive local erosion.

This sequence of development continues in an orderly manner until continued sedimentation overwhelms the riffles, and the channel becomes constricted. Sedimentation on riffle crests and in areas of flow expansion produce a similar effect, but these events are less common. The dominant spacing of the major riffles, 1500 m, or half the meander wavelength, controls the spacing of major bars and bar / island complexes on the river. These features are

mobilized downstream as the riffles themselves migrate. Since the magnitude of sediment transport is small relative to the total volume of sediment stored in the reach, large bar and island assemblages can persist for many decades to centuries before they are completely reworked as new deposits evolve. Compound forms that remain attached to the floodplain, or are protected from direct attack by the prevailing channel alignment, are the most stable forms.

2. Historic patterns of morphodynamic change can be used to predict locations and rates of future instability. Given the somewhat regular sequence of morphologic development on wandering channels, it has been demonstrated that large scale channel developments such as avulsions and erosion of channel deposits can be reasonably predicted over periods from several years to a decade. Sequences of low-water aerial photographs were examined to relate the downstream transfer of bed material to associated channel changes, including sites of probable erosion (including avulsions) and downstream deposition. Monitoring the evolution of local channel alignment — the direct consequence of bed material deposition – is key to successfully predicting significant changes to channel morphology. This knowledge has important implications for riverine management, since it can help identify sites where targeted gravel removals or channel re-alignment would provide the greatest benefit, for reducing compensating erosion.

3. Past gravel removals, construction of flood dykes and riprap bank protection, and a reduction of naturally occurring woody debris deposits have significantly altered the morphology and sediment transport regimes of the river over the past century. Although it is exceedingly difficult to isolate the individual effects of these practices, there is compelling evidence to support this claim in general. An exception is noted for woody debris, which has been greatly reduced by trapping since 1979, but there has been no corresponding impact on the establishment or maintenance of channel islands. Overall, the channel has narrowed by 22% since 1912, even though flood flows have decreased only by 5% over the same period and the channel is in gradual transition to a single-thread channel meandering between large ‘mega-islands’.

Because lateral confinement and gravel mining are known to reduce topographic complexity, these activities may have negatively impacted habitat quality on lower Fraser River. Of particular concern is the apparent reduction of shallow, low-velocity waters at intermediate to high discharges as this represents a deleterious impact on juvenile and rearing fish (Rempel and Church, 2003). A reduction of available habitat types may also affect the capacity of the channel to sustain diverse populations of fishes and other aquatic species (Ward et al., 2002). However, in

the absence of long-term surveys on species density and diversity, there is no obvious method for quantifying the impacts on habitat degradation that may have occurred.

The alluvial gravel floodplain within which the modern channel is found is also being degraded as channel constrictions have increased the ratio of sand and gravel erosion to deposition. Analysis of the channel long-profile, changes in cross-section area and the sediment budget all confirm that reaches upstream of Agassiz-Rosedale Bridge are degrading faster than downstream reaches, resulting an an overall flattening of the channel. This evidence is, however, based strictly on a comparison of 1952 and 1999 survey data. The 1952 data are not well-distributed upstream of the Agassiz-Rosedale Bridge, so extracted cross-sections and sediment budget estimates are not as reliable as for downstream reaches. The long-profile, extracted from actual survey data, provides the best support for this hypothesis, but does not capture all details of topographic variability within the uper reach. The assertion should be viewed cautiously.

There is also no strong evidence to demonstrate that sedimentation rates have been significantly altered over the past half-century. Although the transport rate is estimated to be increasing over this time (a possible response to upstream confinement), this finding must also be more carefully reviewed. Indeed, the result is contrary to additional lines of evidence suggesting the channel is becoming increasingly stable, a condition that should correspond to reduced sediment influx and transfer. The supply of potential sediment that enters the upstream limit of the reach (at Laidlaw) is not, however, well quantified. It would be a worthwhile exercise to determine whether upstream inputs remain artifically high due to anthropogenic disturbances, or are becoming exhausted. Despite efforts to adjust for weaknesses in early surveys, and correct for several potential sources of error, remaining uncertainty in the sediment budgets undermines complete confidence in the results. These concerns are discussed in more detail in the following section of this chapter.

7.3 Summary and evaluation of the sediment budget

Although the association between sediment transport and channel deformation has been successfully demonstrated (cf. Chapter 6), accurate quantification of the actual magnitude of sand and gravel volumes that enter, and are transferred through the reach over time, has proven difficult despite a considerable effort to establish these values. This thesis has demonstrated a number of concerns related to sources of error that ultimately produce uncertainty in the results. While the lack of confidence in the sediment budget results is not a weakness of this thesis, *per se*, it does

indicate a potential weakness in the applicability of the sediment budget approach itself for large, wandering gravel-bed rivers. The difficulties encountered in establishing sand and gravel transport rates through the development of sediment budgets are reviewed below.

Construction of period sediment budgets is ultimately derived from available topographic survey data, which are interpolated as a three-dimensional digital representation of an actual river channel. While the precision of individual survey points is known or can be estimated, it is assumed that these errors are random, and become reduced during the initial modeling process (although the reliability of the historic data must also be considered). The main source of error relates to the actual modeling of individual bed surfaces, since all subsequent computations are based upon these surfaces. It is estimated that each surface has a pooled error of 210,000 m^3 based on the Topogrid modeling procedure, while surfaces of difference have a combined error of 297,000 m^3. Both values are small relative to the volume of sediment that moves through the system, indicating that modeling bias is a small component of overall uncertainty. An additional check of model precision was made by comparing known survey elevations with modeled elevations, and calculating the estimated precision between surveys using the RMS statistic. Dividing this value by the number of independently determined points in each surface of difference gives the RMS error of the mean difference in elevation, yielding an estimated imprecision in the volumetric estimates of roughly 500,000 m^3 for each computing period (although the result is reduced to 160,000 m^3 from 1999 to 2003). If we were simply interested in the net volumetric change of all sediment between surveys, the precision between surveys would quantify all the known error that can be measured. While it would be desirable to calculate the accuracy of our models by comparing them to a true model (i.e. to estimate bias, cf. Lane et al., 2004), no true model exists, and so RMSE is adopted as a single measure of data quality.

Most of the uncertainty in the period sediment budget estimates arises through a series of computing steps necessary to convert bulk volumetric changes into corresponding estimates of sand and gravel, because these steps introduce a series of assumptions. Surfaces of difference were first superimposed with a morphologic change map to categorize the type of channel change between survey dates (i.e. bank erosion) since the steps to parse gross changes into volumes of coarse sand and gravel vary by type. These adjustments introduce bias where the estimated thickness of overbank sand and silt does not correspond to the true thickness of eroded and deposited island and floodplain elements. Amplifying this bias is uncertainty in the assumed constant proportion of washload (sediment that is eliminated from the calculations) in the overbank

material, since spatial variations may genuinely exist. Although this uncertainty could be reduced with further field sampling, the large size of the channel would make this an onerous activity, and potential temporal changes in sand and gravel proportions would still remain unknown.

Following these adjustments, summary sediment budgets were developed to isolate the bed material fraction from the total sediment load that is deposited in the gravel reach. For this calculation, bed material transport into the gravel reach is equivalent to the net volumetric change of bed material over time because a zero downstream transport boundary was assumed (so all the material transported into the reach from upstream, or from bank erosion, becomes 'trapped'). However, strict summation of the period budgets did not equal the direct difference over the full survey interval, implying either that the sand fraction was incorrect, or that gravel actually does move past Mission (the assumed zero downstream boundary). Although there are no data with which to resolve this problem, and field sampling in this location of channel would be particularly difficult, the result implies a temporal bias. This bias occurs during transitions from bar to island to bar, or from island to bar to island, since the erosional thickness of overbank sediments is much larger than the depositional thickness, so the adopted adjustment for the wash material fraction violates mass continuity. The apparent increase in sediment influx over time, where the highest rates are associated with the shortest computing period (1999-2003) provides a further indication of some time-dependent bias. This possibility was investigated by extrapolating the transport rate for a single year when no compensating scour and fill (the likely cause of undetected transport) would occur. However, these 'unbiased' volumes were found to be so large that they could not be real, so the possibility for unmeasured flux was further investigated.

Accumulated sediment budgets were next constructed by adding stored sand and gravel volumes upstream of Mission over successive 1-km long computing cells. This step allows the transport rate to be determined at different locations along the channel, and delineates major zone of storage and transport. Except for the most recent (1999-2003) computing period, these budgets revealed large negative transport rates (which are not physically reasonable) near the downstream limit of the gravel reach. Since these patterns are also consistent with undetected transport, several possible explanations for the negative transport rates were reviewed. By analyzing published records of actual bedload and bed material samples collected by the Water Survey of Canada, it was found that the zero downstream transport boundary assumption was invalid, and while an applied adjustment reduced the magnitude of negative transport, it did not fully resolve the problem. The possibility for sounding errors was also investigated because the location of cells

with the greatest 'negative' storage rates (between 1984 and 1999) were consistent in location with high 'positive' storage rates from 1999 to 2003. This circumstance could occur if there was a survey error in 1999 (an underestimate of bed elevations) which would suppress storage volumes in the early period, and inflate them in the later period. As a direct comparison of 1984 with 2003 surveys partly confirmed this potential survey error, an iterative procedure was followed to estimate the potential error (found to be roughly 15 cm) but negative transport rates could not be eliminated.

Additional remaining sources of error include the potential for survey error in 1984 in the same location, unreported (and unknown) sand and gravel dredging, and the uncertainty in the sand and gravel fractions, especially along the lower computing cells where the budget issues are largely confined. As there is no practical (or possible?) means to estimate the magnitude of, hence correct for these errors, the sediment budgets presented in this thesis are not precise. Consequently, the long-term summed budget (1952-1984 + 1984-1999) of 262,000 ± 15,000 m^3 (which includes adjustments for 1999 sounding errors and downstream transport past Mission) is proposed as the most conservative estimate of bed material influx for riverine management purposes. The long-term budget also averages short-term variability in sediment transport rates (cf. 1999-2003) which are not appropriate metrics for understanding sedimentation patterns on such a large river.

7.4 Management implications

At present, lower Fraser River is characterized by a relatively pristine environment compared to most large, navigable rivers throughout the urbanized world. Nevertheless, flooding and erosion concerns have led to a number of engineering solutions since the late 1800s to combat these impacts. Development on the floodplain is apt to continue, prompting future calls for additional bank hardening to protect new and existing infrastructure. Similarly, knowledge that sedimentation continues to raise the flood level is certain to increase pressure on local land and dyking authorities to press for targeted sediment removals. Both strategies have been demonstrated to have a negative impact on morphologic complexity, hence the quality of available fisheries habitat.

There are additional options that could be pursued, but it is not clear that the existing institutional framework is sufficient to address them. An obvious solution to these problems would be to simply give the river more 'room' by restricting development within the limits of the flood dykes, or rebuilding dykes farther back from the active channel to increase flood conveyance. This

should be viewed strictly as a long-term solution, however, because the strategy involves acquisition or leasing of currently occupied lands, for which there are neither funding programs, nor likely public support at present. Raising the existing dykes is also possible, but this option is expensive, would inevitably lead to additional bank-hardening to protect the investment, and would eventually fail if aggradation in lower reaches continued. In the short-term, it seems inevitable that gravel mining remains the most prudent option for reducing water levels at targeted locations. Modest removals that do not exceed the annual recruitment rate to the river have not been demonstrated to have significant detrimental impacts on the aquatic ecosystem. Further, removals at sites where constrictions are developing could be used to partly address persistent bank erosion problems. Regardless of how we proceed, a long-term monitoring strategy seems essential to ensuring that these activities are conducted in a manner that balances engineering concerns with habitat maintenance. Negative experience on other rivers tells us what will happen if we do not.

References

[1] Abbe, T.B. and Montgomery, D.R. (1996). Large woody debris jams, channel hydraulics and habitat formation in large rivers. *Regulated Rivers: Research and Management*, 12, 201-221.

[2] Allen, J.R.L. (1965). Origin and characteristics of recent alluvial sediments. *Sedimentology*, 5, 89-191.

[3] Armstrong, J.E. (1981). Post-Vashon Wisconsin glaciation, Fraser Lowland, British Columbia. *Geological Survey of Canada Bulletin 322*, 34 p.

[4] Armstrong, J.E. (1984). Environmental and Engineering Applications of the Surficial Geology of the Fraser Lowland, British Columbia. *Geological Survey of Canada Paper 83-23*, 54 p + map.

[5] Ashmore, P.E. (1991). How do gravel rivers braid? *Canadian Journal of Earth Sciences*, 28, 326-341.

[6] Ashmore, P.E. and Church, M. (1998). Sediment transport and river morphology: a paradigm for study. In Gravel Bed Rivers in the Environment (GBR IV), Peter C. Klingemen, Robert L. Beschta, Paul D. Komar and Jeffrey B. Bradley [Eds.]. Highland Ranch, CO: Water Resources Publications, LLC, 115-148.

[7] Beck, S. (1984). Mathematical modelling of meander interaction. In River meandering: proceedings of the Conference Rivers '83, New Orleans, Charles M. Elliott [Ed.]. Waterway, Port, Coastal and Ocean Division of the ASCE and International Association for Hydraulic Reseach, 932-941.

[8] Bishop, T.F.A. and McBratney, A.B. (2002). Creating field extent digital elevation models for precision agriculture. *Precision Agriculture*, 3, 37-46.

[9] Boniface, C. (1985). Vegetation succession on mid-channel bars of the Fraser River, British Columbia. Unpublished M.Sc. thesis, Department of Geography, Simon Fraser University, 137 p.

[10] Brabets, T.P. (1997). Geomorphology of the Lower Copper River, Alaska. *U.S. Geological Survey Professional Paper 1581*. 89 p.

[11] Braga, G. and Gervasoni, S. (1989). Evolution of the Po River: an example of the application of historic maps. In Historical change of large alluvial rivers: Western Europe, G.E. Petts [Ed.]. Chichester: John Wiley & Sons, 113-125.

[12] Brasington, J. and Smart, R.M.A. (2003). Close-range digital photogrammetric analysis of experimental drainage basin evolution. *Earth Surface Processes and Landforms*, 28, 231-247.

[13] Brasington, J., Rumsby, B.T. and McVey, R.A. (2000). Monitoring and modelling morphological change in a braided gravel-bed river using high resolution GPS-based survey. *Earth Surface Processes and Landforms*, 25, 973-990.

[14] Brayshaw, A.C. (1984). Characteristics and origin of cluster bedforms in coarse- grained alluvial channels. In Sedimentology of Gravels and Conglomerates, Koster, E.H. and Steel, R.J. [Eds.]. Canadian Society of Petroleum Geologists, Memoir 10, 77-85.

[15] Bridge, J.S. (1993). The interaction between channel geometry, water flow, sediment transport and deposition in braided rivers. In Braided Rivers, J.L. Best and C.S. Bristow [Eds.]. Geological Society Special Publication 75, 13-71.

[16] Brierley, G.J. (1989). River planform facies models: the sedimentology of braided, wandering and meandering reaches of the Squamish River, British Columbia. *Sedimentary Geology*, 61, 17-35.

[17] Brierley, G.J. (1996). Channel morphology and element assemblages: a constructivist approach to facies modelling. In Advances in Fluvial Dynamics and Stratigraphy, P.A. Carling and M.R. Dawson [Eds.]. Chichester: John Wiley & Sons Ltd., 263-298.

[18] Bristow, C.S. (1987). Brahmaputra River: channel migration and deposition. In Recent Developments in Fluvial Sedimentology, F.H. Ethidge, R.M. Flores and M.D. Harvey [Eds.]. SEPM Special Publication 39, 63-74.

[19] Burrough, P.A. and McDonnell, R.A. (1998*)*. Principles of Geographic Information Systems. Oxford University Press, 333 p.

[20] Carr, J.R. (1995). Numerical Analysis for the Geological Sciences. Englewood Cliffs, NJ: Prentice Hall Inc. 592 p.

[21] Carson, M.A. (1984). The meandering-braided river threshold: a reappraisal. *Journal of Hydrology*, 73, 315-334.

[22] Carson, M.A. and Griffiths, G.A. (1987). Influence of channel width on bed load transport capacity. *Journal of Hydraulic Engineering*, 113, 1489-1509.

[23] Carson, M.A. and Griffiths, G.A. (1989). Gravel transport in the braided Waimakariri River. *Journal of Hydrology*, 109, 201-220.

[24] Chandler, J. (1999). Effective application of automated digital photogrammetry for geomorphological research. *Earth Surface Processes and Landforms*, 24, 51-63.

[25] Charlton, M.E., Large, A.R.G. and Fuller, I.C. (2003). Application of airborne Lidar in river environements: the River Coquet, Northumberlands, UK. *Earth Surface Processes and Landforms*, 28, 299-306.

[26] Church, M.A. (1983a). Pattern of instability in a wandering, gravel-bed channel. In Modern and ancient fluvial systems, J.D. Collinson and J. Lewin [Eds.]. *Int. Assoc. Sedimentology, Special Pub. 6*, 169-180.

[27] Church, M.A. (1983b). River channel changes from maps and photographs. *Association of Canadian Map Libraries Bulletin*, 48, 8-19.

[28] Church, M. (1985). Bed load in gravel-bed rivers: observed phenomenon and implications for computation. *Canadian Society for Civil Engineering Annual Conference*, Saskatoon, SK, 17-37.

[29] Church, Michael (1990). Fraser River in Central British Columbia. In Surface Water Hydrology, M.G. Wolman and H.C. Riggs [Eds]. Boulder, Colorado: Geological Society of America, The Geology of North America, V 0-1, 282-287.

[30] Church, M. (1992). Channel morphology and typology. In The River Handbook Vol. 1, P. Calow and G.E. Petts [Eds.]. Oxford: Blackwell, 126-143.

[31] Church, M. (2001a). Estimation of annual gravel influx to the gravel-bed reach of Fraser River. Report prepared for Technical Advisory Committee, Fraser River Management Plan: Hope to Mission, Fraser Basin Council. Department of Geography, The University of British Columbia. 8 p.

[32] Church, M. (2001b). River science and Fraser River: who controls the river? In Gravel-Bed Rivers V, M.P. Mosley [Ed]. Wellington: New Zealand Hydrological Society, 607-631.

[33] Church, Michael (2002). Geomorphic thresholds in riverine landscapes. *Freshwater Biology*, 47, 541-557.

[34] Church, M. and Ryder, J.M. (1972). Paraglacial Sedimentation: A Consideration of Fluvial Processes Conditioned by Glaciation. *Geological Society of America Bulletin*, 83, 3059-3072.

[35] Church, M. and Jones, D. (1982). Channel bars in gravel-bed rivers. In Gravel-bed Rivers. R.D. Hey, J.C. Bathurst and C.R. Thorne [Eds]. Chichester: Wiley, 291-338.

[36] Church, M. and Slaymaker, O. (1989). Disequlibrium of Holocene sediment yield in glaci-

ated British Columbia. *Nature*, 337, pp 452-454.

[37] Church, M. and McLean, D.G. (1994). Sedimentation in Lower Fraser River, British Columbia: Implications for Management. In *The Variability of Large Alluvial Rivers*, S.A. Schumm and B.R. Winkley [Eds]. New York: American Society of Civil Engineers Press, 221-241.

[38] Church, M. and Ham, D.G. (2004). Atlas of the alluvial gravel-bed reach of Fraser River in the Lower Mainland showing channel changes in the period 1912-1999. Department of Geography, The University of British Columbia. 55 p.

[39] Church, M., Miles, M. and Rood, K. (1987). Sediment transfer along Mackenzie River: A feasibility study. Rep. IWD-WNR(NWT)-WRB-SS-87-1, Environment Canada, Inland Waters Directorate, Western and Northern Region, Sediment Survey Section, Ottawa.

[40] Church, M., Hassan, M.A. and Wolcott, J.F. (1998). Stabilizing self-organized structures in gravel-bed stream channels: Field and experimental observations. *Water Resources Research*, 34, 11, 3169-3179.

[41] Church, M., Ham, D. and Weatherly, H. (2001). Gravel management in lower Fraser River. Report prepared for The City of Chilliwack. Department of Geography, The University of British Columbia. 110 p.

[42] Church, M., Ham, D., Hassan, M. and Slaymaker, O. (1999). Fluvial clastic sediment yield in Canada: scaled analysis. *Canadian Journal of Earth Sciences*, 36, 8, 1267- 1280.

[43] Clague, J.J. (1989). Introduction. In Quaternary Stratigraphy and History, area of Cordilleran Ice sheet, Chapter 1 of Quaternary Geology of Canada and Greenland, R.J. Fulton [Ed.]. Geological Survey of Canada, Geology of Canada, also Geological Society of America, The Geology of North America, K-1, 48.

[44] Clague, J.J. (1993). Mountain Paleoenvironments of Western Canada. In Canada's Cold Environments, Hugh M. French and Olav Slaymaker [Eds.]. McGill-Queens University Press, 223-245.

[45] Collins, B. and Dunne, T. (1990). Fluvial geomorphology and river-gravel mining: a guide for planners, case studies included. California Department of Conservation, Division of Mines and Geology, 29 p.

[46] Collins, B.D., Montgomery, D.R. and Haas, A.D. (2002). Historical changes in the distribution and functions of large wood in Puget Lowland rivers. *Can. J. Fish. Aquat. Sci.*, 59, 66-76.

[47] Crowley, K.D. (1983). Large-scale bed configurations (macroforms), Platte River Basin,

Colorado and Nebraska: primary structures and formative processes. *Geological Society of America Bulletin*, 94, 117-133.

[48] Davis, J.C. (1986). Statistics and Data Analysis in Geology. New York: John Wiley & Sons. 646 p.

[49] Decamps, H., Fortune, M. and Gazelle, F. (1989). Historic changes of the Garonne River, Southern France. In Historical change of large alluvial rivers: Western Europe, G.E. Petts [Ed.]. Chichester: John Wiley & Sons., 249-267.

[50] Desloges, J.R. and Church, M. (1987). Channel and floodplain facies in a wandering gravel-bed river. In Recent Developments in Fluvial Sedimentology: contribution from the Third International Fluvial Sedimentology Conference, F.G. Ethridge, R.M. Flores and M.D. Harvey [Eds.]. Society of Economic Paleontologists and Mineralogists, Special Publication 39, 99-109.

[51] Desloges, J.R. and Church, M. (1989). Wandering gravel-bed rivers. *The Canadian Geographer*, 33, 4, 360-364.

[52] Deutsch, C.V. and Journel, A.G. (1992). Geostatistical Software Library and User's Guide. New York: Oxford University Press. 340 p.

[53] Dunne, T. and Leopold, L.B. (1978). Water in Environmental Planning. New York: W.H. Freeman and Company. 818 p.

[54] Dykaar, B.B. and Wigington, P.J. (2000). Floodplain formation and cottonwood colonization patterns on the Willamette River, Oregon, USA. *Environmental Management*, 25, 1, 87-104.

[55] Eaton, B.C. and Lapointe, M.F. (2001). Effects of large floods on sediment transport and reach morphology in the cobble-bed Sainte Marguerite River. *Geomorphology*, 40, 291-309.

[56] EGIS (1997). Morphological dynamics of the Brahmaputra - Jamuna River. Report prepared for Water Resources Planning Organization, Ministry of Water Resources, Government of Bangladesh by Environment and GIS Support Project for Water Sector Planning and Delft Hydraulics. 76 p + appendices.

[57] EGIS (2002). Developing and updating empirical methods for predicting morphologic changes of the Jamuna River. Environment and GIS support for Water Sector Planning, Ministry of Water Resources, Government of Bangladesh. EGIS Technical Note Series 29. 78 p + appendices.

[58] Englund, E.J. (1990). A variance of geostatisticians. *Mathematical Geology*, 22, 4, 417-455.

[59] ESRI (1991) Surface Modeling with TIN: surface analysis and display. Redlands, California: Environmental Systems Research Institute, Inc.

[60] ESRI (1992) GRID command references. Redlands, California: Environmental Systems Research Institute, Inc.

[61] Ferguson, R.I. (1987).Hydraulic and sedimentary controls of river pattern. In River channels: environment and process, K.S. Richards [Ed.]. Oxford: Blackwell,129-158.

[62] Ferguson, R.I. and Werrity, A. (1983). Bar development in the River Feshie. In Modern and Ancient Fluvial Systems, J.D. Collinson and J. Lewin [Eds.]. *Int. Assoc. Sedimentology, Special Pub. 6*, 181-193.

[63] Ferguson, R.I. and Ashworth, P.J. (1992). Spatial Patterns of Bedload Transport and Channel Change in Braided and Near-braided Rivers. In Dynamics of Gravel-bed Rivers, P. Billi, R.D. Hey, C.R. Thorne and P. Tacconi [Eds.]. Chichester: Wiley, 477-496.

[64] Forbes, D.L. (1983). Morphology and sedimentology of a sinuous gravel-bed channel system: lower Babbage River, Yukon coastal plain, Canada. In Modern and Ancient Fluvial Systems, J.D. Collinson and J. Lewin [Eds.]. *Int. Assoc. Sedimentology, Special Pub. 6*, 195-206.

[65] Fraser Basin Management Program (1994). Review of the Fraser River flood control program, Task Force Report, 82 p.

[66] Fraser River Flood Control Program (1968). Information guide. 25 p.

[67] French, J.R. (2003) Airborne Lidar in support of geomorphological and hydraulic modelling. *Earth Surface Processes and Landforms*, 28, 321-335.

[68] Friedman, J.M., Osterkamp, W.R. and Lewis, W.M.Jr. (1996). The role of vegetation and bed-level fluctuations in the process of channel narrowing. *Geomorphology*, 14, 341-351.

[69] Fuller, I.C., Large, A.R.G., Charlton, M.E., Heritage, G.L. and Milan, D.J. (2003). Reach-scale sediment transfers: an evaluation of two morphological budgeting approaches. *Earth Surface Processes and Landforms*, 28, 889-903.

[70] Gaeuman, D.A., Schmidt, J.C. and Wilcock, P.R. (2003). Evaluation of in-channel gravel storage with morphology-based gravel budgets developed from planimetric data. *Journal of Geophysical Research - Earth Surface*, 108, F1, 2-1: 2-16.

[71] Gilvear, D., Winterbottom, S. and Sichingabula, H. (2000). Character of channel planform change and meander development: Luangwa River, Zambia. *Earth Surface Processes and Landforms*, 25, 421-436.

[72] Goff, J.R. and Ashmore, P. (1994). Gravel transport and morphological change in braided Sunwapta River, Alberta, Canada. *Earth Surface Processes and Landforms*, 19, 195-212.

[73] Gomez, B. (1991). Bedload transport. *Earth-Science Reviews*, 31, 89-132.

[74] Gottesfeld, A.S. and Gottesfeld, L.M.J. (1990). Floodplain dynamics of a wandering river, dendrochronology of the Morice River, British Columbia, Canada. *Geomorphology*, 3, 159-179.

[75] Graf, W.L. (2000). Locational probability for a dammed, urbanizing stream: Salt River, Arizona, USA. *Environmental Management*, 25, 3, 321-335.

[76] Gran, K. and Paola, C. (2001). Riparian controls on braided stream dynamics. *Water Resources Research*, 37, 12, 3275-3283.

[77] Guenther, G.C., Brooks, M.W. and LaRocque, P.E. (2000). New capabilities of the "SHOALS" airborne lidar bathymeter. *Remote Sensing of Environment*, 73, 247-255.

[78] Hales, W.J. (2000). The impact of human activity on deltaic sedimentation, marshes of the Fraser River Delta, British Columbia. Unpublished PhD thesis, Department of Geography, The University of British Columbia. 153 p.

[79] Ham, D.G. (1996). Patterns of channel change on Chilliwack River, British Columbia. Unpublished M.Sc. Thesis, Department of Geography, The University of British Columbia. 164 p.

[80] Ham, D.G. and Church, M. (2000). Bed-material transport estimated from channel morphodynamics: Chilliwack River, British Columbia. *Earth Surface Processes and Landforms*, 25, 1123-1142.

[81] Ham, D. and Church, M. (2002). Channel island and active channel stability in the lower Fraser River gravel reach. Department of Geography, University of British Columbia: Fraser River Research Group Report. 34 p.

[82] Ham, D.G. and Church, M. (2003). The sediment budget in the gravel-bed reach of Fraser River: 2003 revision. Department of Geography, The University of British Columbia. 19 p.

[83] Harrison, C.G.A. (1998). The hypsography of the ocean floor. *Phys. Chem. Earth*, 23, 7, 761- 774.

[84] Haschenburger, J.K. and Church, M. (1998). Bed material transport estimated from the virtual velocity of sediment. *Earth Surface Processes and Landforms*, 23, 791-808.

[85] Hassan, M.A. and Church, M. (1992). The movement of individual grains on the streambed. In Dynamics of Gravel-Bed Rivers, P. Billi, R.D. Hey, C.R. Thorne and P. Tacconi [Eds.]. Chichester: John Wiley & Sons Ltd., 159-175.

[86] Hickin, E.J. (1983). River channel changes: retrospect and prospect. In Modern and ancient fluvial systems, J.D. Collinson and J. Lewin [Eds.]. *Int. Assoc. Sedimentology, Special Pub. 6*, pp 61-83.

[87] Hickin, E.J. (1984). Vegetation and river channel dynamics. *Canadian Geographer*, XXVIII, 2, 111-126.

[88] Hickin, E.J. (1995). Hydraulic geometry and channel scour: Fraser River, British Columbia, Canada. In River Geomorphology, E.J. Hickin [Ed.]. Wiley: Chichester, 155-167.

[89] Hickin, E.J. and Nanson, G.C. (1984). Lateral migration rates of river bends. *Journal of Hydraulic Engineering*, 110, 4, 1557-1567.

[90] Higgitt, D.L. and Warburton, J. (1999). Applications of differential GPS in upland fluvial geomorphology. *Geomorphology*, 29,121-134.

[91] Hoey, T. (1992). Temporal variations in bedload transport rates and sediment storage in gravel-bed rivers. *Progress in Physical Geography*, 16, 3, 319-338.

[92] Holland, S.S. (1964). Landforms of British Columbia - A Physiographic Outline. *British Columbia Department of Mines and Petroleum Resources, Bulletin No. 48*, 138 p.

[93] Hooke, J.M. (1980). Magnitude and distribution rates of river bank erosion. *Earth Surface Processes*, 5, 143-157.

[94] Hooke, J.M. (2003). Coarse sediment connectivity in river channel systems: a conceptual framework and methodology. *Geomorphology*, 1337, 1-16.

[95] Hooke, J.M. and Redmond, C.E. (1989). Use of cartographic sources for analysing river channel change with examples from Britain. In Historical change of large alluvial rivers: Western Europe, G.E. Petts [Ed.]. Chichester: John Wiley & Sons, 79-93.

[96] Hubbell, D.W. (1987). Bed load sampling and analysis. In Sediment Transport in Gravel-bed Rivers, C.R. Thorne, J.C. Bathurst and R.D. Hey [Eds]. New York: John Wiley, 89- 118.

[97] Hughes Clarke, J.E. (2000). *Personal communication*. Senior Research Associate, Ocean Mapping Group, Dept. Geodesy and Geomatics Engineering, University of New Brunswick.

[98] Hutchinson, M.F. (1996). A locally adaptive approach to the interpolation of digital elevation models. In Proceedings, Third International Conference / Workshop on Integrating GIS and Environmental Modeling, Santa Fe, NM, January 21-26, 1996. Santa Barbara, CA: National Center for Geographic Information and Analysis.

[99] Isaaks, E.H. and Srivastava, R.M. (1989). An Introduction to Applied Geostatistics. New York: Oxford University Press. 561 p.

[100] Jackson, R.G. (1975). Hierarchial attributes and a unifying model of bedforms composed of cohesionless material produced by shearing flow. *Geological Society of America Bulletin* 86, 1523-1533.

[101] Jackson, R.G. (1978). Preliminary evaluation of lithofacies models for meandering alluvial streams. In Fluvial Sedimentology, A.D. Miall [Ed.]. *Can. Soc. Petrol. Geol. Mem. 5*, 543-576.

[102] Johnston, W.A. (1921). Sedimentation of the Fraser River Delta. *Geological Survey of Canada Memoir 125*, 46 p.

[103] Keller, E.A. and Melhorn, W.N. (1978). Rythmic spacing and origin of riffles and pools. *Geological Society of America Bulletin*, 89, 723-730.

[104] Kellerhals Engineering Services (1987). Effects of gravel mining on the salmonid resources of the Lower Fraser River. Report prepared for Department of Fisheries and Oceans, Habitat Management Division. 43 p.

[105] Kellerhals, R. and Church, M. (1989). The morphology of large rivers: characterization and management. In Proceedings of the International Large Rivers Symposium, D.P Dodge [Ed.]. *Special Publication of the Canadian Journal of Fisheries and Aquatic Sciences*, 106, 31-48.

[106] Kellerhals, R. and Miles, M. (1996). Fluvial geomorphology and fish habitat: implications for river restoration. In Proceedings of the 2nd IAHR Symposium on habitat hydraulics. Ecohydraulics 2000, M. Leclerc *et al*. [eds.], pp. 261-279.

[107] Kellerhals, R., Church, M. and Bray, D.I. (1976). Classification and analysis of river processes. *Journal of the Hydraulics Division*, ASCE, 102, HY7, 813-829.

[108] Kelsey, H.M., Lamberson, R. and Madej, M. (1987). Stochastic model for the long-term transport of stored sediment in a river channel. *Water Resources Research*, 23, 9, 1738- 1750.

[109] Knighton, A.D. (1998). Fluvial Forms & Processes. London: Arnold Publishers, 383 p.

[110] Knighton, A.D. and Nanson, G.C. (1993). Anastomosis and the continuum of channel pattern. *Earth Surface Processes and Landforms*, 18, 613-625.

[111] Kondolf, G.M. (1998). Lessons learned from river restoration projects in California. *Aquatic Conservation: Marine and Freshwater Ecosystems*, 8, 39-52.

[112] Kondolf, G.M. and Wilcock, P.R. (1996). The flushing flow problem: defining and evaluating objectives. *Water Resources Research*, 32, 8, 2589-2599.

[113] Kondolf, G.M., Piégay, H. and Landon, N. (2002). Channel response to increased and decreased bedload supply from land use change: contrasts between two catchments. *Geomorphology*, 45, 35-51.

[114] Kopaliani, Z.D. and Romashin, V.V. (1970). Channel Dynamics of Mountain Rivers. *Soviet Hydrology: Selected Papers*, 5, pp. 441-452. Reprinted in *Transactions of the State Hydrologic Institute* (Trudy GGI), 183, 81-97.

[115] KWL (2001). 2002 Fraser River Gravel Removals. Final report submitted to British Columbia Ministry of Water, Land and Air Protection by Kerr Wood Leidal Consulting Engineers.

[116] Lane, E.W. (1957). A study of the shape of channels formed by natural streams flowing in erodible material. US Army Corps of Engineers, Missouri River Diversion, Sediment Series 9.

[117] Lane, S.N. (1998). The use of digital terrain modelling in the understanding of dynamic river systems. In Landform Monitoring, Modelling and Analysis, S.N. Lane, K.S. Richards and J.H. Chandler [Eds.]. Chichester: Wiley, 311-342.

[118] Lane, S.N. (1997). The reconstruction of bed material yield and supply histories in gravel-bed streams. *Catena*, 30, 183-196.

[119] Lane, S.N., Chandler, J.H. and Richards, K.S. (1994). Developments in monitoring and modelling small-scale river bed topography. *Earth Surface Processes and Landforms*, 19, 349-368.

[120] Lane, S.N., Richards, K.S. and Chandler, J.H. (1995). Morphological estimation of the time-integrated bed load transport rate. *Water Resources Research*, 31, 3, 761- 772.

[121] Lane, S.N., Westaway, R.M. and Hicks, D.M. (2003). Estimation of erosion and deposition volumes in a large, gravel-bed, braided river using synoptic remote sensing. *Earth Surface*

Processes and Landforms, 28, 249-271.

[122] Lane, S.N., Reid, S.C., Westaway, R.M. and Hicks, D.M. (2004). Remotely sensed topographic data for river channel research: the identification, explanation and management of error. In Spatial Modelling of the Terrestrial Environment, R.E.J. Kelly, N.A. Drake and S.L. Barr [Eds.]. Chichester: Wiley, 113-136.

[123] Lawler, D.M. (1993). The measurement of river bank erosion and lateral channel change: a review. *Earth Surface Processes and Landforms*, 18, 777-821.

[124] Leliavsky, S. (1955). An Introduction to Fluvial Hydraulics. London: Constable & Company, Ltd. 255 p.

[125] Leopold, L.B., Wolman, M.G. and Miller, J.P. (1964). Fluvial Processes in Geomorphology. San Fransisco: W.H. Freeman & Co. 522 p.

[126] Leopold. L.B., and Wolman, M.G. (1957). River channel patterns: braided, meandering and straight. *United States Geological Survey Professional Paper 282-B*, 39-85.

[127] Leys, K.F. and Werrity, A. (1999). River channel planform changes: software for historical analysis. *Geomorphology*, 29, 107-120.

[128] Li, S. and Millar, R.G. (2004). A computational distributed gravel budget for the lower Fraser River, British Columbia. Draft submitted for review and presentation at Riverflow 2004, Naples Italy, June 2004.

[129] Lindsay, J.B. and Ashmore, P.E. (2002). The effects of survey frequency on estimates of scour and fill in a braided river model. *Earth Surface Processes and Landforms*, 27, 27-43.

[130] Lisle, T.E. (1987a). Using "residual depths" to monitor pool depths independently of discharge. USDA, Pacific Southwest Forest and Range Experiment Station Research Note PSW-394, 4 p.

[131] Lisle, T.E. (1987b). Channel morphology and sediment transport in steepland streams. Erosion and Sedimentation in the Pacific Rim (Proceedings of the Corvallis Symposium, August, 1987). IAHS Publ. 165, 287-297.

[132] Lisle, T.E. (1989). Sediment transport and resulting deposition in spawning gravels, north coastal California. *Water Resources Research*, 25, 6, 1303-1319.

[133] Livingstone, D., Raper, J. and McCarthy, T. (1999). Integrating aerial videography and digital photography with terrain modelling: an application for coastal geomorphology. *Geomorphology*, 29, 77-92.

[134] Lyons, J.K. and Beschta, R.L. (1983). Land use, floods, and channel changes: Upper Middle Fork Willamette River, Oregon (1936-1980). *Water Resources Research*, 19, 2, 463-471.

[135] Macklin, M.G., Passmore, D. and Newson, M.D. (1998). Controls of short- and long-term river instability: processes and patterns in gravel-bed rivers, Tyne Basin, England. In Gravel Bed Rivers in the Environment (GBR IV), Peter C. Klingemen, Robert L. Beschta, Paul D. Komar and Jeffrey B. Bradley [Eds.]. Highland Ranch, CO: Water Resources Publications, LLC, 257-278.

[136] Madej, M. (1999). Temporal and spatial variability in thalweg profiles of a gravel- bed river. *Earth Surface Processes and Landforms*, 24, 1153-1169.

[137] Martin, Y. and Church, M. (1995). Bed material transport estimated from channel surveys: Vedder River, British Columbia. *Earth Surface Processes and Landforms*, 20, 347-361.

[138] Martin, Y. and Ham, D. (in press). Testing bedload transport formulae using morphologic transport estimates and field data: lower Fraser River, British Columbia. Forthcoming in *Earth Surface Processes and Landforms*.

[139] McLean, D.G. (1990). Channel Instability on lower Fraser River.. Unpublished PhD thesis, University of British Columbia, 290p.

[140] McLean, D.G. and Church, M. (1986). A re-examination of sediment transport observations in the lower Fraser River. Environment Canada, Water Resources Branch, Sediment Survey Section. Report IWD-HQ-WRB-86-62. 56 p + figs + tables.

[141] McLean, D.G. and Tassone, B. (1987). Discussion of: Bed-load sampling and analysis by David Hubbell. In Gravel-bed Rivers, C.R. Thorne, R.D. Hey and J.C. Bathurst [Eds.]. Chichester: Wiley, 109-113.

[142] McLean, D.G. and Church, M. (1999). Sediment transport along lower Fraser River 2. Estimates based on the long-term gravel budget. *Water Resources Research*, 35, 8, 2549-2559.

[143] McLean, David G., Church, M. and Tassone, B. (1999). Sediment transport along lower Fraser River 1. Measurements and hydraulic computation. *Water Resources Research*, 35, 8, 2533-2548.

[144] Meade, R.H. (1985). Wavelike Movement of Bedload Sediment: East Fork River, Wyoming. *Environmental Geology and Water Science*, 7, 215-225.

[145] Meade, R.H. Yuzyk, T.R. and Day, T.J. (1990). Movement and storage of sediment in rivers of the United States and Canada. In Surface water hydrology, M.G. Gordan and H.C. Riggs [Eds.]. Boulder: Geol. Soc. Am., 255-280.

[146] Meyer, T.H. (2004). The discontinuous nature of kriging interpolation for digital terrain modeling. *Cartography and Geographic Information Science*, 31, 4, 209-216.

[147] Miall, A.D. (1977). A review of the braided-river depositional environment. *Earth Science Reviews*, 13, 1-62.

[148] Micheli, E.R. and Kirchner, J.W. (2002). Effects of wet meadow riparian vegetation on streambank erosion. 1. Remote sensing measurements of streambank migration and erodibility. *Earth Surface Processes and Landforms*, 27, 627-639.

[149] Millar, R.G. (2000). Influence of bank vegetation on alluvial channel patterns. *Water Resources Research*, 36, 4, 1109-1118.

[150] Millar, R.G. and Quick, M.C. (1993). Effect of bank stability on geometry of gravel rivers. *Journal of Hydraulic Engineering*, 119, 12, 1343-1363.

[151] Milne, J.A. and Sear, D.A. (1997). Modelling river channel topography using GIS. *Int. J. Geographical Information Science*, 11, 5, 499-519.

[152] Mlynarczyk, Z. and Rotnicki, K. (1989). Flood and vortex scour of the channel bed of the Prosna river, and their depth range. *Earth Surface Processes and Landforms*, 14, 365-373.

[153] Mollard, J.D. (1973). Airphoto interpretation of fluvial features. *Proceedings of the 9th Canadian Hydrology Symposium, Edmonton, Alberta*. National Research Council of Canada, 341-380.

[154] Montgomery, D.R., Buffington, J.M., Smith, R.D., Schmidt, K.M. and Pess, G. (1995). Pool spacing in forest channels. *Water Resources Research*, 31, 4, 1097-1105.

[155] Moore, R.D. (1991). Hydrology and water supply in the Fraser River basin. In Water in sustainable development: exploring our common future in the Fraser River basin, A.H.J. Dorcey and J.R. Griggs [Eds.]. Westwater Research Centre, Vancouver, 21-40.

[156] Moore, R.D. (2004). *Personal communication*. Associate Professor of Forest Hydrology, Department of Geography, The University of British Columbia.

[157] Morningstar, O.R. (1987). Floodplain construction and overbank deposition in a wandering reach of the Fraser River, Chilliwack, B.C. Unpublished M.Sc. thesis, Department of Geography, Simon Fraser University. 129 p.

[158] Mosselman, E., Huisink, M., Koomen, E. and Seijmonsbergen, A.C. (1995). Morphological changes in a large braided sand-bed river. In River Geomorphology, E.J. Hickin [Ed.]. John Wiley & Sons, 235-247.

[159] Murray, A.B. and Paola, C. (1994). A cellular model of braided rivers. *Nature*, 371, 54-57.

[160] Murray, A.B. and Paola, C. (2003). Modelling the effects of vegetation on channel pattern in bedload rivers. *Earth Surface Processes and Landforms*, 131-143.

[161] Nanson, G.C. and Hickin, E.J. (1986). A statistical analysis of bank erosion and channel migration in western Canada. *Geologial Society of America Bulletin*, 97, 497-504.

[162] Nanson, G.C. and Knighton, A.D. (1996). Anabranching rivers: their cause, character and classification. *Earth surface Processes and Landforms*, 21, 217-239.

[163] Neill. C.R. (1971). River bed transport related to meander migration rates. *Journal of the Waterways, Harbors and Coastal Engineering Division, ASCE*, 97, WW4, 783-786.

[164] Neill, C.R. (1973). Hydraulic and Morphologic Characteristics of Athabasca River near fort Assiniboine - the anatomy of a wandering gravel river. Alberta Cooperative Research Program, Highway and Engineering Division, Report REH/73/3.

[165] Neill. C.R. (1987). Sediment balance considerations linking long-term transport and channel processes. In Sediment Transport in Gravel-bed Rivers, C.R. Thorne, J.C. Bathurst and R.D. Hey [eds]. New York: John Wiley, 225-240.

[166] Nicholas, A.P., Ashworth, P.J., Kirkby, M.J., Macklin, M.G and Murray, T. (1995). Sediment slugs: large-scale fluctuations in fluvial sediment transport rates and storage volumes. *Progress in Physical Geography*, 19, 4, 500-519.

[167] Norcliffe, G.B. (1982). Inferential statistics for geographers. London: Hutchinson & Co. 263 p.

[168] North, M.E.A. and Teversham, J.M. (1984). The vegetation of the floodplains of the Lower Fraser, Serpentine and Nicomekl Rivers, 1959 to 1890. *Syesis*, 17, 47-66.

[169] North, M., Holdsworth, D. and Teversham, J. (1977). A brief guide to the use of land surveyor's notebooks in the lower Fraser Valley, B.C., 1859-1890. *British Columbia Studies*, 34, 45-60.

[170] Paige, A.D. and Hickin, E.J. (2000). Annual bed-elevation regime in the alluvial channel of Squamish River, southwestern British Columbia, Canada. *Earth Surface Processes and Landforms*, 25, 991-1009.

[171] Paola, C. (2001). Modelling stream braiding over a range of scales. In Gravel-Bed Rivers V, New Zealand Hydrological Society, M.P. Mosley [Ed.]. Christchurch: The Caxton Press, 11-46.

[172] Payne, B.A. and Lapointe M.F. (1997). Channel morphology and lateral stability: effects on distribution of spawning and rearing habitat for Atlantic salmon in a wandering cobble-bed river. *Can. J. Fish. Aquat. Sci.*, 54, 2627-2636.

[173] Popov, I.V. (1962). Application of morphological analysis to the evaluation of the general channel deformations of the river Ob'. *Trans. State Hydraulic Institute*, 94, 22-86.

[174] Public Works Canada (1949). Fraser River System, Province of British Columbia: History of Improvements, 1871 to date. Dominion Public Works Department, New Westminster, B.C. Report submitted to Dominion-Provincial Board, Fraser River Basin. 66p + 13 diagrams + appendix.

[175] Pyrce, R.S. and Ashmore, P.E. (2003). The relation between particle path length distributions and channel morphology in gravel-bed streams: a synthesis. *Geomorphology*, 56, 167-187.

[176] Reid, I. and Frostick, L.E. (1994). Sediment Transport and Depositional Processes. In Sediment Transport and Depositional Processes, K. Pye [Ed.]. Oxford: Blackwell Scientific Publications, 89-155.

[177] Reiser, D.W. (1998). Sediment in gravel-bed rivers: ecological and biological considerations. In Gravel Bed Rivers in the Environment (GBR IV), Peter C. Klingemen, Robert L. Beschta, Paul D. Komar and Jeffrey B. Bradley [Eds.]. Highland Ranch, CO: Water Resources Publications, LLC, 199-228.

[178] Rempel. L. and Church, M. (2003). The Harrison Bar gravel removal experiment: final report. Department of Geography, University of British Columbia, 104 p + appendices.

[179] Rennie, C.D., Millar, R.G. and Church, M.A. (2002). Measurement of Bed Load Velocity using an Acoustic Doppler Current Profiler. *Journal of Hydraulic Engineering*, 128, 5, 473-483.

[180] Rennie, C.D. and Millar, R.G. (2004). Measurement of the spatial distribution of fluvial bedload transport velocity in both sand and gravel. *Earth Surface Processes and Landforms,* 29, 10, 1173-1193.

[181] Rice, S.P. and Church, M. (2001). Longitudinal profiles in simple alluvial systems. *Water Resources Research*, 37, 2, 417-426.

[182] Richards, K.S. (1976). The morphology of riffle-pool sequences. *Earth Surface Processes*, 1, 71-88.

[183] Richards, K.S. (1982). Rivers: form and process in alluvial channels. London: Methuen.

358 p.

[184] Roberts, M.C. and Morningstar, O.R. (1989). Floodplain formation in a wandering gravel-bed river: lower Fraser River, British Columbia, Canada. *GeoArchaeoRhein*, 2, 63-70.

[185] Roy, P.E. (1966). The changing role of railways in the Lower Fraser Valley, 1885- 1965. In *Lower Fraser Valley - Evolution of a Cultural Landscape*, B.C. Geographical Series, No. 9, Alfred H. Siemens [Ed.]. Vancouver: Tantalus Research Ltd., 51-67.

[186] Ryder, J.M. and Clague, J.J. (1989). British Columbia. In Quaternary Stratigraphy and History, area of Cordilleran Ice sheet, Chapter 1 of Quaternary Geology of Canada and Greenland, R.J. Fulton [Ed.]. Geological Survey of Canada, Geology of Canada, 1, also Geological Society of America, The Geology of North America, K-1, 48-58.

[187] Schumm, S.A. (1963). A tentative classification of alluvial river channels. *Bulletin of the Geological Society of America*, 74, 1089-1100.

[188] Schumm, S.A. (1977). The Fluvial System. New York: John Wiley & Sons. 338 p.

[189] Schumm, S.A. (1985). Patterns of alluvial rivers. *Ann. Rev. Earth Planet Sci.*, 13, 5-27.

[190] Schumm, S.A. and Winkley, B.R. (1994). The character of large alluvial rivers. In The Variability of Large Alluvial Rivers, S.A. Schumm and B.R. Winkley [Eds.]. New York: ASCE Press, 1-9.

[191] Sedell, J.R. and Froggatt, J. (1984). Importance of streamside forests to large rivers: The isolation of the Willamette River, Oregon, U.S.A., from its floodplain by snagging and streamside forest removal. *Verh. Internat. Verein. Limnol.*, 22, 1828-1834.

[192] Sewell, W.R.D. (1965). Water management and floods in the Fraser River Basin. Department of Geography, University of Chicago. 163 p + figs.

[193] Siemens, A.H. (1966). The processes of settlement in the Lower Fraser Valley — in its Provincial context. In *Lower Fraser Valley - Evolution of a Cultural Landscape*, B.C. Geographical Series, No. 9, Alfred H. Siemens [Ed.]. Vancouver: Tantalus Research Ltd., 27- 49.

[194] Sinclair, F.N. (1961). A history of the Sumas Drainage, Dyking and Development District. Chilliwack Historical Society, Chilliwack, B.C. 20 p.

[195] Slama (1980). Manual of Photogrammetry. Slama, C.C. [Principle Ed.], Theurer, C. and Henrikson, S.W. [Contributing Eds.]. Falls Church Va: American Society of Photogrammetry, 1056 p.

[196] Slater, P.N. (1975). Photographic Systems for Remote Sensing. In Manual of Remote Sensing, Volume I:Theory, Instruments and Techniques, Frank J. Janza, Harold M. Blue and John E. Johnston [Eds.]. American Society of Photogrammetry, Falls Church, Virginia, 235-323.

[197] Smith, N.D. (1978). Some comments on terminology for bars in shallow rivers. In Fluvial Sedimentology, A.D. Miall [Ed.]. *Can. Soc. Petrol. Geol. Mem. 5*, 85-88.

[198] Steiger, J., Gurnell, A.M., Ergenzinger, P. and Snelder, D. (2001). Sedimentation in the riparian zone of an incising river. *Earth Surface Processes and Landforms*, 26, 91-108.

[199] Sterling, S.M. and Church, M. (2002). Sediment trapping characteristics of a pit trap and the Helley-Smith sampler in a cobble gravel bed river. *Water Resources Research*, 38, 8, **19**-1-**19**-11.

[200] Strahler, A.H. and Strahler, A.N. (1991). Modern Physical Geography. New York: John Wiley & Sons. 656 p.

[201] Strahler, A.N. (1952). Hypsometric (area-altitude) analysis of erosional topography. *Bulletin of the Geological Society of America*, 63, 1117-1142.

[202] Sundborg, A. (1956). The River Klaralven: a study of fluvial processes. *Geografisca Annaler*, 38, 127-316.

[203] Surian, N. and Rinaldi, M. (2003). Morphological response to river engineering and management in alluvial channels in Italy. *Geomorphology*, 50, 307-326.

[204] Tamburi, A.J. (1979). Sediment and morphologic studies of the lower Fraser. Fourth National Conference on river basin management, Vancouver, B.C., May 7-8, 1979. Canadian Society for Civil Engineering, 4, 2, 566-581.

[205] Tiegs, S.D. and Pohl, M. (in press). Planform dynamics of the lower Colorado River, 1976-2000. Forthcoming in *Geomorphology.*

[206] Tywoniuk, N. (1973). Sediment budget of the lower Fraser River. Fluvial Processes and Sedimentation, Proceedings of the Hydrology Symposium, University of Alberta, May 7-8, 1973, 624-638.

[207] UMA Engineering (2001). Fraser and Harrison Rivers hydrologic and hydraulic investigations. Final report prepared for The City of Chilliwack by UMA Engineering Ltd., Victoria.

[208] UMA Engineering Ltd. (2002). Fraser River gravel reach 1952 conditions study. Final report prepared for Ministry of Water, Land and Air Protection.

[209] UMA Engineering Ltd. (2004). Fraser River gravel reach sedimentation scenario modelling. Report prepared for Ministry of Water, Land and Air Protection. 12 p + 11 figs.

[210] Van den Berg, J.H. (1995). Prediction of alluvial channel pattern of perennial rivers. *Geomorphology*, 12, 259-279.

[211] Vandernerghe, J. and Maddy, D. (2000). The significance of fluvial archives in geomorphology. *Geomorphology*, 33, 3-4, 127-130.

[212] Veregin, Howard (1988). Error modeling for the map overlay operation. Accuracy of Spatial Databases Meeting, Montecito, CA, December 1988, 3-18.

[213] Vitek, J.D., Giardino, J.R. and Fitzgerald, J.W. (1996). Mapping geomorphology: a journey from paper maps, through computer mapping to GIS and virtual reality. *Geomorphology*, 16, 233-249.

[214] Warburton, J. (1996). Active braidplain width, bed load transport and channel morphology in a model braided river. *Journal of Hydrology (NZ)*, 35, 2, 259-285.

[215] Ward, J.V., Tockner, K., Arscott, D.B. and Claret, C. (2002). Riverine landscape diversity. *Freshwater Biology*, 47, 517-539.

[216] Weatherly, H. and Church, M. (1999). Gravel extraction inventory for Lower Fraser River (Mission to Hope) - 1964 to 1998. Report prepared for District of Chilliwack. Department of Geography, The University of British Columbia. 18 p.

[217] Westaway, R.M., Lane, S.N. and Hicks, D.M. (2000). The development of an automated correction procedure for digital photogrammetry for the study of wide, shallow, gravel-bed rivers. *Earth Surface Processes and Landforms*, 25, 209-226.

[218] Westaway, R.M., Lane, S.N. and Hicks, D.M. (2003). Remote survey of large-scale braided, gravel-bed rivers using digital photogrammetry and image analysis. *Int. J. Remote Sensing*, 24, 4, 795-815.

[219] Willgoose, G. and Hancock, G. (1998). Revisiting the hypsometric curve as an indicator of form and process in transport-limited catchment. *Earth Surface Processes and Landforms*, 23, 611-623.

[220] Williams, P.F. and Rust, B.R. (1969). The sedimentology of a braided river. *Journal of Sedimentary Petrology*, 39, 649-679.

[221] Winkley, B.R. (1994). Response of the lower Mississippi River to flood control and navigation improvements. In The Variability of Large Alluvial Rivers, S.A. Schumm and B.R. Win-

kley [Eds.]. New York: ASCE Press, 45-74.

[222] Winter, G.R. (1966). Agricultural development in the Lower Fraser Valley. In *Lower Fraser Valley - Evolution of a Cultural Landscape*, B.C. Geographical Series, No. 9, Alfred H. Siemens [Ed.]. Vancouver: Tantalus Research Ltd., pp 101-115.

[223] Winterbottom, S.J. and Gilvear, D.J. (2000). A GIS-based approach to mapping probabilities of river bank erosion: regulated River Tummel, Scotland. *Regulated Rivers: Research & Management*, 16, 127-140.

[224] Wolman, M.G. and Leopold, L.B. (1957). River flood plains: some observations on their formation. U.S. Geological Survey Professional Paper 282-C.

[225] Wooldridge, C. (2002). Channel bar radar archirecture and evolution in the wandering gravel-bed Fraser and Squamish Rivers, British Columbia, Canada. Unpublished M.Sc. Thesis, Department of Geography, Simon Fraser University. 122p.

[226] Zar, J.H. (1984). Biostatistical analysis. Prentice Hall: Englewood Cliffs, New Jersey, 718 p.

[227] Zrymiak, P. (1984). 1984 Fraser River hydrographic survey field trip report. Canada Department of Environment, Water Resources Branch, Sediment Survey Section. Unpublished report, 17p + appendix.